Università di Pisa

SCUOLA DI INGEGNERIA

DIPARTIMENTO DI INGEGNERIA CIVILE ED INDUSTRIALE

Corso di Dottorato in Ingegneria Chimica e dei Materiali

Anno Accademico 2014/2015

Diagnostica Avanzata di Sistemi di Controllo di Processi Industriali

Candidato

Riccardo Bacci di Capaci

Relatori

Prof. Ing. **Claudio Scali**

Dott. Ing. **Gabriele Pannocchia**

Controrelatore

Prof. Ing. **Alberto Landi**

University of Pisa

School of Engineering

DEPARTMENT OF CIVIL AND INDUSTRIAL ENGINEERING

Advanced Diagnosis of Industrial Process Control Systems

Riccardo Bacci di Capaci

Degree of Doctor of Philosophy in Chemical and Materials Engineering

2016

Abstract

This PhD work aims to develop an advanced monitoring and diagnostic system for industrial process control loops. This study is based on techniques and algorithms which make use of data available in industrial plants in order to evaluate performance of control loops, detect and distinguish different causes of malfunction, and suggest counteractions to perform.

The overall activity includes modeling and simulation in MATLAB™, experimentations on pilot plants, analysis of industrial data, and implementations in process plants.

The whole PhD activity is framed in a series of projects for development and analysis of monitoring systems, carried out in the last 15 years within the Laboratory of Control of Chemical Processes (CPCLab).

The software developed in this thesis is an evolution of the monitoring system, called *PCU* (Plant Check Up), which has formed a subject of research in the past several years. Different versions of this monitoring system are now available, which vary depending on equipments and devices used in the plants and on variables and measurements available from DCS.

Different collaborations and partnerships with Italian industrial companies (as ENI and ENEL) have been established in the last years. Industrial implementations constitute an interesting source of inspiration on real problems and a mean of validation of the actual operating ability of the system, as well as a large data base valuable to test new monitoring and diagnostic techniques. These activities are usually accompanied by technical reports, and may also originate scientific papers for the most significant results and applications.

Contents

Chapter 1

Introduction

1.1 Motivation

Performance monitoring/assessment of control systems of industrial plants is an important topic in the discipline of Process Control. The common acronym which indicates this fruitful research area is Control Performance Monitoring/Assessment (CPM/CPA).

The term *monitoring* means the action of watching out for changes in a statistic that reflects the control performance over time. The term *assessment* refers to the action of evaluating a statistic that reflects control performance at a certain point in time. Note, however, that both terms are used somewhat interchangeably in the literature [83].

CPM/CPA typically allows one to maintain quality specifications and to limit products cost. Performance deterioration is, in fact, quite common and appears with too oscillating or too slow trends of the controlled variables. Oscillations in control loops cause many issues which can disrupt the normal plant operation. Typically fluctuations increase variability in product quality, accelerate equipment wear, move operating conditions away from optimality, and generally they cause excessive or unnecessary energy and raw materials consumption.

The four main causes of control loop malfunctions – which may also happen simultaneously – are:

- wrong design/tuning of controllers,
- problems (friction) in actuators,
- external perturbations,
- interactions between variables.

Therefore, an automatic monitoring system becomes essential in order to find out which control loops work away from optimal conditions, to identify root causes of malfunctions and to suggest the most appropriate corrective actions.

Nowadays, control loop performance monitoring is an established area of research, and many effective and sophisticated methods to detect malfunctioning loops have been developed. Nevertheless, easiest and most practical methods still tend to be most successful in industrial environments. Often, there are additional aspects - often quite trivial - such as organizational issues, data availability and access that can compromise the use of CPM. Among others, well established works of review, of survey, and of industrial applications are [83, 58, 38, 113]. In [36], very recent results of surveys amongst CPM users have been reported.

1.2 Activity Overview

The present PhD activity is based on two main topics:

1. the so called “standard” diagnosis,

2. the so called "advanced" diagnosis.

This study is limited to performance monitoring and diagnosis of singular control loops, that is, singular input singular output (SISO) systems; therefore, assessment of multivariate systems with emphasis on the presence of interactions is not considered and it may represent a topic of future developments.

The general approach of this thesis is quite practical and specifically oriented to industrial applications and on-line implementations. Anyway, also general and theoretical aspects have been properly studied and presented.

The first activity of the PhD concerned the *standard* diagnosis, with applications on basic control systems present in traditional process plants, that make available only three variables for each control loop: set point (SP), process (or controlled) variable (PV), controller output (OP). Feedback controllers are of PID type which generally act on pneumatic control valves.

One of most common causes of low performance is proved to be the presence of friction in valves, known with the term *stiction* (static friction). Different models for the description of this phenomenon have been developed in the literature of the last 20-30 years. Moreover, numerous techniques for an automatic detection have been proposed in most recent years and, then, various methods for its quantification and for compensation of oscillations on controlled variable have been developed. Approximately, 150 research works concerning valve stiction have been reviewed and classified in these years of PhD studies.

The core of the first activity has focused on the quantification of friction in control valves, which, unlike detection, is little consolidated. There are still several open issues; for example, a reliable prediction of the position of the valve stem (MV) – signal otherwise not measured; the identification of regular and sustained oscillations in controlled variables; the quantification of friction in the presence of additional perturbations, such as a aggressive tuning of controllers and external stationary and non-stationary disturbances.

The second line of research of this PhD, the *advanced* diagnosis, has involved smart instrumentation devices and innovative communication protocols, as Fieldbus. Numerous variables – available through these new technologies – permit one to develop an advanced diagnosis which takes into account the dynamics of internal elements of the actuator (especially the positioner), and allow one also to manage alarms and check-backs from devices. In particular, the measurement of the actual position of the valve (MV) and, consequently, the valve position error allows one to realize a more accurate diagnosis, which separately evaluates specific problems of the actuator from the external loop, and which identifies a higher number of causes of malfunctioning with more reliability.

1.3 Thesis Overview

This thesis consists of 6 chapters, based on one or more original papers, produced during the PhD activity. A fair effort has been made to get a homogeneous and straightforward text, which did not seem simply a miscellany of different works. Each chapter starts with an abstract and a brief introduction, and ends with conclusions. Anyway, these parts might unavoidably contain some repetitions of problems and methodologies.

Chapter 2 acts as introductory part, to present the core of the whole PhD: friction in control valves. This chapter has the form of a review, by describing the state of the art about valve stiction from its basic characterization through its different aspects: modeling, detection, quantification, compensation, smart diagnosis, and commercial software packages. The most significant works appeared in the recent literature have been analyzed, by pointing out analogies and differences among various techniques, and by showing more appealing features and possible points of weakness. The five following chapters focus on some specific topics only

revised in Chapter 2.

Chapter 3 and **Chapter 4** focus on stiction quantification. Different techniques, based on Hammerstein models, have been developed in order to perform process identification and valve stiction estimation. A nonlinear block describes valve friction, while a linear block is used for process dynamics. A grid method is employed to estimate stiction parameters, while different least squares methods (linear or recursive) identify process parameters.

In **Chapter 3** a first couple of nonlinear and linear model has been used. In addition, a general methodology has been proposed in order to discard data for which is very likely to get incorrect stiction estimates and in order to limit application to appropriate cases. Particular attention is devoted to the fact that these estimates can be negatively affected by the inevitable presence of further perturbations on process variables such as set point variations, incorrect tuning of controllers and external disturbances. This basic algorithm of stiction quantification has been then implemented into a new specific analysis module inside the latest version of *PCU* software.

Afterwards, in **Chapter 4** the additional presence of disturbances has been managed with the use of specific (extended) process models. Different quantification techniques – from literature and personally developed – have been tested and their performance have been compared by means of various types of data sets: simulation examples, experiments on pilot plants and data obtained from industrial plants.

Chapter 5 concerns stiction compensation. Fast responses as well as a complete removal of the oscillations on process variable induced by valve stiction are removed by means of a specific technique. This new approach is based on estimate of the appropriate controller output, associated with the desired valve position at the steady-state, by using the amplitude of oscillation before compensation and through the estimate of valve stiction. In addition, set point tracking and disturbance rejection are guaranteed, by monitoring the control error and by switching temporarily to a standard PI(D) controller.

Chapter 6 regards smart diagnosis of pneumatic control valves. The use of additional variables, available by intelligent instrumentations and field bus communication systems, allows one to assess not only valve stiction, but also other malfunctions of the whole actuator. Different types of malfunctions have been introduced and suitable indices have been defined through experimental runs on a pilot plant scale. The valve position error allows specific evaluation of valve status, and detection of different causes of malfunctioning. The same logic has been then implemented in the advanced version of *PCU* software and advantages in the accuracy of diagnosis are shown. Finally, the system has been successfully validated by on-line implementation for control loops assessment of an industrial power plant.

Chapter 7 presents main features of a dedicated version of the system *PCU*, delivered to different companies with the objective of analyzing the most critical control loops of their industrial plants. As example, a comprehensive case of application of the software is described. Two complex plants of the chemical industry, for a total of about 100 loops and 1000 data acquisitions, have been monitored and assessed. Interesting indications of causes of low performance - controller tuning, valves, disturbances - have been obtained and also different strategies to adopt - retuning, valve maintenance, upstream actions - have been given.

Chapter 8 sums up conclusions from the thesis and tries to propose some directions of future works. Then, 3 appendices concerning stiction quantification have been included.

Appendix A contains additional issues not specifically included in Chapter 4 about stiction quantification methods by means of Hammerstein models. Appendix B proposes another approach of estimation by involving Expectation Maximization algorithms. Appendix C compares several stiction quantification methods on further examples of industrial applications.

Finally, an unified bibliography ends this thesis.

Preliminary versions or parts of the different chapters have been presented at conferences

or published in journals, as listed below; some of them have been submitted or will be asap.

- Chapter 2 [27]: To be submitted as soon as possible, 2016.
- Chapter 3 [22]: Chemical Engineering Transactions, 32: 1201–1206, 2013.
  [25]: Industrial & Engineering Chemistry Research, 53: 7507–7516, 2014.
  [23]: In Proceedings of the 19th IFAC World Congress, 2014.
- Chapter 4 [29]: In Proceedings of 9th IFAC ADCHEM, 2015.
  [30]: Submitted to Journal of Process Control, 2016.
- Chapter 5 [28]: Submitted to 11th IFAC DYCOPS, 2016.
- Chapter 6 [31]: In Proceedings of 10th IFAC DYCOPS, 2013.
- Chapter 7 [33]: Chemical Engineering Transactions, 43: 1369–1374, 2015.
- Appendix C [26]: to be submitted as soon as possible, 2016.

1.4 Collaborations

1.4.1 Academic collaborations

During these three years of PhD studies, some international activities of academic collaboration have been established.

First of all, a period of abroad research stay has been conducted for the last part of the PhD. Five months (June - October 2015) have been spent by the research group of Prof. Biao Huang of Chemical and Materials Engineering of University of Alberta (Edmonton, Canada). A research activity has been defined, by merging the areas of interest of the Canadian team with the topics of PhD in the field of control loops monitoring.

In this context, some new specific topics, such as Bayesian statistics, Hidden Markov models, and Expectation Maximization (EM) algorithms, have been examined. These issues are usually exposed and discussed during weekly presentations and meetings taking place within the research group. The main activity of has been two-fold.

The first part has regarded stiction compensation. The whole activity presented in Chapter 5 has been conducted during the abroad research stay. In particular, experimentations have been carried out on a pilot plant in Laboratory of Process Control of Prof. Huang.

The second part, which is still underway, aims to develop an EM algorithm applied to the problem of identification and estimation of friction in control valves. Some details of this activity are reported in Appendix B.

Other academic collaborations have concerned:

- Prof. Q. P. He of Tuskegee University (Alabama, USA). A comparison of performance of techniques for stiction quantification has been carried out. This activity has ended with an acknowledgment inside a paper published in an international journal [75], and it has been then the source of inspiration for a larger comparison of methods for stiction quantification (see Appendix C). This work might also represent the starting point of further collaborations in the fields of control loops monitoring and valve diagnosis.
- PhD student M. Daneshwar of the Universiti Sains Malaysia (Malaysia). The idea was to model the control loop with a mixed approach (white and black box), using Neural Networks for the description of valve friction. The algorithm - still under development - could be applied to both conventional valves and smart valves, for which the position of the stem is measurable.
- an extensive activity of peer reviewing for international journals and conferences, for a total of about 40 papers in different areas of process control.

1.4.2 Industrial collaborations

In parallel, some activities of industrial collaboration and partnership with Italian companies have been carried out. All these activity are finalized to development and analysis of control loop monitoring systems, which are gathered under the name *PCU* (Plant Check Up). Different versions of this monitoring system have been developed, depending on equipments and devices used in the industrial plants and on variables and measurements available from DCS.

In details:

- with ENI, the Italian multinational oil and gas company, to develop and maintain the base monitoring system, called *Loop Control* and implemented in ENI R&M refinery of Livorno since 2007;
- with ENEL, the largest Italian energy company, to develop the system of advanced diagnosis, object of experimentations in a pilot plant (IdroLab), and then implemented in the energy plant of La Casella - Piacenza;
- with CLUI-EXERA, an international association of industrial users of control systems, for which a dedicated version of the system PCU was developed.

These activities have been accompanied by technical reports, which for the most significant results and applications have then originated some scientific papers in national (e.g, [21], [24], [32]) and international (e.g., [31], [33]) field.

Chapter 2

Loop Monitoring and Valve Stiction

Abstract [1]

Valve stiction is indicated as one of the main problems affecting control loop performance and then product quality. Therefore, it is important to detect this phenomenon as early as possible, distinguish it from other causes, and suggest the correct action to the operator in order to fix it. It is also very desirable to give an estimate of stiction amount, in order to be able to follow its evolution in time to allow the scheduling of valve maintenance or different operations, if necessary.

This chapter is a review of the state of the art about the phenomenon of stiction from its basic characterization to smart diagnosis, including modeling, detection techniques, quantification, compensation and a description of commercial software packages.

In particular, this study analyzes the most significant works appearing in the recent literature, pointing out analogies and differences among various techniques, showing more appealing features and possible points of weakness. The review also includes an illustration of main features of performance monitoring systems proposed by major software houses. Finally, the chapter gives indications on future research trends and potential advantages for loop diagnosis when additional measurements are available, as in newly designed plants with valve positioners and smart instrumentation.

Each of the five subsequent chapters of the thesis broadens one topic firstly introduced in this chapter.

[1] This chapter is based on [27]: *Evolution from classical to advanced valve stiction diagnosis.*

2.1 Introduction

Valve malfunctions, hysteresis, backlash, dead-band, and especially stiction, have been known since early times to be important causes of performance deterioration in control loops [120]. They affect plant routine operation and force periodical shutdown to remove them; therefore, they influence the overall product quality and plant economy.

Oscillations in process variables, induced by stiction, can be confused with other causes as incorrect tuning, presence of external disturbances, multi loop interaction and other valve internal problems. In addition they cannot be completely eliminated by controller detuning or by the presence of valve positioners.

Therefore, the problem must be diagnosed as early as possible and appropriate actions to take should be suggested to the plant operator. This explains the large research effort on the subject, carried out by academic research in the last years, facing different aspects of the phenomenon. As fall out, the techniques originated by research work have been adopted in most commercial software packages, initially proposed mostly for retuning purposes.

Several review works also appeared in the literature, even though mostly devoted to specific issues: on stiction detection techniques [78, 48, 86, 54]; on stiction models [64], and on stiction compensation methods [54, 131]. Global reviews, not including smart diagnosis, have been recently proposed by [19, 39].

Following this short recall about the impact of valve stiction, this chapter aims to be a comprehensive survey of the most significant works concerning the phenomenon of valve stiction, starting from modeling and ending with potentiality made possible by smart instrumentation. This chapter follows the structure of the more recent review paper [39], with a detailed updating on last publications, new insights in the comparison of techniques and in perspective open by smart diagnosis.

The survey consists of pointing out analogies and differences among several recent techniques and showing their more appealing features and possible weak points. Results from the comparison of different approaches are synthesized in tables reporting significant indices of merit. Section 2.2 presents an illustration of basic aspects of the phenomenon and related oscillations in the control loop, while Section 2.3 presents more established models to reproduce its effects. Section 2.4 is devoted to the illustration of stiction detection techniques, to recognize its presence since the early stage, and Section 2.5 covers stiction quantification methods which allow one to estimate the amount of stiction and its evolution in time. Section 2.6 deals with compensation techniques, and Section 2.7 with possibilities created by the availability of additional measurements (smart instrumentation). The chapter ends with Section 2.8, where features of different commercial and academic software packages are synthesized, followed by Section 2.9 where conclusions are drawn.

2.2 Phenomenon Description

The term *stiction* - contracted form of static friction - was coined in the process industry to emphasize the difference between static and dynamic friction [120]. Although friction is a long-time-studied topic, the stiction phenomenon has been defined formally only quite recently. Choudhury et al. [47] have proposed a comprehensive description of the mechanism, thus differentiating it from similar valve malfunctions, as backlash, hysteresis, dead-band.

Stiction is defined as a "property of an element such that its smooth movement in response to a varying input is preceded by a sudden abrupt jump called the 'slip-jump', which is expressed as a percentage of the output span. Its origin in a mechanical system is static friction which exceeds the dynamic friction during smooth movement" [47].

The phenomenon is measured as the difference between the final and initial position values required to overcome static friction. For instance, 5% of stiction means that when the valve gets

stuck, it will restart to move and then to vary its true position (MV) only after a cumulative change in control signal (OP) exceeding 5% [47].

In Figure 2.1, the four main variables of a "standard" control loop are indicated. Set Point (SP), Controlled Variable (PV) and Controller Output (OP) are usually recorded, while valve stem position (MV) is not available in general.

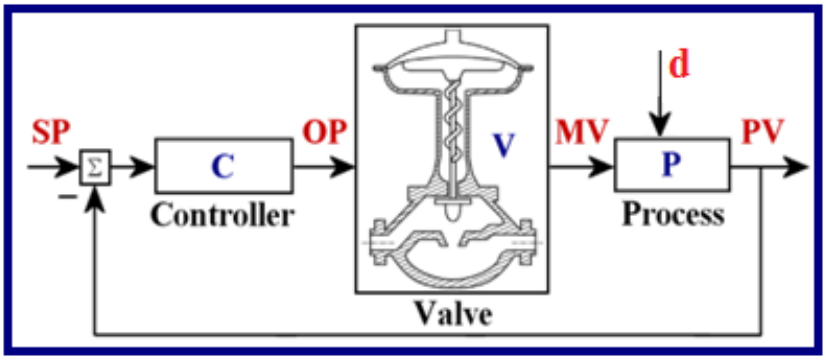

Figure 2.1: The reference scheme for a "standard" control loop.

Pneumatic control valves are the most commonly used valves in process industry due to their high performance. However, some practical issues as seal degradation, unnecessary tightening, expanded metal at high working temperature, and lubricant depletion may result in valve stiction [85].

For a normal valve, MV and OP signal are equal (or proportional) at all times. But in the case of stiction, the valve acts like a nonlinear element and these two signals clearly differ. Stiction in control valve may cause significant degradations in the behavior of the whole control loop, even leading to stability problems. Note that 1% of stiction is considered enough to cause performance problems [85].

Typically, steady-state control errors or unwanted oscillations and limit cycles in all variables are registered (see Figure 2.2). Ideally, distinctive wave shapes characterize the limit cycles caused by stiction. Since the stem velocity remains at zero for a certain period of time, a square-shaped MV signal is generated. This can be considered the "sign" of stiction, as other sources of loop malfunction generate limit cycles behaving more as sinusoidal waves.

Note that increasing the amount of stiction, the amplitude and the period of oscillation of OP and PV signals increase significantly, and the oscillation behavior is also altered [50]. The distinctive signature of a control valve affected by stiction can be also observed in the MV(OP) diagram: a parallelogram-shaped pattern is registered (Figure 2.2, bottom right). The valve is stuck even though the integral component of the controller increases the active force on the stem. Then, the valve jumps abruptly when the active force overcomes friction forces (marked as A in Figure 2.2), and it moves with a offset respect with the desired position.

Note that this signature is typical both of a sticky pneumatic valve and a sticky electric valve. These two types of valve differ only for the actuator, while the valve body, subjected to the majority of friction forces, is the same, as shown in Figure 2.3.

Unfortunately, MV signal is hardly available in practice; therefore MV(OP) diagrams are rarely accessible. Flow control loops, with fast (linear) dynamics, allow one to approximate MV with PV and to assess stiction presence on PV(OP) diagram. Conversely, loops with slower dynamics (level control, temperature control) show PV(OP) diagrams having elliptic shapes also in the case of stiction (Figure 2.2, top right).

Nevertheless, similar paths on PV(OP) are obtained also for other types of oscillating loops: external stationary disturbance or aggressive controller tuning. Furthermore, the presence of field noise and the cases of simultaneous sources of oscillation can significantly alter waveforms. This is the reason why making stiction diagnosis simply by using OP and PV signals can be a very difficult task.

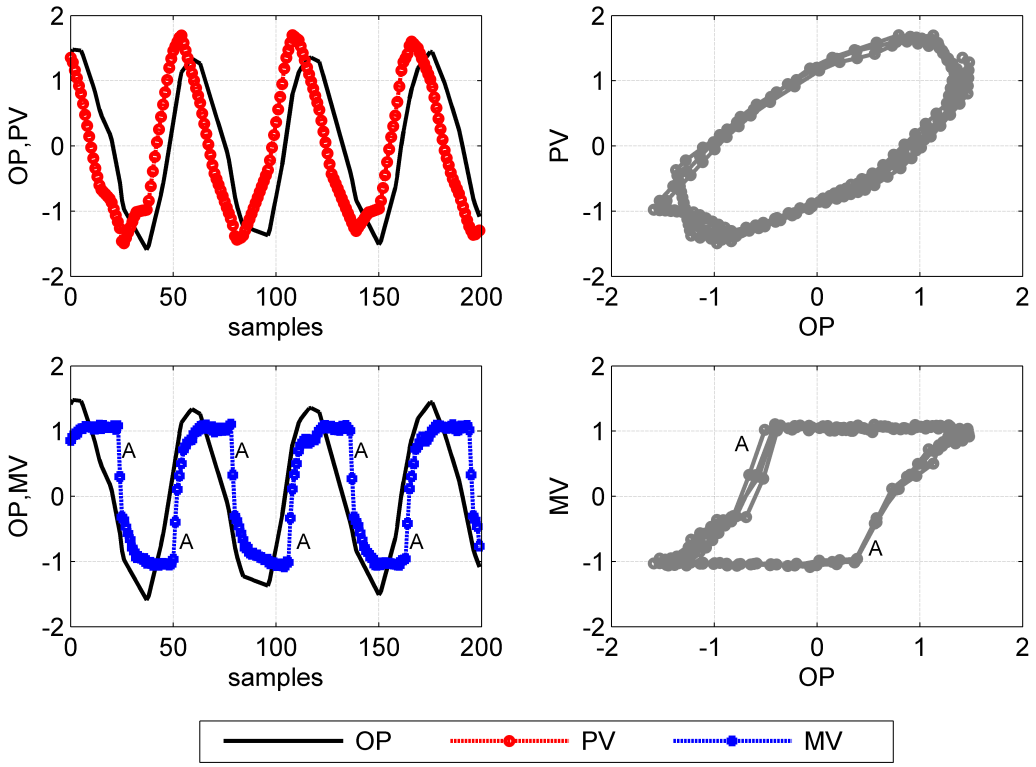

Figure 2.2: Limit cycles of a sticky valve: (left panels) oscillating time trends of OP, PV, and MV; (top right) PV(OP) diagram; (bottom right) MV(OP) diagram.

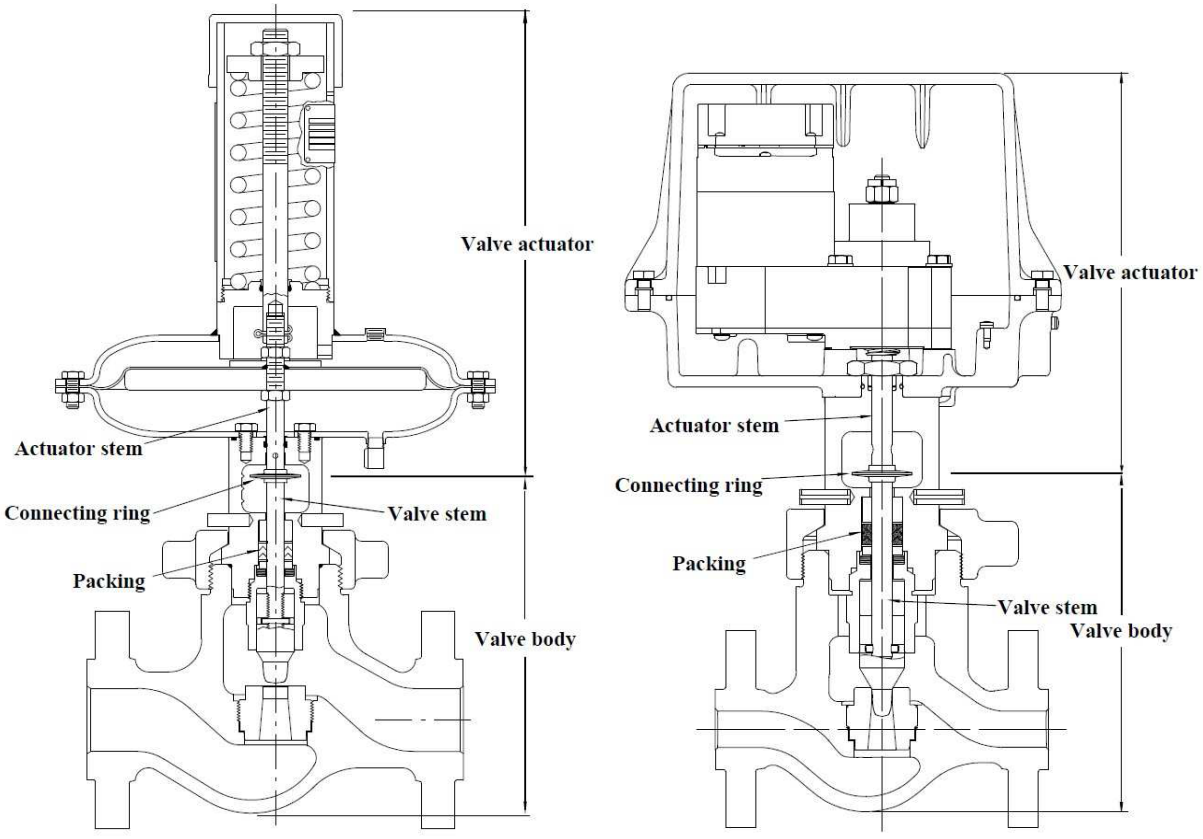

(a) Pneumatic control valve **(b)** Electric control valve

Figure 2.3: Configurations of different types of control valves.

However, the very first challenge for process control purposes is to evaluate the significance of the oscillation in the registered variables. Therefore, also for the analysis of stiction-induced oscillations, only significant oscillations should be evaluated.

Techniques which detect significant loop oscillation can be broadly classified into the following categories [156]: (i) time-domain approaches, e.g., integral absolute error (IAE) and autocorrelation function (ACF) methods; (ii) frequency domain approaches, e.g., fast Fourier transform (FFT) method; and (iii) hybrid approaches including wavelet transform (WT) method. Once single/multiple significant oscillations have been identified, the hard following step is to assess the sources (root-causes) of these malfunctions, that is, the loop(s) where the oscillation started. Finally, the causes of oscillation have to be diagnosed. Therefore, stiction analysis is also strictly linked with the more general issue of oscillation detection and diagnosis. The main techniques for oscillation detection are briefly reviewed below.

Firstly, Hägglund [67], and Thornhill and Hägglund [155] proposed a simple oscillation detection technique based on the IAE of subsequent zero-crossings of the control error (e), between Set Point (SP) and Controlled Variable (PV). The industrial implementation of this method has been discussed by Hgglund in [70]. Then, Forsman and Stattin [63] improved this method by regularizing the upper and lower IAEs. In parallel, Miao and Seborg [105] developed a technique using a decay ratio index of the autocorrelation coefficients of the control error. Later, Thornhill et al. [157] introduced a regularity index of the zero-crossings in the ACF to assess loop oscillation, but its accuracy is limited by the manual choice of band pass filters in the case of multiple oscillations. In the meanwhile, Matsuo et al. [103] presented an oscillation detection approach with the wavelet transform. Later, Salsbury and Singhal [122] have developed a method based on the poles of autoregressive and moving-average models (ARMA).

More recent techniques include discrete cosine transform (DCT) by Li et al. [99], and empirical mode decomposition (EMD) by Srinivasan R. et al. [147], and by Srinivasan B. and Rengaswamy [139], which also provide solutions for nonstationary data. Zakharov and Jämsä-Jounela [176] proposed a method by identifying peak positions of the dominant frequency component in oscillating signals. The technique is compared against five other methods reported in the literature and also introduced two indices to quantify the mean-non stationarity and the presence of noise. In addition, Tikkala et al. [158] have developed a technique for detecting nonstationary oscillations based on a robust zero-crossing method which computes the moving trend of the signal and some specific statistics.

Very recent techniques are able to detect multiple oscillations in control loops. Naghoosi and Huang [108] detect and cluster the peak values of the ACF of the variables. No frequency-selection filtering is required in order to separate different oscillations. In parallel, Guo et al. [66] propose a detection technique of nonstationary multiple oscillations based on an improved wavelet packet transform (WPT), which integrates Shannon Entropy with a non-Gaussianity test and a quasi-intrinsic mode function index. Recently, Srinivasan B. et al. [138] also developed an integrated approach to identify and detect single and multiple sources of loop oscillation.

In the next four sections, the main techniques for stiction modeling, detection, quantification, and compensation will be reviewed.

2.3 Stiction Modeling

Stiction models can be classified into two major categories: *first-principle* and *data-driven* models [47]. It is important to note that all stiction models are a trade off between accuracy and simplicity.

First-principle stiction models describe accurately the physics of phenomenon and fall ba-

sically into two classes: *static* and *dynamic* friction models. Newton's second law of motion and classical balance of forces on the valve are used. The static models describe the friction force using time-invariant (static) functions of the valve stem velocity. Conversely, in the dynamic models time-varying parameters are employed. Two well-known examples of first-principle stiction models are introduced in pioneering works by Karnopp [88] and Canudas de Wit et al. [42] (known as LuGre model).

However, two are the main disadvantages of first-principle models. Firstly, several parameters, such as the diaphragm area, the air pressure, the spring constant and the stem mass, that are actually difficult to estimate, must be known. Secondly, computational times may be too long for practical purposes because cumbersome numerical integrations are necessary. Therefore, first-principle models are usually of scarce practical use for loop monitoring purpose and industrial applications.

On the opposite, data-driven (empirical) modeling approaches can get over the previous two drawbacks, by limiting the number of parameters and the computational burden. However, such empirical models also present some disadvantages. In fact, they cannot fully capture the dynamics of the valve, since - for example - not all the proposed models passed the specific tests applied by following the standards of International Society of Automation (ISA) [64]. An exhaustive review of first-principle stiction models can be found in [39].

Only data-driven models will be discussed in the sequel of this section, being this type largely studied in the last decade, and considered that the scope of Chapter 4 is to make use of practical stiction models in order to compare different quantification techniques based on them.

Nowadays, widely adopted data-driven models are Stenman's, Choudhury's, Kano's, and He's models.

The first model, proposed by Stenman et al. [149], reproduces the jump of the valve stem after the stickband through the use of a single parameter (d). However, this very simple model was proved to be quite inaccurate. In particular, it cannot predict the observed behaviors in the case of a sticky valve excited with a sinusoidal input [47], and it also fails to pass many ISA tests [64].

Therefore, in order to improve the description of stiction phenomenon, a different model was introduced by Choudhury et al. [47], by having the Karnopp's model [88] as reference base. Two parameters are now introduced: the amplitude of deadband plus stickband (S), and the amplitude of the slip-jump (J).

In parallel, a similar stiction model was introduced by Kano et al. [87]. Unlike Choudhury's model, which proves to cope accurately only with deterministic signals, this model handles also stochastic inputs. In this case, S and J coincide with the sum and the difference of static and dynamic friction, respectively. Note that these parameters are quantitatively equivalent to those of Choudhury's model, but, for a given input signal OP, the two models can produce different MV signals with the same values of parameters.

An alternative model was introduced by He et al. [76] in order to reduce the complexity of the two previous formulations. The use of a temporary variable, that represents the accumulated static force, allows one to implement a more straightforward logic and to handle stochastic signals. Two different parameters are used: static f_s and dynamic f_d friction, which make the model closer to the first-principle-based description.

Ideally, these three two-parameters models describe the behavior of a sticky valve on the MV(OP) diagram through a sequence of three components (see Figure 2.4):

1. *Deadband + stickband.* When the valve stem arrives to a rest position or changes the direction, the valve sticks (point A). While it does not overcome the frictional forces, the valve maintains the position (AC) resulting in deadband (AB) and stickband (BC).

2. *Slip-jump.* After overcoming the static friction, the valve converts the potential energy stored in the actuator into kinetic energy, jumping in an abrupt way to a new position (from C to D).

3. *Moving phase.* Once the stem jumps, it continues to move until it eventually sticks again because of a stop or inversion of the direction of the movement (between G and H). During the moving phase, the stem may have a reduced velocity. This condition may stick the valve again while it keeps its traveling direction; in this case, only stickband is present (between E and F).

The parameters of He's model have their equivalent in Kano's and Choudhury's models, according to simple equations: $S = f_s + f_d$; $J = f_s - f_d$ (Figure 2.4). However, due to different logics, He's stiction model can generate a very different MV sequence for a given OP signal and with equivalent stiction parameters.

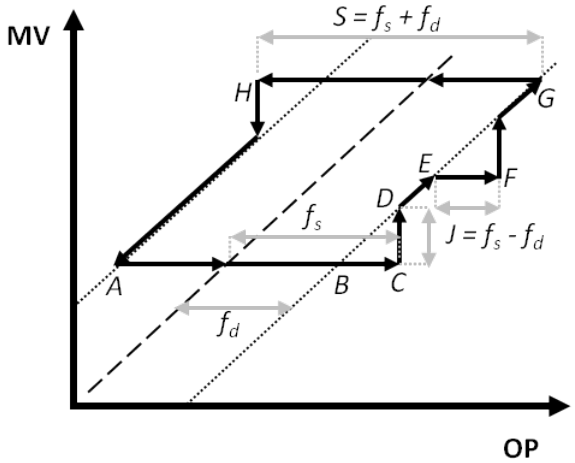

Figure 2.4: MV(OP) Diagram: Modeling a sticky valve with a standard two-parameters model.

Choudhury's and Kano's models were subsequently compared in [85] (Chap. 2): both proved to predict satisfactorily the stiction effects. It is worth underlining that these two models assume that the valve moves slowly and stops only when the control signal changes its direction or the same signal is applied for two consecutive sampling intervals. Conversely, He's model specifically assumes that the static friction is associated with all valve movement, that is, the valve is sufficiently fast - and not *sluggish* as in the other two models - to stop at the end of each sampling interval. In practice, the moving (slipping) phase is actually absent in He's stiction model.

Following this line, He and Wang [74] have then proposed a semi-physical model which can better reproduce the behavior of the first-principle (Classical) model. Three parameters are now used: K, the overshoot observed in the physical model, which is proved to be substantially constant ($K = 1.99$), f_s, the static friction force, and f_d, the dynamic friction force.

On the opposite, Chen et al. [43] modified the first He's model [76] by introducing a two-layer binary tree logic. Although two extra variables are added, the approach generalized static and dynamic friction, improving the inclusion of various types of stiction patterns. The comparison performed by [43] confirms that the path shown in Figure 2.4 on MV(OP) diagram can be actually obtained only using Choudhury's or Kano's model. Conversely, He's model produce a staircase-shaped path along the moving phase of the valve. Note that, since the valve has two states (stick and slip), there are four possible state transitions: stick to slip, keep sticking, slip to stick, and keep slipping [43]. He's model only covers the first two possible state transitions, that is it assumed that the static friction affects every valve movement. Therefore, the moving phase of He's model can be only "jumpy".

Other data-based models have also been presented in the literature. Ivan and Lakshminarayanan [82] simplified the first He's model proposing a one-parameter model (f), specifically oriented to stiction quantification and compensation. This model can simulate only the case of pure stick-slip, in which the valve, after overcoming the stiction band, immediately jumps to the desired position as specified by controller output.

An improved version of Choudhury's model, termed as the XCH model, has been proposed by Xie et al. [166]. This model passed all the ISA standard tests providing a more accurate simulation of a real industrial valve affected by stiction.

Karthiga and Kalaivani [91] proposed a novel model considering three parameters: the deadband (d), the maximum pressure required to move the stem (u_{max}), and the stick-slip magnitude (f). However, explanations provided appear incomplete, thus this model seem to be not applicable for purposes of stiction detection and estimation.

Li et al. [100] revised and refined the previous model of Chen et al. [43] to overcome its limitations in handling instantaneous input commands on reverse motion. The accuracy of the revised model is validated using the full set of ISA standard tests.

Very recently, Tang et al. [152] have proposed a new semiphysical model for sticky pneumatic control valves, based on the study of signal conversion processes among basic components. This semi-physical model contains some major differences and some appealing features with respect to the other data-driven models. Specific experimental tests seems to demonstrate the effectiveness and superiority of the method.

Note that all the previous data-driven stiction models imply uniform parameters for the whole valve span. Conversely, stiction could be inhomogeneous, having various amounts for different operating conditions - that is, different OP values - and then producing complicated signatures on MV(OP) diagram.

In order to overcome these limitations, Wang and Zhang [163] proposed two point-slope models to describe the ascending and descending paths of valve stem, so that asymmetric stiction can be captured. An even more flexible model has been recently introduced by Fang and Wang [59]. This new type of model (Preisach-type), can deal with complicated patterns of sticky control valves and encloses the classical data-driven stiction models as special cases, at the expense of a very complex and non-parametric modeling.

An alternative approach for stiction modeling consists in a pure black-box strategy based on artificial Neural Networks (NNs). Firstly, Zabiri et al. [175] have tested two different types of Neural Networks, by comparing and validating their performance with Choudhury's model. Only the recurrent NN with Nonlinear Autoregressive structure with eXogenus inputs and with Series Parallel architecture (NARXSP) is proved to sufficiently predict the valve behavior in all different stiction situations. Afterwards, Zabiri and Mazuki [172] have extended this approach by testing six other types of NNs. The NARXSP Neural Network is confirmed to be the only structure which can track accurately the sticky valve behavior. A fair robustness of NARXSP-based stiction model is also shown against uncertainty in stiction parameters and situations.

However, it is important to note that these specific good results are obtained, since NARXSP-NN is the only case in which the real output (MV) is fed back to the network feature along with the input (OP) during the training phase. That is, MV signal is predicted only one step ahead in the future. Therefore, such NN cannot be used in a pure modeling mode, to generate the entire valve output from the input. Alternatively, a trained NARXSP network can be used in the parallel (feedback) architecture, where the predicted output from the network is being delayed and fed back along with the input to the network. In this framework, an accurate multi-steps ahead prediction seems to be achieved. Anyway, the actual MV signal has to be known at least in the training phase.

Recently, Daneshwar and Noh [55] developed a model for the whole process with sticky valve, which can be used in controller design to mitigate stiction-induced oscillations. A dynamic fuzzy model of Takagi–Sugeno-type is derived through an iterative well-developed fuzzy clustering algorithm; model parameters are then estimated through least-squares regression.

In Table 2.1, all stiction models reviewed in this survey are synthetically compared, showing their more appealing features and possible weak points.

Table 2.1: Synthesis of data-driven stiction models.

Model	Features				
	Stiction Parameters	Auxiliary Variables	Application on Industrial Data	Pros	Cons
Stenman et al. [149]	1 (d)	-	✓	simple	inaccurate
Choudhury et al. [47]	2 (S, J)	I, x_{ss}	✓	established	no stochastic signals
Kano et al. [87]	2 (S, J)	stp, d, u_s	✓	accurate	-
He et al. [76]	2 (f_s, f_d)	-	✓	accurate	-
He and Wang [74]	3 (f_s, f_d, K)	-	✓	accurate	recently stated
Chen et al. [43]	2 (f_s, f_d)	$stop, cum_u$	✓	accurate	-
Ivan and Lakshminarayanan [82]	1 (f)	-	✓	simple	partially accurate
Xie et al. [166]	2 (S, J)	I, x_{ss}	✗	accurate	recently stated
Karthiga and Kalaivani [91]	3 (d, u_{max}, f)	-	✗	accurate	recently stated
Li et al. [100]	2 (f_s, f_d)	$stop, cum_u$	✗	accurate	recently stated
Tang et al. [152]	7 (f_s, f_d, ...)	several	✗	accurate	recently stated
Wang and Zhang [163]	many	-	✓	flexible	recently stated
Fang and Wang [59]	many	-	✓	flexible	very complex
Zabiri et al. [175, 172]	-	-	✗	flexible	black-box
Daneshwar and Noh [55]	many	-	✓	flexible	very complex

Symbols: "✗", no; "✓", yes

Observing Table 2.1, it is clear that first stiction models (e.g., [47, 149]) are more established in the literature, but, at the same time, they show some basic inaccuracies. Conversely, more recent models potentially allow better performance but should be further applied to industrial data for a complete validation.

Nine of the previous data-driven stiction models are further compared by using some simulation examples. The following models are considered: Stenaman [149], Choudhury [47], Kano [87], classical He [76], semi-physical He [74], Chen [43], XCH [166], Li [100], and Ivan & Lakshminarayanan [82].

Test #1 Figure 2.5 shows a comparison of the results of the models obtained in open-loop (OL), for the same OP signal which consists in a simple sinusoidal input. The stiction parameters are equivalent between all models: $f_s = 5$; $f_d = 3$; $S = 8$; $J = 2$; $d = 6$; $f = 3$.

In the top panel, MV signals obtained with Choudhury's model [47], Kano's model [87], Chen's model [43], XCH model [166], and Li's model [100] are reported.

To better visualize the similarities and differences, the last four MV signals are shifted down by 3, 6, 9 and 12%, respectively. Note that all of these four models produce exactly the same MV signal, while Choudhury's model gives the same stationary oscillation, but a slightly different dynamics for the transitory phase. This peculiar behavior is proved to be incorrect if compared with the MV obtained with physical models [64, 74].

In bottom panel of Figure 2.5, the results of Stenman's model [149], classical He's model [76], semi-physical He's model [74], and Ivan & Lakshminarayanan model [82] are shown. The MV signals are not shifted, since each stiction model generates a very distinctive waveform. Note also the "jump" feature of the wave obtained with Stenman's model and with the two He's models.

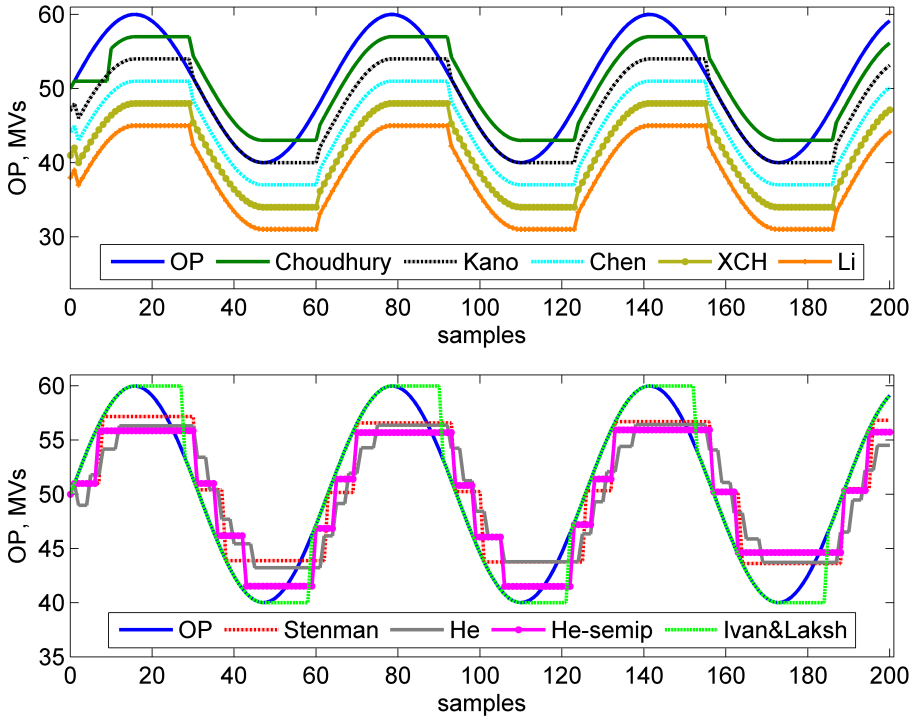

Figure 2.5: Test #1: MV signals for 9 different data-driven stiction models for the same sinusoidal input.

Test #2 In Figure 2.6, to further compare the same nine data-driven stiction models, the closed-loop (CL) behavior of a simulated control loop, with a PI controller $C(s)$, a process model $G(s)$ under a step change of the reference $r(s)$ is then reported. The parameters are fixed in all cases: $C(s) = 0.1(s + 0.5)/s$, $G(s) = 3e^{-5s}/(5s + 1)$, and $r(s) = 1/s$; the same white noise with zero-mean and variance $\sigma_n = 0.01$ is added. The stiction parameters are equivalent between all models: $f_s = 0.35$; $f_d = 0.15$; $S = 0.5$; $J = 0.2$; $d = 0.30$; $f = 0.15$. SP and PV, OP, and MV signals are plotted in the first, second and third column respectively.

The results of Stenman's and Choudhury models are reported along the first row of Figure 2.6. Stenman's model generates peculiar wave shapes with respect to the other models. Choudhury's model gives oscillations with higher frequency and amplitude. The results of the classical and semiphysical He's models, and of the model of Ivan and Lakshminarayanan [82] are shown along the second row of Figure 2.6. In this case, the two He's models produce a perfect square wave on MV. Classical He's model gives PV and MV signals of lower amplitude and frequency. Finally, the other four models are given along the third row of Figure 2.6. To better visualize them, the signals of the last three models are shifted down by 1, 2, 3%, respectively. Note that all of these three produce exactly the same signals (PV, OP, MV) for each sample. Kano's model produces similar stationary oscillations, but due to its different dynamics along the transitory samples, it results slightly out of phase with respect to the other three cases.

Test #3 The results of another example of CL simulation are reported in Figure 2.7. The following parameters are now changed: $r(s) = 2/s$, $\sigma_n = 0.05$. The new stiction parameters - equivalent between all models - are: $f_s = 5$; $f_d = 3$; $S = 8$; $J = 2$; $d = 6$; $f = 3$. Here follow some observations: the waves obtained with Choudhury's model become much asymmetric and less accurate; the model of [82] gives oscillations of excessive amplitude and frequency; the phase shift between the signals obtained with Kano's model and the other three models of the last group appears now much more evident.

Even though these three cases represent specific numerical examples, they are already sufficient to confirm that different data-driven stiction models, even with analogous parameters,

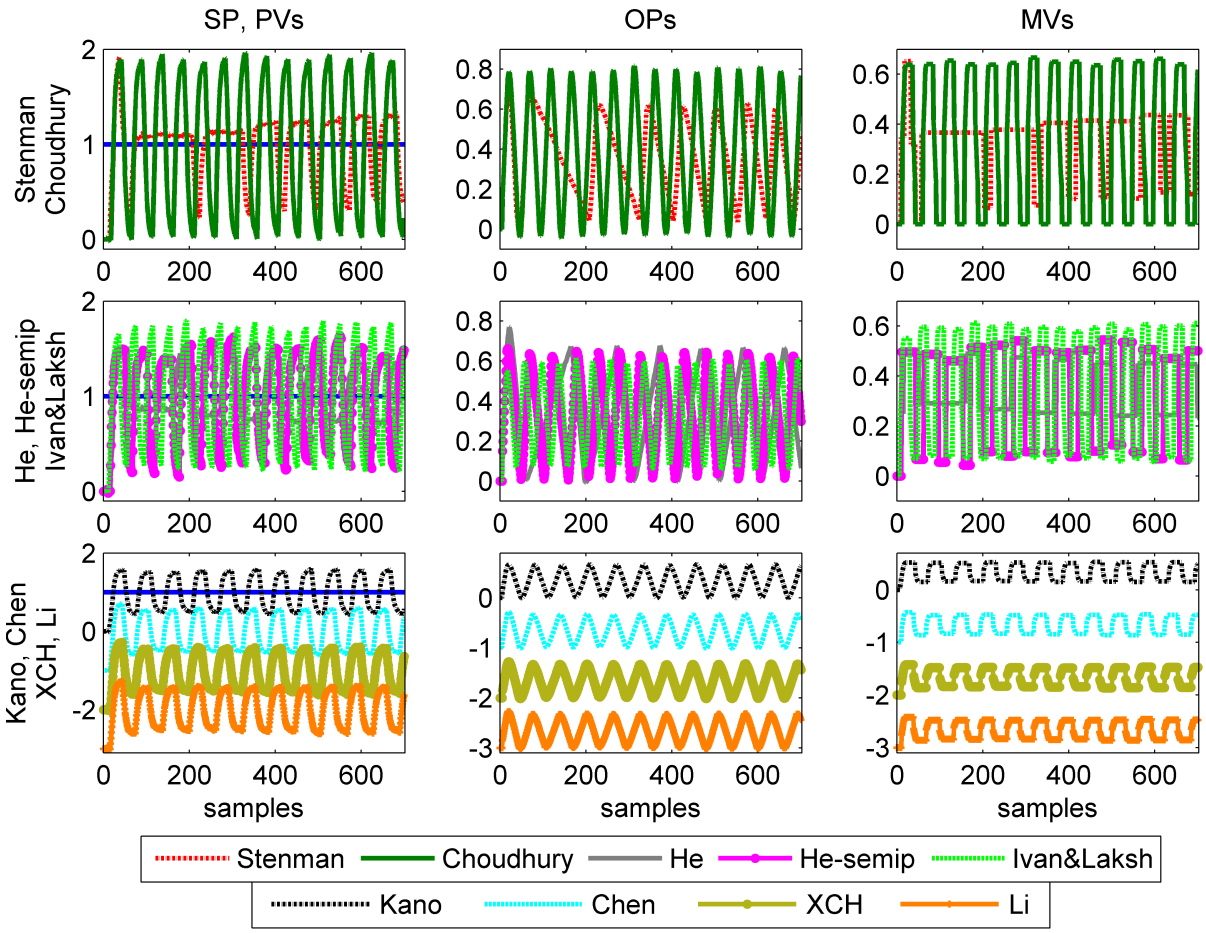

Figure 2.6: Test #2: MV signals for different data-driven stiction models for the same control loop.

may produce very different outputs, both in OL and in CL operation. Only the models of Chen, XCH, and Li appear totally equivalent in these practical situations. To conclude, it is worth noting that:

- the simple Stenman's model reproduces reasonable time trends under CL condition, as confirmed and validated also in the studies of Srinivasan R. et al. [148, 143];
- Kano's model and the most recent models of Chen, XCH and Li seem to give the most accurate and robust description of a real sticky valve.

Anyway, as pointed by He and Wang [75], since the actual valve position is not usually measurable in industrial plants, there is no definitive conclusion on which model signature is absolutely correct.

2.4 Stiction Detection

Many techniques for stiction detection have been proposed in the literature. Following Jelali and Huang [85], they can be broadly classified into four main categories: cross-correlation function-based [77], limit cycle patterns-based (e.g., [87, 168, 124]), nonlinearity detection based (e.g., [46, 154]), and waveform shape-based (e.g., [76, 146, 119]). Note that techniques which simultaneously identify a process dynamics and estimate the stiction amount are elsewhere classified as model-based detection techniques [54, 39]. In this survey, this type of techniques are revised in Section 2.5, which specifically concerns stiction quantification methods.

In a typical stiction detection technique, specific indices are computed using recorded time trends of OP and PV; thresholds values are then established after simulations and applications

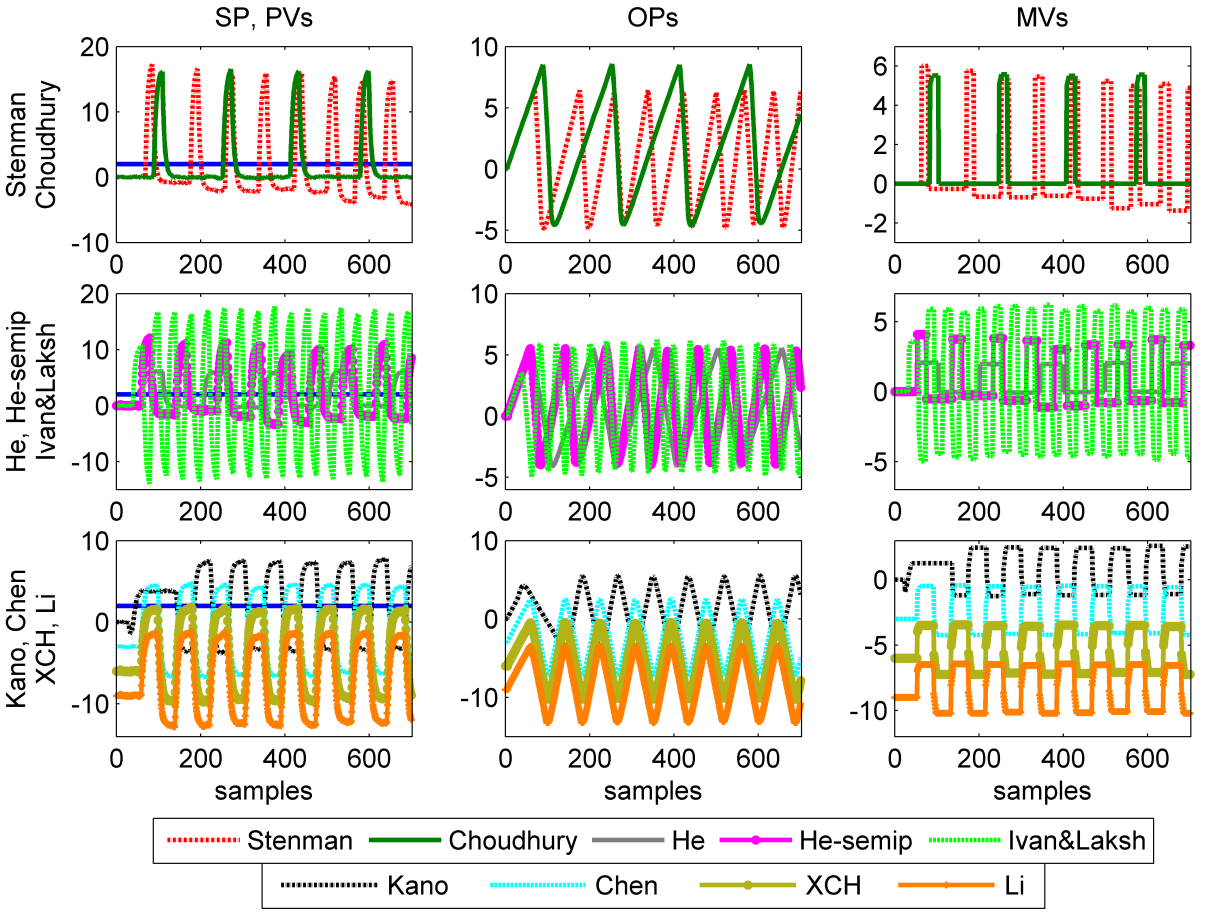

Figure 2.7: Test #3: MV signals for different data-driven stiction models for the same control loop.

on industrial data. Most of these methods, by assuming the presence of a significant oscillation in the control loop, have the main objective of operating a distinction between external disturbance and valve stiction. Reliability is usually reduced in the case of contemporary presence of stiction and disturbances.

Table 2.2 briefly lists all stiction detection techniques reviewed in this section, reporting the category which they belong to or the specific type of algorithm which is used, and also the field of application.

Historically, the first technique to diagnose oscillations can be considered the method of Horch [77], based on the cross-correlation between OP and PV signals. This method is very simple and accessible, but is applicable only to non integrating processes controlled by proportional - integral (PI) controllers, and, in addition, good performance can be achieved only for very periodical oscillations.

Afterwards, Horch [79] has proposed a method specific for integrating processes. The probability density function (PDF - approximated with the normalized raw histogram) of the second derivative of the process output (PV) is used. In the theoretical case of stiction, PDF is close to Gaussian, otherwise it shows two peaks. Stiction presence is assessed on the basis of the best fitting of measured PV. Similarly, PDF of the first derivative of the error signal can be also used for self-regulating processes.

From Table 2.2, it is clear that detection techniques based on typical patterns on MV(OP) diagram are suited only for flow rate control loops (FC).

Kano et al. [87] firstly proposed two methods based on the relationship between the valve input OP and the valve output MV. As shown in Figure 2.4, the MV(OP) diagram produces a

Table 2.2: Synthesis of stiction detection methods.

Method	Features	
	Type	Loop Applicability
Horch [77]	cross-correlation	no LC
Horch [79]	statistics	all type
Kano et al. [87]	MV(OP) patterns	all (better FC)
Yamashita [168]	MV(OP) patterns	only FC
Scali and Ghelardoni [124]	MV(OP) patterns	only FC
Daneshwar and Noh [56]	MV(OP) patterns	only FC
Yamashita [169]	statistics	only LC
Farenzena and Trierweiler [62]	waveform shape	only LC
Brásio et al. [41]	limit cycle patterns	only LC
Choudhury et al. [46]	NL detection	all
Thornhill [154]	NL detection	all
Rengaswamy et al. [116]	waveform shape	all
Srinivasan R. et al. [146]	waveform shape	all
Rossi & Scali [119]	waveform shape	all
He et al. [76]	waveform shape	all
Singhal and Salsbury [132]	waveform shape	no LC
Hägglund [72]	waveform shape	all
Zabiri and Ramasamy [173]	waveform shape - NL detection	all
Ahmed et al. [13]	waveform shape	all
Stockmann et al. [150]	waveform shape	no LC
Ahammad and Choudhury [12]	harmonics based	all
Xu et al. [167]	wavelet technology	all
Zakharov et al. [177]	algorithms combination	all
Pozo Garcia et al. [114]	algorithms combination	all

parallelogram-shaped limit cycle in case of a sticky valve, while it would be linear without stiction. However, since MV is frequently unmeasured, this signal is substituted by the controlled variable PV. This approximation can be considered reasonable for the case of fast dynamics (FC loops), whereas it may yields large errors in the case of loops with slower dynamics (level control LC, temperature control TC), for which PV(OP) diagram shows cycles with elliptic shapes.

Another detection method focused on patterns of the MV(OP) plot was developed by Yamashita [168]. The valve movements are distinguished between I (increasing), D (decreasing), and S (steady). The stiction patterns are assessed for specific sequences of these letters. Three weighted indices are computed on the basis of number of periods of sticky movements. Stiction is detected if these indices, which vary between 0 and 1, overcome the threshold value of 0.25, typical of a random signal.

Scali and Ghelardoni [124] investigated the performance of Yamashita's method using a large number of industrial flow rate control loops and concluded that the method correctly identifies the presence of stiction in 50% of the cases. The authors improved also the original method introducing additional MV(OP) reference patterns and computing corresponding detection indices.

Very recently, Daneshwar and Noh [56] presented a stiction detection technique for FC loops based on a well-developed fuzzy clustering approach, by using typical sticky patterns on MV(OP). Observing a dramatic change of the slope of the lines obtained from successive cluster centers in the presence of stiction, a performance index to distinguish different causes

of oscillation is proposed.

From Table 2.2, three other techniques are specifically addressed to stiction detection in level control loops (LC) [169, 62, 41]. Yamashita [169] developed a statistical analysis based on a simple index that evaluates the excess kurtosis on PV signal. A level control loop affected by stiction presents a two-peak distribution of the first derivative of PV, which means a negative large value of excess kurtosis.

Farenzena and Trierweiler [62] used the PV patterns of a valve affected by backlash or stiction to detect and even distinguish these two phenomena. An index is computed on the first-order derivatives, but the diagnosis seems to be disrupted by the sampling time and the tuning of the controller.

Recently, Brásio et al. [41], proposed a detection technique exploiting the direct proportionality between valve position (MV) and the first derivative of the level (PV) in LC loops. The traditional patterns of the first technique of Yamashita [168] can be then fitted using the OP signal and the first derivative of PV.

Since valve stiction is a highly nonlinear phenomena, the presence of nonlinearity in the signals can mean that stiction is the possible source of loop oscillation [46, 154]. Choudhury et al. [46] proposed a method based on higher-order statistical techniques, as cumulants, bispectrum, and bicoherence of the control error signal in order to infer two metrics: the non-Gaussianity index (NGI) and the nonlinearity index (NLI).

Thornhill [154] developed a method to compare predictability of the original signal and its surrogates using a specific index, based on the fact that a nonlinear signal is more predictable than its surrogates. In particular, a nonlinearity is inferred when the prediction error for the original signal is smaller than the mean of the reference distribution of its surrogates by more than three standard deviations.

According to Table 2.2, ten different stiction detection techniques are based on the comparison between measured signals and reference waveform shapes. The first technique based on the analysis of qualitative waveforms was presented by Rengaswamy et al. [116]. Seven types of primitives and a complex neural network were used to detect and diagnose different kinds of oscillations.

Srinivasan R. et al. [146] have then proposed a pattern recognition approach using the dynamic time warping technique. An optimal fitting between measured data and a stiction template pattern for each oscillating cycle and a global pattern for the whole dataset is performed. The method was tested on datasets of varying complexity as non constant behavior, intermittent stiction, and external disturbances.

The Relay technique, developed by Rossi and Scali [119], is based on the fitting of significant half cycles of the oscillation by means of three different models: a sine wave, a triangular wave and the output response of a first order plus time delay under relay control. The last one is specifically suitable to approximate square waves shapes generated by stiction and modified by the process dynamics. Once fittings have been performed, a Stiction Identification Index (SI) is defined.

This technique presents analogies with the Curve Fitting method proposed by He et al. [76] in which, assuming that stiction is associated to a square wave in MV, a triangular wave is looked for as the distinctive feature of stiction after the first integrator element of the loop. This means in the OP signal (for self regulating processes) or in the PV signal (for integrating processes). On the opposite, the Relay method [119] always analyses the PV signal and uses the relay shape as an additional primitive.

Another approach, based on the ratio (R) between areas before and after the peak of an oscillating signal has been presented by Singhal and Salsbury [132]. The decision rule is sum-

marized as: if $R > 1$, the valve is sticky, but if $R \approx 1$, the controller is aggressive. The method is very simple, but is not applicable to integrating processes (LC loops) and, in addition, shows high sensitivity to noise and different sampling times.

In the shape-based detection method of Hägglund [72], the final decision relies on the averaged value of a normalized index, which involves the fitting of the control error signal between two consecutive zero crossings. If the fitting corresponds best to a sine wave, no stiction is assessed; otherwise, if a square wave is best fitted, stiction is detected.

The approach of Zabiri and Ramasamy [173] involves an index based on nonlinear principal components analysis (NLPCA). Distinctive shapes of the signals caused by stiction and other sources are used. Along with its coefficient of determination, the index quantifies the degree of nonlinearity thus determining the presence of stiction.

Ahmed et al. [13] also presented a stiction detection technique based on waveform shapes. Data compression is used to compare patterns of a sinusoidal or exponential signal with a triangular signal. The basic idea is that triangular signals can be better compressed, since they can be approximated by a combination of straight line segments. A relative compressibility index is specifically defined so that a positive value is an indicator of integrating process with stiction and a negative value means self-regulating process with stiction; a close-to-zero value indicates no stiction.

Finally, Stockmann et al. [150] have developed a method of pattern recognition by using principal component analysis (PCA). PCA allows a clustering procedure which classifies between the typical stiction oscillation and the sinusoidal shape for non integrating processes. Main disadvantages of this method is that many reference simulations with great data variance have to be done once, and then merged in a reference matrix. Anyway, if the matrix has been created successfully, it could be used for all future analysis of industrial datasets.

An alternative method based on harmonics analysis was developed by Ahammad and Choudhury [12]. The control error signal is decomposed using Fourier series. Amplitude, frequency and phases of each term of Fourier series expansion are estimated using least-squares regression technique. Then, the harmonic relationship among the frequencies is examined: odd harmonics indicate the presence of stiction.

Xu et al. [167] presented an approach by using wavelet technology. The key idea is to analyze the signal at various resolution scales to achieve different levels of localization, so that noise and disturbances can be effectively separated from real valve stiction patterns. PV jumps are detected by estimating the Lipschitz regularity of the signal using the discrete dyadic wavelet transform (DDWT) coefficients at multiple resolution scales. Then, an adaptive wavelet denoising method is also applied to the data, preserving stiction patterns while removing the noise. Sticky features are then extracted from the denoised data, and three indexes are calculated. Finally, an overall stiction probability is determined based on these indexes.

Zakharov et al. [177] proposed a stiction detection system that selects four detection algorithms based on characterizations of the data. Five novel indices are proposed: the presence of oscillations, data-sampling resolution, mean nonstationarity, noise and nonlinearities are quantified. The selection is then performed according to the conditions on the index values in which each method can be applied successfully. Finally, the stiction detection decision is given by combining the detection decisions made by the selected methods. The whole algorithm is validated with benchmark industrial data of [85]. In parallel, Pozo Garcia et al. [114] have developed a similar system which combines four stiction detection methods and computes a reliability index for each diagnosis. Each detection method and the whole integrating system are applied to industrial data of a paperboard machine.

Finally, note that all the previously reviewed methods employ only measurements available in process plants. It is important to recall that, once stiction is detected, it is common practice

to *confirm* stiction by means of specific tests on the field. Among others well-established methods, Choudhury et al. [45] have proposed a controller gain change method. This technique employs the peculiar variation of the frequency of oscillation due to changes in the controller gain when valve stiction is the cause malfunction. Different behaviors are registered for the case of aggressive tuning of the controller and external periodical disturbances. A full industrial application has been used to show how the proposed method can identify the root cause of plant-wide oscillations.

Later, Yu et al. [73] showed that the previous method of [45] may give incorrect or inconclusive confirmations in the case of interacting multi-input multi-output systems. In particular, the oscillation frequency seems to change even when the controller gain of a loop not containing a sticky valve is changed. A strategy based on the magnitude of relative change in oscillation frequency due to changes in controller gain is proposed to overcome previous limitations. Nevertheless, only simulation examples are shown.

In conclusion, stiction detection can be considered an established research area, even though different diagnosis techniques may not give the same verdict once applied on industrial data. Examples of inconsistent assessments are widely illustrated in Chap. 13 of [85]. Therefore, knowing the strengths and the weaknesses of different methods, it is possible to obtain a more reliable final detection decision by combining and weighting verdicts of different techniques.

2.5 Stiction Quantification

The ability of providing an estimate of stiction amount is a crucial step before scheduling valve maintenance or performing on-line compensation. While stiction modeling and detection can be considered relatively mature topics, stiction quantification should be regarded still an open issue [85] and, consequently, a fervent research area.

Some techniques perform detection and quantification of stiction in a single stage, while other methods can be applied only once stiction is clearly detected. Table 2.3 summarizes the main features of the quantification techniques reviewed in this survey in terms of kind of approach, type of model (linear and nonlinear part) used to describe the control loop with the sticky valve, and application on industrial data.

The first contributions about stiction quantification have proposed simple metrics to infer the amount of stiction basing on the PV(OP) plot and without requiring the use of specific models of valve stiction and process dynamics. Firstly, Choudhury et al. [49] quantified stiction by fitting an ellipse on the PV(OP) diagram and computing the maximum width of this ellipse. The authors also proposed two other simple algorithms, c-means and fuzzy c-means clustering, to estimate the degree of stiction on PV(OP) plot.

Afterwards, following this line, Cuadros et al. [51] presented an improved algorithm which fits an ellipse just using the most significant points of OP and PV signals, that is, the datasets characterized by large PV variations in response to small OP changes. The method is applicable only to flow stream control loops (FC), where the PV(OP) plot is similar to a parallelogram. For these cases, the procedure seems to have more precision than the previous approaches of [49].

Also Yamashita [170], by extending his first diagnostic method [168], has evaluated the amount of stiction simply basing on the width of the sticky pattern on PV(OP) diagram. To emphasize, these three techniques give a relative estimate of stiction, termed as *apparent* stiction, which represents only an indication of its severity. Indeed, this value is influenced by all other loop parameters, such as controller and process gain. As they may change in time, these techniques cannot be considered completely reliable for stiction quantification.

Techniques which estimate the parameters of a data-driven stiction model and predict the (unmeasured) MV signal, from OP and PV, are much more effective. Significant developments

Table 2.3: Synthesis of stiction quantification methods.

Method	Features			
	Type	Blocks		Application on
		NL Model	LIN Model	Industrial Data
Choudhury et al. [49]	PV(OP) fitting	-	-	✓
Cuadros et al. [51]	PV(OP) fitting	-	-	✗
Yamashita [170]	PV(OP) fitting	-	-	✗
Stenman et al. [149]	Hammerstein Id.	Stenman	ARX	✗
Srinivasan R. et al. [146]	Hammerstein Id.	Stenman	ARMAX	✓
Lee et al. [95]	Hammerstein Id.	He	ARX	✓
Choudhury et al. [50]	Hammerstein Id.	Choudhury	ARX	✓
Jelali [84]	Hammerstein Id.	Kano	ARMAX	✓
Farenzena and Trierweiler [61]	Hammerstein Id.	Kano	ARMAX	✓
Ivan and Lakshminarayanan [82]	Hammerstein Id.	He (modified)	ARMAX	✓
Karra and Karim [90]	Hammerstein Id.	Kano	EARMAX	✓
Sivagamasundari and Sivakumar [133, 134]	Hammerstein Id.	He	ARX	✓*
Shang et al. [129]	Hammerstein Id.	Chen	ARX	✓*
Brásio et al. [40]	Hammerstein Id.	Chen	ARX	✗
Srinivasan B. et al. [138, 137]	Hammerstein Id.	Stenman	ARMAX	✓
Bacci di Capaci and Scali [25]	Hammerstein Id.	Kano	ARX	✓
Bacci di Capaci et al. [29]	Hammerstein Id.	Kano/He	5 types	✓*
Li et al. [98]	Hammerstein Id.	Choudhury	ARX	✗
Wang and Zhang [163]	Hammerstein Id.	Asymmetric	ARX	✓
Fang and Wang [59]	Hammerstein Id.	Preisach	ARX	✓
Wang and Wang [160]	Hamm.-Wiener	Chen	Wiener	✗
Romano and Garcia [118]	Hamm.-Wiener	Kano	Wiener	✓
Ulaganathan and Rengaswamy [159]	Volterra model-based	Stenman	Volterra	✓
Nallasivam et al. [109]	Volterra model-based	Stenman	Volterra	✓
Chitralekha et al. [44]	unknown input observer	(Choudhury)	-	✓
Zabiri et al. [171]	Neural Network	Choudhury	-	✗
Araujo et al. [16]	Describing Function	DF	ARX	✓
He and Wang [75]	Semiphysical stiction mod.	He (3 par.)	-	✓

Symbols: "✗", no; "✓", yes; "✓*", on pilot plant data

were achieved by means of system identification using a *Hammerstein* model, composed of a nonlinear block in series with a linear dynamic block. The nonlinear element models the sticky valve, while the linear part describes the process dynamics. From Table 2.3, it can be observed that the Hammerstein system identification is definitely the most common type of approach (19 different methods), and maybe also the most robust and effective.

The first example of Hammerstein system identification is the method of Stenman et al. [149], where Stenman's stiction model and an ARX process model are used. Stiction is quantified through a segmentation-based method inspired by multi model mode estimation techniques. Also Srinivasan R. et al. [148] fitted OP and PV signals using Stenman's model [149], but - in this case - plus a linear ARMAX model. A grid search algorithm is exploited to estimate the single parameter of the stiction model, while the process parameters are identified through separable least-squares method.

Afterwards, several variants of Hammerstein approach have been proposed. Lee et al. [95] used the ordinary least-squares method to identify the entire model. He's model was chosen as stiction model and the process was assumed having fixed structure: first or second order plus time delay models. In addition, a bounded search region for the stiction parameters was defined and a constrained optimization problem was formulated.

Choudhury et al. [50] improved the approach of [148] by using their two-parameter stiction model [47], which proved to capture more accurately the real stiction behavior. Therefore, both the stiction and the process model parameters were estimated using a two-dimensional (S and J) grid search method.

The method of Jelali [84] used a global optimization by means of genetic and path search algorithms. This approach proved to be robust, but high computational times are required. The

technique of Farenzena and Trierweiler [61] is considered to be an improvement over Jelali's method. A one-stage identification is performed by means of a deterministic algorithm of global optimization that is no longer dependent on the initial guess.

An alternative method was proposed by Ivan and Lakshminarayanan [82] with the objective of an unified approach for stiction quantification and compensation. A modified version of He's stiction model, a refined ARMAX model for the linear part, and some algorithms of data preprocessing, such as data isolation and denoising, are used.

A nonstationary disturbance term in the structure of the process model is the peculiarity of the technique presented by Karra and Karim [90]. This E(xtended)-ARMAX linear model allows one also to detect external disturbances, even when acting simultaneously with valve stiction. A new grid search algorithm is used to determine all the system parameters: Kano's stiction model plus the extended linear model.

Sivagamasundari and Sivakumar [133] presented a method for stiction quantification based on particle swarm optimization. PV and OP data are used to estimate the parameters of the Hammerstein system, consisting of He's stiction model and ARX linear model. Afterwards, these two authors proposed a hybrid procedure combining the fundamental elements of standard genetic algorithms with Nelder-Mead simplex algorithm [134]. These two methods have been also compared and validated on a laboratory control facility.

Particle swarm optimization was also applied by Shang et al. [129]. In this case, Chen's stiction model [43] and an ARX model form the two parts of Hammerstein configuration to be estimated. Brásio et al. [40] also introduced a one-stage optimization technique, by identifying a Hammerstein model composed by Chen's model and a first-order linear model. In order to simplify the identification procedure, the discontinuity of the stiction model is smoothed by means of a continuous function.

Srinivasan B. et al. [137] presented a methodology which combines a Hammerstein model and a Hilbert-Huang Transform with the purpose of root cause analysis. Detection and estimation of stiction are performed using the method developed by Srinivasan R. et al. [148], while oscillations distinction - that is, stiction from aggressively tuned controller and external disturbances - is possible through the nonparametric transform.

Recently, Srinivasan B. et al. [141] improved their previous technique developing an integrated framework for a comprehensive diagnosis of single and multiple causes of oscillation. The problem is addressed integrating a multiple oscillation detection algorithm [136], a model based stiction estimation [148], and additional information obtained by analyzing the data-driven model obtained from Hammerstein method.

Bacci di Capaci and Scali [25], based on Kano's stiction model and an ARX linear model, proposed a filtering methodology which detects and estimates stiction discarding outliers and restricting application to appropriate cases. Recently, Bacci di Capaci et al. [29] have presented a comparison of different combinations of linear and nonlinear models to perform stiction quantification also in the presence of external disturbances.

Within the framework of identification of Hammerstein system, Li et al. [98] have considered a method based on criteria in both the time domain and in the frequency domain in order to improve accuracy and reliability of parameters estimates.

Wang and Zhang [163] introduced a Hammerstein identification algorithm applied to their new asymmetric stiction model and to an ARX model for the process dynamics. More recently, Fang and Wang [59] have developed an identification method based on their flexible Preisach model that can capture complicated patterns of a sticky valve. An iterative methodology estimates the parameter vectors in two iterative linear steps. Parallel to the advantages of this method, a limitation involves stiction quantification: being nonparametric, the Preisach model does not have an index to directly establish the stiction amount.

From Table 2.3, it is clear that while there are a lot of studies modeling processes as linear,

nonlinear processes have not received the same attention, despite many potential benefits. Some of the few approaches to handle nonlinearity are based on the *Wiener* model, which is composed of a linear dynamic block connected to a nonlinear static part. Overall, the control loop is described by a *Hammerstein-Wiener* model, which accounts for the valve stiction and the nonlinear process dynamics; in some cases, they can also address external disturbances. Next four contributions belong to this class.

The method of Wang and Wang [160], considered an extension of Jelali's technique, used Chen's stiction model and a non linear process model in a Wiener-type structure. A new global search grid identification algorithm is then used.

Afterwards, Romano and Garcia [118] described stiction with Kano's model, the linear process with an ARMAX model, and also external disturbances with transfer models of nth order. Piecewise polynomials of the third degree are employed to model the nonlinear block, in the case of unknown nonlinear process dynamics. The optimal couple of stiction parameters is obtained through the Nelder-Mead Simplex algorithm. Despite reasonable results, the procedure seems too complex to be suitable for on-line industrial applications; the large number of parameters to be estimated also may restrict the method utility.

Finally, the nonlinearity of the process was also addressed by Ulaganathan and Rengaswamy [159]. Stenman's stiction model is followed by a nonlinear process composed by a second-order Volterra model. A moving average model for the external disturbance is considered. A solution approach is proposed in the case of known model dynamics.

Later, Nallasivam et al. [109] extended a very similar approach to the case of unknown model dynamics. The parameters of process model and disturbance model are identified, and the single stiction model parameter [149] is identified.

Other stiction estimation approaches have been developed in the literature, few of them are briefly reviewed in the sequel. Chitralekha et al. [44] applied the method of unknown input estimation using a Kalman filter type recursive estimator. After the estimation of MV signal, a trapezoid is fitted on MV(OP) plot. A constrained optimization problem to find the four corner points of the polygon is solved. Note that no specific stiction model is directly assumed in the identification stage; Choudhury's model is only used for the final validation of the technique.

A technique based on six different types of neural networks was introduced by Zabiri et al. [171]. Valve stiction is described by Choudhury's model, while the most suitable neural network algorithm is assessed. Being a black-box approach, this method is applicable to all types of processes, but no deterministic process model is identified.

Araujo et al. [16] developed a technique for stiction quantification based on the harmonic balance method and the describing function (DF) of the stiction nonlinearity. The DF method, a well-established approach to predict the period and amplitude of limit cycles in control loops, shows good performance also in the presence of model uncertainty and for processes with unknown models.

He and Wang [75] have presented an alternative stiction estimation technique which is based on their new semiphysical stiction model [74]. Linear and nonlinear least-squares methods and simplifying assumption on the oscillations of OP and PV signals are exploited.

More recently, in order to make the diagnosis more reliable, some authors have suggested an evaluation of the uncertainty associated with the stiction parameters estimate. Qi and Huang [115] introduced a bootstrap based approach to establish the statistical distribution of stiction estimations. For example, if the 95% confidence intervals of stiction parameters include 0, it is possible that there is no stiction. Once again, a Hammerstein model identification and a grid search algorithm are used.
Afterwards, Srinivasan B. et al. [140, 141] have proposed an algorithm to measure the reliability of the results provided by any Hammerstein-based stiction detection and estimation

method. This measure, using the frequency domain analysis of closed-loop systems, is applicable only to linear process dynamics. Basically, it is showed that if the controller cutoff frequency is much smaller than that of the process, and this latter is also much greater than the loop oscillation frequency, then stiction is likely to be correctly identified, if present. On the opposite, if the process cutoff frequency is not much greater than the oscillation frequency, the presence of stiction is much less likely to be correctly detected. The method addresses also the problem of determining a reliable search space for the linear model components of any Hammerstein system.

To conclude, as for stiction detection, in order to get a more reliable final estimation, combining and weighting the verdicts of different types of techniques - even the simplest ones - can be suggested as the best solution.

In Chapter 3 a first method for stiction quantification is proposed; while in Chapter 4 and then in Appendix C, some well-established methods for stiction quantification are compared by applications to large industrial datasets.

2.6 Stiction Compensation

Repair and maintenance are the definitive solutions to fix a sticky valve. However, these actions may not be practicable between two consecutive plant shutdowns; therefore, as matter of principle, stiction compensation can be a valid option to relieve negative effects of stiction on loop performance.

A first classification of stiction compensators, derived from mechanical and robotics engineering, divided them into model-based and non-model-based.

Although a stiction model is not directly employed by non-model-based compensators, it may be anyway needed to predict operating point stability, limit cycle stability, or to analyze performance [39]. In order to delete the stiction force, many feedforward and feedback strategies based on stiction models were proposed. However, in general, these models are very complex, which restricts significantly the possibility of industrial applications. For example, the well-established method of Kayihan and Doyle [92] uses a first-principle stiction model (the Classical model) to describe stiction and estimates the immeasurable states providing a robust control action. All valve parameters are to be available, but such detailed information is hardly possible in practice. A detailed review of model-based compensation methods can be found in [39].

On the opposite, most recent stiction compensation techniques, specifically oriented to control loop monitoring and assessment, follow data-driven approaches and thus result much more simple and accessible. Only these methods will be discussed in the sequel of this section.

Six different categories can be established [131, 39]: compensation through controller retuning (e.g., [65]), knocker method (e.g., [69]), constant reinforcement (CR) [82], alternate knocker method [142], two- or three-move compensators (e.g., [145, 52]), and optimization approaches [145].

Two other basic approaches, namely dithering and impulsive control, have been reported in the literature for stiction compensation in electro-mechanical systems. Unfortunately, pneumatic valves, that constitute about 90% of actuators used in control loops, filter such high frequency dither signals, making dithering techniques ineffective. A similar problem exists with impulsive control technique [52].

Table 2.4 summarizes the features of the reviewed compensation methods, in terms of reduction of PV oscillation, reduction of valve movement, and no a priori process knowledge

requirement - except for routinely available operating data, and set point tracking and disturbance rejection.

Table 2.4: Synthesis of stiction compensation methods.

Method	Type	Features			
		Reduction of PV Oscillation	Reduction of Valve Movement	no a-Priori Process Knowledge Requirement	Set Point Tracking and Disturbance Rejection
Gerry and Ruel [65]	Retuning	✓	✓	✓	✗
Mohammad and Huang [15]	Retuning	✓	✓	✓	✗
Hägglund [69]	Knocker	✓	✗✗✗	✓	✓
Srinivasan R. and Rengaswamy [143, 144]	Knocker	✓	✗✗	✓	✓
Cuadros et al. [53]	Knocker	✓	✗	✓	✓
Arumugam et al. [20]	Knocker	✓	✗✗	✓	✓
Ivan and Lakshminarayanan [82]	Constant Reinf. (CR)	✓	✗✗	✓	✓
Hägglund [71]	Constant Reinf. (CR)	✓	✗✗	✓	✓
Srinivasan R. and Rengaswamy [142]	Alternate Knocker	✓	✗	✓	✗
Srinivasan R. and Rengaswamy [145]	2-Moves	✓	✓	✗	✗✗
Farenzena and Trierweiler [60]	2-Moves	✓	✓	✗	✗
Cuadros et al. [52]	2-Moves (i)	✓	✓	✗	✗
	2-Moves (ii)	✓	✓	✗	✓
Wang [161]	2-Moves	✓	✓	✗	✓
Karthiga and Kalaivani [91]	3-Moves	✓	✓	✗	✓
Wang et al. [164]	2-Moves	✓	✓	✓	✗✗
Tang and Wang [153]	2-Moves	✓	✓	✓	✗✗
Srinivasan R. and Rengaswamy [145]	Optimization	✓	✓	✓	✓
Sivagamasundari and Sivakumar [135]	Mixed	✓	✓	✓	✓
Mishra et al. [106, 107]	Advanced Controller	✓	✓	✓	✓
Arifin et al. [17]	Mixed	✓	✓	✓	✓

Symbols: "✗", no/low; "✗✗", bad; "✗✗✗", very bad; "✓", yes/good

From Table 2.4, it is worth noting that all methods exhibit good capacity in reducing PV oscillation, but most of them also shows some drawbacks regarding other issues. For example, knocker approaches tend to produce a too fast motion of the valve, while two-moves techniques usually require a priori process knowledge and may not achieve good set point tracking and disturbance rejection. Each compensation method is briefly reviewed below.

Simple and practical techniques for facing stiction on-line were firstly proposed by Gerry and Ruel [65]. Basically, a set of retuning rules for the controller are introduced to decrease the impact of the stiction-induced oscillations at the expense of a slower response (detuning) or steady-state control errors (switching from PI to P action).

Afterwards, Mohammad and Huang [15] suggested a stiction compensation framework based on the oscillation condition proposed in their previous work [14], which is also suited for systems with multiple sticky valves. By using frequency analysis and harmonic balance, and by following some guidelines of controllers retuning, the occurrence and the amplitude of oscillations can be predicted and then stiction can be reduced or eliminated for different process and controller dynamics. For example, for a PI controller and a first-order process with time delay, integral time T_i must be greater than the sum of the process time constant τ and its time delay θ to avoid oscillations.

Very recently, Li et al. [97] analyzed stiction induced oscillation in cascade control loops by using frequency analysis. A set of practical techniques of oscillation compensation through outer and inner controller tuning, and through changes of control strategies were proposed. Theoretical results are then validated through experiments on a pilot scale flow-level cascade control.

The knocker approach consists of adding a predefined signal to the control signal (OP) before entering the valve in order to prevent oscillations in the process output (PV). These meth-

ods, producing a faster motion of the valve, however, can cause mechanical problems even worse than the normal operating. Therefore, they should be considered just short-term solutions. The first knocker developed by Hägglund [69], specifically targeting stiction in control valves, produces short pulses with constant amplitude, width, and duration. PV oscillations are removed at the expense of a faster and wider motion of the valve stem, which involves a much higher wear rate (compare Table 2.4).

To overcome these disadvantages, some guidelines for the automated choice of the compensation parameters of the knocker were suggested by Srinivasan R. and Rengaswamy [143, 144]. This revised knocker approach, which integrates two stiction detection techniques, shape-based [146] and model-based [148], proved to reduce PV variability ensuring less aggressive valve movements compared to Hägglund's formulation.

Another method based on the knocker approach was presented by Cuadros et al. [53]. A supervision layer analyzes the control error and interacts with the proportional-integral-derivative (PID) controller. This integrated strategy shows a lower integral absolute error and even a reduced number of valve movements (compare Table 2.4).

Finally, the most recent technique inspired by the knocker method has been proposed by [20]. Instead of a pulse signal, a pure sine wave is added to the controller output. Amplitude and frequency of the compensating signal are tuned on the basis of uncompensated control variable. PV oscillations are reduced and MV movements are limited. The additional signal does not contain harmonics which cause sudden changes in valve input and increase variability of the valve output. The technique seems to overcome results of standard knocker; anyway, only few simulation examples are shown, while no practical application is provided.

An alternative compensation approach was suggested by Ivan and Lakshminarayanan [82]. The compensating signal is now a constant reinforcement, added to the valve input only when the OP signal varies, whose value is related to the estimated amount of the single stiction parameter (f). The method appears very useful to reduce variability of PV, but does not significantly decrease the valve aggressiveness.

This method is actually similar to the one proposed by Hägglund [71] for backlash compensation. Note that the term "backlash" in the context of linear motion control valves has to be interpreted as the deadband, which is a special case of stiction, that is when $J = 0$. In [71], the compensating signal, to be added to OP, is the product of estimated amount of backlash and the variation of the control error.

The alternate knocker method of Srinivasan R. and Rengaswamy [142] includes the addition of a special block to the nominal PID algorithm. However, since the nominal controller is unaware of this adaptation of control signal, its performance may be negatively affected. Moreover, instability and/or additional wear of the valve may even occur.

The two-moves compensation method aims to keep the valve at its steady-state position, by performing at least two stem moves in opposite directions. In this approach, first proposed by Srinivasan R. and Rengaswamy [145], the magnitude of the compensating signal should be large enough to exceed stiction and move the valve, but not too large to saturate it. Considerable limitations arise in the case of set point tracking and disturbance rejection, hindering on-line implementation of the method. Also the use of the one-parameter stiction model [145] reduces accuracy. In addition, this method [145] relies on the assumption that the measurements are represented by deviation variables and the steady-state value of MV is known, which is rarely feasible, mainly because the loop to be compensated is under oscillatory behavior [52].

Afterwards, another two-moves method was presented by Farenzena and Trierweiler [60]. Instead of using an additional compensator block, the traditional PI controller block is modified. The technique can achieve closed-loop performance faster than open-loop and efficient

rejection of load disturbances. Unlike the previous method of Srinivasan R. and Rengaswamy [145], a fair set point tracking, with a small offset is possible, and a significant reduction of valve travel is showed.

Two improved versions of the two-moves compensation method were then developed by Cuadros et al. [52], in order to overcome the drawbacks concerning the set point tracking. An exact knowledge of the plant model is not required and set point changes can be tackled by detecting increases in the control error. However, the first method, consisting of four movements, is sensitive to load disturbances. On the opposite, the second method, based on two movements and four states, and especially suited to tackle disturbances, proves more robust. Anyway, the requirement of having similar control valve and process dynamics is a limitation of this second approach.

Also Wang proposed a compensation method based on two movements [161]. A short-time rectangular wave is added to the set point in two distinct movements and the valve is moved to the desired position, avoiding high variability. Robustness against modeling errors and against measurement noise seems to be the main advantages of this method; also the fact that two-movements are applied in closed-loop is an appealing feature.

A alternative method that involved not two but three movements was presented Karthiga and Kalaivani [91]. This approach, exhibiting a lower overshoot and settling time than the previous ones, seems to impose a smoother valve operation, which results in a longer valve life.

Very recently, Wang et al. [164] have presented a new implementation of the open-loop two-moves compensation method, which performs actually six movements. The period of oscillation of the controller output before compensation and the estimated amount of stiction are employed to assess the value of OP associated with the desired valve position. Therefore, no a priori assumption of the valve position in oscillation is required, as in the case of standard two-movement method [145]. This implementation outperforms the standard two-moves method in terms of velocity and lower amplitude of the response. However, set point tracking and disturbance rejection are still poor.

Following this line, Tang and Wang [153] have proposed an improved version of the two-moves method, which uses really only two movements in open-loop mode. A revised approach is presented to estimate the value of OP associated with the desired valve position to be applied at steady-state. A simplified method to estimate amount of valve stiction is also given, and the time of implementation seems shorter than the technique of [164].

An optimization-based approach was also developed by Srinivasan R. and Rengaswamy [145], with the idea of balancing between less-aggressive valve movements, reduced PV variability, and less energy in the signal added to OP. An objective function is minimized using the compensator moves as optimization variables. Compared to the classical approaches, significant improvements are obtained, but the need for analyzing the model mismatch effect, the incorrect stiction measurement, and the real-time issues before on-line implementation are pointed out. In addition, the method is computationally expensive and, since the objective function is not smooth, a local minimum might be attained and an offset between PV and SP may arise.

Based on previous knocker techniques, Sivagamasundari and Sivakumar [135] introduced a model-based compensation approach. He's model is employed to estimate the stiction amount, and, subsequently, few rules to build the waveform of the compensating signal are suggested. This mixed approach seems to give a non oscillatory PV without involving faster and wider moves of the valve. Moreover, no information of process or controller is required, and good tracking of the set point changes is achieved.

Among other approaches of compensation, a model predictive control formulation, based on mixed-integer quadratic programming (MIQP), was developed by Zabiri and Samyudia

[174]. Since valve stiction is taken into account explicitly in the optimization problem, closed-loop performance are proved to be significantly improved. However, a priori knowledge of the stiction parameters is required. In addition, due to the high computational burden and the resulting feedback latency, this formulation may not perform well in the case of highly nonlinear or highly dimensional systems.

Recently, Mishra et al. [106] introduced a stiction combating intelligent controller (SCIC) based on fuzzy logic. No additional compensator is required, since the SCIC is a fuzzy PI controller with variable integral gain, making use of Takagi-Sugeno scheme. The instantaneous integral gain depends upon the value and upon the rate of change of the control error. This novel approach, being also independent of the stiction band value, seems to outperform a traditional PI controller, yielding less variability in PV and less aggressiveness in the valve input, both in the case of set point tracking and disturbance rejection.

Afterwards, the same authors [107] have proposed another compensation solution, by using a nonlinear PI controller (NPIC), which is tuned on-line through a Differential Evolution algorithm for ITAE as a cost function to be minimized. Again, a nonlinear control law is employed to vary the PI integral gain, based on the error and its rate of change. Similarly to [107], pilot plant experiments reveal good performance for the NPIC with respect to all features of Table 2.4.

In parallel, a model free approach for stiction compensation was developed by Arifin et al. [17]. Also this scheme proves to attain all the characteristics listed in Table 2.4. In particular, both oscillation amplitude and frequency are reduced, and good set point tracking and disturbance rejection are obtained. No precise knowledge of process model, but only minimal information about stiction-induced oscillation is required. Also simplicity in on-line implementation is shown by applications on a pilot plant.

A comprehensive comparative study of different stiction compensation methods was presented by Silva and Garcia [131]. The performance were evaluated using some metrics: the integral absolute error, a factor related to the stem position variation, the valve actuator pressure variation, and the rising time. The methods were tested in the case of set point tracking and through various regulatory experiments, by using a flow rate control loop in a pilot plant. The best solutions proved to be the knocker method [69] and the two constant reinforcement methods of [82] and [71], applied along with a slightly modified version of the method of Cuadros et al. [53] based on the monitoring of control error (called as *control freezing*).

In this section, a brief comparison of five different stiction compensation techniques is now presented (see Figure 2.8). The following methods are compared: the retuning method of Mohammad and Huang [15], the knocker of Srinivasan R. and Rengaswamy [143], the constant reinforcement (CR) of Ivan and Lakshminarayanan [82], the CR of Hägglund [71], and the two-movements method of Wang et al. [164].

The methods are applied to the same control loop, with a PI controller and a process model $G(s)$, under two step changes of the reference (at time $t_{sp} = 4000$, and 6000), and a load disturbance (at time $t_d = 8000$). Before the onset of the compensators (at time $t_{on} = 2000$), the parameters are fixed in all cases: $C(s) = 0.1(s + 0.1)/s$, $G(s) = 3e^{-5s}/(10s + 1)$; the same white noise with zero-mean and variance $\sigma_n = 0.005$ is added. Stiction is simulated by Chen's model [43], with the following parameters: $f_s = 0.2$; $f_d = 0.1$. SP, PV, and OP, MV signals are plotted in the first and second column, respectively.

In particular, by using the method of [15], the controller is retuned following some basic rules: the proportional gain is reduced (here by a factor of 4), and the integral time is increased (here to $T_i = 60$) to be greater than the sum of the process time constant ($\tau = 10$) and its time delay ($\theta = 5$). The parameters of the Knocker pulses are set according to the suggestions given in [143]: amplitude $a_k = (f_s + f_d)/2$, width $\tau_k = 2T_c$, and duration $h_k = 5T_c$, where $T_c = 1$ is the time sampling. For both CR methods, the amplitude of the compensating signal is set to

$a = (f_s + f_d)/2$, as suggested in [82]. Finally, the parameters of the two-moves compensator of Wang et al. are set to their default values [164].

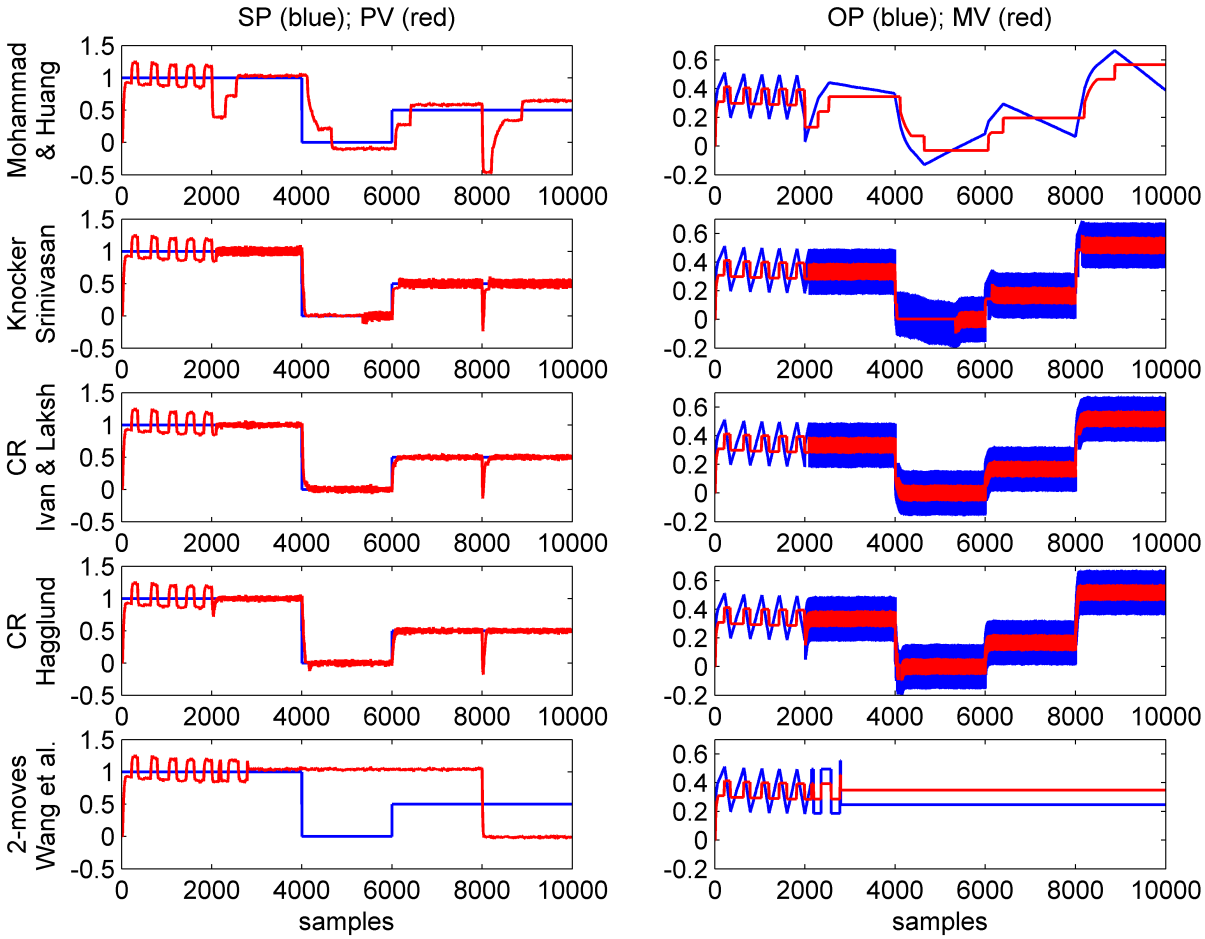

Figure 2.8: Time trends for different stiction compensation methods for the same control loop.

The features of performance of different compensation methods, previously reported in Table 2.4, are now confirmed in Figure 2.8. All methods allow a reduction of PV oscillation in the case of constant set point, that is until $t_{sp} = 4000$. In particular, the retuning (detuning) method of [15] shows poor closed-loop performance, typical of a sluggish controller. The knocker and the two CR methods involve also a significant increase of OP variability, which causes a higher MV variability and a faster valve wear. The two-moves method of [164] leads the PV signal close to its reference, by also reducing the OP variability; however, being a fully open-loop method, it does not guarantee any set point tracking and disturbance rejection.

Table 2.5 compares these five methods, by using simple indices computed before and after the onset of compensation, similarly to what extensively presented by [131].

These performance indices are the reduction ratio of the integral absolute error, the reduction ratio of OP variability, and the reduction ratio of MV variability, defined respectively

as:

$$IAE_{rr} = \frac{IAE_{\text{bef}}}{IAE_{\text{aft}}} = \frac{\sum_{k=1}^{t_{on}} |e_k| T_c}{t_{on}} \frac{(t_{fin} - t_{on})}{\sum_{k=t_{on}}^{t_{fin}} |e_k| T_c} \tag{2.1}$$

$$OP_{rr} = \frac{OP_{\text{bef}}}{OP_{\text{aft}}} = \frac{\sum_{k=1}^{t_{on}} |OP_k - OP_{k-1}|}{t_{on}} \frac{(t_{fin} - t_{on})}{\sum_{k=t_{on}}^{t_{fin}} |OP_k - OP_{k-1}|} \tag{2.2}$$

$$MV_{rr} = \frac{MV_{\text{bef}}}{MV_{\text{aft}}} = \frac{\sum_{k=1}^{t_{on}} |MV_k - MV_{k-1}|}{t_{on}} \frac{(t_{fin} - t_{on})}{\sum_{k=t_{on}}^{t_{fin}} |MV_k - MV_{k-1}|} \tag{2.3}$$

Table 2.5: Performance Indices for different compensation method.

Method	IAE_{rr}	ΔOP_{rr}	ΔMV_{rr}
Mohammad and Huang [15]	0.828	4.674	4.166
Srinivasan R. and Rengaswamy [143]	3.855	0.036	0.065
Ivan and Lakshminarayanan [82]	5.489	0.012	0.014
Hägglund [71]	5.258	0.012	0.015
Wang et al. [164]	0.285	6.941	7.882

From Table 2.5, it can be observed that the knocker and the two CR methods yield a significant reduction of the integral absolute error at the expense of a high increased variability in OP and MV. The opposite happens for the retuning method and the 2-moves technique. To conclude, also by basing on the proposed simple simulation example, it is confirmed that different compensation methods have good compensation capacity; however, they all present some specific drawbacks. Therefore, the choice of the best technique is due to a trade off between all the analyzed issues.

In Chapter 5 a new method for stiction compensation is illustrated.

2.7 Smart Diagnosis

It is important to note that all techniques described in previous sections have been developed for traditional control plant design, with ordinary valves and communication systems with analog signals in 4 – 20 mA. Being the manipulated variable (valve stem position - MV) not known, stiction must be detected and quantified on the basis of available measurements of the controlled variable (PV) and controller output (OP).

However, in newly designed plants, the adoption of intelligent instrumentation, valve positioner and field bus communication systems increases the number of variables that can be acquired and analyzed by the monitoring system. This fact enlarges the potentialities of performing a more precise diagnosis of actuator problems which are not only limited to the presence of valve stiction (and related problems, as deadband, hysteresis, backlash), but can also include other causes (changes in spring elasticity, dynamic friction (jamming), membrane wear or rupture, leakage in the air supply system). The positioner itself can also be the source of other specific faults that can upset loop performance. All these malfunctions require specific actions to be counteracted by operators and, once more, it is very important to be able to diagnose different sources.

Diagnosis of smart actuators has been recently addressed in literature, but it can be observed that comprehensive connection with the traditional research on control loop assessment

and valve diagnosis is still lacking; some of the few works about smart diagnosis are briefly reviewed in the sequel.

Koj [93] firstly distinguished 19 different faults in a smart industrial actuator composed by control valve, pneumatic servo-motor, and positioner. Then, Bartyś and Kościelny [34] applied four different fuzzy logic methods to diagnose and isolate some of these faults. A minimum, a multiplicative, an additive, and a mixed approach were developed and specifically applied to monitor the smart actuator studied in [93]. Also Ould Bouamama et al. [111] dealt with fault detection and isolation (FDI) of smart actuators. They combined bond graphs and external models to assess different faults. An external model is a generic method which can be used to verify the functional specifications of a smart equipment. This technique has been applied to monitor the same valve with positioner of [93].

Bartyś et al. [35] provided the description and presentation of the actuator benchmark used in fault diagnosis studies within the Development and Application of Methods for Actuator Diagnosis in Industrial Control System (DAMADICS) European Research Training Network. This system is openly available, is FDI method-independent, and based on an accurate study of the phenomena that can lead to likely faults in valve actuator systems. The industrial application is focused on the sugar factory Cukrownia Lublin SA, Poland. This actuator benchmark can be used either for testing, evaluation, or ranking of different FDI methods.

Mendonça et al. [104] also proposed a FDI method based on fuzzy logic approach. Nonlinear models for the process running in normal condition and for each fault were derived. When a fault occurs, fault detection and isolation is performed using the model residuals. This method, applied to the actuator benchmark [35], was able to detect and isolate 10 abrupt and incipient faults.

In parallel, Huang and Yu [81] presented a simple method specifically addressed to detection of stick-slip fault. This approach requires only valve position set OP and actual valve position signal MV; specific indices are defined, and an on-line sliding window algorithm is developed. Huang et al. [80] also proposed a series of methods based on trend analysis to detect different faults. Stick-slip fault, constant bias fault, change of valve gain, serious hysteresis, and stuck condition can be inferred by using OP, MV and PV signals. Industrial data sets from a power plant were used to test the methods' efficiency.

Recently, Subbaraj and Kannapiran [151] proposed an Adaptive Neuro-Fuzzy Inference System to detect and diagnose the occurrence of various faults in a smart pneumatic valve of a cooler water spray system in cement industry. The training and testing data required for model development were generated at normal and faulty conditions in a laboratory setup.

Other interesting results about smart actuators were presented by Scali et al. [126]. In the framework of a cooperation with ENEL (major Italian electricity producer company), a pilot plant scale apparatus is appropriately equipped to reproduce different types of malfunctions for a pneumatic valve. The availability of MV allows one to compute TD (Travel Deviation), defined as the difference between real and desired valve position ($TD = MV–OP$). On the basis of different patterns and range of values of TD, stiction can be clearly detected and also other causes of malfunctions affecting the valve can be distinguished (see Chapter 6). An example is reported in Figure 2.9.

As final result, by defining few Key Performance Indices (as simple metrics of TD), and fixing low and high thresholds for them, it is possible to assess valve status as Good, Alert, Bad, thus giving very specific indications to the operator about troubles affecting the valve and actions to perform. The same logics has been exported and validated on industrial processes (power plants), after a field calibration of some KPIs, by Bacci di Capaci et al. [31].

Referring to Figure 2.9, it is worth putting into evidence that typical waveforms and distinctive limit cycles on PV(OP) and MV(OP) diagrams generated by a traditional sticky valve (cfr. Figure 2.4) are no more observed in the case of a sticky valve augmented by smart in-

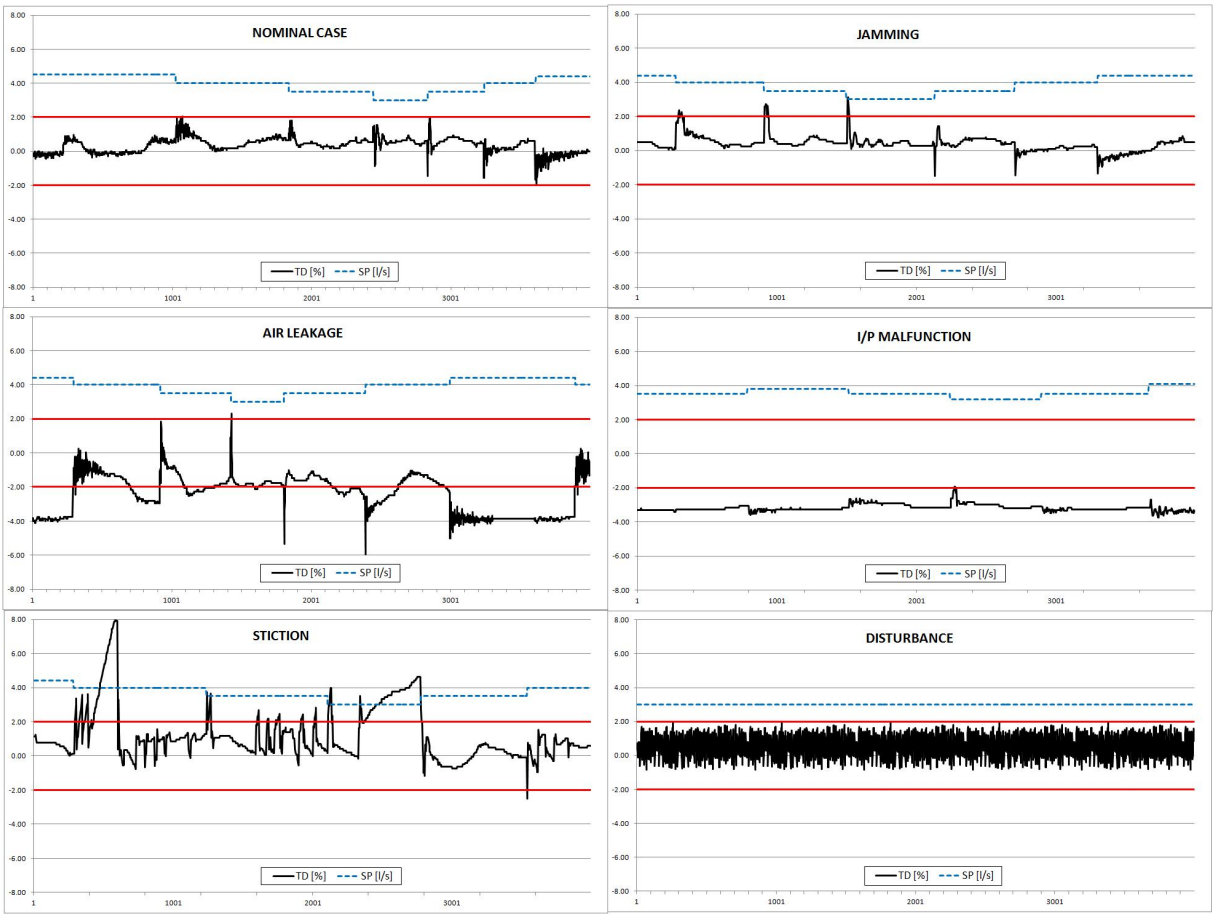

Figure 2.9: TD time trends for nominal case and different malfunctions: jamming, air leakage, I/P malfunction, stiction and disturbance.

strumentation. The positioner, performing an additional control action as an internal cascade controller, can significantly alter frequencies and amplitudes of oscillation, even though, contrary to popular belief, it does not allow elimination of oscillations.

2.8 Software Packages

Many software packages, addressing the issue of control loop performance assessment (CLPA), have been proposed in recent years by major companies. Among the few surveys including software packages, papers by Shardt et al. [130] and Brásio et al. [39] should be mentioned. Historically developed for controller re-tuning, nowadays these tools not only detect loops needing attention and/or maintenance but also include different features for a more general diagnosis of loop status.

Detailed illustrations of these systems can be found on the appropriate company web sites. Unfortunately, in most cases the available documentation is oriented towards a commercial approach rather than a scientific one. It is possible to find an indication of the main features and tackled issues, lists of successful implementations, benefits in terms of Return On Investment and enthusiastic comments by users. It is very unusual to have a complete explanation that includes theoretical issues (the problem, basic techniques and performance indicators) and practical issues to focus on for the success of the implementation (system architecture, key parameter calibration, field validation).

For this reason, a detailed analysis of all software packages for CLPA not being possible, basic features of 15 different systems today present in the market are reported following the

approach of our review in Table 2.6 that highlights various options of stiction analysis: modeling, detection, quantification, compensation, and smart diagnosis.

From Table 2.6, it can be seen that stiction detection is a feature common to almost all packages (11/15), thus confirming to be now a mature subject; in general, no information about the adopted technique is available: about this point, the *PCU* software makes use of multiple techniques to get a more reliable final verdict in terms of oscillation detection and stiction diagnosis. Very few packages perform quantification (4/15), to indicate that there is still research to be carried out. Only 2/15 deal with modeling and only one with compensation: in our experience, this fact confirms the scarce interest of industry about these two subjects. On the contrary, it is a bit surprising that only one package (the PCU software [31]) includes smart diagnosis, taking into consideration the proved advantages by its adoption: this is probably due to the relatively few plants fulfilled with advanced instrumentation, but this feature will certainly find a place in future packages.

In Chapters 6 and 7 two examples of software packages for monitoring and assessment of control loops are illustrated.

Table 2.6: Synthesis of Performance Assessment Software.

Software	Organization	Features of Stiction Analysis				
		Modeling	Detection	Quantification	Compensation	Smart Detection
Control Performance Assessment [121]	Petroleum University of Technology, Iran	✗	✓	✗	✗	✗
Plant Check–Up (PCU) [31, 123, 23]	University of Pisa, Italy	✓	✓	✓	✗	✓
Process Assessment Technologies and Solutions [96]	University of Alberta, Canada	✓	✓	✓	✓	✗
Aspen Watch Performance Monitor [1]	AspenTech	✗	✓	✗	✗	✗
Automatic Control Loop Monitoring and Diagnostics [10]	PAPRICAN	✗	✗	✗	✗	✗
Condition Data Point Monitoring [7]	Flowserve	✗	✓	✗	✗	✗
Control Monitor [3]	Control Arts, Inc.	✗	✓	✗	✗	✗
Control Performance Monitor (Process Doctor) [9]	Matrikon–Honeywell	✗	✓	✓	✗	✗
Control Loop Optimisation [11]	PAS	✗	✗	✗	✗	✗
EnTech Toolkit (DeltaV Inspect) [5]	Emerson Process Management	✗	✗	✗	✗	✗
INTUNE [4]	ControlSoft	✗	✗	✗	✗	✗
Loop Scout [8]	Honeywell	✗	✓	✗	✗	✗
LPM, Loop Performance Manager [37]	ABB	✗	✓	✗	✗	✗
Plantstreamer Portal [2]	Ciengis	✗	✓	✓	✗	✗
Plant Triage [6]	Expertune	✗	✓	✗	✗	✗

Symbols: "✗", no; "✓", yes

2.9 Conclusions

A review of research works on valve stiction is indeed a heavy burden to carry out, owing to very large efforts devoted to this phenomenon in the last years. This is certainly an indication

of its relevance as issue affecting loop performance and then the global efficiency of the plant.

In this first part of the study, we tried to give a general overview starting from basic aspects of the problem, analyzing different techniques, and ending with possibilities open by smart instrumentation. We can now make some final considerations, based on personal experience as researchers and, more, on familiarity with end-user expectations: therefore, more attention is paid to the perspective of their impact in industrial applications.

Characterization of the phenomenon and its modeling has certainly reached an almost complete stage. While from the academic side many issues can still attract interest (for instance basic principle models), the adoption of data-driven model can be considered fully satisfactory for the evaluation of stiction effects.

Stiction detection techniques, based on available measurements in old-design plants (SP, PV, OP), can also be considered a mature research topic, even though a combined application of more than one technique is recommended to reduce possible errors in distinguishing stiction from similar causes of oscillations.

Stiction compensation techniques are certainly a valid help to mitigate the problem when a direct action is not possible; despite their potentiality, in our experience, very seldom are they implemented in the plant.

Smart instrumentation creates the opportunity for a very innovative scenario in the diagnosis of different problems which may affect the valve and their distinction from other troubles. While all other diagnosis approaches remain valid for classical plants, techniques which make use of additional measurements will be used more and more in the next few years.

About closed-loop performance systems, understandably, techniques included in commercial packages are not illustrated with all details: it seems that they follow with some time delay the advances in research. At the moment, very few of them feature approaches that include benefits deriving from the availability of smart instrumentation.

Being able to quantify the amount of stiction is very important in order to follow its evolution in time and to predict the moment of valve maintenance; this is a field where all previous aspects play a role and where there is still research to do in order to improve reliability of estimations.

To the comparison results of emerging quantification techniques on industrial data is devoted the second part of this review.

Chapter 3

Stiction Quantification - part I

Abstract [1]

Valve stiction is one of the most common causes of poor performance in control loops. This chapter presents a first procedure which allows stiction quantification. The method describes the control loop by means of a Hammerstein model: a non-linear block for valve stiction followed by a linear block for process dynamic. A two-parameters empirical model is used to reproduce accurately the valve behavior and a linear least square identification is performed. A grid search method allows one to estimate process and stiction parameters. This technique permits one to predict the unknown real stem position (MV), and moreover, it does not need any process knowledge and requires only the data normally registered in industrial plants. It is pointed out that the real problem consists of the lack of knowledge about the *true* value of stiction.

In addition, quantification of valve stiction can be heavily affected by the presence of unavoidable perturbations in loop variables, such as set point variations, controller tuning and external disturbances, which could affect the stiction estimation obtained by this inherently robust technique. A general filtering procedure is proposed to discard data for which quantification is very likely to give wrong indications and to restrict its application to appropriate cases.

Simulations show that several sources of perturbations can be eliminated, thus improving the reliability of stiction evaluation. Results are confirmed by application to industrial data: a significant number of valves are analyzed for repeated acquisitions before and after plant shutdown. The proposed procedure seems to be a valid methodology to monitor valve stiction and to schedule and check valve maintenance.

The last part of this chapter presents main features of the new version of *PCU* software, a performance monitoring system which allows stiction quantification. This system implements the whole methodology previously presented: the estimation algorithm and the corresponding filtering procedure.

[1] This chapter is based on three different papers: [22], [25], [23].

3.1 Introduction

Performance monitoring plays an important role in process industries because poor performance considerably reduces their profitability and competitiveness. A control loop performance monitoring system detects poor performance loops, indicates different sources of malfunction and suggests appropriate ways of correction. Control valves are said to be the cause of oscillations and poor performance in control loops for a significant number of cases (about 30%, according to [85]). In particular, the most common problem is *stiction* (static–friction). An accurate characterization of this phenomenon was performed by Choudhury et al. [47], and since then research on this topic has found new emphasis. The research on valve stiction can be broadly categorized into the following four topics: modeling, detection or confirmation, quantification, and compensation. In this Section, the existing research on stiction modeling, detection, and quantification is briefly reviewed to illustrate the motivations and scope of this chapter.

Basically, two types of models are used to describe stiction: models derived from physical principles and models derived from process data. Physical models (e.g., Karnopp [88]) are certainly more accurate, but owing to the large number of unknown parameters, they are not considered convenient for the purpose of stiction detection and quantification. Simplicity in the structure is the main reason why data-driven models are preferred (Choudhury et al. [47], Kano et al. [87], He et al. [76]). More details will be given in Section 3.2 when presenting the proposed methodology.

Many stiction detection techniques have been proposed in the literature. These techniques distinguish two common causes of oscillation: external disturbance and valve stiction. They can be broadly classified into four categories: cross-correlation function-based (Horch [77]), waveform shape-based (Kano et al. [87], Srinivasan et al. [146], Singhal and Salsbury [132], Rossi and Scali [119], Yamashita [168], and He et al. [76]), nonlinearity detection-based (Choudhury et al. [46]), and model-based algorithms (Karra and Karim [90]). A performance comparison of the most recent techniques on a large benchmark (93 loops) of industrial data is reported in Jelali and Huang [85]. In conclusion, these problems can be considered almost solved, even though different stiction models and diagnosis techniques cannot always give the same results once they are applied on industrial data. Therefore, it is important to know the strengths and the weaknesses of different models and methods.

On the contrary, stiction quantification should be considered an open issue [85]. Knowing the value of stiction is very important in order to follow its evolution in time, to compare it with acceptable thresholds, and to be able to schedule valve maintenance.

Both stiction detection and quantification techniques do not require invasive procedures for the plant. They only require algorithms based on data usually recorded for control and monitoring purposes, that is Set-Point (SP), Controlled Variable (PV), and Controller Output (OP). The measure of the stem position (MV) is not generally available, and it must be estimated from the other available measurements. Once MV is recorded, owing to the availability of smart equipment (valve positioners) and advanced communication systems (Field Bus), the task is quite easier. Not only can stiction be detected and quantified directly on an MV(OP) diagram, but also other causes of malfunction can be indicated (for instance, air leakage, I/P converter troubles, etc.). Details can be found in Scali et al. [126] and Bacci di Capaci et al. [31].

In one of the first significant papers on stiction quantification, Choudhury et al. [49] proposed fitting the limit cycle on PV(OP) with a geometrical ellipse in a least-squares sense. A stiction index is evaluated as the ellipse width in the OP direction. This technique gives a relative estimate of stiction, called *apparent*, which represents only an indication of stiction severity. Indeed, this value is influenced by all other loop parameters (starting from controller and process gain). As they may change in time, this technique cannot be considered completely reliable for stiction quantification. Techniques which estimate the parameters of a data-driven

stiction model and predict the MV signal are much more effective. In stiction quantification, the objective function does not generally have a concave shape but shows many flat regions where the gradient is zero or close to zero. A global search algorithm for the minimum is necessary; a gradient method would be too influenced by the initial guess and would stop in a local minimum. In many techniques, the control loop is modeled by a *Hammerstein* system: a nonlinear block for valve stiction, followed by a linear block for the process. Some of these techniques are briefly reviewed in the sequel.

First, Srinivasan et al. [148] used a one-parameter stiction model, and the linear dynamics was identified using an ARMAX (AutoRegressive Moving Average with eXternal input) model. Choudhury et al. [50] performed a grid search of the two stiction parameters of Choudhury's model. The stiction parameters combination and the corresponding process parameters vector which minimize mean squared error on PV are evaluated. Jelali [84] used a stochastic optimization approach for the nonlinear part. A two-stage quantification is performed: stiction parameters are obtained with genetic algorithms or pattern search methods, then the linear part is identified using ARX or ARMAX models and a time delay estimation algorithm. The method of Farenzena and Trierweiler [61] is said to be an improvement over Jelali's method. It performs a one-stage identification of stiction and process parameters by means of a deterministic algorithm of global optimization which is no longer dependent on the initial guess. Lee et al. [95] described valve stiction with the He et al.[76] model and identified a linear process model of first or second order plus time delay. A triangular search grid is a remarkable improvement because it constrains the search space of stiction parameters and fastens the method. Romano and Garcia [118] modeled the control loop with a Hammerstein-Wiener structure: the valve nonlinear block precedes the process represented by a linear block and a nonlinear static block. Process identification is performed with ARMA or ARMAX models for the linear part and third grade spline functions for the nonlinear part. This approach avoids a possible process nonlinearity to be wrongly included in the stiction model. Karra and Karim [90] described the control loop with Kano's stiction model and a specific linear model (E(xtended)-ARMAX type), which also accounts for nonstationary disturbances entering the process.

Regarding quantification, the main difficulty to put into evidence is that the *true* value of stiction is not known in industrial data (rather, it may be known in *ad hoc* experiments or in simulations). Therefore, the validation of a proposed technique on a single set of industrial data can be incomplete, apart from the mathematical elegance of the solution. This is confirmed by the fact that different quantification techniques can strongly disagree when applied on the same benchmark of industrial data (Chapter 13 in [85]). Recently, methods to evaluate the reliability of stiction detection and quantification techniques have been presented. Qi and Huang [115] have proposed a *bootstrap* method to obtain the statistical distribution of stiction estimation. They defined a region for stiction parameters with 95% confidence. Srinivasan et al. [140] have performed a frequency domain analysis of loop oscillation and determined a confidence function for the estimated stiction parameters.

Finally, as previously seen in Section 2.8, it is worth to notice that possibility of diagnosing stiction is included in several systems of closed loop performance monitoring (CLPM), proposed nowadays by major software houses. On the opposite, to the best of the author's knowledge, no commercial tool performs stiction quantification or estimation.

Following these considerations, the objective of this chapter is three-fold:

(i) to overcome the problem that the *true* value of stiction is not known, the proposed methodology will be performed on many applications available for long periods of time (before and after plant shutdown) and for a significant number of valves;

(ii) to show how the most common causes of loop perturbation may influence stiction estimation, a robust methodology is proposed, including a filtering procedure able to discard data for which stiction quantification is very likely to fail.

(iii) to propose a tool which performs stiction quantification and process identification.

This chapter is organized as follows: in Section 3.2, the proposed method for stiction quantification is illustrated; Section 3.3 presents the results in simulation; in Section 3.4, the technique is analyzed on a large number of industrial data; Section 3.5 illustrates the new tool of performance monitoring and stiction quantification; and in Section 3.6, conclusions are drawn.

3.2 The First Proposed Method

The first proposed stiction quantification technique is based on a grid search, a method which is simple and mathematically sound but may require quite a long computational time. The choice of a grid technique is on purpose, to show that even in this case, unreliable estimates may be caused by the presence of perturbations in the data. Long computational times do not represent a disadvantage for three reasons: the technique is oriented toward an off-line application which requires data registered for hours (versus minutes of computational time), the wear phenomena in valves occur slowly (weeks or months), and valve maintenance usually occurs periodically every few years on occasion of a plant shutdown.

3.2.1 The Hammerstein system

The control loop is modeled by a Hammerstein system (Figure 3.1a). Kano's stiction model describes the nonlinear valve dynamics, and an ARX (Auto Regressive model with eXternal input) model describes the linear valve and the process dynamics. More details about the model are added here to better understand the algorithm.

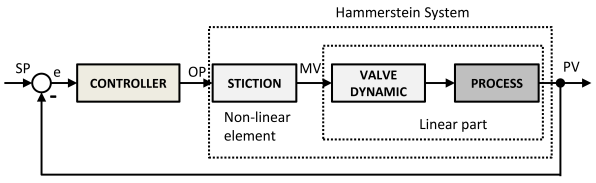

(a) Hammerstein system: control loop with valve stiction.

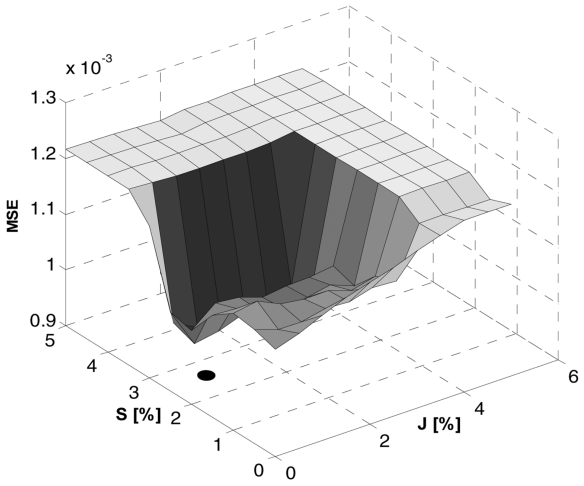

(b) Grid search of stiction parameters.

The relation between the controller output (desired valve position) OP and the real valve position MV is described in three phases (Figure 3.2a):

1. *Sticking*: MV is steady and the valve does not move, owing to the static friction force (deadband + stickband, S).
2. *Jump*: MV changes abruptly because the active force unblocks the valve, J.
3. *Motion*: MV changes gradually, and only the dynamic friction force can possibly oppose the active force acting on the valve diaphragm (the valve stops again when the force generated by the control action decreases under the stiction force).

Valve stiction produces an offset between control variable PV and Set Point SP, and this causes loop oscillation because the valve is stuck even though the integral action of the controller acts and increases the pressure on the valve diaphragm. The MV(OP) diagram shows a parallelogram–shaped limit cycle, while MV(OP) would be perfectly linear without valve stiction. Figure 3.2b

represents the PV(OP) plot for a case of flow control loop, for which the fast dynamics allows one to approximate MV(OP) with PV(OP), since MV is usually not measured.

It should be recalled that also in the case of stiction, loops with slow dynamics (PC, LC, TC) show PV(OP) diagrams having elliptic shapes. Similar paths on PV(OP) are obtained for other types of oscillating loops (external stationary disturbance or aggressive controller tuning), and this creates some problems in assigning causes. It is worth saying that the value of J is critical to inducing limit cycles (Choudhury et al. [50]). However, while S is easy recognizable, J is hardly detectable in industrial data, owing to its small value and the presence of field noise (see Figure 3.2b).

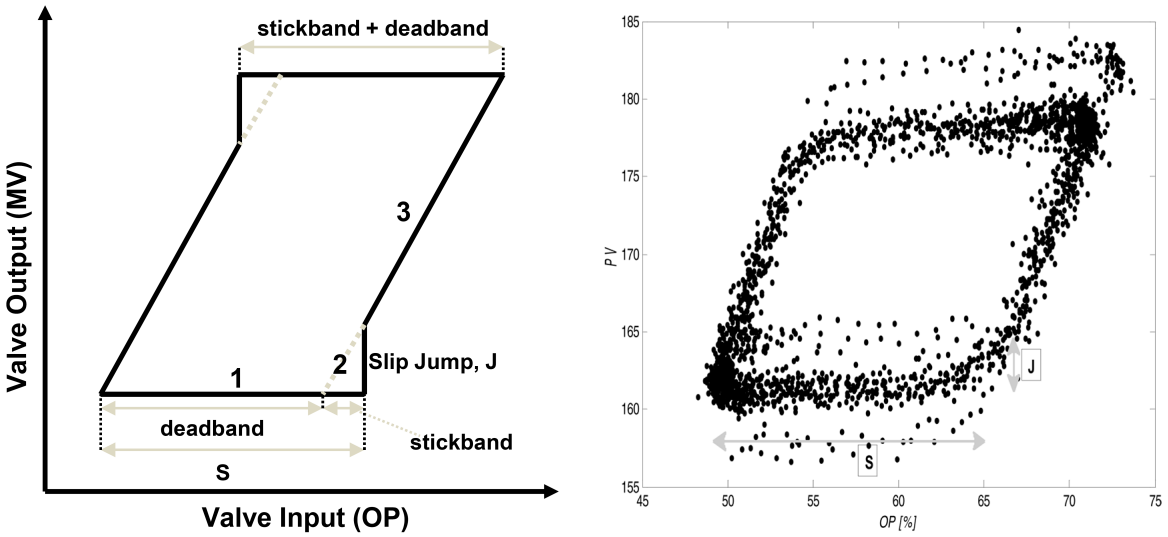

(a) Valve stiction modeling: MV(OP) diagram. **(b)** Industrial PV(OP) diagram.

Figure 3.2: Typical limit cycles.

The ARX model used has the following structure in discrete time form:

$$y_k = \sum_{j=1}^{n} -a_j \cdot y_{k-j} + \sum_{j=1}^{m} b_j \cdot u_{k-j-L} + e_k \tag{3.1}$$

where y_k denotes the measured value of controlled variable PV at time k-th, u_k is the value of manipulated variable MV at time k-th, a_j are the coefficients of the vector for PV, b_j are the coefficients of the vector for MV, and e_k is the error committed in the prediction. The (n,m) pair is the order of the model, and L represents the time-delay units of the process.

The proposed method goes as follows: A grid of the two stiction parameters S/J is built (Figure 3.1b), and for each possible combination, the MV signal is generated from the measured OP signal using Kano's stiction model. Another grid of possible process time delay L is performed: L is taken as a multiple of the sampling time. For every triad $S/J/L$, the overall vector θ of the coefficients of the ARX model is identified in a linear least-squares sense based on MV and measured PV. The range of the grid, as well as the order of the ARX model, are discussed afterward.

The following maximization problem is stated:

$$\begin{aligned} (\overline{S},\overline{J},\overline{\theta},\overline{L},) &= \max_{S,J,\theta}(\max_{L}(F_2)) \\ F_2 &= 100 \cdot \left(1 - \frac{\|\widehat{PV} - PV\|^2}{\|PV - PV_m\|^2}\right) \end{aligned} \tag{3.2}$$

F_2 is a fitting index related to the mean squared error between measured (PV) and predicted

($\widehat{PV}$) control variables; PV_m is the mean value of PV. F_2 is equal to 1 in the case of perfect estimation and tends to $-\infty$ for large errors.

The stiction parameter grid has a triangular shape to restrict the search space. Overshoot stiction cases ($J > S$) are excluded because the waveforms generated for these combinations are rarely observed in practice. The largest value of S (and J) is the OP oscillation span. Therefore, under boundary conditions (when $S = J$ and $S = OP$ span), the valve jumps between two extreme positions, generating an exactly squared wave for MV.

To avoid different estimations depending on the examined time window, data are divided into two sets, and the method is applied separately. Two stiction models (S_1/J_1; S_2/J_2) and two linear ARX models (θ_1/L_1; θ_2/L_2) are identified; consequently, two fitting indices are calculated ($F_{2,1}$; $F_{2,2}$).

Then, a comparison of the two data windows is performed using the two specific indices defined below:

$$\begin{aligned} MD_{NL} &= 1 - \frac{\|MV_1^{OL} - MV_2^{OL}\|^2}{\|MV_{1,2}^{OL}\|^2} \\ MD_{LIN} &= 1 - \frac{\|PV_1^{sr} - PV_2^{sr}\|^2}{\|PV_{1,2}^{sr}\|^2} \end{aligned} \tag{3.3}$$

MD_{NL} is a deviation index between nonlinear models. MV_1^{OL} and MV_2^{OL} are respectively the output signals of the first and the second estimated stiction model in response to a specific sinusoidal OP input signal. $MV_{1,2}^{OL}$ is the mean signal of these two. MD_{LIN} is a deviation index between linear models. The output signals of the first (PV_1^{sr}) and the second (PV_2^{sr}) linear model in response to a unitary step are compared; $PV_{1,2}^{sr}$ is the mean signal of these two.

MD_{NL} and MD_{LIN} are equal to 1 when the two responses are exactly the same, that is, when the two couples of stiction parameters and the two linear models perfectly correspond; MD_{NL} and MD_{LIN} tend to $-\infty$ when differences become significant. The identified stiction and linear model parameters are related to the best data set, that is, the one with the highest F_2 index (between $F_{2,1}$ and $F_{2,2}$). In the calibration step, it was found that, to obtain reliable results from the algorithm, the three following conditions have to be satisfied:

$$MD_{NL} > 0.95 \qquad MD_{LIN} > 0.80 \qquad \min\{F_{2,1}, F_{2,2}\} > 0.80 \tag{3.4}$$

Concerning the choice of model type, Srinivasan et al. [148] have shown that the accuracy of identification of the nonlinear part is not affected by the complexity of the linear model structure. This statement justifies the use of a simple model to describe linear dynamics. The adoption of an ARX model gives an exact solution for the least-squares problem and, differently from an ARMAX, implies only an iterative estimation of nonlinear parameters. Concerning model order, intensive simulations have shown that an ARX(2, 2) model is suitable to quantify stiction with good precision even for complex process dynamics, with acceptable computational times.

The step size of stiction parameters (S,J) plays a key role: small values allow one to increase accuracy, avoiding the effect of local minima, at the expense of longer computational times. By assuming as acceptable an error on the estimation of S and J equal to 0.1 (which is 1/1000 of stroke of valve stem, 0-100%), according to simulation results, a step size equal to 0.05 can be considered adequate. The technique also shows robustness to noise; the errors become significant only in case of a Signal to Noise Ratio (SNR) equal to or smaller than 2.

These considerations concern the mathematical statement and the solution of the problem. In the perspective of application on industrial data, there are some practical issues which might affect the accuracy of stiction quantification. They are mainly correlated to the presence of different sources of oscillation (with or without valve stiction): irregular oscillations, periodic external disturbances, variable set point loops, and incorrect controller tuning can be seen as unavoidable phenomena in industrial situations.

3.2.2 The filtering procedure

To reduce the impact of these practical issues on the reliability of stiction estimation, a systematic procedure is proposed as described in the sequel (compare Figure 3.3). First, two ap-

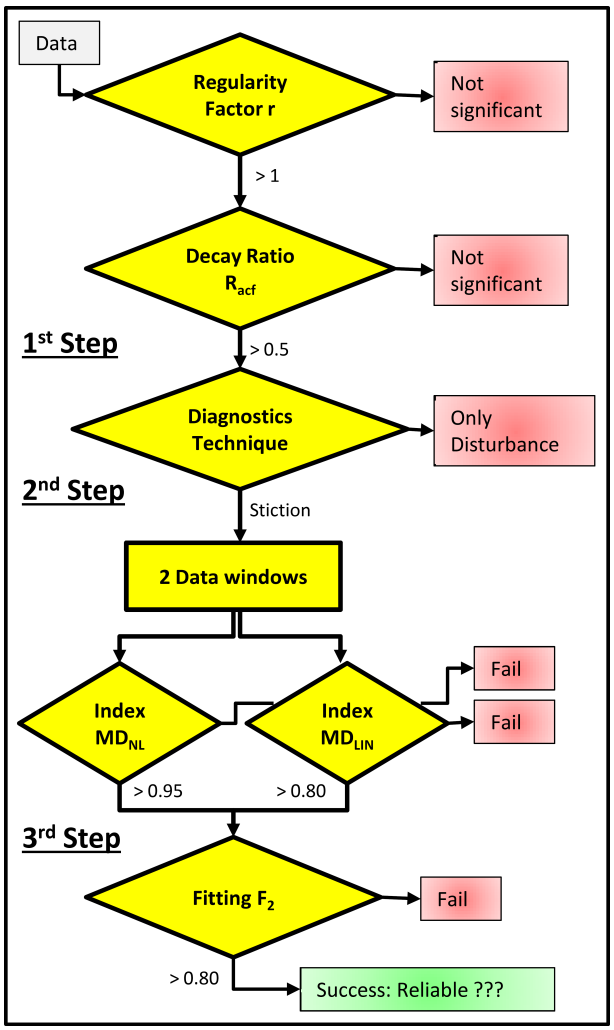

Figure 3.3: Flow diagram of the proposed technique:
oscillation detection, stiction detection, data division, and stiction quantification.

propriate techniques to detect significant loop oscillations are applied. Loop oscillation is, in fact, the main reason for stiction detection. The regularity factor r (Thornhill et al., [157]) and decay ratio R_{acf} (Miao and Seborg, [105]) of the autocorrelation function (ACF) of control error ($e = PV - SP$) are calculated. If these two indices exceed threshold values, set respectively to 1 and 0.5, as suggested by the authors, the control loop is considered to oscillate significantly (that is, regularly and steadily), and the quantification continues; otherwise the analysis should be stopped, because it is assumed that non-substantial stiction is present.

Second, a stiction diagnostic technique is applied to avoid the application of the algorithm when a periodic disturbance is the unique source of oscillation. Among several available techniques (see the list reported in the Introduction 3.1), for the first two papers [22, 25] composing this chapter, the relay-based technique developed in our laboratory a few years ago was adopted [119]. Afterwards in [23], in the perspective of industrial applications, the suggestion is to adopt more different techniques of only when stiction is clearly detected. More details about this point are given in Section 3.5 where the monitoring system *PCU* is described. Anyway, when stiction is not clearly detected, the procedure should be stopped, since the estimated values can be unreliable.

Subsequently, when stiction is detected, data are divided into two sets; stiction quantification is applied separately, and results are compared in terms of the indices previously defined. It is worth saying that the appropriate number of data samples and data sets depends on the whole data length. Usually, a number of data samples which includes at least 4-5 periods of oscillation is needed to have a significant data window; therefore the number of data windows can be just one, two, or even more. In the last case, the proposed procedure compares the two best windows in terms of fitting indices F_2. The next Section 3.3 illustrates the effectiveness of the proposed procedure on simulation results and Section 3.4 on industrial data.

3.3 Simulation Results

Two different examples of simulations are here reported. In Section 3.3.1 the proposed quantification algorithm is tested for different sources of loop perturbations. Then, in Section 3.3.2 the focus is on the additional presence of external disturbances.

3.3.1 Applications for different sources of oscillation

As first illustrative example, a control loop is simulated, where the process P is described by a First Order Plus Time Delay (FOPTD) transfer function and the controller C has PI tuned by the Continuous Cycling method of Ziegler-Nichols[22, 25]. Valve stiction is described with Kano's model. Sampling time is set to 1 s. This loop is a specific case study, but the results have general validity, as verified by other extensive simulations; other types of process models were used and different values for stiction parameters were adopted.

$$P(s) = \frac{1}{15s+1}e^{-5s} \qquad C(s) = 2.44\left(1 + \frac{1}{14.9s}\right) \tag{3.5}$$

The methodology is applied to different sources of oscillation, as described above. In detail, 10 different cases have been examined (see Table 3.1). In cases 1 and 2, the stiction is the only source of oscillation; different amounts of stiction in the valve have been simulated. In case 3, the loop oscillates due to set point sinusoidal variation, and the valve has no stiction. Case 4 is equal to case 3, but the valve has low stiction. In case 5, the loop oscillates due to aggressive controller tuning ($K_c = 4.15$), which causes a marginal stability condition (no stiction). In case 6, an aggressive tuning ($K_c = 3.66$) acts together with high valve stiction. In case 7, an external sinusoidal disturbance is the unique cause of loop oscillation. In cases 8 and 9, an external sinusoidal disturbance acts respectively with low and high valve stiction. In case 10, an irregular disturbance acts with low valve stiction.

Results are reported in Table 3.1. In columns from left to right are given the simulated stiction parameters (S^o, J^o), regularity and decay ratio factors (r, R_{acf}), diagnosis verdicts issued by the relay technique [119], estimated stiction parameters (S, J), models' deviation indices (MD_{NL}, MD_{LIN}), and the F_2 index.

It can be seen that the oscillation is regular and steady for all cases (except for case 10), as indicated by values of r and R_{acf} above thresholds. In cases from 1 to 6, the procedure perfectly succeeds and gives good stiction estimations, both in the presence of stiction and not. In the case of pure disturbance (7), stiction quantification might fail (nonzero S and J estimation), but the relay technique indicates disturbance (not stiction), so these data should not be examined by the stiction estimation algorithm. In cases of simultaneous stiction and disturbance (8 and 9), the relay technique correctly indicates stiction but the estimated stiction parameters are always wrong. In case 8, the low value of MD_{LIN} (< 0.80) gives an indication of scarce accuracy, while in case 9, both indices are above thresholds, but a wrong stiction estimation is obtained. In case 10, stiction and disturbance act simultaneously, producing an irregular oscillation; therefore the procedure is stopped.

Table 3.1: Simulation Examples: Different Sources of Loop Oscillation.

	case	S^o	J^o	r	R_{acf}	verdict	S	J	MD_{NL}	MD_{LIN}	F_2
1	low stiction	0.5	0.5	9.8	0.98	stiction	0.5	0.46	0.99	0.83	0.97
2	high stiction	4	1	2.32	0.96	stiction	4.02	1.08	0.98	0.89	0.96
3	SP variation	0	0	21.4	0.97	no stiction	0	0	0.99	0.82	0.95
4	SP variation + low stiction	0.5	0.5	21.2	0.97	stiction	0.46	0.42	0.99	0.83	0.95
5	aggressive tuning (marginal stability)	0	0	12.1	0.99	no stiction	0.04	0.04	0.99	0.84	0.97
6	aggressive tuning + high stiction	4	1	14.4	0.97	stiction	3.84	0.88	0.99	0.89	0.97
7	sinusoidal disturbance	0	0	8.6	0.99	no stiction	0.36	0.14	0.99	0.87	0.97
8	disturbance + low stiction	0.5	0.5	6.92	0.93	stiction	0	0	0.99	0.46	0.94
9	disturbance + high stiction	6	4	12.9	0.98	stiction	4.98	4.98	0.97	0.91	0.95
10	irregular disturbance + low stiction	0.5	0.5	0.47	0.35	-	-	-	-	-	-

The first conclusions after these simulations are as follows:

(i) It is confirmed that the proposed methodology is able to give a correct stiction estimation when stiction is the only source of oscillation.

(ii) The procedure continues to be correct even in case of oscillations caused by set point variations and incorrect tuning, with or without the presence of stiction.

(iii) On the contrary, in the presence of external sinusoidal disturbances, the methodology may give wrong stiction estimations. The screening by means of relay diagnosis technique and checks on the deviation indices of models in the data windows are not enough to eliminate the problem completely, but they can reduce the number of wrong evaluations, sometimes allowing one to reject the (wrong) estimated stiction parameters.

(iv) In the presence of irregular or nonsteady oscillation, the procedure is stopped because both stiction diagnosis technique and stem position estimation give unreliable results. Stiction detection and quantification are postponed to a later data registration with significant oscillation.

3.3.2 Applications in the presence of disturbances

As second illustrative example, a control loop is simulated: the process P is described by a First Order Plus Time Delay (FOPTD) transfer function and the controller C has PI algorithm with Closed Loop Ziegler-Nichols tuning [23]. Sampling time is set to 1 second. Valve stiction is described with Kano model.

$$P(s) = \frac{1}{10s+1}e^{-5s} \qquad C(s) = 1.73\left(1 + \frac{1}{14.25s}\right) \qquad S = 4; \quad J = 1 \tag{3.6}$$

This loop is a specific case study, but the results have absolutely general validity: other process models were used and different values for stiction and disturbance parameters were applied; they are not reported for sake of brevity.

Three simple cases study of simulation are illustrated below:

- In case 1 valve stiction is the only source of oscillation.
- In case 2 the same valve stiction acts with external disturbance: a sinusoidal input with a frequency of 0.2 rad/s and amplitude of 1.
- In case 3 the same valve stiction acts with a higher disturbance: a sinusoidal input with a frequency of 0.05 rad/s and amplitude of 5.

In case 1, the proposed method perfectly succeeds: it gives a good stiction estimation ($S = 4.01$; $J = 0.85$) and an accurate MV prediction (compare Figure 3.4). In case 2, the amplitude and frequency of the disturbance do not alter too much stiction quantification ($S = 3.95$; $J = 1.47$) and the estimation of MV is still effective (Figure 3.5a). On the contrary, in case 3 the external

disturbance significantly degrades stiction estimation ($S = 0.56$; $J = 0.05$) and prediction of MV is really inaccurate (Figure 3.5b).

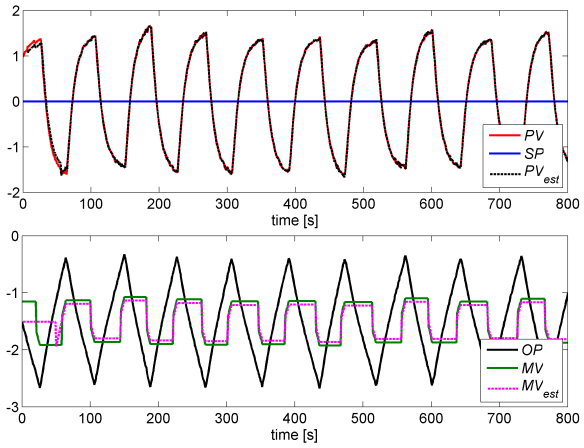

Figure 3.4: Case 1. Only valve stiction: good prediction of MV.

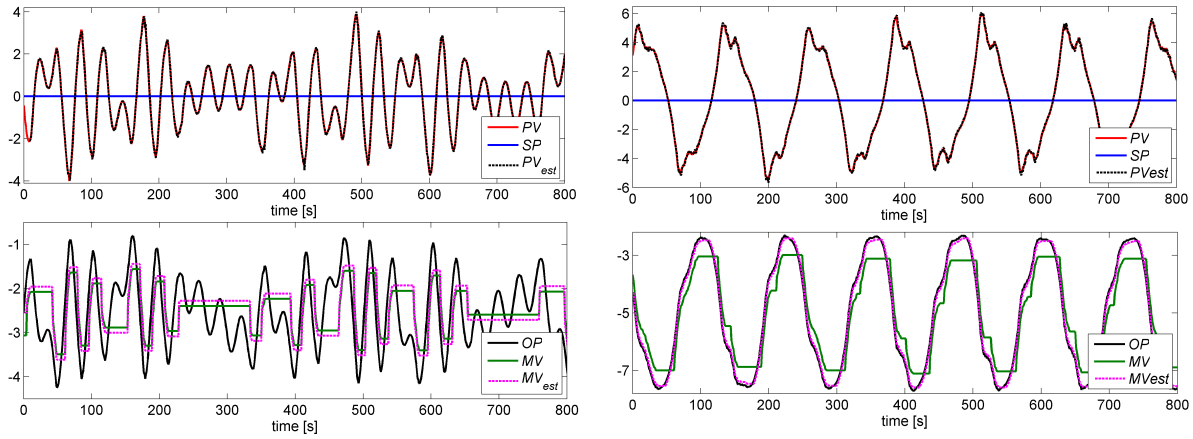

(a) Case 2. Good prediction of MV.

(b) Case 3. Inaccurate prediction of MV.

Figure 3.5: Sticky valve + external disturbance.

Therefore, this second example of simulation confirms that the proposed stiction quantification methodology is able to give a correct stiction estimation when valve stiction is the only source of oscillation. On the contrary, in the presence of external disturbances, the methodology may give wrong stiction estimations.

In the next section, the proposed methodology has been checked on a large number of industrial loops with sticky valves.

3.4 Application to Industrial Data

As stated in the Introduction 3.1, the main problem with stiction detection and quantification is that, in industrial data, the *true* position of the valve stem (MV) and the *true* value of stiction are not known. Therefore, stiction quantification of an industrial valve based on a single set of data can be insufficient, as one single result can be inaccurate and meaningless. On the contrary, the analysis of a large number of valves, under repeated acquisitions, before and after plant shutdown, can be suggested as a sound procedure to validate the proposed technique.

In fact, before valve maintenance, constant or increasing trends of stiction parameters are expected and after maintenance, negligible oscillations and low stiction values are recorded.

Repeating the procedure for different acquisitions allows one to follow the evolution of stiction values in time and to disregard anomalous cases, which appear as *outliers* with respect to the main trend.

The effectiveness of the proposed stiction quantification technique has been checked by its application on a wide set of acquisitions before and after plant shutdown for periodic maintenance. The availability of industrial data is made possible by referring to the archives of the performance monitoring system (*PCU*, [123]) implemented on refinery units for continuous loop assessment.

In this section, two first examples of industrial loops are presented to show the details of the proposed deviation indices between models [22]. Afterwards, as further examples of successful application of the whole methodology, four other control loops are analyzed [25]. The results can be considered representatives of many practical situations.

3.4.1 Loop #1 & #2

Two different flow rate control loops are here considered [22]. Figure 3.6 shows the results for Loop #1, a clear case of success of the procedure. On the opposite, Figure 3.7 shows the results for Loop #2, a case of failure. On the left of these two Figures, time trends of SP, PV, PV_{est}, and OP, MV, MV_{est} are reported, while on the right the step responses of the two linear models identified are reported.

For the Loop #1, the deviation indices between models are both very high: $MD_{NL} = 0.99$ and $MD_{LIN} = 0.95$; also the fitting index is above its threshold: $F_2 = 0.90$. The two step responses of Figure 3.6b are pretty similar, and this explains the high value of MD_{LIN} index.

For the Loop #2, the nonlinear part index and the fitting index are high: $MD_{NL} = 0.95$, and $F_2 = 0.85$. Nevertheless, the index for the linear dynamics is far below the threshold: $MD_{LIN} = -0.45$. As shown by 3.7b, the two step responses are very different and this explains the low value of MD_{LIN} index. This industrial case might correspond to the simulation typology 8: a situation of valve stiction and external disturbance, which can be anyway filtered by the proposed methodology.

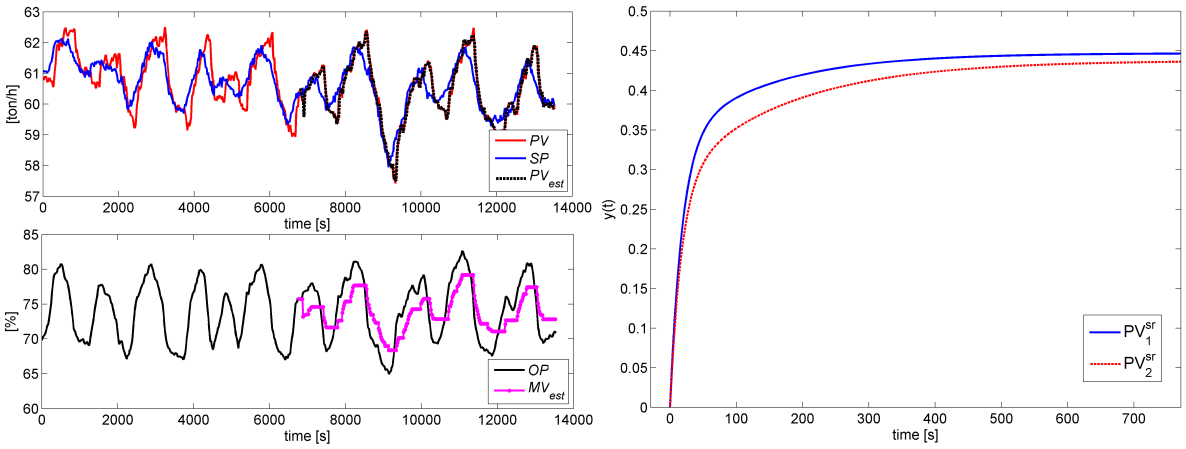

(a) Time trends: two similar windows. **(b)** Step responses for MD_{lin}: successful.

Figure 3.6: Loop #1: a successful application.

3.4.2 Loop #3

This case refers to a pressure loop where the presence of stiction is also evident from visual inspections; two different registrations of data are available before valve maintenance (MTA) and one after MTA. The controller has a PI algorithm with parameters set to $K_c = 1$ and $T_i = 0.4$.

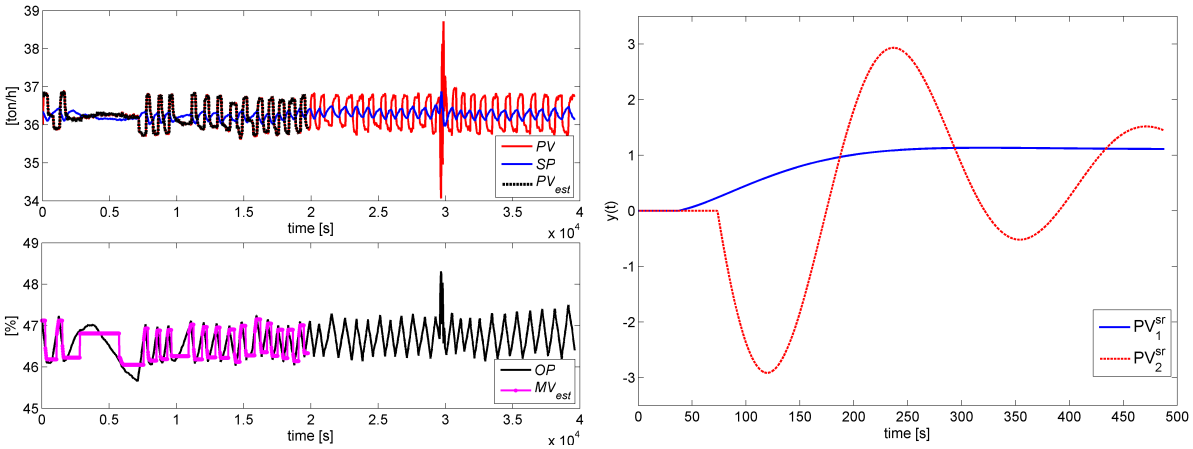

(a) Time trends: two different windows.

(b) Step responses for MD_{lin}: unsuccessful.

Figure 3.7: Loop #2: an unsuccessful (filtered) application.

The first two registrations show oscillations with wide amplitudes, regular ($r > 1$) and steady ($R_{acf} > 0.5$). Large values of stiction parameters are estimated. The procedure gives reliable results because uniform values of the S parameter are quantified (see Table 3.2).

After valve maintenance, no significant oscillation is detected ($r < 1$ and $R_{acf} < 0.5$), and no stiction estimation is performed: the valve operates correctly.

Table 3.2: Loop #3: Valve Stiction Estimation.

time	run #	r	R_{acf}	verdict	S	J	MD_{NL}	MD_{LIN}	F_2
before MTA	i	6.35	0.93	stiction	27.8	4.3	0.98	0.83	0.98
before MTA	ii	5.96	0.94	stiction	25.9	0.9	0.99	0.97	0.97
after MTA	iii	0.43	0.11	-	-	-	-	-	-

The removal of the stiction problem is also confirmed by the comparison of time registrations of SP, PV, OP, and estimated values of PV and MV (PV_{est}, MV_{est}) for one set of data collected before and the one collected after valve maintenance, as shown in Figure 3.8.

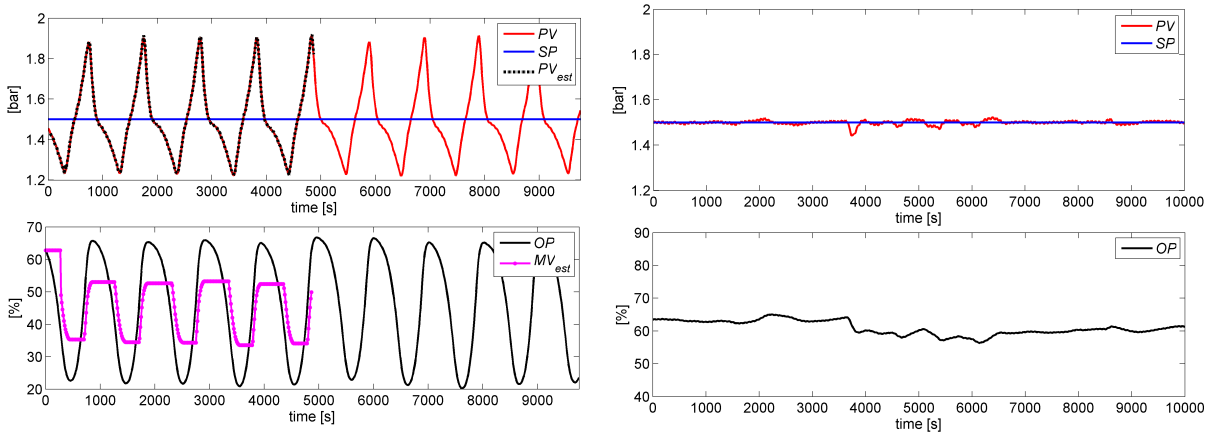

(a) Run i (before MTA):
wide oscillations due to valve stiction.

(b) Run iii (after MTA):
no significant oscillation.

Figure 3.8: Trends for Loop #3.

3.4.3 Loop #4

For this level loop, four different registrations of data are available before valve maintenance and four after (see Table 3.3). The controller has a PI algorithm with parameters always set to $K_c = 4$ and $T_i = 400$.

The first four registrations show oscillations with wide amplitudes, regular ($r > 1$) and steady ($R_{acf} > 0.5$), and the stiction diagnosis is always positive. Therefore, the proposed methodology can always be applied, and it estimates large values of stiction. In particular, an increasing trend of the S parameter is quantified. Note that the methodology is performed on a unique data window because only a few peaks are available due to the long period of oscillation compared to the whole data length available. Therefore, the two deviation indices between models (Eq. 3.4) are not calculated. It is worth noticing that these four data registrations are close in time (4 months); the set point is constant (always $SP_m = 40\%$), and the valve works around 15% of its span. Therefore, the stiction estimations are particularly reliable: the phenomenon is rapidly increasing in time.

The data collected after valve maintenance are completely different. The methodology does not detect any significant oscillation, and no stiction estimation is performed. The loop is no longer oscillating because the valve now operates correctly (due to effective valve maintenance).

Table 3.3: Loop #4: Valve Stiction Estimation.

time	run #	SP_m	OP_m	r	R_{acf}	verdict	S	J	F_2
before MTA	i	40	13.0	2.97	0.78	stiction	7.0	5.0	0.98
before MTA	ii	40	11.5	1.55	0.56	stiction	7.4	7.4	0.98
before MTA	iii	40	11.8	2.94	0.89	stiction	9.0	1.1	0.99
before MTA	iv	40	17.1	1.44	0.80	stiction	13.1	8.5	0.98
after MTA	v	50	19.3	0.42	0.25	-	-	-	-
after MTA	vi	50	19.1	0.83	0.31	-	-	-	-
after MTA	vii	55	18.5	0.37	0.36	-	-	-	-
after MTA	viii	50	15.8	0.70	0.47	-	-	-	-

The removal of stiction is also confirmed by the comparison of time registrations of SP, PV, OP, and estimated values of PV and MV (PV_{est}, MV_{est}), and PV(OP) diagrams for a set of data collected before and a set collected after valve maintenance (see Figure 3.9).

3.4.4 Loop #5

For this pressure loop, seven different registrations of data are available before valve maintenance and four after. The controller has a PI algorithm with parameters set to $K_c = 1$ and $T_i = 24$, apart from acquisition number vii: $K_c = 1.2$ and $T_i = 36$. In this case, the loop operates under MPC control; therefore, the set point oscillates (low frequency).

Before valve maintenance, significant oscillation is detected in five data sets: regular, $r > 1$, and steady, $R_{acf} > 0.5$, excluding run numbers ii and vi. Significant values of stiction parameters are estimated in four cases; MD_{LIN} is under its threshold (0.80) only for acquisition number v, and this result must be rejected (see Table 3.4). The procedure gives overall reliable results because uniform values of the S parameter are quantified, with the mean value equal to 4.9 and a little deviation of 0.6. As illustrated in previous simulations, the causes of these three unreliable results might be seen in the presence of perturbations and stiction acting simultaneously.

After valve maintenance, the loop shows good performance and the error signal is close to zero. The procedure detects no significant oscillation.

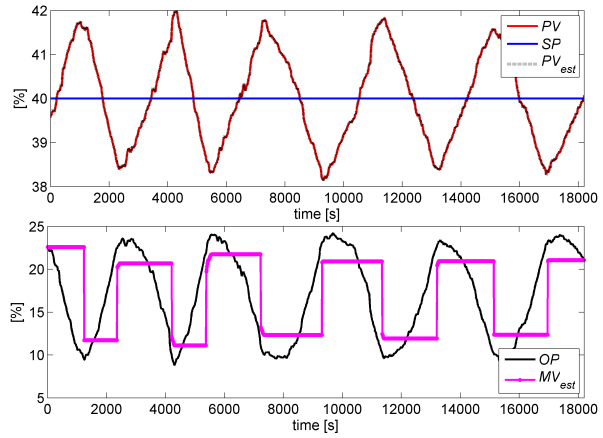

(a) Run iv (before MTA): wide oscillations due to valve stiction.

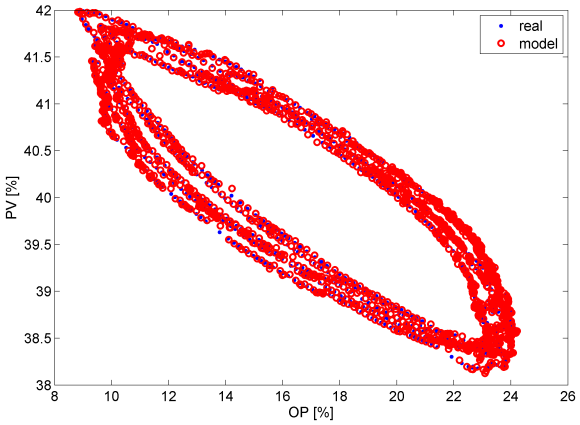

(b) Run iv (before MTA): large PV(OP) ellipse-shaped diagram.

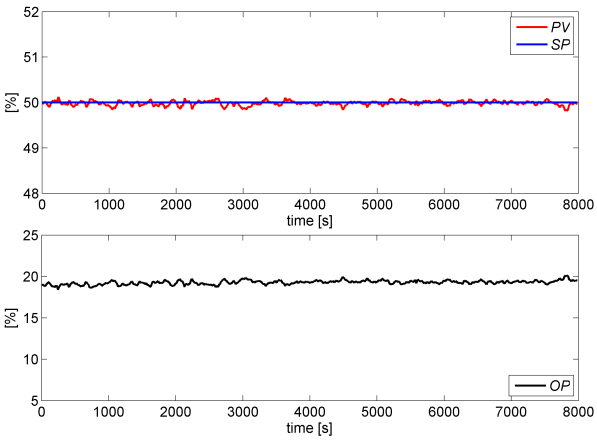

(c) Run v (after MTA): no significant oscillation.

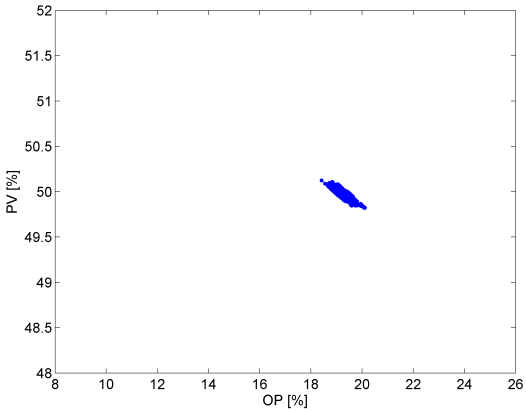

(d) Run v (after MTA): no limit cycle.

Figure 3.9: Trends for Loop #4.

The removal of the stiction problem is also confirmed by the comparison of time registrations for a set of data collected before and a set collected after valve maintenance, as shown in Figure 3.10.

3.4.5 Loop #6

For this pressure loop, ten different registrations are available before valve maintenance and three after (see Table 3.5). The controller has a PI algorithm with parameters always set to $K_c = 1$ and $T_i = 21$.

Before valve maintenance, regular and steady oscillation is detected in eight data sets, except run numbers iii and ix. For acquisitions numbers v and viii, MD_{LIN} is under its threshold, and these results must be rejected. Stiction parameters are accepted in the other six cases, but uniform values of parameter S are quantified only in five registrations. Number vi seems to be a case of unreliable results, because its value differs a lot from the general stiction trend (mean value of 15 with deviation of 1). The proposed filtering methodology allows one to discard only registration numbers v and viii but would accept results for number vi. Also for this loop, the causes of unreliable results might be seen in the presence of perturbations and stiction acting simultaneously.

Unlike the previous three loops, this loop still shows significant oscillation in all three acquisitions after valve maintenance and uniform values (9-10%) of stiction are now quantified. A possible explanation could be unresolved stiction despite valve maintenance or a recurrence

Table 3.4: Loop #5: Valve Stiction Estimation.

time	run #	r	R_{acf}	verdict	S	J	MD_{NL}	MD_{LIN}	F_2
before MTA	i	2.1	0.62	stiction	5.5	2.6	0.98	0.88	0.93
before MTA	ii	0.61	0.56	-	-	-	-	-	-
before MTA	iii	4.56	0.71	stiction	5.3	0.8	0.99	0.97	0.93
before MTA	iv	3.0	0.50	stiction	4.3	0.05	0.98	0.91	0.93
before MTA	v	4.52	0.61	stiction	(3.8)	(0.05)	0.99	0.62	0.93
before MTA	vi	1.15	0.40	-	-	-	-	-	-
before MTA	vii	1.75	0.55	stiction	4.4	0.3	0.99	0.86	0.91
after MTA	viii	1.27	0.47	-	-	-	-	-	-
after MTA	ix	0.49	0.24	-	-	-	-	-	-
after MTA	x	0.47	0.45	-	-	-	-	-	-
after MTA	xi	0.62	0.67	-	-	-	-	-	-

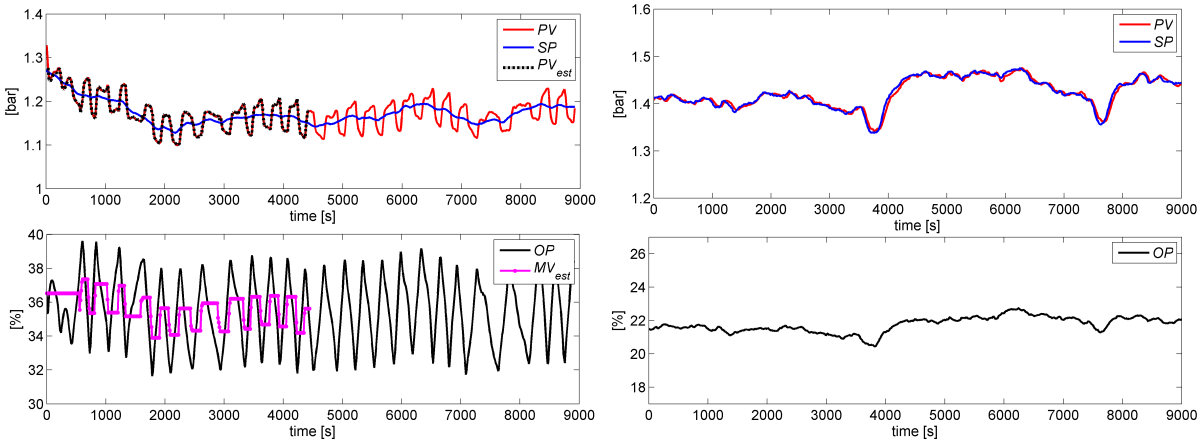

(a) Run iv (before MTA): wide oscillations due to valve stiction.

(b) Run ix (after MTA): no significant oscillation.

Figure 3.10: Trends for Loop #5.

of stiction. It is worth noticing that, in this case, after plant shutdown, the loop starts to operate under MPC control, and this explains why set point oscillates (low frequency). The presence of stiction, both before and after valve maintenance, is confirmed by the comparison of time registrations, as shown in Figure 3.11.

3.4.6 General Discussion

Results for the last four (#3 - #6) control loops illustrated above are synthesized in Figure 3.12, where values of the stiction parameter S are reported for different time acquisitions. Before valve maintenance (MTA), loops #3, #5, and #6 have almost constant values of stiction, while loop #4 shows an increasing trend.

Trends are drawn only on the basis of values considered reliable; disregarded cases and motivations are repeated here: runs ii and vi for loop #5 and runs iii and ix for loop #6 (irregular oscillations); run v for loop #5 and runs v and viii for loop #6 (different results in the two windows of data); run vi for loop #6 (outlier with respect to the main trend).

After maintenance, no significant oscillation is detected for loops #3, #4, and #5, and negligible values of stiction are estimated; on the contrary, significant values of stiction are still quantified for loop #6.

As stated before, the significance of the proposed filtering procedure in the analysis of industrial data has been checked by application on a wide number of valves. Data consist in

Table 3.5: Loop #6: Valve Stiction Estimation.

time	run #	r	R_{acf}	verdict	S	J	MD_{NL}	MD_{LIN}	F_2
before MTA	i	1.09	0.56	stiction	15.3	7.1	0.99	0.88	0.85
before MTA	ii	1.11	0.66	stiction	16.5	11.0	0.93	0.84	0.87
before MTA	iii	1.41	0.38	-	-	-	-	-	-
before MTA	iv	1.02	0.56	stiction	15.2	2.59	0.99	0.89	0.92
before MTA	v	3.36	0.61	stiction	(13.3)	(0.2)	0.96	0.01	0.87
before MTA	vi	1.38	0.57	stiction	[6.3]	[0.1]	0.99	0.90	0.84
before MTA	vii	2.24	0.63	stiction	14.0	7.0	0.99	0.82	0.95
before MTA	viii	1.36	0.62	stiction	(13.4)	(3.2)	0.94	-0.26	0.87
before MTA	ix	0.47	0.25	-	-	-	-	-	-
before MTA	x	0.95	0.68	stiction	14.2	1.26	0.97	0.87	0.85
after MTA	xi	19.4	0.88	stiction	10.6	2.2	0.99	0.86	0.96
after MTA	xii	0.79	0.57	stiction	9.1	1.0	0.98	0.96	0.94
after MTA	xiii	4.28	0.61	stiction	9.3	4.5	0.99	0.94	0.95

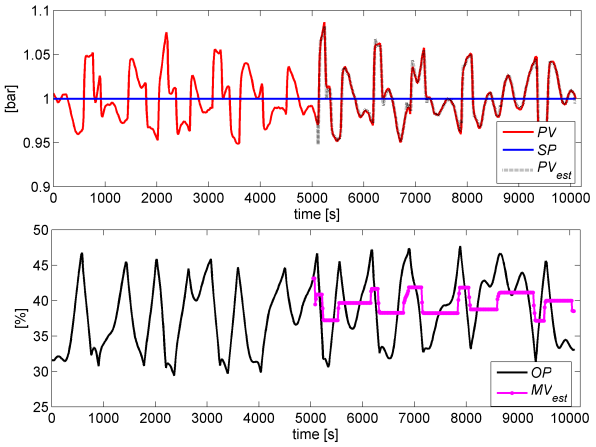

(a) Run x (before MTA): wide oscillations due to valve stiction

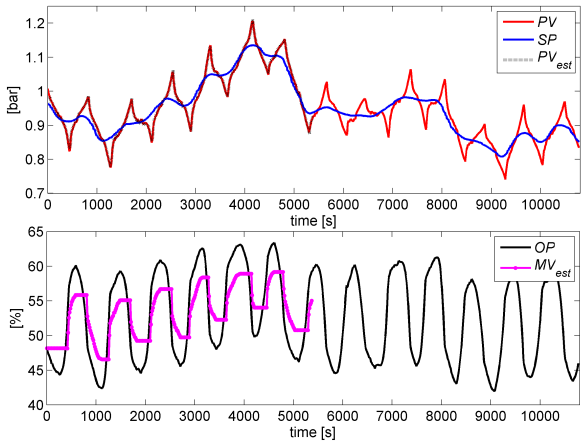

(b) Run xi (after MTA): still significant oscillation – again valve stiction.

Figure 3.11: Trends for Loop #6.

about 800 acquisitions before and after plant shutdown for periodic maintenance. The reliability criterion was the repeatability and homogeneity of stiction values estimation in different acquisitions for the same valve.

As global considerations, the proposed procedure has allowed one to issue results which are considered reliable for 43 out of 62 industrial loops examined. The other 19 loops are cases of unreliable results probably due to the presence of perturbations and stiction acting simultaneously. This result can be considered encouraging, taking into account that different perturbations may be present in an industrial environment.

3.5 The Updated Performance Monitoring Tool

Afterwards, the proposed stiction quantification methodology has been included in the new architecture of the control loop performance monitoring system *PCU* (Plant Check Up) [23]. Figure 3.13 shows the architecture of the system, while the new structure of the module devoted to analysis of stiction (diagnosis + quantification) is reported in Figure 3.14.

A full description of the previous version of *PCU* is reported in Scali and Farnesi [123]; a synthesis is reported below.

The *Initialization Module* imports parameter values from DCS and performs a first check on

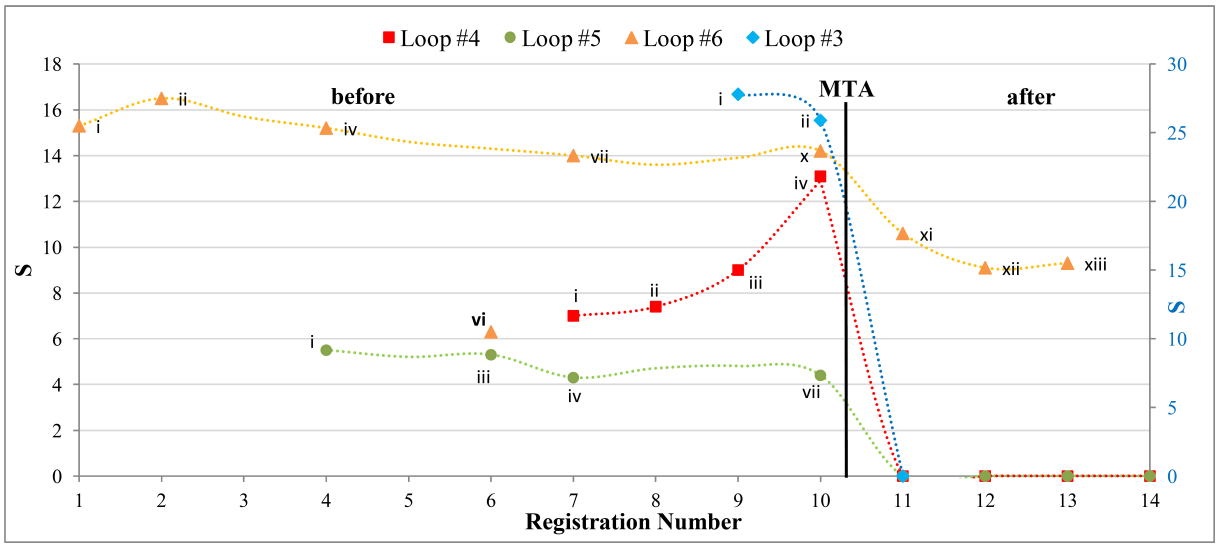

Figure 3.12: Trends of stiction parameter S before and after valve maintenance.

loop status; if the quality of the data is not good, or a change of configuration is detected, or the valve is operating manually, the analysis stops. In these cases, the loop receives a (definitive) label (**NA**: *Not Analyzed*) and the analysis is stopped. Otherwise, all recorded data are imported and performance analysis begins.

The *Anomaly Identification Module* performs a first assignment of performance with verdicts: such as **G** (*Good*), **NG** (*Not Good*). Loops subject to excessive set point changes (amplitude or frequency) are temporarily labeled as **NC** (*Not Classified*) and sent to the identification module (I&R). For loops not in saturation, after a data pre-treatment, tests to detect oscillating or sluggish loops are executed; these tests refer to the Hägglund's approach ([67, 68]), with suitable modifications of internal parameters, based on field calibration [125]. In the case of both tests resulting negative, the loop is classified as well-performing and a definitive label **G** is assigned. Slow loops can only be caused by the controller: therefore they receive a **NG** label and are sent to the Identification and Retuning Module (I&R). Oscillating loops can be caused by aggressive tuning, external disturbance or valve stiction: for this reason, they are primarily sent to FAM, for a frequency analysis.

The *Identification & Retuning Module* accomplishes process identification and, if successful, controller retuning and evaluation of performance improvements. It receives from the AIM module loops with constant SP labeled as **NG** (*Not Good*) caused by improper tuning and loops labelled as **NC** (*Not Classified*) with variable SP. The two possibilities of constant and variable Set Point are treated differently, the second case being typical of secondary loops under cascade control.

The *Frequency Analysis Module* has the scope of separating irregular oscillations from regular ones on the basis of a power spectrum which computes dominant frequencies; irregular loops are labeled **NG**, without any further inquiry about causes. Regular loops with deteriorating oscillations are sent to the I&R Module, otherwise - in the case of loops showing permanent oscillations - to the SAM for stiction/disturbance detection.

The *Stiction Analysis Module* analyses data of **NG** oscillating loops and performs different tests to detect the presence of valve stiction and to quantify its amount. Following previous results and considerations about the effect of external disturbances, this module has been significantly changed (Figure 3.14). Two techniques to detect significant loop oscillations are firstly applied. Regularity factor r (Thornhill et al. [157]) and decay ratio R_{acf} (Miao and Seborg [105]) of autocorrelation function (ACF) of the control error are calculated. If the control loop is considered to not oscillate regularly and non-substantial stiction is present.

About stiction detection, tests consist in the application of four techniques: the relay-based

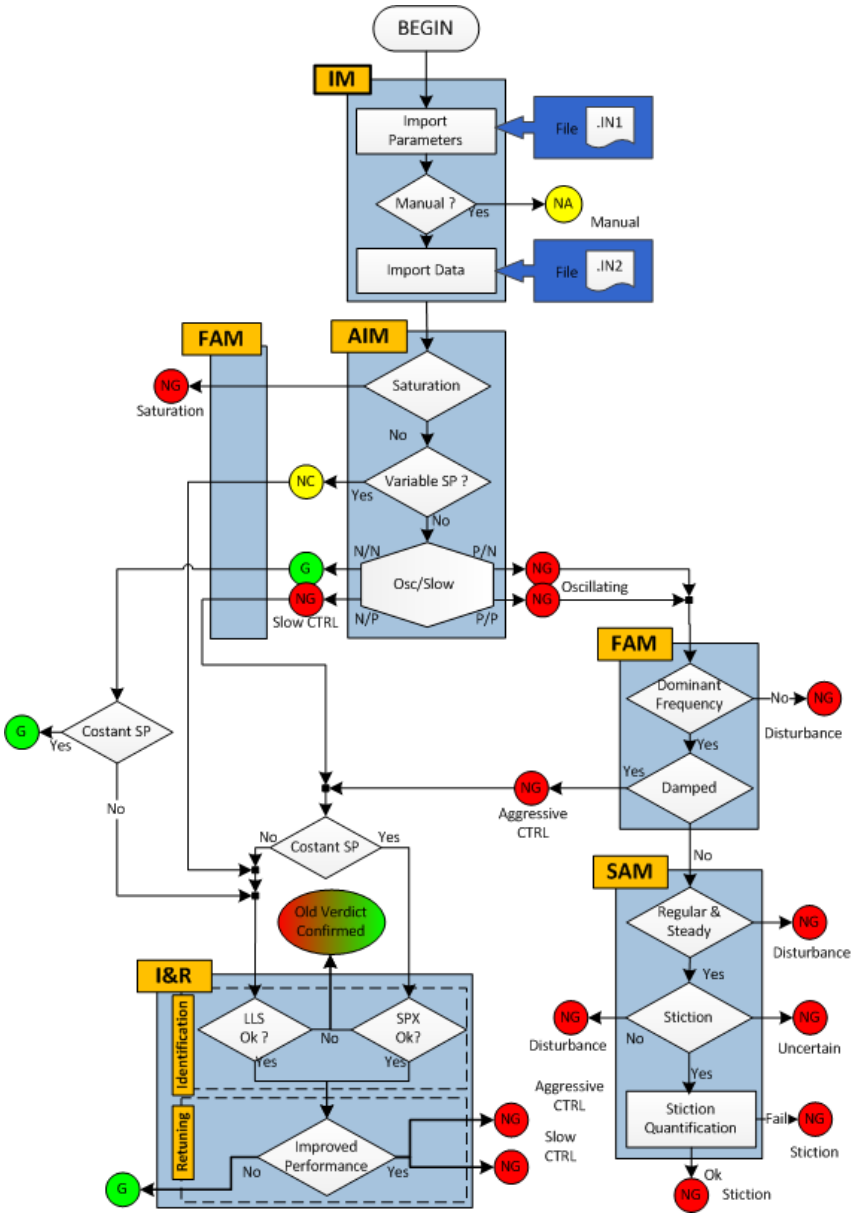

Figure 3.13: Schematic representation of the new PCU system.

fitting of values of the controlled variable (PV) (Rossi and Scali [119]), the improved qualitative shape analysis (Scali and Ghelardoni, [124]), the Cross-Correlation (Horch, [77]), which is the simplest (and probably most widely used) test, and the Bicoherence (Choudhury et al., [46]), which allows to put into evidence non-linear characteristics of loop data. The appropriate technique is automatically selected by the system, as well as the "weight" to be assigned to the different techniques, depending on the type of loop. Final verdict takes into account indications coming from different techniques and from other auxiliary indices: the cause Stiction or Disturbance is assigned to the exit loop in cases of strong evidence; otherwise the cause is Uncertain.

The stiction quantification procedure (Section 3.2) is applied only to loops clearly indicated as affected. To increase the reliability of stiction estimations, data can be divided into sets and the method can be applied separately. The appropriate number of data sections depends on the whole data length; in general, at least 4-5 periods of oscillation are needed. For each data window, a stiction model and a linear model are identified. Then, a comparison of the data windows is performed using two specific indices, which separately evaluate deviations

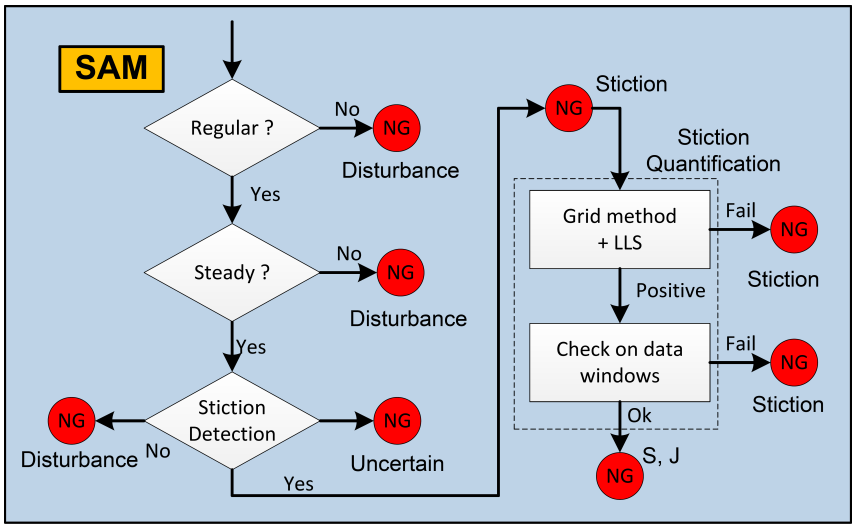

Figure 3.14: Flow diagram of the Stiction Analysis Module.

between non-linear and linear models [25].

Note that the screening by means of diagnosis techniques and the check on the indices of models deviation are not sufficient to assure always an exact diagnosis and an accurate estimation of stiction, but the number of wrong evaluations can be significantly reduced, as reported in the next section.

Many other industrial loops have been analyzed by means of the new version of the monitoring system *PCU* . No additional result is here presented for the sake of brevity.

3.6 Conclusions

Stiction quantification is certainly important for valve monitoring and maintenance scheduling. In the perspective of application on industrial data, the first problem consists of the lack of knowledge about the *true* valve stem position (MV) and the *true* stiction values. In addition, the presence of irregular perturbations and of different sources of oscillation acting simultaneously might affect the accuracy of any estimation technique.

The proposed technique models the control loop as a Hammerstein system and it is based on a grid search and a systematic filtering procedure, which permits one to discard data for which stiction quantification is very likely to fail. The methodology allows reliable quantification when stiction is the only cause of oscillation and even in the case of stiction together with incorrect tuning and set point variation. However, the technique may fail in the case of simultaneous presence of disturbances and stiction. Therefore, even though not sufficient to eliminate the problem completely, the methodology is able to reduce the number of wrong evaluations.

Repeating the procedure for different acquisitions for the same valve allows one to follow the evolution of stiction values in time and to disregard anomalous cases (*outliers*). Successful applications and reliable results for 43 out of 62 industrial loops demonstrate the effectiveness of the proposed method.

The procedure for stiction quantification, and its implementation in the performance monitoring system (*PCU*), is indeed a valid tool to check valve stiction and to schedule valve maintenance. The possible drawback seems to be a preliminary assessment of the presence of stiction by means of diagnosis techniques, because the simultaneous presence of external disturbances may alter results. This is a common feature for the majority of stiction quantification techniques and further activity has been devoted to overcome this problem.

Chapter 4

Stiction Quantification - part II

Abstract [1]

This chapter presents a comparative study of different models and identification techniques applied to the quantification of valve stiction in industrial control loops, with the specific objective of taking into account for the presence of external disturbances.

As in Chapter 3, a Hammerstein system is used to model the controlled process (linear block) and the sticky valve (nonlinear block). Nevertheless in this case, five different candidates for the linear block and two different candidates for the nonlinear block are evaluated and compared in terms of achievable performance. In particular, the capability to cope with the presence of nonstationary disturbances is analyzed.

Two of the five linear models include a nonstationary disturbance term that is estimated along with the input-to-output model, and these extended models are meant to cope with situations in which significant nonzero mean disturbances affect the collected data. The comparison of the different models and identification methods is carried out thoroughly in three steps: simulation, application to pilot plant data and application to industrial loops.

In the first two cases (simulation and pilot plant) the specific source of fault (stiction with/without external disturbances) is known and hence a validation of each candidate can be carried out more easily. Nonetheless, each fault case considered in the previous two steps has been found in the application to a large number of datasets collected from industrial loops, and hence the merits and limitations of each candidate have been confirmed.

As a result of this study, extended models are proved to be effective when large, time varying disturbances affect the system, whereas conventional (stationary) noise models are more effective elsewhere.

[1] This chapter is based on two different papers: [29], [30].

4.1 Introduction

Oscillations in control loops cause many issues which can disrupt the normal plant operation. Typically fluctuations increase variability in product quality, accelerate equipment wear, move operating conditions away from optimality, and generally they cause excessive or unnecessary energy and raw materials consumption.

The common sources for oscillatory control loops can be found in poor design of the process and of the control system, e.g. choice and pairing of controlled and manipulated variables, from one hand. From another hand, poor controller tuning, oscillatory external disturbances, and control valve nonlinearities such as stiction, backlash and saturation, are frequent causes of excessive loop oscillations. Therefore, control loop monitoring and assessment methods are recognized as important means to improve profitability of industrial plants. An effective monitoring system should, first of all, detect loops with poor performance. Then, for each faulty loop, it should indicate the sources of malfunction (among possible causes) and suggest the most appropriate way of correction.

Among actuator problems, valve stiction is said to be the most common cause of performance degradation in industrial loops [85]. An extensive characterization of this phenomenon was firstly given in [47]. Two kinds of models are commonly used to describe stiction: models derived from physical principles and models derived from process data. Physical models are more accurate, but owing to the large number of unknown parameters, they may not be convenient for practical purposes [88, 42]. This is the main reason why data-driven models are typically preferred [47, 149, 87, 76, 43].

A review of a significant number of stiction detection techniques recently presented in the literature is reported in [85]; among them: cross-correlation function-based [77], waveform shape-based [87, 146, 132, 119, 168, 76, 124], nonlinearity detection-based [46], and model-based algorithms [90]. In [85] a comparison of performance is also presented by applications on a large benchmark (93 loops) of industrial data.

Following their conclusions, research on stiction *modeling* and *detection* (i.e. confirmation of its presence) has to be considered a mature topic, even if it may happen that different results are obtained once applied on the same industrial dataset, owing to complexity and superposition of different phenomena. Stiction *quantification* instead has to be regarded as an area where research contributions are still needed. As seen in Chapter 3, the main difficulty in quantifying the amount of stiction arises from the fact that the valve stem position (MV) is not measured and recorded in many (old designed) industrial control systems [25], and then it must be reconstructed from available measurements (controlled variable, PV, and controller output, OP) by using a data driven stiction model.

In stiction quantification techniques, the control loop is often modeled by a Hammerstein system: a nonlinear block for valve stiction, followed by a linear block for the process. This approach was firstly used in [148] along with a one parameter stiction model given in [149]. However this method may not capture the true stiction behavior since the nonlinear model is not always very accurate. Subsequently, other techniques have been proposed [50, 84, 95, 61]. A specific linear model was used in [90], which also accounts for nonstationary disturbances entering the process. The control loop was modeled as a Hammerstein-Wiener structure also in [118]. More recently, a technique based on harmonic balance method and describing function identification was proposed in [16]. A simplified method based on a new semi-physical valve stiction model was illustrated in [75].

Chapter 3 pointed out that, while simulation is the first necessary step to check mathematical consistency of a proposed identification technique, its validation on a single set of industrial data can be pointless due to the superposition of unknown effects, such as nonstationary disturbances [25]. As a confirmation, results obtained by different quantification techniques can be very inconsistent once applied on the same set of industrial data (as it happened in benchmark presented by [85], Chp. 13). To overcome this problem, it has been suggested to

repeat stiction estimation for different data acquisitions for the same valve, in order to follow the time evolution of the phenomenon and to disregard anomalous cases (*outliers*) [25]. The comparison of reasonable values of stiction with predefined acceptable thresholds allows one to schedule valve maintenance in a reliable way; on-line stiction compensation is also an alternative, though not very popular in industry (compare Chapter 5).

Following the above considerations, this chapter represents a continuation of the work reported in Chapter 3. The new objectives to be addressed are:

i) comparing some different identification techniques (of the linear model in the Hammerstein system) when applied on the same dataset;

ii) showing how external nonstationary disturbances can influence stiction estimation and system identification. Both aspects were not considered in the methodology presented in [22, 25] where a single (ARX) model structure and a single identification technique were developed, and nonstationary disturbances were not modeled.

Note that this chapter collects the results of [29] and [30], here merged in an application-oriented direction. Simulation examples and datasets of pilot plant presented in both papers are here illustrated. Mostly, results obtained from several registrations of industrial control loops are shown. [2]

The remainder of this chapter is organized as follows. In Section 4.2, five different models and identification methods of the linear block (in the Hammerstein system) and two models for the stiction nonlinear are illustrated. The merits of each model and identification method are firstly assessed in simulation in Section 4.3, and then validated in a pilot plant in Section 4.4. Section 4.5 is dedicated to applying and evaluating the different techniques to several industrial data sets. Finally, conclusions are drawn in Section 4.6.

4.2 Hammerstein System: Models and Identification Methods

As in Chapter 3, the control loop is here modeled by a Hammerstein system as depicted in Figure 4.1. In details, v and y are the linear process input and output (that is, MV and PV respectively), u is the controller output (that is, OP), r is the loop set point, e is a Gaussian white noise, and η is a time varying bias representing the additive nonstationary external disturbance.

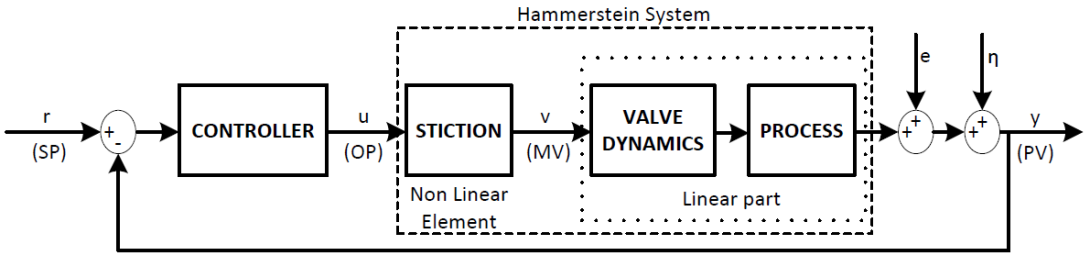

Figure 4.1: Hammerstein system representing the (sticky) control valve followed by the linear process, inserted into the closed-loop system.

Two well-established stiction models are used to describe the nonlinear valve dynamics: Kano's [87], and He's [76] model.

Five different models describe the linear process dynamics:

- ARX (Auto Regressive model with eXternal input),
- ARMAX (Auto Regressive Moving Average with eXternal input),
- SS (State Space model),

[2] Preliminary results of the study of [30] have been previously presented in [29].

- EARX (Extended Auto Regressive model with eXternal input),
- EARMAX (Extended Auto Regressive Moving Average with eXternal input, [89]).

4.2.1 Nonlinear stiction models

In Kano's stiction model [87], the relation between the controller output (the desired valve position) OP and the actual valve position MV is described in three phases (Figure 4.2):

I. *Sticking*: MV is steady (*A*-*B*) and the valve does not move, due to static friction force (dead-band + stick-band, *S*).

II. *Jump*: MV changes abruptly (*B*-*C*) because the active force unblocks the valve, which jumps of an amount *J*.

III. *Motion*: MV changes gradually, and only the dynamic friction force can possibly oppose the active force; the valve stops again (*D*-*E*) when the force generated by the control action decreases under the stiction force.

In He's stiction model the relation between OP and MV is slightly different and simpler [76]. The model uses static f_S and dynamic f_D friction parameters and is closer to the first-principle-based formulation. It uses a temporary variable that represents the accumulated static force. Note that parameters of He's model have their equivalent in Kano's model and vice versa, according to the following equations (cfr. also Figure 4.2):

$$\begin{cases} S = f_s + f_d \\ J = f_s - f_d \end{cases} \quad \text{or} \quad \begin{cases} f_s = \dfrac{S+J}{2} \\ f_d = \dfrac{S-J}{2} \end{cases} \tag{4.1}$$

However, due to different logics, the two stiction models can generate different MV sequences for a given OP and with equivalent parameters. Note also that Kano's and He's models are quite simple, since they imply uniform stiction parameters for the whole valve span. Stiction could be really inhomogeneous, having various amounts for different operating conditions (that is different OP values) and then producing complicated signatures on MV(OP) diagram. In order to overcome these limitations, recent works which implement flexible stiction models have been proposed [163, 59].

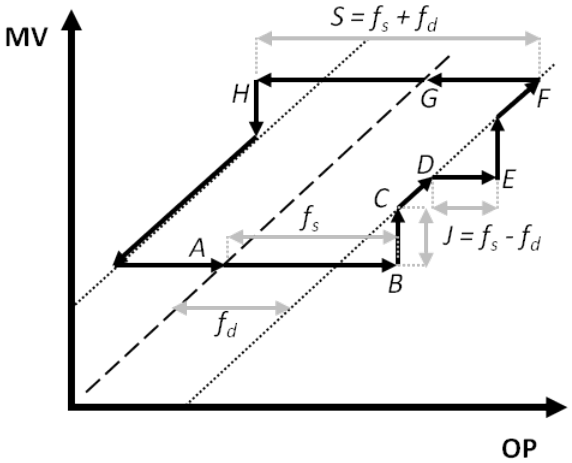

Figure 4.2: Valve stiction: theoretical behavior of MV vs. OP, and graphical representation of Kano's and He's model parameters.

Valve stiction produces an offset between controlled variable PV and Set Point SP, and this causes loop oscillations because the valve is stuck even though the integral action of the controller increases (or decreases) OP. The MV(OP) diagram shows a parallelogram-shaped limit

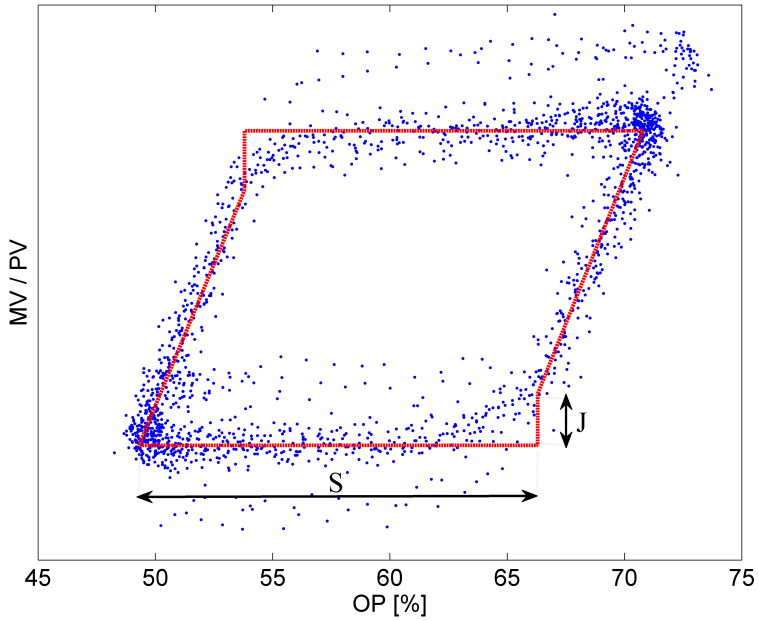

Figure 4.3: Valve stiction: typical industrial behavior of PV vs. OP.

cycle, while MV(OP) would be perfectly linear without valve stiction. Figure 4.3 represents the PV(OP) plot for a case of flow rate control loop, for which the fast linear dynamics allows one to approximate MV(OP) with PV(OP), since MV is usually not measured. Figure 4.3 shows also the signature obtained with Kano's stiction model by fitting the industrial data.

It should be recalled that also in the case of stiction, loops with slower dynamics (level control, temperature control) usually show PV(OP) diagrams having elliptic shapes. Similar PV(OP) diagrams are obtained for other types of oscillating loops (external stationary disturbance or aggressive controller tuning), and therefore assigning causes is not straightforward.

It is also worth saying that the value of J is critical to induce limit cycles [50, 84]. In addition, while S can be often easily recognized on PV(OP) diagram, since limit cycles show clear horizontal paths, on the opposite, the process dynamics or the presence of high level noise make PV trend deviate significantly from MV trend, and make J almost hidden [85] (see Figure 4.3).

Finally, note that $S \simeq 1\%$ is considered enough amount of stiction to cause performance problems [85]. Increasing the amount of stiction (associated to the ratio S/J), the amplitude and the period of oscillation of OP and PV signals increase significantly, thus leading to particularly poor performance. For these reasons, being able to quantify and predict the evolution of stiction in time is important in order to schedule maintenance action on more critical valves.

4.2.2 Linear process models

The linear part of the Hammerstein system has one of the following structures, in discrete-time form.

- ARX:

$$A(q^{-1})y_k = B(q^{-1})v_{k-t_d} + e_k \tag{4.2}$$

where v_k and y_k are the linear process input and output; $A(q^{-1})$ and $B(q^{-1})$ are polynomials in time shift operator q (i.e. such that $q\,v_k = v_{k+1}$), and given as:

$$\begin{aligned} A(q^{-1}) &= 1 + a_1 q^{-1} + a_2 q^{-2} + \ldots + a_n q^{-n} \\ B(q^{-1}) &= b_1 q^{-1} + b_2 q^{-2} + \ldots + b_m q^{-m} \end{aligned} \tag{4.3}$$

where e_k is white noise, t_d is the time delay of the process, (n, m) are the orders on the auto-regressive and exogenous terms, respectively.

- ARMAX:
$$A(q^{-1})y_k = B(q^{-1})v_{k-t_d} + C(q^{-1})e_k \tag{4.4}$$
where $A(q^{-1})$ and $B(q^{-1})$ are defined in (4.3), whereas:
$$C(q^{-1}) = 1 + c_1 q^{-1} + c_2 q^{-2} + ... + c_p q^{-p} \tag{4.5}$$
in which p is the order of the moving average term.

- SS:
$$\begin{aligned} x_{k+1} &= \mathbf{A}x_k + \mathbf{B}v_k + \mathbf{K}e_k \\ y_k &= \mathbf{C}x_k + e_k \end{aligned} \tag{4.6}$$
where $\mathbf{A} \in \mathbb{R}^{n\times n}$, $\mathbf{B} \in \mathbb{R}^{n\times 1}$, $\mathbf{C} \in \mathbb{R}^{1\times n}$, $\mathbf{K} \in \mathbb{R}^{n\times 1}$, and n is the model order.

- EARX:
$$A(q^{-1})y_k = B(q^{-1})v_{k-t_d} + e_k + \eta_k \tag{4.7}$$
where η_k is the time varying bias representing the additive nonstationary external disturbance, to be estimated along with the polynomials $A(q)$ and $B(q)$ (see Figure 4.1).

- EARMAX:
$$A(q^{-1})y_k = B(q^{-1})v_{k-t_d} + C(q^{-1})e_k + \eta_k \tag{4.8}$$

4.2.3 Hammerstein system identification

The proposed stiction quantification techniques are based on a grid search over the space of the nonlinear model parameters. The computational time of the methodology may be long, but it does not represent a disadvantage for three main reasons: the procedure is oriented toward an off-line application which requires data registered for hours, the wear phenomena in valves occur slowly (weeks or months), and valve maintenance usually occurs periodically on the occasion of a plant shutdown.

In details, the system identification is carried out according to the following procedure.

(i) A 2-D grid of stiction parameters (S, J) is built; for each possible combination of (S, J), MV signal is generated from (measured) OP using Kano's model. For He's model, MV is generated using the corresponding parameters (f_s, f_d) according to (4.1).

(ii) Coefficients of the linear models are identified using different techniques on the basis of (generated) MV and (measured) PV sequences.

The overall model fit is quantified by F_{PV}:

$$F_{PV} = 100 \cdot \left(1 - \frac{\|PV_{est} - PV\|^2}{\|PV - PV_m\|^2}\right) \tag{4.9}$$

where PV, PV_m and PV_{est} are vectors containing values of the measured output, measured output average and estimated output sequences, respectively. The symbol $\|\cdot\|$ denotes the Euclidean norm. Thus, for each considered linear model, the optimal combination of (S, J) is computed as the one that maximizes the fitting index F_{PV}.

Note that the stiction parameters grid has a triangular shape, since $f_s \geq f_d \geq 0$ (or $S \geq J$). Thus, overshoot stiction cases ($J > S$) are excluded; actually waveforms generated for these combinations are rarely observed in practice. The largest value of S (and J) is the OP oscillation span. Therefore, under boundary conditions, when $S = J = \Delta OP$ (the span of OP), the valve jumps between two extreme positions, generating an exactly squared MV signal.

4.2.4 Identification algorithms

The five linear process models are identified by means of different algorithms.

ARX model coefficients are estimated by least-squares regression. SS model coefficients are identified using a subspace identification method, the PARSIM-K technique [112]. ARMAX, EARX and EARMAX models are estimated using the recursive least-squares (RLS) identification algorithm proposed (for EARMAX model) by [89].

For EARX and EARMAX, a decoupled parameter covariance update procedure with variable forgetting factors is developed to identify the process parameters and the bias term [89]. To the best of the author's knowledge, this is the first time that a SS model and an EARX model are used for Hammerstein system identification applied to valve stiction estimation.

The proposed RLS identification algorithm is based on the one of [89], and can be summarized as follows.

Model Order: Choose a model order (e.g., (n, m, p) for EARMAX) from the model order library and estimate the model parameters using the following algorithm.

Initiation: The recursive estimator is initiated with the following covariance and parameter estimates.

$$\begin{aligned} P_\theta(0) = \beta I_{n_t \times n_t}, \quad P_\eta(0) = \beta; \quad \beta = 10^4, \\ \hat{\theta}(0) = \bar{0}_{n_t \times 1}, \quad \hat{\eta}(0) = 0, \\ \lambda_\theta(0) = 1, \quad \lambda_\eta(0) = 0.84, \\ \{\varepsilon(t)\} = \bar{0}. \end{aligned} \tag{4.10}$$

where n_t is the total number of model parameters to be estimated inclusive of both LTI and time varying parameter η.

Propagation: Steps i to vi are to be performed for $t = 1, ..., N$.

- Step i. Formulate the regressor vector.

  EARMAX:

$$\varphi(t) = [-\hat{y}(t-1), ..., -\hat{y}(t-n),\, u(t-t_d), ..., u(t-t_d-m+1),\, \varepsilon(t-1), ..., \varepsilon(t-n_h)] \tag{4.11}$$

  EARX:

$$\varphi(t) = [-\hat{y}(t-1), ..., -\hat{y}(t-n),\, u(t-t_d), ..., u(t-t_d-m+1)] \tag{4.12}$$

- Step ii. Gain update,

$$\begin{aligned} K_\theta(t) = P_\theta(t-1)\varphi(t)(\lambda_\theta(t-1) + \varphi^T(t)P_\theta\varphi(t))^{-1} \\ K_\eta(t) = P_\eta(t-1)(\lambda(t-1) + P_\eta(t-1))^{-1} \end{aligned} \tag{4.13}$$

- Step iii. Parameter update,

$$\begin{bmatrix} \hat{\theta}(t) \\ \hat{\eta}(t) \end{bmatrix} = \begin{bmatrix} I_{n-1} & K_\theta(t) \\ K_\eta(t)\varphi^T(t) & 1 \end{bmatrix}^{-1} \times \begin{bmatrix} \hat{\theta}(t-1) + K_\theta(t)(y(t) - \varphi^T\hat{\theta}(t-1)) \\ \hat{\eta}(t-1) + K_\eta(t)(y(t) - \hat{\eta}(t-1)) \end{bmatrix} \tag{4.14}$$

- Step iv. A posteriori prediction error,

$$\varepsilon(t) = y(t) - \varphi^T\hat{\theta}(t) \tag{4.15}$$

- Step v. Parameter estimate covariance update,

$$\begin{aligned} P_\theta(t) = \frac{1}{\lambda_\theta(t-1)}(I - K_\theta(t)\varphi^T(t))P_\theta(t-1), \\ P_\eta(t) = \frac{1}{\lambda_\eta(t-1)}(I - K_\eta(t))P_\eta(t-1), \end{aligned} \tag{4.16}$$

- Step vi. Forgetting factor update,

$$\lambda_\theta(t) = 1,$$
$$\lambda_\eta(t) = 1 - \frac{(y(t-1) - \varphi^T(t-1)\hat{\theta}(t-1) - \hat{\eta}(t-2))^2}{(1 + P_\eta(t-1))\sigma_e}; 0.72 \leq \lambda_{eta}(t) \leq 0.9 \tag{4.17}$$

If the objective is to obtain the non-stationary additive disturbance, the recursive identification algorithm may be carried in two or more iterations, where the initial parameter estimates for jth iteration are chosen as the parameter estimates obtained at the end of $(j-1)$th iteration.

4.2.5 Specific issues in identification of the stiction plus process system

It is worth to underline that the exact stiction estimates depend on several issues. In addition to some general aspects (e.g., the dataset used in identification, choice of loss function, identification algorithm), in the case of Hammerstein system identification with grid search algorithm, also the following issues are important: type, order, and time delay of the linear (process) model; type of the nonlinear (stiction) model; step size of the grid. Only some of these aspects will be analyzed hereinafter in the text.

Moreover, the way in which the stiction model is initialized must be attended. This issue could seem a negligible aspect, but in reality, as it has been verified by a large number of simulations and applications, it is an important point, as discussed next and in the application results. In particular, the identification results can be sensitive to the initialization of the Kano's model. On the opposite, the He's model does not present these problematics.

Given an OP sequence and fixed (S, J) parameters, different MV sequences can be produced, simply by changing the initial values of the auxiliary parameters of the Kano's model: u_s, stp, d [87]. Figure 4.4 shows that, for the same triangular OP wave, given a combination of stiction parameters $(S = 1, J = 0.5)$, four different MV sequences can be generated using different values of *stp* and d. Only after several samples, all MV sequences coincide perfectly with each other.

This *stationary time* depends on the specific OP sequence and the (S, J) combination. Therefore, during the identification procedure, three choices are possible for the initialization of Kano's model states:

In.1 The auxiliary variables are initialized arbitrarily, the same for each combination;

In.2 A threshold stationary time is fixed *a priori* and an average MV sequence is considered after this time;

In.3 The stationary time is computed for each (S, J) combination and only the steady sequence of MV is considered.

According to the results of extensive simulations that have been carried out, the third (or at least the second) choice should be preferred.

4.3 Simulation Study

The objective of this section is to investigate the impact of different factors on the effectiveness of the methods to yield accurate estimation. To this aim, simulation results are provided to describe the capabilities of the compared algorithms for Hammerstein system identification. The systems are simulated in closed-loop operation, which is known to be a difficult task as compared to open-loop identification, because of the correlation between process noise and input sequences. OP and PV sequences are used without any filtering in the identification methodologies, which fall under the class of direct identification techniques.

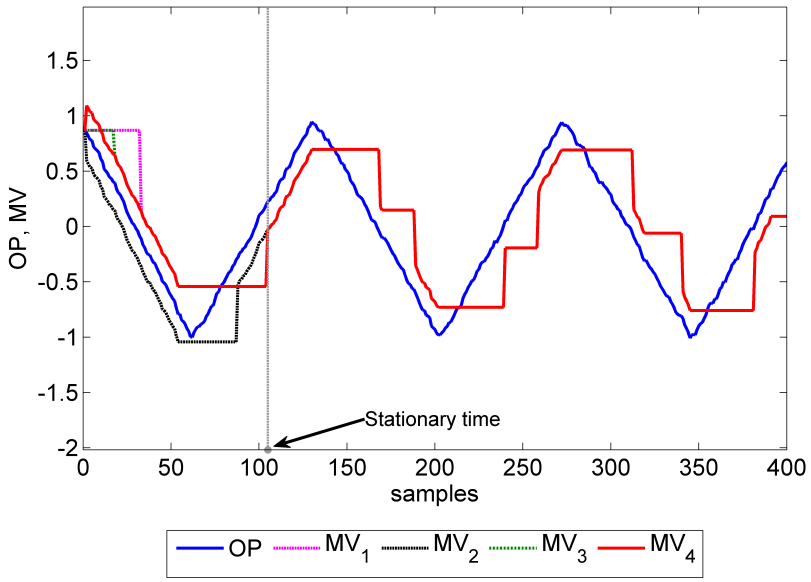

Figure 4.4: Ambiguity in the nonlinear model initialization (data of CHEM 10, benchmark of [85]).

4.3.1 Effect of stiction amount and disturbance presence

Firstly, the impact of stiction amount and of external disturbance presence is investigated. Two different simulation examples are here considered: the first one previously presented in [29], the second one in [30].

Example #1

As first example, the following ARMAX process, with $(n, m, p) = (2, 2, 2)$ and subject to an external disturbance, is considered in discrete-time form [90, 29]:

$$\begin{aligned} y_k = {} & 0.7358 y_{k-1} - 0.1353 y_{k-2} + 0.2642 u_{k-1} \\ & + 0.1353 u_{k-2} + e_k + 0.7 e_{k-1} - 1.3 e_{k-2} + \eta_k \end{aligned} \tag{4.18}$$

where:

$$\eta_k = a\Big(sin(0.02\,k) + 0.5 sin(0.05\,k)\Big) \tag{4.19}$$

with $a \geq 0$. Stiction parameters are varied to cover a wide range of phenomena ($S \in [2, 12]$, $J \in [1, 4]$) using Kano's model. The stationary disturbance $\{e_k\}$ is a normally distributed white noise signal with standard deviation $\sigma_e = 0.1$. The process is in closed-loop with a proportional-integral (PI) controller having proportional gain $K_C = 0.4$, and integral gain $K_I = 0.3$ (values which allow stable response with acceptable performance).

The system is excited by introducing a random-walk signal, as controller set-point, which varies as follows:

$$SP_k = \begin{cases} SP_{k-1} + 2(R_{2k} - 0.5) & \text{if} \quad R_{1k} > 1 - \delta_{sw} \\ SP_{k-1} & \text{otherwise} \end{cases} \tag{4.20}$$

where δ_{sw} is the average switch probability and R_{1k}, R_{2k} are two random numbers drawn, at time k, from a uniform distribution in $[0, 1]$. This type of set-point is thought to reproduce an industrial scenario of a control loop with variable reference commanded by a higher level Model Predictive Controller.

One hundred Monte-Carlo simulations are carried out, using different realizations of white noise $\{e_k\}$, for each set of stiction parameters and disturbance amplitude. The linear process

model orders and the time delay are fixed a-priori in performing identification steps, namely $t_d = 0$, $(n, m) = (2, 2)$ for ARX and EARX, $(n, m, p) = (2, 2, 2)$ for ARMAX and EARMAX, $n = 2$ for SS. No structural error is present in the nonlinear part: Kano's model is also used to generate MV sequences.

Note that data of PV and OP are divided into two sets. The first two-thirds of data are used as identification data set; the last third of data is used as validation set in order to test the models previously identified. As in (4.9), a fitting index for the estimation data set, $F_{PV}^{(id)}$, and for the validation data set, $F_{PV}^{(val)}$, can be defined. The linear model fit is quantified by the scalar E_G given as:

$$E_G = 100 \cdot \left(1 - \frac{\|G_{est}(z) - G(z)\|_\infty}{\|G(z)\|_\infty}\right) \tag{4.21}$$

where $G(z)$ and $G_{est}(z)$ are the true process and the identified model discrete-time transfer functions, respectively, and $\|g(z)\|_\infty = \max_{\omega \in [0, 2\pi]} |g(e^{i\omega})|$. The nonlinear model fit is quantified by F_{MV}:

$$F_{MV} = 100 \cdot \left(1 - \frac{\|MV_{est} - MV\|^2}{\|MV - MV_m\|^2}\right) \tag{4.22}$$

where MV, MV_m and MV_{est} are vectors containing values of the actual valve position, average actual valve position and the estimated valve position.

Figure 4.5 shows a summary of the results for the case of $a = 0$ in (4.19), that is when valve stiction is the only source of oscillation. Top panels show the various simulated stiction cases (S, J) and the corresponding estimated parameters (S_{id}, J_{id}). Bottom panels show the values of the fitting indices E_G and $F_{PV}^{(val)}$ using the different proposed techniques.

Figure 4.6 shows a summary of the results for the case of $a = 0.25$ in (4.19), that is when an external disturbance acts simultaneously with stiction.

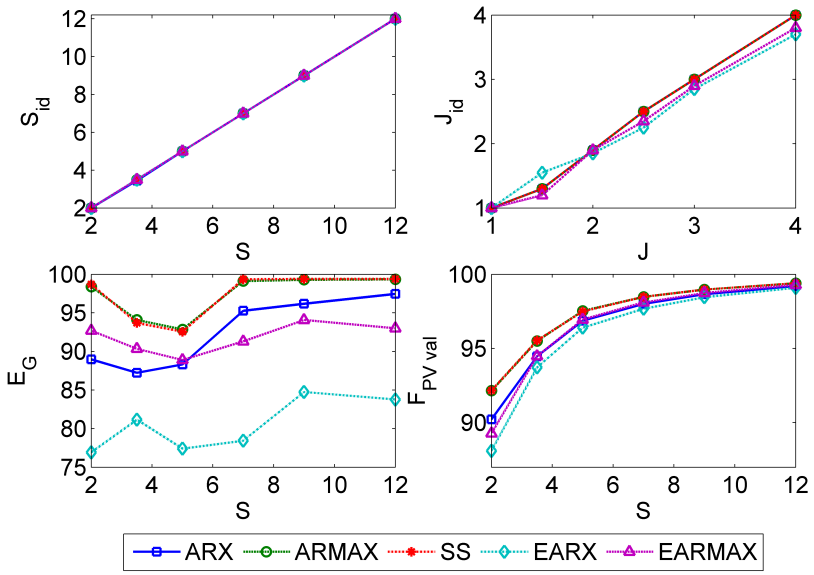

Figure 4.5: Simulation example #1: identification results for $a = 0$: top panels, left: S_{id} vs S, right: J_{id} vs J; bottom, left E_G vs. S, right $F_{PV}^{(val)}$ vs. S.

It can be clearly seen that, in the case of pure stiction oscillation, ARX, ARMAX and SS models ensure a more accurate stiction estimation and, mostly, perform a better linear model identification: E_G values are higher, especially for ARMAX and SS. On the other hand, in the presence of external disturbance, the stiction parameters and the linear model identified using EARMAX and EARX are of higher accuracy as compared to the other identification techniques: E_G and $F_{PV}^{(val)}$ values are higher.

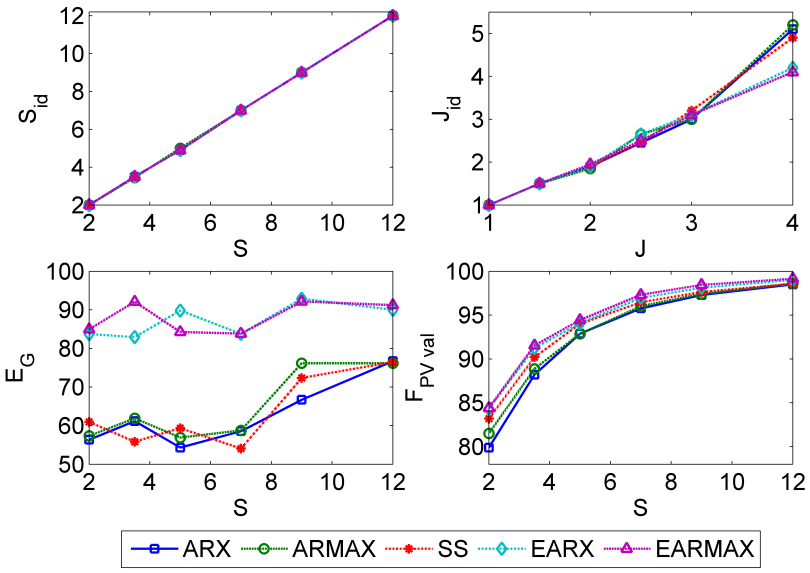

Figure 4.6: Simulation example #1: identification results for $a = 0.25$: top panels, left: S_{id} vs S, right: J_{id} vs J; bottom, left E_G vs. S, right $F_{PV}^{(val)}$ vs. S.

Example #2

As second example, the following ARMAX process, with $(n, m, p) = (3, 3, 3)$ and subject to an external disturbance, is considered in discrete-time form [30]:

$$\begin{aligned} y_k = {} & 0.5215y_{k-1} - 0.0590y_{k-2} + 0.0009y_{k-3} \\ & + 0.2836u_{k-1} + 0.2442u_{k-2} + 0.0088u_{k-3} \\ & + e_k + 0.5e_{k-1} + 1.0e_{k-2} - 1.0e_{k-3} + \eta_k \end{aligned} \quad (4.23)$$

where η_k is the external (unmeasured) disturbance given by:

$$\eta_k = a\Big(sin(0.03\,k) + 0.5sin(0.07\,k)\Big) \quad (4.24)$$

with $a \geq 0$. Stiction parameters are varied to cover a wide range of phenomena ($S \in [1, 12]$, $J \in [0.5, 4]$) using Kano's model. The stationary disturbance $\{e_k\}$ is a normally distributed white noise signal with standard deviation $\sigma_e = 0.1$. The process is in closed-loop with a Proportional-Integral (PI) controller having the following transfer function $C_{PI}(q) = K_c + \frac{K_I}{1-q^{-1}}$, with proportional gain $K_C = 0.5$ and integral gain $K_I = 0.5$ (values which allow stable response with acceptable performance).

The system is excited by introducing a random-walk signal, as controller set-point, which varies as in (4.20).

As in example #1, one hundred Monte-Carlo simulations are carried out, using different realizations of white noise $\{e_k\}$, for each set of stiction parameters and disturbance amplitude. The orders and the time delay of the linear process models are fixed a-priori in performing identification steps, namely $t_d = 0$, $(n, m) = (2, 2)$ for ARX and EARX, $(n, m, p) = (2, 2, 2)$ for ARMAX and EARMAX, $n = 2$ for SS. Therefore, in this second example, a little mismatch in the orders of the linear part is present. Conversely, no structural error is present in the nonlinear part: Kano's model is also used to generate MV sequences.

The first two-thirds of data are used as identification data set; the last third of data is used as validation set in order to test the models previously identified. As in (4.9), a fitting index for the estimation data set, $F_{PV}^{(id)}$, and for the validation data set, $F_{PV}^{(val)}$, can be defined.

The linear model fit is quantified by the scalar E_G, as given in (4.21); while the nonlinear model fit is quantified by F_{MV}, as given in (4.22).

Figure 4.7 shows a summary of the results for the case of $a = 0$ in (4.24), that is when valve stiction is the only source of loop oscillation. Top panels show the various simulated stiction cases (S, J) and the corresponding estimated parameters (S_{id}, J_{id}). Bottom panels show the values of the fitting indices E_G and $F_{PV}^{(val)}$ using the different proposed techniques.

Figure 4.8 shows a summary of the results for the case of $a = 0.25$ in (4.24), that is when an external disturbance acts simultaneously with valve stiction.

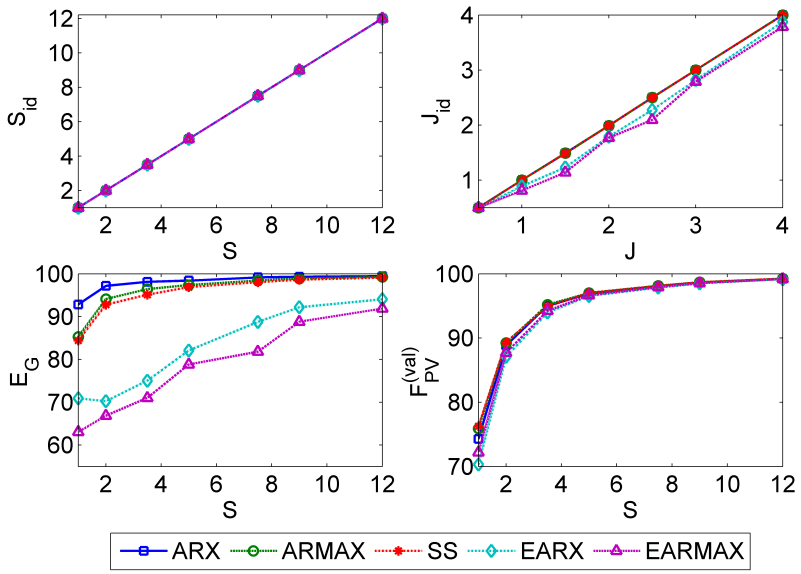

Figure 4.7: Simulation example #2: identification results in absence of the external disturbance ($a = 0$). Top panel, left: S_{id} vs S, right: J_{id} vs J; bottom panel, left E_G vs. S, right $F_{PV}^{(val)}$ vs. S.

As seen for the example #1, it can be now clearly seen that, in the case of pure stiction oscillation ARX, ARMAX and SS models ensure a more accurate stiction estimation and, mostly, perform a better linear model identification: E_G values are higher. On the other hand, in the presence of external disturbance, the stiction parameters and the linear model identified using EARMAX and EARX are of higher accuracy as compared to the other identification techniques: E_G and $F_{PV}^{(val)}$ values are higher. Moreover, the little mismatch in the orders of the linear model does not sensibly affect the results.

Note also that, both in the case of only stiction and in the case of additive disturbance, a worse model identification arise because J is not perfectly estimated, whereas S is always well estimated. Higher values of $F_{PV}^{(val)}$ are obtained for higher values of S. When the amount of stiction increases (that is the ratio S/J), the amplitude of oscillation increases. Therefore, since the stationary disturbance $\{e_k\}$ has the same standard deviation for each simulation, the higher is stiction, the lower is the noise-to-signal ratio. Anyway, noise-to-signal ratio is significant for all the considered simulations, by ranging in the following interval: $NSR \in [5, 25\%]$.

4.3.2 Effect of controller tuning

In the case of direct identification methods, as the ones presented in this thesis, the impact of controller tuning parameters on the estimation results is proved to be not particularly significant. In general, an aggressive controller tuning makes the input signal (OP) more oscillating and then more persistently exciting for the process to be identified. Whereas, a sluggish tuning produces a slowly-varying input, which is less exciting for the process, and possibly less

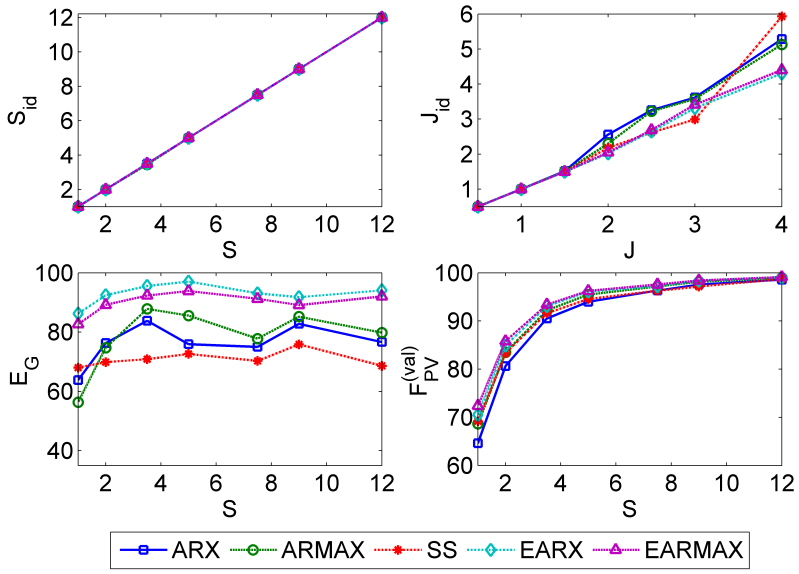

Figure 4.8: Simulation example #2: identification results in the presence of external disturbance ($a = 0.25$). Top panel, left: S_{id} vs S, right: J_{id} vs J; bottom panel, left E_G vs. S, right $F_{PV}^{(val)}$ vs. S.

informative for any identification procedure.

The impact of controller tuning has already been studied by [89], for the identification of a pure linear dynamics without considering the problem of valve stiction. In addition, the same authors ([90], and Chp. 12 in [85]), in the framework of a Hammerstein system, considered the case of double source of loop oscillation (aggressive tuning and valve stiction), by showing that the estimates of stiction parameters are still accurate.

In the present study, good performances are possible for reasonably large ranges of controller parameters around nominal values, both for nonextended and extended process models. The effect of poor controller tuning has been analyzed, by using extensive simulation data. Also pilot plant data have been evaluated (see Appendix A, Section A.6).

Here below only the same linear process of example #2 of Section 4.3.1 is presented. A case of pure valve stiction, described by Kano's model with $S = 9$ and $J = 3$, is studied; no external disturbance (η) is present. Firstly, the controller parameters are set to $K_c = 1.2$ and $K_i = 1.2$, which represent an aggressive tuning. Then, the parameters are changed to $K_c = 0.2$ and $K_i = 0.2$, which compose a sluggish tuning. Note that an appropriate tuning should be $K_c = 0.5$ and $K_i = 0.5$. For both tuning settings, one hundred Monte-Carlo (MC) simulations are carried out, by using different realizations of white noise $\{e_k\}$.

Figure 4.9a shows the results of one identification in the case of aggressive tuning, by using Kano stiction model and ARX linear model. Figure 4.9b reports results of one identification in the case of sluggish tuning, by using Kano stiction model and EARX linear model. In both cases, PV and MV signals are well estimated. Similar results have been obtained for the other linear process models. Indeed, Table 4.1 and 4.2 show the overall results obtained for the two different tuning settings. Average estimates of stiction parameters ($\bar{S}$, $\bar{J}$) with corresponding standard deviations (σ_S, σ_J) are reported. Also average indices of fitting are evaluated: $\bar{F}_{PV}^{(id)}$, $\bar{F}_{PV}^{(val)}$. Therefore, good performance and robustness of the approaches with respect to very different controller tuning parameters are demonstrated.

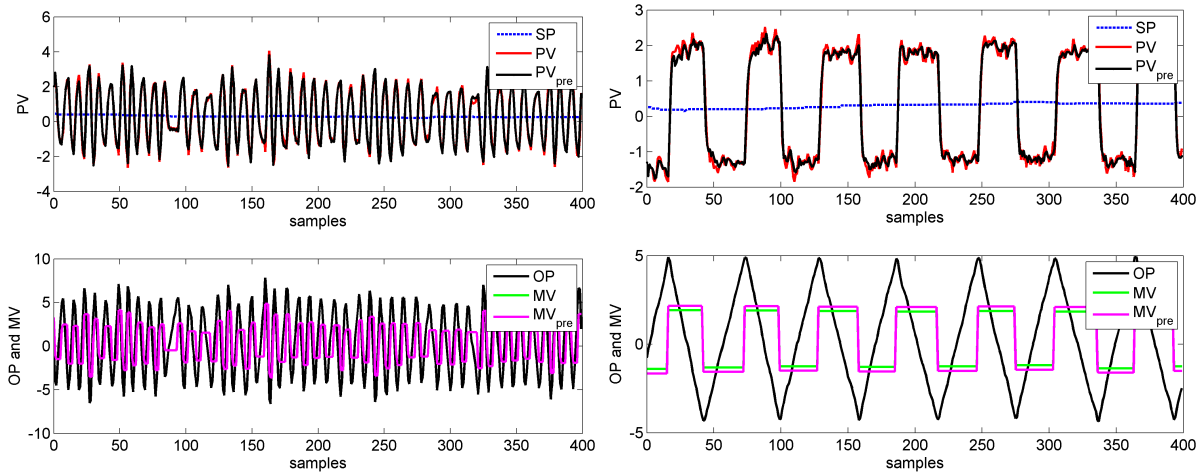

(a) Aggressive tuning. **(b)** sluggish tuning.

Figure 4.9: Simulation data with poor controller tuning.

Table 4.1: Results for MC simulations with aggressive tuning.

LIN model	$\bar{S}$	σ_S	$\bar{J}$	σ_J	$\bar{F}_{PV}^{(id)}$	$\bar{F}_{PV}^{(val)}$
ARX	9.00	0.00	2.97	0.05	99.73	98.71
ARMAX	9.00	0.00	2.90	0.06	98.77	98.75
SS	9.00	0.00	2.88	0.06	98.78	98.76
EARX	9.00	0.00	2.89	0.07	98.98	98.59
EARMAX	9.00	0.00	2.84	0.09	99.01	98.99

Table 4.2: Results for MC simulations with sluggish tuning.

LIN model	$\bar{S}$	σ_S	$\bar{J}$	σ_J	$\bar{F}_{PV}^{(id)}$	$\bar{F}_{PV}^{(val)}$
ARX	8.99	0.01	2.98	0.15	98.60	98.61
ARMAX	8.99	0.03	2.95	0.15	98.65	98.65
SS	8.99	0.03	2.93	0.16	98.67	98.66
EARX	8.99	0.01	2.90	0.27	98.77	98.40
EARMAX	9.00	0.00	2.88	0.23	98.88	98.90

4.3.3 Discussion of results

Main aspects and basic results of the simulation study are discussed below. Firstly, it is worth noting that computational times are different for each technique. The ARX model, with a simple algorithm of LLS identification, requires much shorter times compared to ARMAX, EARX, EARMAX and SS models. There is approximately one order of magnitude: some seconds vs. some minutes.

Note also that through the standard approach, for the sake of simplicity, time delay of the linear process models is never estimated. In particular, time delay is assumed known for the simulation results, and then it is fixed a priori for the pilot plant data and the industrial data.

The impact of time delay could be evaluated by considering another grid of possible time delay L, where $L = T_s t_d$, is taken as a multiple of the sampling time (T_s). For every triple (S, J, t_d), the coefficients of the linear model could be then identified. This approach is robust, but obviously heavy in terms of computational load. Among other standard solutions to estimate the time delay, [95] and [89] have proposed a cross correlation analysis between the input (MV) and the output (PV) sequence. Additional simulations with process time delay have showed that t_d has no significant impact on the identification methods. An example of this study is reported in Appendix A, Section A.5.

In addition, it has to be recalled that the main focus of this chapter is the identification and quantification of a control loop with valve stiction, possibly with the additional presence of external disturbances. So the cases of loop oscillation not due to stiction, that is, only due to aggressive controller or external disturbances or due to both of these sources, are by purpose not considered in Chapter 4, neither in the simulation section nor for real data sets.

Note also that in the industrial practice the proposed identification methods, as almost any stiction quantification method, should be applied only on data where valve stiction has been reliably detected by specific diagnosis techniques. Nevertheless, cases of pure external

disturbance and pure aggressive tuning can be used as negative tests in order to estimate close-to-zero stiction parameters, as it has been verified in additional simulation studies. An example of this analysis is reported in Section A.1.

Finally, as general results from simulation study, nonextended models prove to be better in the case of only valve stiction, while extended models outperform simpler models in the presence of additional nonstationary disturbance. These same outcomes have been obtained using different process dynamics (also with time delay), other disturbance amplitudes and frequencies, other types of slowly-varying nonstationary disturbance (as drift), different types of SP signal (also constant), and with He's stiction model in place of Kano's model. Some details are reported in Appendix A.

Anyway, similar results are to be obtained on real industrial data. Note that, in general, to be able to obtain good model parameter estimates, these data have to be rich enough. Normal operating data may not be persistently exciting, especially if the set point is constant for long periods of time.

4.4 Application to Pilot Plant

In this section, the performance of the considered methods are tested on IdroLab, a pilot plant located in Livorno (Italy), and owned by ENEL, the largest Italian power company. A diagram of the pilot plant used in the experiments is shown in Figure 4.10a. Water circulates between drums *D1* and *D2*, and a pneumatic actuator is coupled to a spherical valve (*V2*) which controls the flow rate. Further details on the experimental apparatus can be found in [31]. The control valve, its stem and the packing are shown in Figure 4.10b.

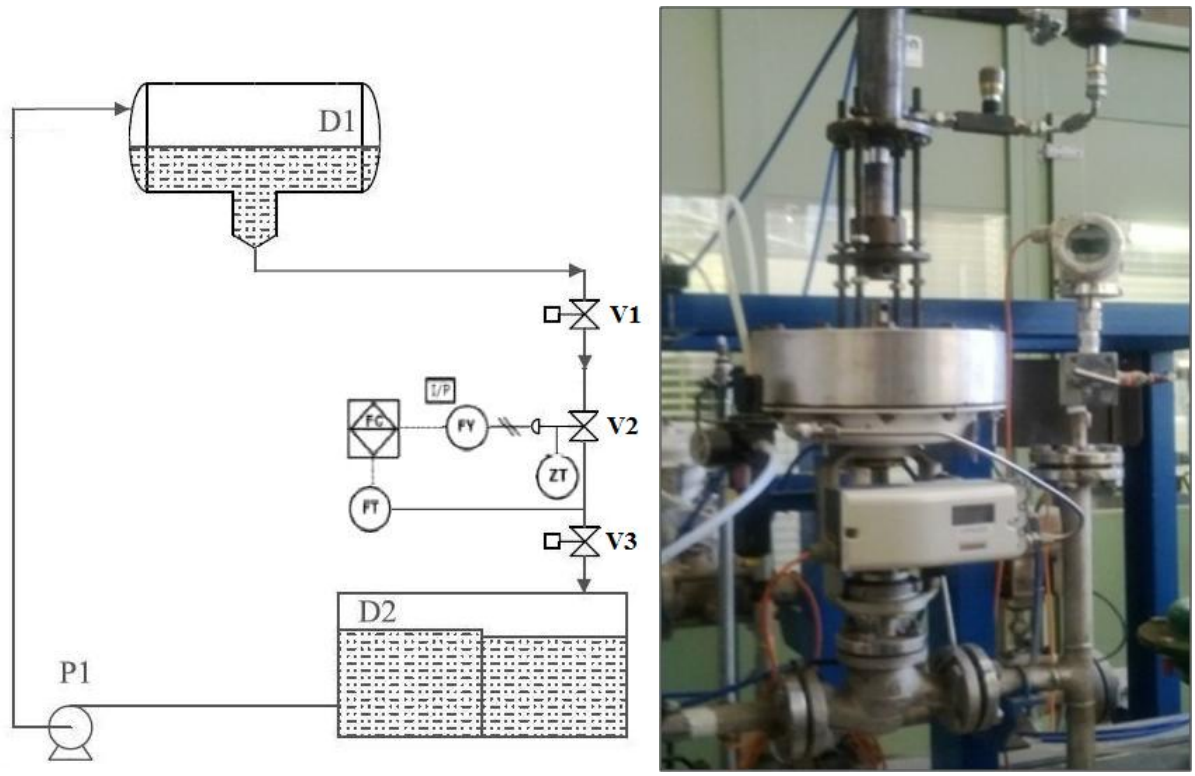

(a) the process diagram. **(b)** the actuator and the sticky valve.

Figure 4.10: Pilot plant:

Friction is "introduced" into the valve by tightening the packing nut by means of a special device. The valve is equipped with a positioner, but the position control loop is open: in this way the actual valve stem position (MV) is measured but the positioner does not perform any

control action. The PV is the flow rate through the valve and the OP is the output signal from a PI controller. The opening of the valve $V3$ (installed downstream the sticky valve $V2$) is changed by imposing, as command (OP), a near sinusoidal profile in order to "generate" the external disturbance.

Four different sets of data are collected with a sampling time of 1 s.

I. A low amount of valve stiction is the only source of oscillation [30].

II. A high amount of stiction is introduced around the valve stem [29, 30].

III. An external disturbance is introduced and acts simultaneously with stiction of low amount [30].

IV. A different external disturbance is introduced and acts simultaneously with stiction of high amount [29].

Figure 4.11a shows the MV(OP) diagram of the valve obtained imposing triangular waves on OP, oscillating from 0 to 100% of the valve span, when a low amount of stiction is applied to the stem. In Figure 4.11b the corresponding diagram is shown, when a high amount of stiction is applied.

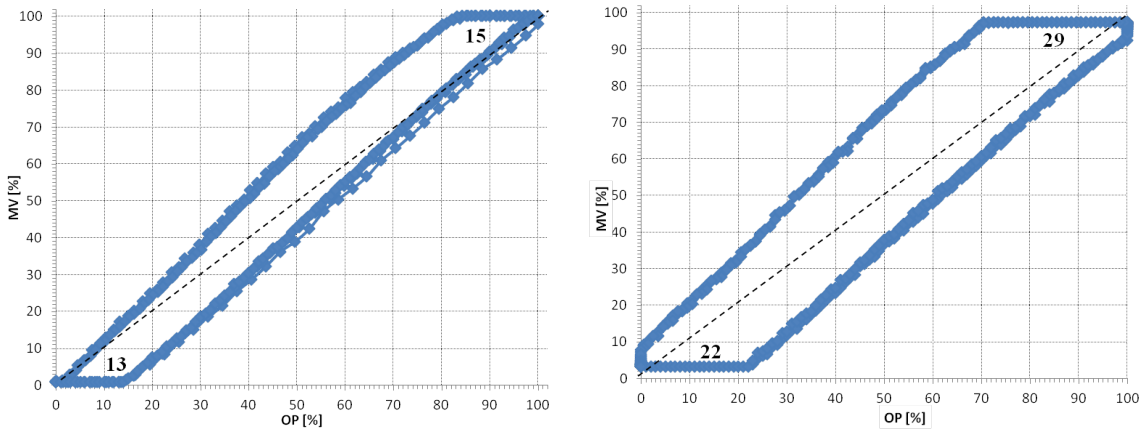

(a) in the case of low stiction. **(b)** in the case of high stiction.

Figure 4.11: Pilot plant: experimental behavior MV vs. OP

The valve shows an asymmetric behavior: S (dead-band + stick-band) is bigger in the closing direction and smaller in the opening direction, while the slip jump J is always really small. The stiction parameters obtained from these off-line (manual) tests on the valve are approximately known: $S \in [13, 15]$, $J \in [0.1, 0.2]$ in the case of low stiction, and $S \in [22, 29]$, $J \in [0.2, 1]$ in the case of high stiction.

Kano's model and He's model are used to fit the *measured* MV signals of the four sets of data collected in closed loop. The best combinations of parameters are, in the case of low stiction, $S = (f_s + f_d) = 12.1$, $J = (f_s - f_d) = 0.1$ (both for Kano's and He's model), with a fitting index $F_{MV} = 71.75\%$. In the case of high stiction, actual stiction parameters are $S = 22.1$, $J = 0.2$ (for Kano's), with a fitting of 76.28%, and $S = 22.0$, $J = 0.1$ (for He's), with a fitting of 76.27%. Therefore, both nonlinear models appear sufficiently adequate.

The five linear process models with the two stiction models are then applied to detect and quantify the amount of stiction without the knowledge of the MV signal. The time delay and the orders of the linear process models are fixed *a priori*, namely $t_d = 5$, $(n, m) = (2, 2)$ for ARX and EARX, $(n, m, p) = (2, 2, 2)$ for ARMAX and EARMAX, $n = 2$ for SS.

Table 4.3, 4.4, 4.5, and Table 4.6 show respectively the results of the comparison for the first, the second, the third and the fourth experimental set.

Test 1 In Table 4.3, identification results obtained with all ten combinations of models are reported. In all cases good estimates of the nonlinearity are established: $F_{MV} \in [60\%, 70\%]$, and (S, J) are close to their actual values. EARMAX and EARX models perform also a better PV fitting.

Figure 4.12 shows the registered time trends of SP, PV, OP, MV and the estimated values of PV and MV (PV_{est}, MV_{est}) of the first experiment when Kano's model for the sticky valve and EARX model for the linear dynamics are used. Both the PV fitting indices are sufficiently high (cfr. Table 4.3): $F_{PV}^{(id)} = 88.31\%$ for the identification dataset and $F_{PV}^{(val)} = 82.95\%$ for the validation dataset. Also the estimation of the valve stem position is quite accurate: $F_{MV} = 69.35\%$. In this first experiment, with only valve stiction, both nonextended (ARX, ARMAX, SS) and extended models (EARX, EARMAX) are appropriate to the purpose.

Table 4.3: Pilot plant first experiment: low amount of valve stiction.

LIN model	NL model	S	J	$F_{PV}^{(id)}$	$F_{PV}^{(val)}$	F_{MV}
ARX	Kano	11.9	0.2	86.03	84.70	69.35
	He	11.8	0.1	86.01	84.63	69.25
ARMAX	Kano	11.9	0.2	86.08	84.72	67.54
	He	11.8	0.2	86.07	84.56	69.05
SS	Kano	12.5	0.1	85.88	84.77	69.09
	He	12.9	1.0	85.88	84.29	60.46
EARX	Kano	11.9	0.2	88.31	82.95	69.35
	He	11.4	0.4	88.49	82.65	60.77
EARMAX	Kano	11.9	0.2	88.52	84.03	69.35
	He	11.4	0.4	88.57	83.74	60.77

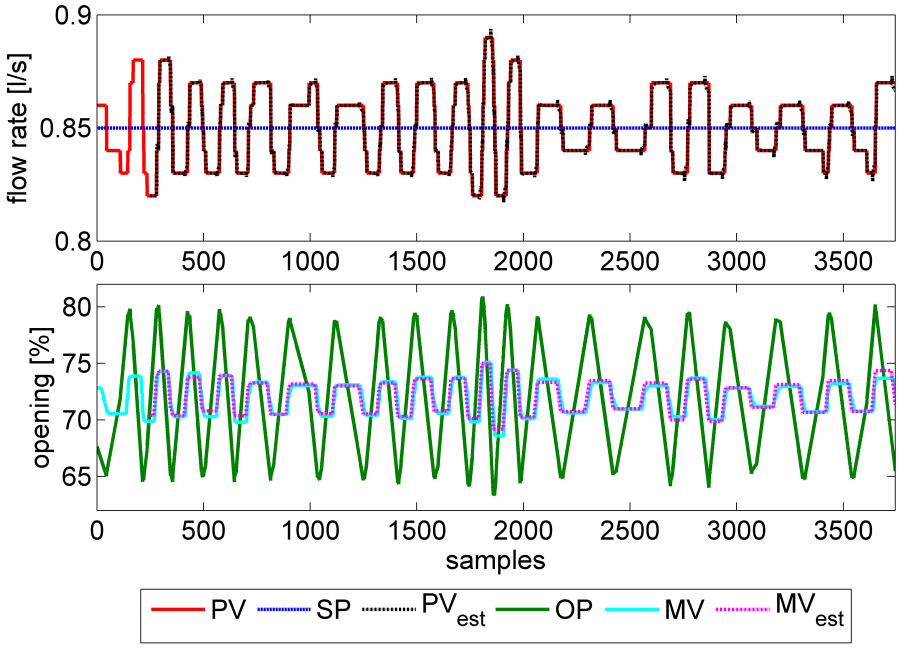

Figure 4.12: Pilot plant first experiment: registered time trends.

Test 2 Table 4.4 shows that good estimation results are obtained again with nonextended (ARX, ARMAX and SS) models. They guarantee a better identification of the nonlinearity:

F_{MV} values are higher. EARMAX and EARX models perform a slightly higher PV fitting but, in this case, produce a significantly worse MV estimation: $F_{MV} \in [25\%, 42\%]$. Since these two models have one more degree of freedom, they tend to generate a bias term (η) even though the external disturbance is not present in order to improve the PV fitting, but this alters the stiction quantification.

Figure 4.13 shows the corresponding registered time trends and estimated signals of the second experiment when He's model and the SS model are used. Both the PV fitting indices are high (cfr. Table 4.4): $F_{PV}^{(id)} = 85.77\%$ for the identification dataset and $F_{PV}^{(val)} = 83.68\%$ for the validation dataset. The estimation of the valve stem position is rather accurate: $F_{MV} = 71.82\%$. Non extended models prove themselves most appropriate when only valve stiction is present in the control loop.

Table 4.4: Pilot plant second experiment: high amount of valve stiction.

LIN model	NL model	S	J	$F_{PV}^{(id)}$	$F_{PV}^{(val)}$	F_{MV}
ARX	Kano	25.2	4.3	85.53	83.57	62.61
	He	23.6	1.5	85.59	83.99	63.44
ARMAX	Kano	24.5	3.5	85.62	84.27	71.85
	He	22.7	2.0	85.77	83.79	71.82
SS	Kano	24.5	3.5	85.67	84.26	71.85
	He	22.7	2.0	85.77	83.68	71.82
EARX	Kano	26.6	0.7	87.07	83.65	28.93
	He	25.0	1.6	87.25	83.63	41.39
EARMAX	Kano	26.8	3.3	87.37	82.22	25.33
	He	25.0	1.6	87.34	83.70	41.39

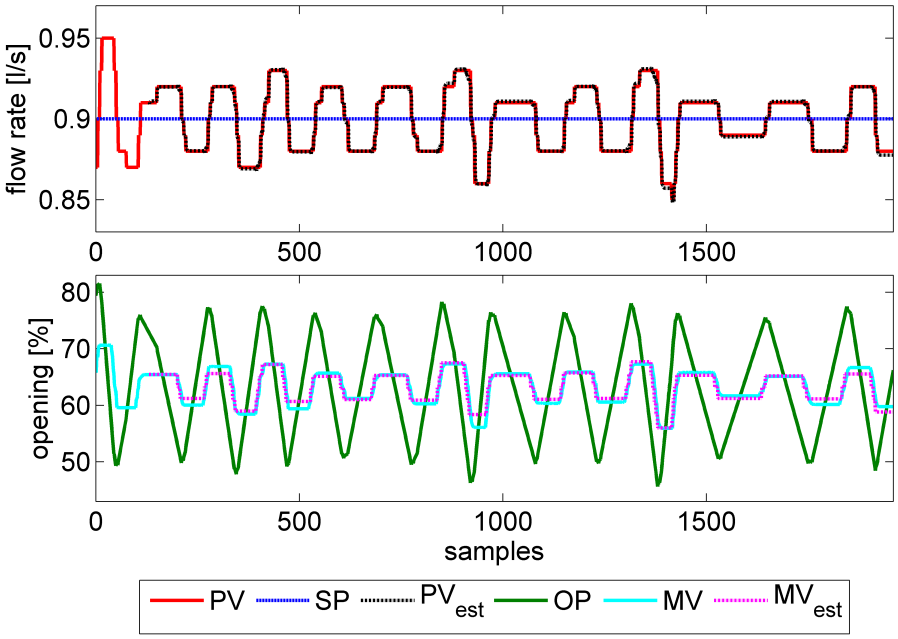

Figure 4.13: Pilot plant second experiment: registered time trends.

Test 3 The results of the third experiment are basically opposite to those of the second experiment (cfr. Table 4.5). EARMAX and EARX models ensure both a better PV fitting and a

higher MV estimation. On the contrary, nonextended models perform a lower identification of the global dynamics and a wrong estimation of the nonlinearity. For the validation dataset, SS model produces instable trends in PV_{est} and $F_{PV}^{(val)}$ indices tend to minus infinite. The presence of a large external disturbance can alter significantly stiction estimation when a nonextended model is used to identify the linear dynamics.

Table 4.5: Pilot plant third experiment: low amount of valve stiction and external disturbance.

LIN model	NL model	S	J	$F_{PV}^{(id)}$	$F_{PV}^{(val)}$	F_{MV}
ARX	Kano	23.7	3.1	84.91	85.19	49.28
	He	22.0	4.4	85.38	83.94	46.86
ARMAX	Kano	23.7	0.7	85.21	84.65	47.37
	He	22.0	4.4	85.46	84.04	46.86
SS	Kano	17.1	2.9	85.50	$-\infty$	69.66
	He	17.0	2.2	85.50	$-\infty$	67.82
EARX	Kano	14.7	0.2	86.12	83.62	74.25
	He	15.2	2.1	86.38	83.80	73.25
EARMAX	Kano	14.8	2.0	86.24	82.93	73.81
	He	12.4	4.3	86.50	83.54	72.10

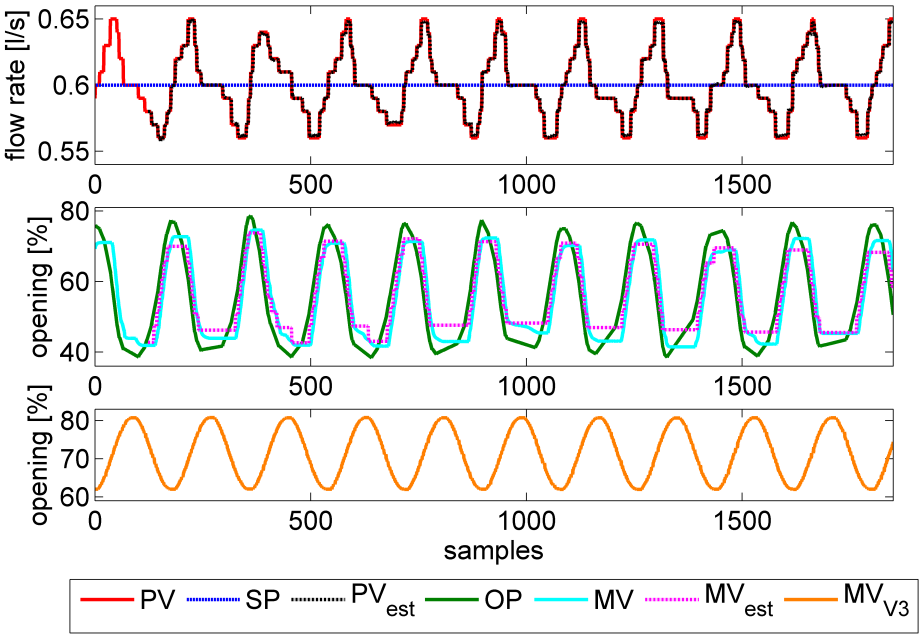

Figure 4.14: Pilot plant third experiment: registered time trends.

Figure 4.14 shows the signals of the third experiment when He's model and the EARMAX model are used. In the bottom panel the stem position of valve $V3$ is reported; this signal is proportional to the disturbance entering the process. The extended model gives an accurate PV fitting (cfr. Table 4.5), $F_{PV}^{(id)} = 86.50\%$, $F_{PV}^{(val)} = 83.54\%$, and a good MV fitting $F_{MV} = 72.10\%$, much higher compared to values obtained with ARX, ARMAX and SS models. The estimated stiction values obtained with EARX and EARMAX are close to the real parameters ($S \simeq 13.1; J \simeq 0.5$) unlike those obtained with nonextended models. Therefore, the additional presence of an external disturbance can be well managed when an extended model is used for stiction estimation.

Test 4 The results of this last experiment are similar to the ones of Test 3 (cfr. Table 4.6). EARMAX and EARX models grant both a better PV fitting and a higher MV estimation. On the opposite, ARX, ARMAX and SS perform a worse identification of the linear dynamics and a completely wrong estimation of the nonlinearity. The presence of the external disturbance can alter stiction estimation when a nonextended model is used to identify the linear dynamics.

Table 4.6: Pilot plant fourth experiment: valve stiction and external disturbance.

LIN technique	NL model	S	J	F_{PV}	$F_{PV}^{(id)}$	$F_{PV}^{(val)}$	F_{MV}
ARX	Kano	13.8	2.7	78.26	78.27	78.20	-131.27
	He	13.1	1.3	78.37	78.22	78.54	-116.95
ARMAX	Kano	12.2	2.7	78.75	78.62	78.88	-163.99
	He	10.2	4.8	78.94	78.97	78.86	-189.26
SS	Kano	10.2	2.7	78.88	78.73	79.03	-203.10
	He	10.4	2.8	79.14	78.85	79.50	-181.10
EARX	Kano	20.6	0.9	78.61	79.81	76.95	39.21
	He	20.2	0.5	78.66	79.83	77.04	38.55
EARMAX	Kano	20.2	0.5	78.79	80.01	77.11	36.71
	He	20.3	2.8	78.74	80.06	76.93	24.89

Figure 4.15 shows the corresponding registered time trends and estimated signals of the second experiment when Kano's model and the EARMAX model are used. In the bottom panel the stem position of valve $V3$ is reported; this signal is proportional to the disturbance entering the process. The extended model gives an accurate overall PV fitting (cfr. Table 4.6) $F_{PV} = 78.79\%$ and a reasonable MV fitting $F_{MV} = 36.71\%$ (especially compared to values obtained with ARX, ARMAX and SS models). The estimated stiction values obtained with EARX and EARMAX are fairly close to the real parameters unlike those obtained with nonextended models (ARX, ARMAX and SS). The presence of the external disturbance does not affect significantly stiction estimation when an extended model is used.

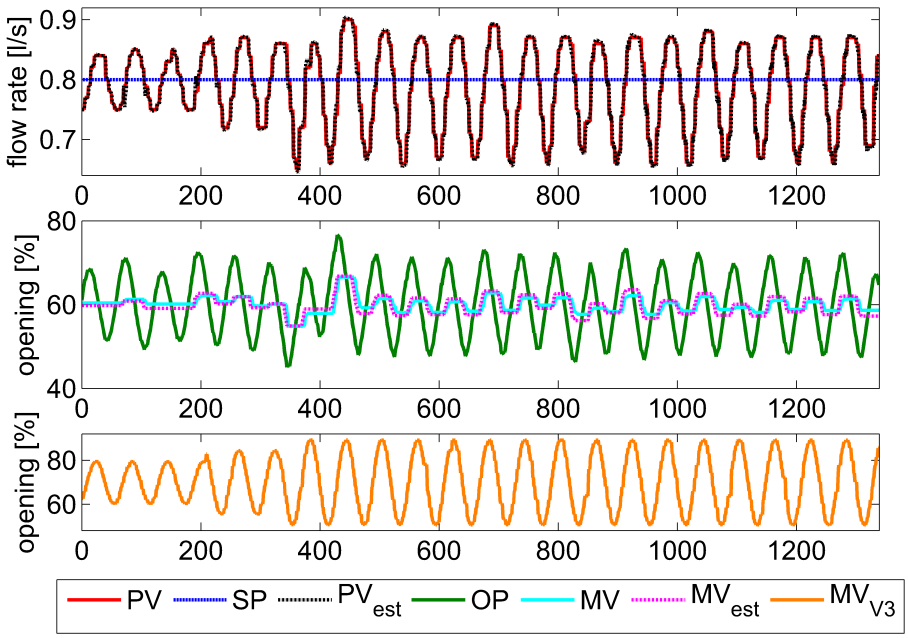

Figure 4.15: Pilot plant fourth experiment: registered time trends.

As general conclusion, the results obtained with pilot plant data have basically confirmed

the ones achieved with simulation data.

4.5 Application to Industrial Data

In this section, the performance of the proposed methods are further compared on some different industrial datasets.

4.5.1 Data from benchmark [85]

Three loops of the dataset of the book of [85], illustrated as a benchmark for stiction detection methods, are firstly used. These three loops are clearly indicated as suffering from valve stiction by several detection methods [85]. The five proposed linear process models are tested, while only Kano's model is used to describe the sticky valve dynamics.

Unless otherwise specified, datasets are used in full: the first two-thirds of data are used as identification set and the last-third is used as validation set. The time delay and the linear models orders are fixed: $t_d = 1$, $(n, m) = (2, 2)$ for ARX and EARX, $(n, m, p) = (2, 2, 2)$ for ARMAX and EARMAX, $n = 2$ for SS. These data are also used purposely to show the effect of the initialization of Kano's model on stiction estimates (see Section 4.2.5).

The results are then compared with the estimates given by some well-established literature procedures: (i) Karra and Karim [90], (ii) Jelali [84], (iii) Lee at. al [95], (iv) Romano and Garcia [118].

CHEM 25 The data of this pressure control loop were obtained from a refinery. Karra and Karim used the following parameters for their EARMAX model: $t_d = 1$ and $(n, m, p) = (2, 2, 2)$. Jelali tested the loop twice using an ARMAX model with: (i) $t_d = 2$, $(n, m, p) = (3, 2, 2)$ and (ii) $t_d = 1$, $(n, m, p) = (2, 2, 1)$. Romano and Garcia used a Hammerstein-Wiener structure on 272 non specified samples without reporting the exact model parameters. Lee et al. used a second order linear model, that is an ARX with $(n, m) = (2, 1)$, and He's stiction model on a specific data window (100 - 350 samples).

Table 4.7 summarizes the estimates obtained using the proposed models and the results available in the literature. The estimates of (S, J) with all methods are really close. Only Lee et al. obtain a higher value of J, probably due to the use of He's model. The proposed EARMAX model (case *a*) gives exactly the same stiction estimate of Karra and Karim once that Kano's model is initialized as in the literature work. Using In.2 initialization discussed in Section 4.2.5, slightly different values of S and J are obtained (case *b*). It should be also noted that the proposed EARX and EARMAX models produce the highest values of PV fitting.

CHEM 10 These data come from a pressure control loop in a chemical process industry. Karra and Karim used the following parameters for their EARMAX model: $t_d = 1$ and $(n, m, p) = (2, 2, 2)$ [85, Chp. 12]. Lee et al. used an ARX$(2, 1)$ and He's stiction model.

Table 4.8 summarizes all the results. The estimates of S are very close in all the five proposed methods, while the estimates of J are bit more variable. These results are obtained with In.2 initialization of Section 4.2.5 setting the *stationary time* of MV at the first tenth of the data length. Also Lee et al. obtained similar values of S and J, while Karra and Karim obtained a similar value of S but a smaller value of slip-jump ($J = 0.05$). In particular, for this dataset, as showed for EARMAX model, different stiction estimates are possible using four different Kano's model initializations of type In.1 (cfr. Figure 4.4). Note that values close to zero of stiction are incorrectly obtained with a specific initialization: $stp = 0; d = -1$.

POW 4 These data are from a level control loop in a power plant. Karra and Karim used an EARMAX model with unspecified parameters applied on an initial data window (1 - 1000

Table 4.7: CHEM 25: comparison of results.

LIN model	NL model	S	J	$F_{PV}^{(id)}$	$F_{PV}^{(val)}$
ARX	Kano	1.8	0.3	74.14	72.96
ARMAX	Kano	1.8	0.2	74.45	73.79
SS	Kano	2.0	0.2	73.88	73.55
EARX	Kano	1.8	0.3	78.67	73.92
EARMAX (a)	Kano	1.8	0.3	78.83	73.95
EARMAX (b)	Kano	1.6	0.0	79.32	74.09
Karra & Karim [90]	Kano	1.8	0.3	-	-
Jelali (i) [84]	Kano	1.80	0.59	-	-
Jelali (ii) [84]	Kano	1.87	0.60	-	-
Romano & Garcia [118]	Kano	1.60	0.44	68.70	-
Lee et al. [85, Chp. 13]	He	1.62	1.62	-	-

Table 4.8: CHEM 10: comparison of results.

LIN model	NL model	S	J	$F_{PV}^{(id)}$	$F_{PV}^{(val)}$
ARX	Kano	1.85	1.70	93.21	92.86
ARMAX	Kano	1.85	1.50	93.50	92.92
SS	Kano	1.85	1.70	93.63	92.87
EARX	Kano	1.90	1.45	93.79	91.33
EARMAX	Kano	1.85	1.35	93.85	92.55
EARMAX ($stp = 1; d = 1$)	Kano	1.85	1.80	93.83	92.55
EARMAX ($stp = 1; d = -1$)	Kano	1.90	1.75	94.10	91.16
EARMAX ($stp = 0; d = 1$)	Kano	1.85	1.65	93.60	92.28
EARMAX ($stp = 0; d = -1$)	Kano	0.20	0.10	93.34	91.63
Karra & Karim [85, Chp. 12]	Kano	1.85	0.05	-	-
Lee et al. [85, Chp. 13]	He	1.77	1.73	-	-

samples). Jelali tested the loop using an ARMAX model of unspecified orders, probably on the first 700 samples. Lee et al. used an ARX$(2, 1)$ and He's stiction model applied on all available data. The proposed identification methods are executed on the first 1000 samples, with In.2 initialization of Section 4.2.5 and setting the *stationary time* of MV at the first tenth of the data length.

Table 4.9 summarizes all the results. For this loop, the estimates of stiction parameters are different with the five proposed methods. ARX, ARMAX and SS models agree and estimate low values of stiction: $S \in [0.8, 0.9]$, $J = 0$. Conversely, EARX and EARMAX models yield larger amounts: $S = 4.1$, $J \in [0.4, 0.7]$. Also Lee et al. obtained low values, while Karra and Karim estimated a much more significant amount of stiction and they also assessed the presence of an external disturbance. For this case, it can be observed that techniques which implement an extended process model yield higher stiction values than techniques which use a nonextended model. The first ones also identify a significant additional disturbance, which alters numerical estimates of stiction. Note that Jelali obtained the largest stiction amount, since his final value of S falls close to the initial guess obtained with ellipse-fitting method ($S_0 = 4.80$).

As overall considerations, since there is no information about the real values of S and J, it is not possible to say exactly which are the best estimates. However, for the first two applications

Table 4.9: POW 4: comparison of results.

LIN model	NL model	S	J	$F_{PV}^{(id)}$	$F_{PV}^{(val)}$
ARX	Kano	0.9	0.0	84.82	84.29
ARMAX	Kano	0.9	0.0	84.80	84.33
SS	Kano	0.8	0.0	85.19	84.78
EARX	Kano	4.1	0.7	85.95	82.37
EARMAX	Kano	4.1	0.4	86.13	82.70
Karra & Karim [85, Chp. 13]	Kano	3.6	1.2	-	-
Jelali [84]	Kano	4.49	2.49	-	-
Lee et al. [85, Chp. 13]	He	0.58	0.39	-	-

(CHEM 25 and CHEM 10), as the stiction estimates in all proposed methods are close and next to the values reported in some well-established literature works, it is possible to conclude that all the techniques give acceptable results. In particular, the estimates of S are very close and therefore really reliable. The estimates of J are more variable and therefore, as expected and previously discussed, more difficult. Moreover, the initialization of Kano's model is proved to be a factor which can alter stiction estimates.

The third application (POW 4) clearly confirms that different techniques can also strongly disagree when applied on the same industrial data [85, Chp. 13]. Some other examples of comparison of selected stiction quantification techniques applied on benchmark data are reported in ...

4.5.2 Data from other industrial loops

The proposed identification techniques are then applied to three datasets obtained during multiannual application of the performance monitoring software (*PCU*) [123] in Italian refinery and petrochemical industries. Data refer to repeated registrations (of PV, OP, SP) for the same loops [30]. The source of malfunction is known to be stiction, but the actual MV signals are not available. Trends of values of parameter S are reported for each combination of nonlinear and linear model. Values of J are not reported since their estimate, as shown previously, is less significant and reliable.

Loop I These data has been previously presented in Chapter 3, as application of the original grid search technique and the first identification method (ARX model) [25]. For this pressure control loop, six different registrations, collected during a month, are available just before the valve maintenance. Four detection techniques ([77, 119, 124, 46]) indicate this loop as always affected by stiction in these acquisitions. Therefore, rather constant stiction values, though unknown, are expected.

In Figure 4.16 pretty uniform values of stiction ($S \in [4, 5.6]$) are obtained for each combination of nonlinear and linear models. Low variability in estimated values of S is given by all linear models plus Kano's model. SS model plus Kano's model gives the lowest variability ($\sigma_S = 0.23$) with a mean value ($\hat{S} = 5.36$) higher than other techniques. Slightly higher variability is obtained with He's model, especially with SS model. Figure 4.17 shows time trends of SP, PV, OP and estimated values of PV and MV (PV_{est}, MV_{est}) of registration # 3 when Kano's model and EARMAX model are used.

The results of this industrial application reproduces the outcome of the first experimental set in the pilot plant (cfr. Table 4.3), where all the linear models are equally valid. In this application, all the identification techniques prove to be sufficiently reliable: constant stiction trends are always estimated.

Note that slightly decreasing trends of stiction are anyway admissible. Here the SP is variable (Figure 4.17), therefore stiction could be not exactly the same for different operating conditions along the same registration or - more likely - along different acquisitions, while Kano's and He's models imply uniform parameters for the whole valve span.

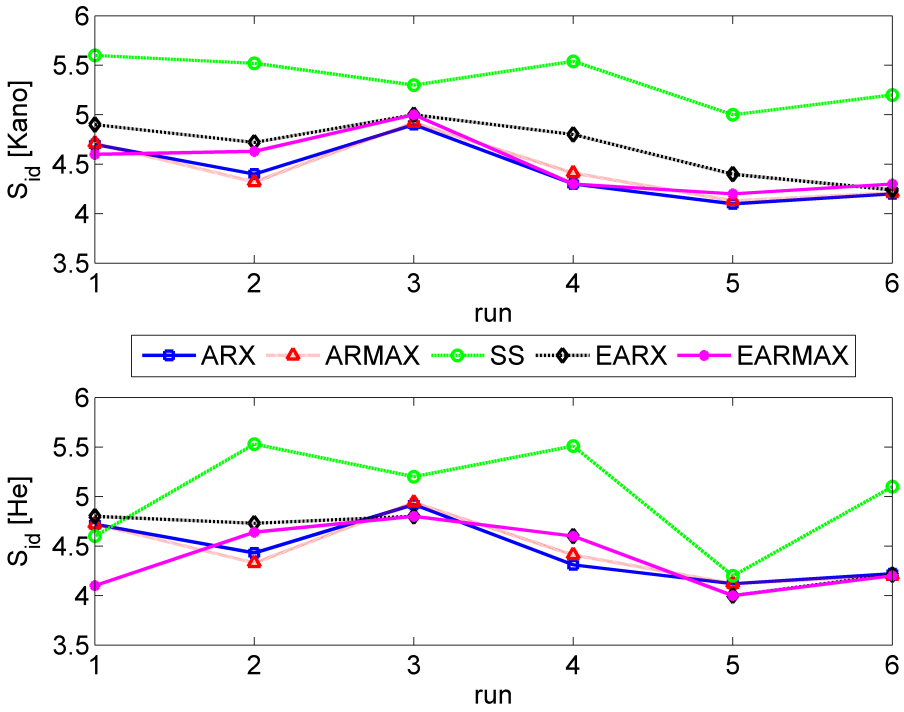

Figure 4.16: Industrial Loop I: Trends of the identified stiction parameter S using different linear models: top, Kano's model; bottom, He's model.

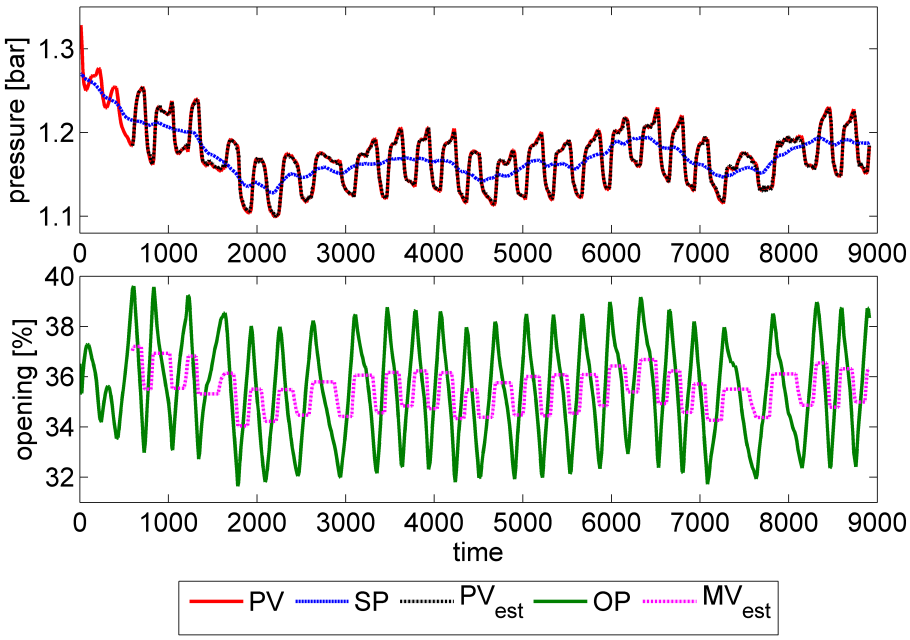

Figure 4.17: Industrial Loop I: time trends for registration # 3.

Loop II These data are from a flow rate control loop with PI-algorithm controller and variable set point. The presence of stiction is clearly recognizable by the PV and OP shapes being close to squared and triangular waves, respectively (Figure 4.18). Moreover, the plot of PV(OP) shows evident stiction characteristics (Figure 4.19), since in FC loops PV is proportional to MV. The same four detection techniques ([77, 119, 124, 46]) indicate this loop as affected by stiction in 11 acquisitions registered along two consecutive days. Therefore, nearly constant stiction values, though unknown, are expected.

From Figure 4.20, rather uniform values of stiction ($S \in [1.8, 2.5]$) are quantified with nonextended models. The lowest variability in estimated values of S is given by ARMAX and SS models plus Kano's or He's model ($\sigma_S \in [0.13, 0.14]$) with a mean value $\hat{S} \in [2.26, 2.30]$. Conversely, an excessively high variability is obtained using extended models: EARX and EARMAX.

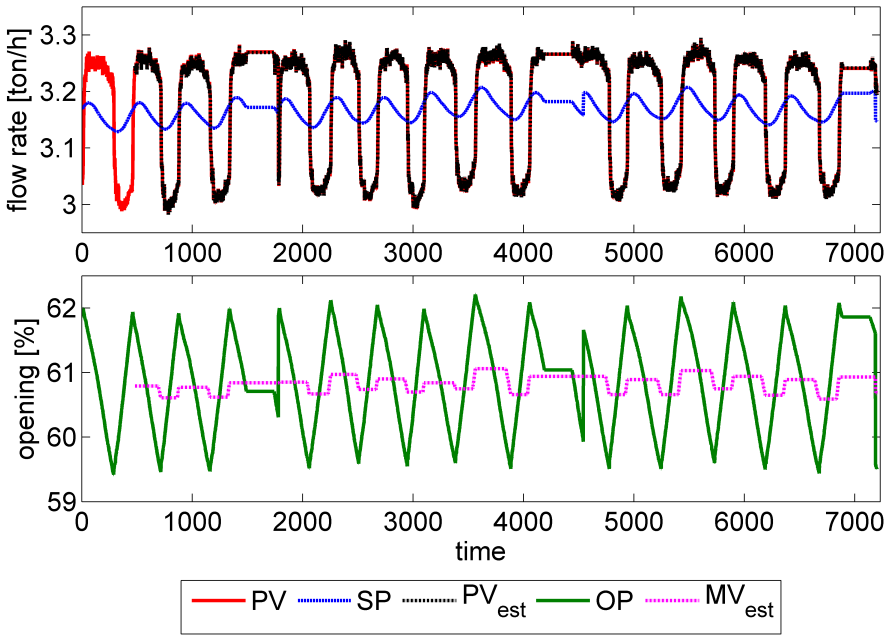

Figure 4.18: Industrial Loop II: time trends for registration # 9.

The results of this industrial application are rather similar to the outcome of the second experimental set in the pilot plant (cfr. Table 4.4), where the nonextended models are more appropriate for the case of only valve stiction. Extended models prove to be not sufficiently reliable: high variable stiction trends are estimated. Sometimes even zero values are obtained: loop oscillation is not associated with valve stiction but wrongly with a significant bias term of external disturbance.

Loop III These data are from a flow rate control loop, the controller has a PID algorithm, and the SP is variable since the loop is the inner part of a cascade control. The same four detection techniques ([77, 119, 124, 46]) indicate stiction in 6 acquisitions registered along four months. Therefore, a constant or increasing trend of stiction is expected.

Once again the presence of stiction is clearly recognizable by the shapes of PV and OP signals, being close to squared and triangular waves, respectively (Figure 4.21). Now, for this loop, the two extended models (EARX and EARMAX) give rather uniform values of stiction ($S \in [2.1, 3.1]$). Conversely, for registration # 4, using ARX and ARMAX models, and for # 5, using all three nonextended models, very low ($S \simeq 0$) or low values are estimated (see Figure 4.22). These estimates appear incorrect since they result as *outliers* with respect to the main stiction

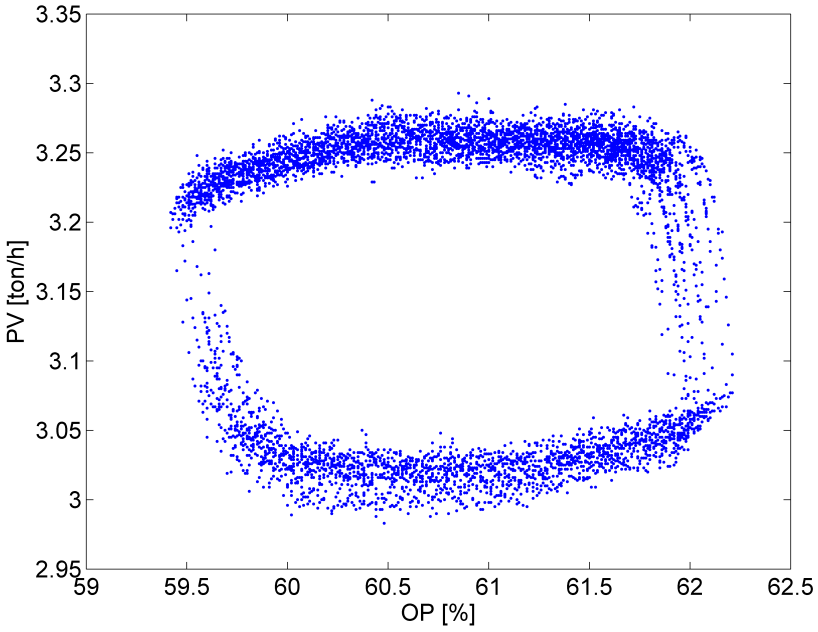

Figure 4.19: Industrial Loop II: experimental behavior MV vs. OP obtained in registration # 9.

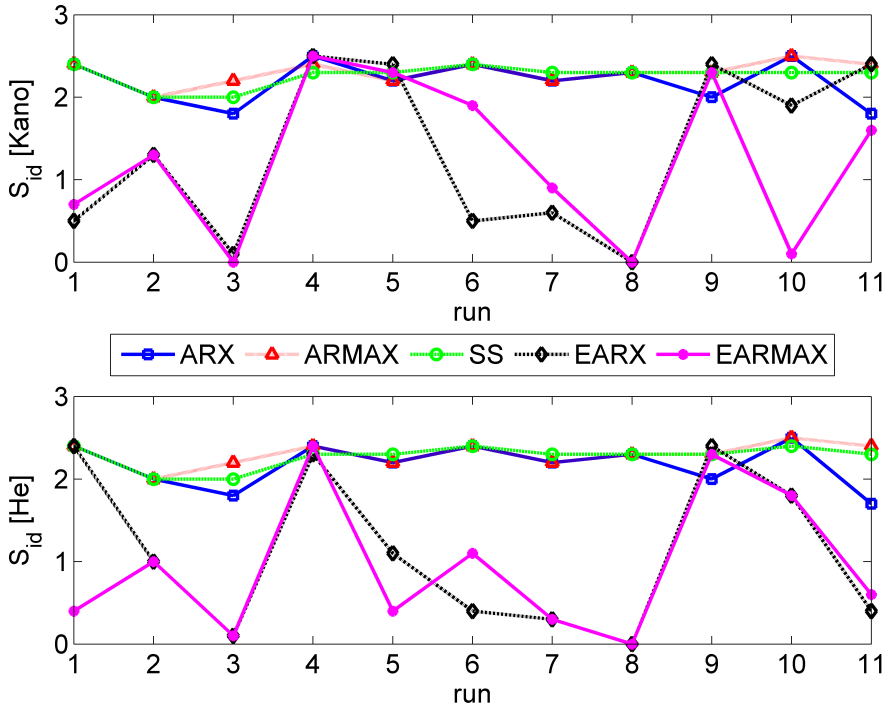

Figure 4.20: Industrial Loop II: Trends of the identified stiction parameter S using different linear models: top, Kano's model; bottom, He's model.

trend. In these two registrations, PV signal does not clearly show a singular frequency of oscillation (cfr. Figure 4.23). An external disturbance might act simultaneously with valve stiction.

The results of this last industrial application are rather similar to the outcomes of Test 3 and 4 in the pilot plant (cfr. Table 4.5 and 4.6), where extended models are to be preferred for the case of simultaneous valve stiction and external disturbance. Non extended models are not sufficiently reliable: inconsistent values of stiction can be estimated. The loop oscillation is not

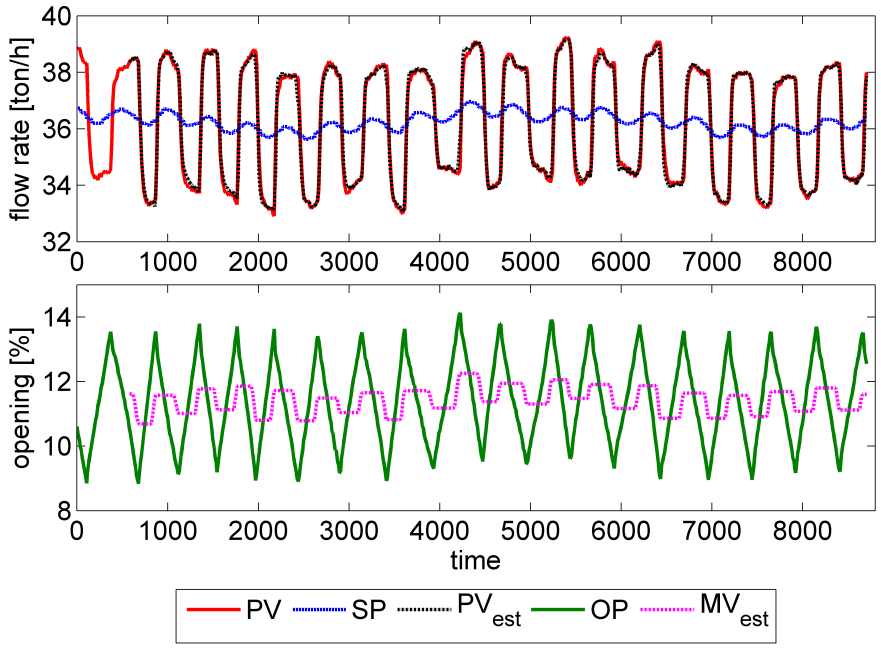

Figure 4.21: Industrial Loop III: time trends for registration # 2.

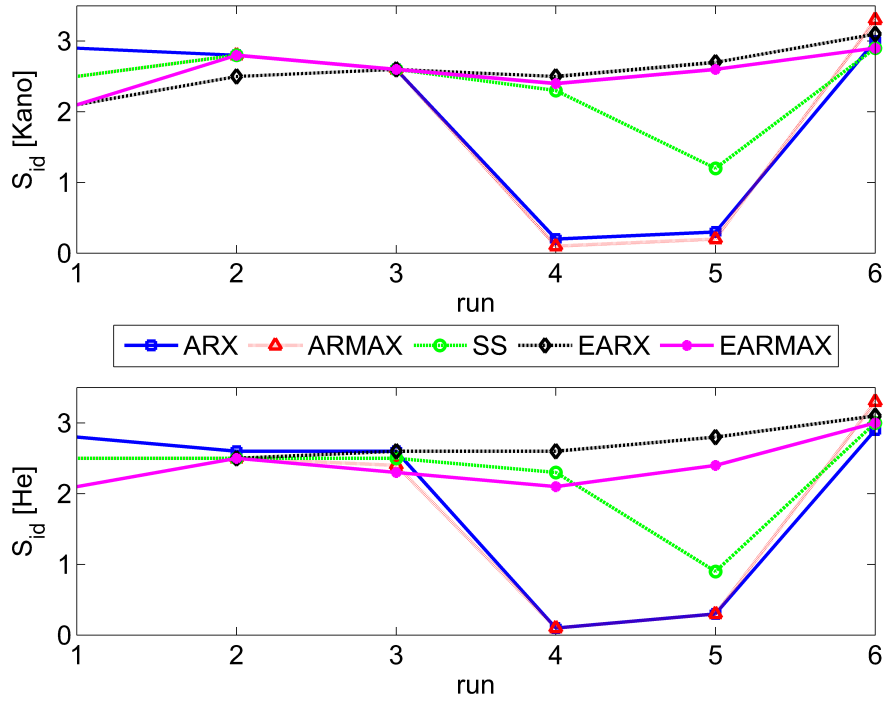

Figure 4.22: Industrial loop III: Trends of the identified stiction parameter S using different linear models: top, Kano's model; bottom, He's model.

due to a singular frequency and external disturbance can alter stiction estimation.

As a general conclusion, the results obtained with industrial data confirm those achieved with pilot plant data. Nonextended models are the best choice when valve stiction is the only source of loop oscillation; extended models are better for the case of simultaneous presence of

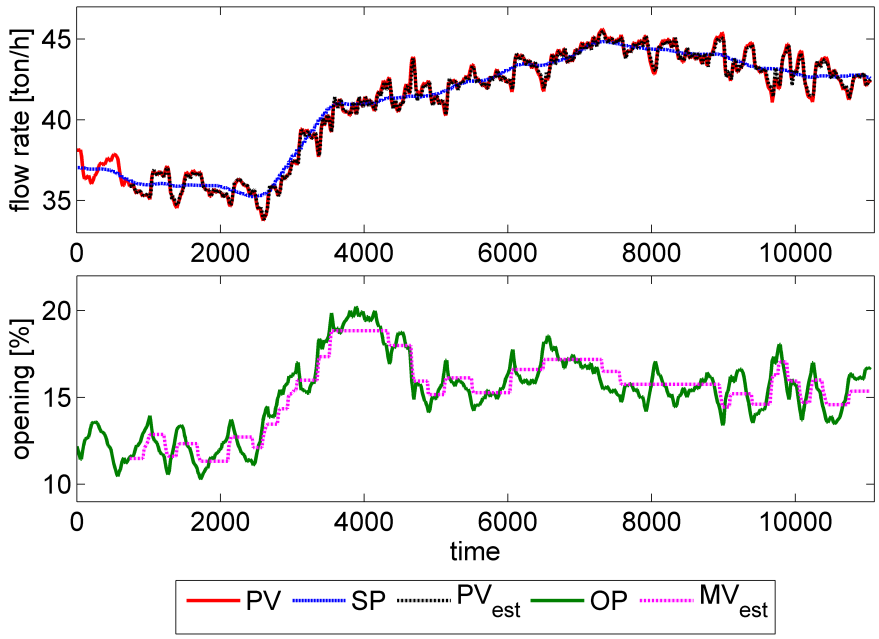

Figure 4.23: Industrial Loop III: time trends for registration # 4.

external disturbances. It is worth noting that for industrial data the presence (or the absence) of non stationary disturbances is not known a priori. Nevertheless, repeated data acquisitions for the same valve can help since they allow one to perform comparable estimates, that is, time evolution of stiction can be followed and eventual anomalous cases can be assessed.

For example, outliers can be ascribed to the presence of disturbances whether non extended models are used, or, on the opposite, the absence of disturbances can be inferred whether inconsistent estimates are obtained when extended models are tested. Anyway, this criterion could be not reasonable when only few acquisitions, or even just one, are available. In such cases a conservative approach should be to test all different models and then emit an average verdict.

Thus, a reliable detection of additional external disturbances seems the definitive solution to this problem. Recent techniques [108, 66] allow one to detect multiple oscillation. Therefore, they could be used as a preliminary step in stiction estimation in order to assess the simultaneous presence of different sources of oscillation (stiction and disturbance) and to direct the choice between simpler and extended process models.

4.6 Conclusions

In this chapter the effect of nonstationary disturbances on estimated amount of stiction has been investigated. For this reason, two different stiction models and five linear models are proposed and compared in order to identify the Hammerstein system of the sticky valve and the process. The identification methods have been validated, firstly, by using closed-loop simulation data in the presence of different faults (low/high stiction, with/without external nonstationary disturbances). Then, practical applicability and significance has been demonstrated through the application of the considered identification methods to data obtained from a pilot plant data and to a large number of industrial data sets.

For the nonlinear part, both Kano's and He's models confirm to be appropriate to model the sticky valve. Simpler models (ARX, ARMAX and SS) appear to be the best choice for linear process dynamics when stiction is the only source of loop oscillation. Extended models (EARX

and EARMAX), incorporating the time varying additive nonstationary disturbance, have one more degree of freedom, i.e. the bias term which is estimated recursively along with the process and stationary noise parameters. When the external disturbance is actually present, extended models prove to be very effective and generate consistent stiction model parameters. As a matter of fact, as verified by different types of industrial data, the extended models ensure a better process identification and a more accurate stiction estimation in the case of significant disturbances acting simultaneously with valve stiction.

Future research directions may include the application of recent techniques aimed at detecting the presence of large external disturbances in order to choose between extended and nonextended models. Furthermore, more complex and flexible stiction models could be used to describe non uniform friction dynamics in order to obtain more consistent estimates when repeated data registrations are analyzed.

Chapter 5

Stiction Compensation

Abstract [1]

A well-established compensation technique to remove oscillations caused by control valve stiction is the two-moves method. However, the actual versions of this technique present major drawbacks, as the long time for implementation and, mostly, some strong assumptions on the valve position in oscillation. A recent version of two-moves compensation has proven to reduce the time of execution. Nevertheless, this method does not allow the control loop to handle set point tracking and disturbance rejection.

The present chapter proposes a revised version of two-moves stiction compensation method, which overcomes previous limitations. This new approach is based on the estimation of controller output associated with the desired valve position at the steady-state, by using the amplitude of oscillation before compensation and through the estimate of valve stiction, obtainable with specific techniques. In this case, fast responses are possible as well as a complete removal of the oscillation. In addition, set point tracking and disturbance rejection are guaranteed, by monitoring the control error and by switching temporarily to a standard PI(D) controller. Simulation examples and applications to a pilot plant show the effectiveness of the proposed method. The effectiveness of the proposed method has been demonstrated through several examples of simulation and subsequently validated by some applications on a pilot plant. In particular, all this study has been conducted during the months of abroad research stay, and the activities of experimentation have been carried out in Laboratory of Process Control at University of Alberta, by Prof. Biao Huang of Department of Chemical and Materials Engineering.

[1] This chapter is based on: [28]: *A Revised Technique of Stiction Compensation for Control Valves*.

5.1 Introduction

Problems in control valve are widely recognized as one of main causes of low performance of base control loops in industrial plants. Well established works [58, 38, 113] indicate that up to 30% of total loops may show persistent oscillation, due to valve problems. The major issues are backlash, hysteresis, dead band, static and dynamic friction, but also variation in the elasticity of the spring, wear or rupture of the membrane, leakage in the air supply system can occur [31].

Among all, static friction (*stiction*) is considered the most common source of sustained oscillations in control loops. Therefore, a major interest has been devoted to its characterization and its diagnosis from routinely acquired data, by means of automatic techniques [85]. Also valve positioners can be the source of other specific causes. For example, in the presence of stiction, too much air is pushed into the actuator causing overshoot that leads to oscillations [145]. Anyway, smart or intelligent positioners can monitor and diagnose valve status and indicate performance deterioration [31].

Repair and maintenance must be considered the only definitive solutions to fix a sticky valve. However, this fact implies to stop the operation of the entire control loop, which is usually practicable only during a plant shutdown. Since the production stops occur generally between every six months and three years, compensation can be a valid alternative to mitigate negative effects of stiction on loop performance.

This chapter is organized as follows. Different stiction compensation methods are briefly revised in Section 5.2. Existing two-moves compensation methods are analyzed and the proposed method is introduced in Section 5.3. Extensive simulation examples are also provided in this section. Section 5.4 illustrates some applications on pilot plant. Finally, conclusions are drawn in Section 5.5.

5.2 Compensation Methods

The most recent stiction compensation methods appeared in the literature are typically data-driven techniques. Firstly, note that two basic approaches - dithering and impulsive control [18] - well-established for stiction compensation in electro-mechanical systems, are not practical in the case of pneumatic valves. This last type of valves, by far the most spread in the process industry, filter such high frequency compensating signals [145]. Afterwards, [92], by using a first-principle stiction model for the valve, estimated the immeasurable states providing a robust control action. However, all parameters of the valve must be known, which is hardly possible in practice.

The knocker compensator proved the first simple viable approach [69]. A predefined signal is added to the controller output (OP) before entering the valve. The knocker produces short pulses with constant amplitude, width, and duration, in the direction of the rate of change of OP. Oscillations on the control variable (PV) are removed at the expense of faster and wider movements of the valve stem, which involve a much higher wear rate. To overcome this disadvantage, [143] suggested some guidelines for the automated choice of the compensation parameters of the knocker. This revised approach, which integrates two stiction detection techniques, proved to reduce PV variability ensuring less aggressive valve movements.

Later, [53] presented a revised knocker compensator based on a supervision layer which analyzes the control error and interacts with the standard PI(D) controller. This integrated strategy shows a lower integral absolute error and even a reduced number of valve movements. Two other simple techniques are the constant reinforcement of [82] and the second method of [71], which is specifically oriented to compensation of backlash (that is, dead band). Both methods prove proficient in removing PV oscillation, but do not yet reduce aggressiveness on the valve.

The controller detuning is another common compensation approach for valve stiction. [15] presented comprehensive rules to detune PI(D) parameters for different process dynamics, by using frequency analysis and harmonic balance. [145] developed also an optimization-based method, which, compared to other approaches, allows significant improvements. However, the need for an exact model of the process, a precise estimate of stiction parameters, and high computational times may limit practical applications. Recently, a model free approach was developed by [17]. This scheme shows to attain both oscillation reduction, and good set point (SP) tracking and disturbance rejection.

The last well-established approach is the so-called two-moves method, which ought to remove oscillations and keep the valve stem (MV) at its steady-state position, by performing at least two moves in opposite directions. The magnitude of the compensating signal should be large enough to exceed stiction and move the valve, but not too large to saturate it.

The aim of this chapter is to introduce a revised version of two-moves method for stiction compensation, which can overcome many limitations of the previous implementations.

5.3 Two-moves Compensation Methods

The existing two-moves methods will be briefly introduced below, in order to highlight their characteristics and to present the features of the proposed method.

5.3.1 The existing methods

The two-moves compensator was introduced by [145]. This first implementation does not need the controller parameters and, most importantly, does not increase the wear rate of the control valve, as the knocker does, since the stem is not constantly forced to move.

The compensating signal (f_k) is added to the output controller (u_c), as in Figure 5.1. The added signal can assume only two values by imposing two consecutive movements to the valve. The first signal moves the stem from its stuck position, according to:

$$f_k(t) = |u_c(t)| + \alpha \cdot d \tag{5.1}$$

and setting:

$$u(t) = u_c(t) + sign\left(\frac{du_c(t)}{dt}\right) \cdot f_k(t) \tag{5.2}$$

where d is the stick band and α is a real number greater than 1. Then, the second signal ought to bring the stem position (u_v) to its steady-state value in order to eliminate the error, by:

$$f_k(t+1) = -u_c(t+1) \tag{5.3}$$

Note that after this second movement, the stem cannot move from the steady-state position since the controller output is canceled by (5.3). The input signal to the valve (u) is thus constant (zero), that is, the controller operates as in open-loop mode.

Anyway, this first version of two-moves method presents several drawbacks, which heavily hinder its on-line implementation. Firstly, accuracy is reduced by assuming the one-parameter (d) model of [149] to predict the valve behavior. Moreover, the steady-state value of valve position (MV_{ss}) is assumed to be known, while MV is not usually measurable in the process plants.

In particular, the method relies on the strong assumption that all measurements are represented by deviation variables and their respective steady-state values are zero [52]. Thus, for the second movement (5.3), it is assumed that $MV = 0$ will make $PV = SP$.

Figure 5.2a verifies this assumption for a generic simulation case. The method proves indeed to be effective only in the case of deviation variables. Just by setting the reference to

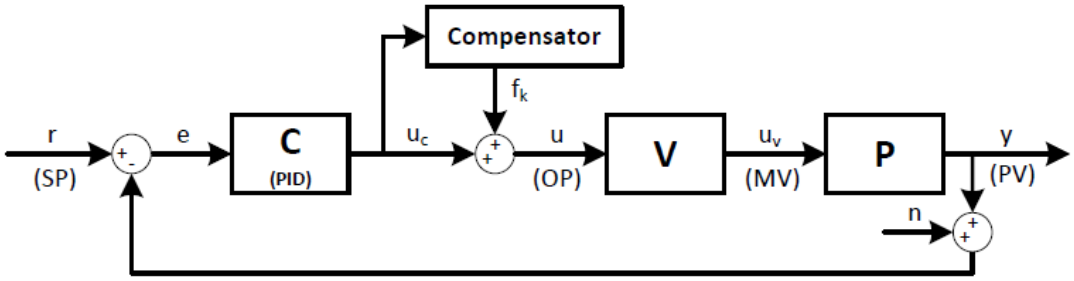

Figure 5.1: Structure of the two-moves compensator [145].

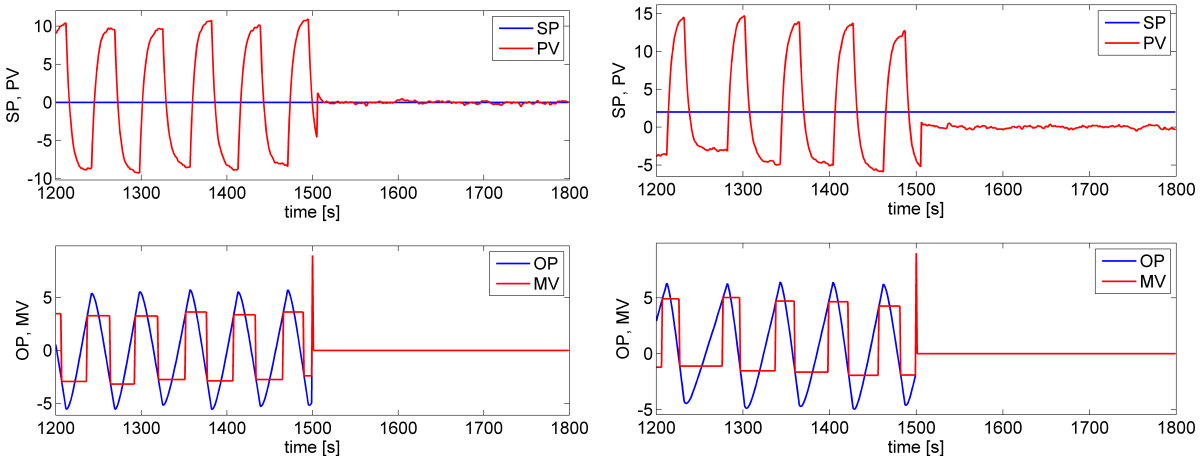

(a) effective for $SP = 0$; **(b)** poor for $SP \neq 0$.

Figure 5.2: Results for the "standard" two-moves compensator.

$SP = 2$, a large steady-state error is obtained (Figure 5.2b). Finally, it is to be noted that, acting partially as in open-loop mode, the method cannot tackle set point changes or disturbances.

Another two-moves method was introduced by [60]. Instead of using an additional compensator block as in Figure 5.1, the traditional PI controller block is modified. This technique seems to achieve faster closed-loop performance and efficient rejection of load disturbances. A fair set point tracking, with a small offset, would be also possible, and a reduction of valve travel is shown.

To overcome previous limitations, [53] revisited the "standard" two-moves approach. Authors showed that assumptions on the knowledge of MV_{ss} that assures $PV = SP$ could be not easily achievable in practice. Significant experimental results on a flow rate control loop of a pilot plant are thus provided. The steady-state value of valve input (OP_{ss}) would be obtained only experimentally and additionally it could be not unique.

Two improved compensation methods are then proposed: the first, consisting of four movements, is sensitive to load disturbances. The second, based on two movements and four states, and especially suited to tackle disturbances, proves more robust. Exact knowledge of the plant model is not required, and loop perturbations (SP changes and disturbances) are handled by monitoring the increase of the control error and by switching back and forth to a standard PI(D) controller. Anyway, both methods can be applied only to self-regulating processes, and the second approach requires similar dynamics between valve and process.

Afterwards, [161] proposed a closed-loop compensation method with the control loop fully operating at the auto mode. A short-time rectangular wave is added to the reference in order to impose two movements to the valve, which so arrives at the desired position. A systematic way to design the parameters of this short-time rectangular wave was also developed.

Very recently, [164] have presented another solution. Three consecutive implementations

of the "standard" two-moves of [145] are used. This technique allows one to estimate online the steady-state value of valve input (OP_{ss}). Therefore, no a priori assumption on MV is required. However, this approach could take a very long time in real applications, since two extra open-loop step responses must be awaited to compute the desired input OP_{ss}.

Simultaneously, the same authors have proposed another implementation which outperforms the three-times two-moves method in terms of velocity and lower amplitude of the response. A practical estimate of the desired valve position MV_{ss} is introduced, thus the value of OP_{ss} to impose to get the steady-state can be computed faster.

In details, the amplitude of oscillation of the controller output before compensation is measured: OP_{min} and OP_{max} are the minimum and maximum value, respectively. Then, the amount of valve stiction is somehow estimated in advance. The objective is to ensure a case that the valve position is bound to stick only at two places. The input OP is changed to guarantee the valve is being moved, but not too large.

In total, the method of [164] imposes six open-loop movements to the valve:

$$OP(kT_s) = \begin{cases} OP_{max} & \text{if} \quad kT_s < T_0 \\ OP_{min} & \text{if} \quad T_0 \leq kT_s < T_0 + T_1 \\ OP_{max} & \text{if} \quad T_0 + T_1 \leq kT_s < T_0 + T_1 + T_2 \\ OP_{min} & \text{if} \quad T_0 + T_1 + T_2 \leq kT_s < T_0 + T_1 + T_2 + T_{sw} \\ OP_{sw} & \text{if} \quad T_0 + T_1 + T_2 + T_{sw} \leq kT_s < T_0 + T_1 + T_2 + T_{sw} + T_h \\ OP_{ss} & \text{otherwise} \end{cases} \tag{5.4}$$

where $T_0 = t_0 + \theta_0$, and T_s is the sampling time (see Figure 5.3). When OP is increasing, close to its peak, the controller is switched into open-loop mode at time t_0, and OP is set to OP_{max} to make the valve move away from the current sticky position. Then, after time interval θ_0, OP is enforced in the opposite direction to OP_{min}. Afterwards, OP switches once again between these two extreme values, for times T_1 and T_2.

Note that T_1 corresponds to the time interval between the second-last peak and the valley, and T_2 corresponds to the time interval between the valley and the last peak, both measured on the oscillation of OP before the compensation starts. Then, after time interval T_{sw}, OP is switched to:

$$OP_{sw} = OP_{ss} - \beta_{sw}(OP_{max} - OP_{min}) \tag{5.5}$$

where T_{sw} does not have to be specific, but only to ensure that PV has changed direction. Likewise, β_{sw} is a coefficient (≥ 1) that enables the valve to overcome the stiction band.

Finally, after time interval T_h, OP is held to a value so that PV is expected to approach SP at the steady-state. The desired steady-state valve position is estimated, according to:

$$MV_{ss} = \frac{OP_{min}T_1 + OP_{max}T_2}{T_1 + T_2} + f_d \frac{T_1 - T_2}{T_1 + T_2} \tag{5.6}$$

If OP is increased first and decreased afterwards, its steady-state value can be computed, by making use of He's stiction model [76], as following:

$$OP_{ss} = MV_{ss} + f_d \tag{5.7}$$

where f_d is the dynamic friction in the valve. In reverse, if the method is implemented in opposite direction, i.e., OP is decreased first and increased afterwards:

$$OP_{ss} = MV_{ss} - f_d \tag{5.8}$$

The interval T_h should be as small as possible, to avoid that PV deviates much from SP value. As seen in Figure 5.3, the method is indeed able to bring the PV close to its reference. However, being a fully open-loop approach, set point tracking and disturbance rejection are still not ensured, as in the case of the "standard" version of [145].

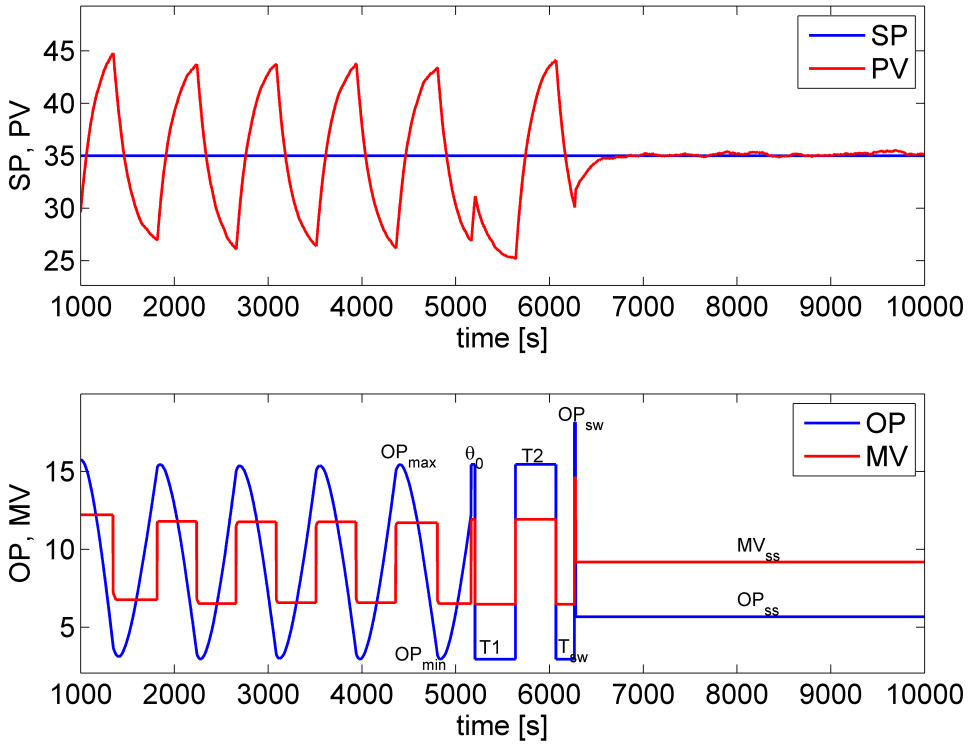

Figure 5.3: Results for the compensator of [164].

5.3.2 The proposed method

The proposed compensation method is based on the approach of [164], by developing some practical simplifications. Only four open-loop movements are now required:

$$OP(kT_s) = \begin{cases} OP_{max} & \text{if} \quad kT_s < T_0 \\ OP_{min} & \text{if} \quad T_0 \leq kT_s < T_0 + T_{sw} \\ OP_{sw} & \text{if} \quad T_0 + T_{sw} \leq kT_s < T_0 + T_{sw} + T_h \\ OP_{ss} & \text{otherwise} \end{cases} \tag{5.9}$$

where $T_0 = t_0 + \theta_0$, and T_s is the sampling time (see Figure 5.4). The first two moves are as in (5.4). When OP is increasing, close to its peak, the controller is switched into open-loop mode at time t_0, and OP is set to OP_{max}. Then, after time interval θ_0, OP is enforced to OP_{min}. Now it comes to the difference. Note that, if one chooses to impose symmetrical movements to OP, that is $T_1 = T_2$, (5.6) can be simplified, resulting:

$$MV_{ss} = \frac{OP_{min} + OP_{max}}{2} \tag{5.10}$$

Therefore, the steady-state valve position is now estimated according to (5.10). This relation is consistent with the fact that, when a "standard" data-driven stiction model is used (e.g., [76, 43]), the valve position typically oscillates between the two extremes of the input signal OP. Then, equations (5.5) and (5.7 or 5.8) are still employed to directly compute OP_{sw} and OP_{ss}, which requires an estimate of stiction parameter f_d. Note also that the time interval T_{sw} does not need to be specific. A safe choice is $T_{sw} \approx T_{op}$, where T_{op} is the average half-period of oscillation of OP. In this case too T_h should be as short as possible.

The results of Figures 5.3 and 5.4 have been obtained in simulation by using the same parameters [164], so as to allow a direct comparison between different methods. The process

model is a first order plus time delay (FOPTD):

$$P(s) = \frac{3.8163}{156.46\,s+1} e^{-2.5s} \tag{5.11}$$

The PI controller is:

$$C(s) = 0.25\left(1 + \frac{1}{50\,s}\right) \tag{5.12}$$

Valve stiction is described by Chen's model [43], which is an extension of He's model, setting the following parameters: $f_s = 8.4$, $f_d = 3.5243$. A white noise with zero-mean and standard deviation $\sigma = 0.01$ is added. For both compensators, the following parameters are used: $T_s = 0.5$, $\theta_0 = 40$, $T_{sw} = 200$ and $T_h = 10$ seconds, and $\beta_{sw} = 1$.

Note that the compensator of [164] starts at $t_0 = 5165$ and sets the steady-state at time $t_{ss} = 6278$, by imposing $OP_{ss} = 5.668$, which moves the valve to $MV_{ss} = 9.192$ (see Figure 5.3). The mean steady-state error results: $e_{ss} = SP - PV_{ss} = -0.157$. The two time intervals last $T_1 = 420$ and $T_2 = 434$ seconds, respectively.

On the contrary, the proposed compensator starts at time $t_0 = 5132$ and stops already at time $t_{ss} = 5382$, for a duration of only 250 seconds with a saving of around 850 (see Figure 5.4). The steady-state valve input and output are $OP_{ss} = 5.665$ and $MV_{ss} = 9.189$, respectively. The mean steady-state error results $e_{ss} = -0.023$. Note also that $T_{sw} \simeq T_{op}/2 \simeq 430/2$ seconds.

Overall, by using the proposed method, two valve movements can be avoided, and a significant time (equal to $T_1 + T_2$) can be saved. Therefore, the whole compensation procedure proves to be much simpler and faster than the one of [164]. Note that the previous one is just a numerical example. However, the same general result can be obtained by using different values of process, controller, and stiction parameters.

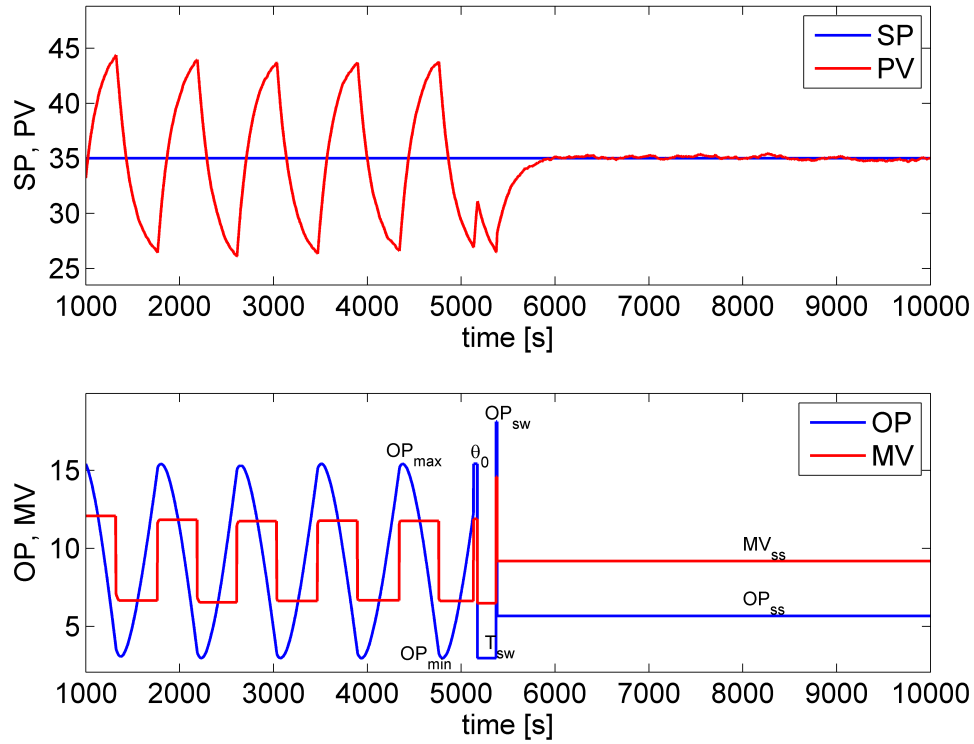

Figure 5.4: Results for the proposed compensator.

Another improvement of the proposed compensator with respect to the implementation of [164] is the ability to address loop perturbations. In particular, SP changes and load distur-

bances can be tackled by monitoring the control error ($e = SP - PV$), similarly to what proposed by [52].

The compensating signal (u_k) is not added to the controller output (u_c), but the valve input (u) is switched between these two signals (see Figure 5.5). When sustained oscillations are detected, the compensator is activated by using the moves in (5.9). Once the steady-state is reached, if somehow PV diverges and the error passes a predetermined threshold (e_{lim}), or if a SP change is detected, the loop is switched back to the standard PI(D) controller. Then, once the oscillation has returned stable, a certain number of periods are counted before reactivating the compensator. Note that when the compensator takes control, PI(D) controller tracks the valve input, in order to avoid abrupt changes in OP and PV once the control is switched again.

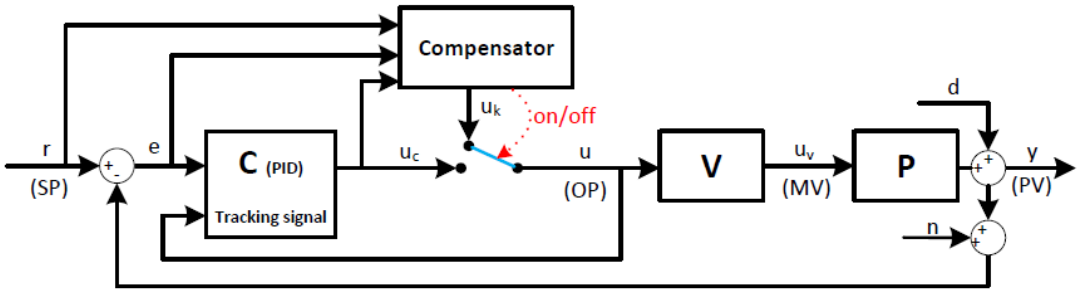

Figure 5.5: Structure of the proposed compensator.

Figure 5.6 shows the behavior of the proposed compensator in the presence of such perturbations. All the parameters are set as in the case of Figure 5.4, except for the stiction parameters: $f_s = 5$, $f_d = 2$. The compensation is activated in four different occasions (marked as black spots in Figure 5.6), at the time instants $t_{on} = 5714$, 14220, 24220, and 34290. Two set point changes occur at the time instants 10000 and 20000. A step disturbance of amplitude -0.05 affects the output at time 30000. The error threshold is set to $e_{lim} = 1.5\,A_{PV}$, where A_{PV} is the average amplitude of oscillation of PV before the start of compensation.

The extremes of oscillation of OP are recomputed each time to get the desired steady-state valve position MV_{ss} by using (5.10). As a set point change is detected or the threshold is violated, the PI controller is resumed. Then, compensation is renewed and removes again the oscillation. In this case, 10 half-periods of sustained oscillation are awaited every time before the compensation restarts.

Therefore, the proposed implementation outperforms previous two-moves methods in the presence of loop perturbations. Note also that it requires only easily-tunable parameters, unlike other anyway appealing solutions [52, 17].

5.3.3 Sensitivity analysis

For a more complete evaluation of performance achievable by the proposed compensator, a sensitivity analysis has been carried out. Some results are briefly reported below.

Different process and controller parameters. A different control loop is simulated: the process model is a FOPTD with $P(s) = \frac{2}{100\,s+1}e^{-5s}$, while the controller is now a PI with $C(s) = 0.75\left(1 + \frac{1}{25\,s}\right)$. The stiction parameters of Chen's model are $f_s = 5$, $f_d = 2$. As can be seen from (5.7), (5.8), and (5.10), the design of the proposed four moves (5.9) does not depend on the process and controller parameters, therefore they cannot influence the compensation results.

Figure 5.7 shows that the compensator is indeed able to bring PV close to the reference and move the stem to its correct steady-state value ($MV_{ss} = 12.54$). The mean steady-state error

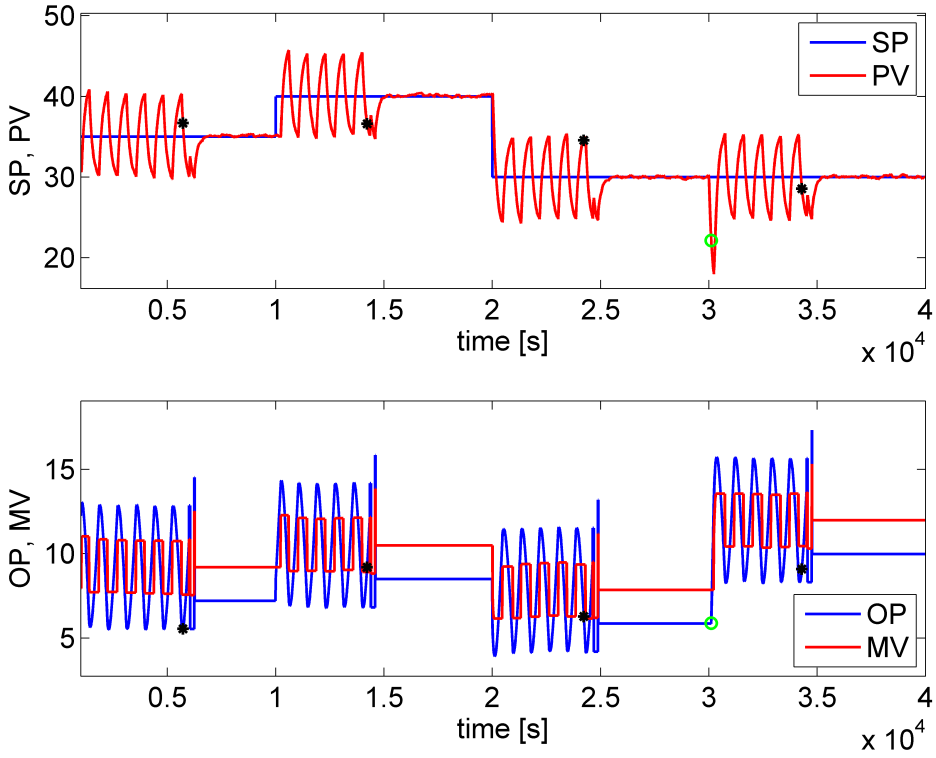

Figure 5.6: Stiction compensation in the case of perturbations.

is $e_{ss} = -0.062$. Thus the compensation is not affected by the specific process and controller parameters.

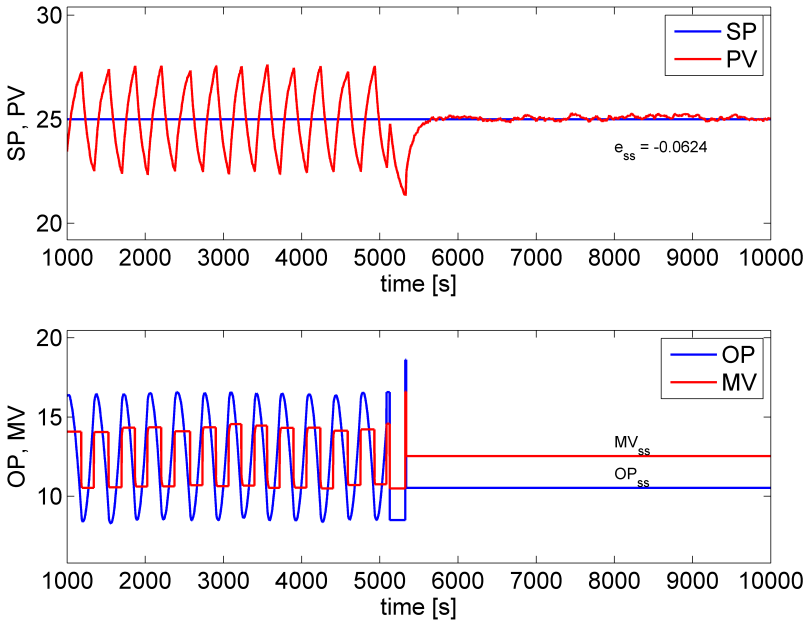

Figure 5.7: Results with different process and controller parameters.

Note that the compensator has good performance also for other types of controllers and self-regulating processes. However, it does not work for the case of pure integral processes, as level control loops, since no open-loop steady-state value for PV is permissible.

To this aim, the case of control loop formed by a process with IPTD model $P(s) = \frac{1}{50\,s}e^{-5s}$,

and a PI controller with $C(s) = 0.25\left(1 + \frac{1}{50\,s}\right)$ is considered. The stiction parameters of Chen's model are $f_s = 5$, $f_d = 2$. Figure 5.8 shows that after the compensator is activated and once that OP is fixed and MV is steady, PV keeps on increasing, that is, the level is out of control.

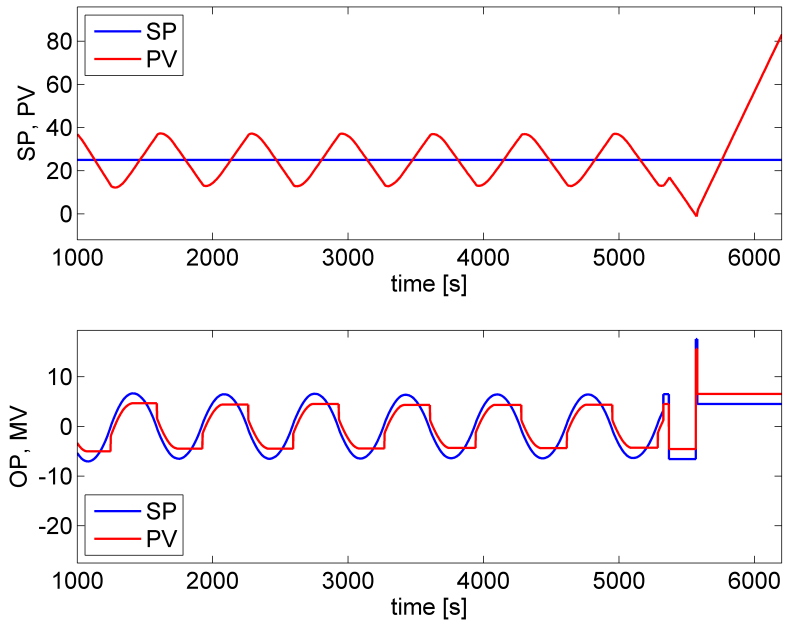

Figure 5.8: Ineffective results for a pure integral process.

Uncertainty in stiction value f_d. On the opposite, it is important to state that the proposed method, as the one introduced by [164], is strictly dependent on the estimate of stiction parameter f_d, as seen in (5.7) and (5.8). Note that stiction parameters can be obtained in advance through quantification methods, as the ones presented in Chapter 4. In addition, an accurate stiction detection is assumed a priori in this approach, since the compensation procedure should not start in the case that oscillations are not due exclusively to stiction. Anyway, it is important to stress that the proposed method is not based on the knowledge of MV.

Here the effect of an incorrect stiction estimate on the compensator performance is analyzed (see Figure 5.9). Valve is simulated using a dynamic friction of $f_d = 2$, while the estimated value for designing the steady-state input (OP_{ss}) is $\hat{f}_d = 1$, that is, a 50% mismatch. The other parameters are set as in the previous simulation case (of FOPTD type). The compensator cannot bring the PV to the reference, and the mean steady-state error is quite high: $e_{ss} = -1.919$. Note that the desired steady-state valve position, estimated from (5.10), is anyway accurate: $MV_{ss} = 12.48$. Nevertheless, due to the wrong estimate of f_d, the steady-state valve input is $OP_{ss} = 11.48$ and the actual final position is higher: $MV_{ss} = 13.48$. The correct input value ($\simeq 10.5$) should have moved the valve to $MV_{ss} \simeq 12.5$, as shown in Figure 5.7.

Effect of the noise level. The magnitude of the noise added to the control feedback is also studied. The same system of Figure 5.7 is considered, and 100 Monte Carlo simulations have been performed for six different levels of white noise. The average absolute value of the control error obtained at steady-state ($\overline{|e|}_{ss}$) is computed for each noise level. Table 5.1 summarizes the complete results. It can be observed that an acceptable stiction compensation is still possible for a significant level of noise.

It is also worth noticing that the estimate of the extremes of oscillation of OP, computed before the onset of compensation, can be a key factor for a good performance, as seen in (5.10). Extensive simulations have shown that the best outcomes are possible by considering the mean

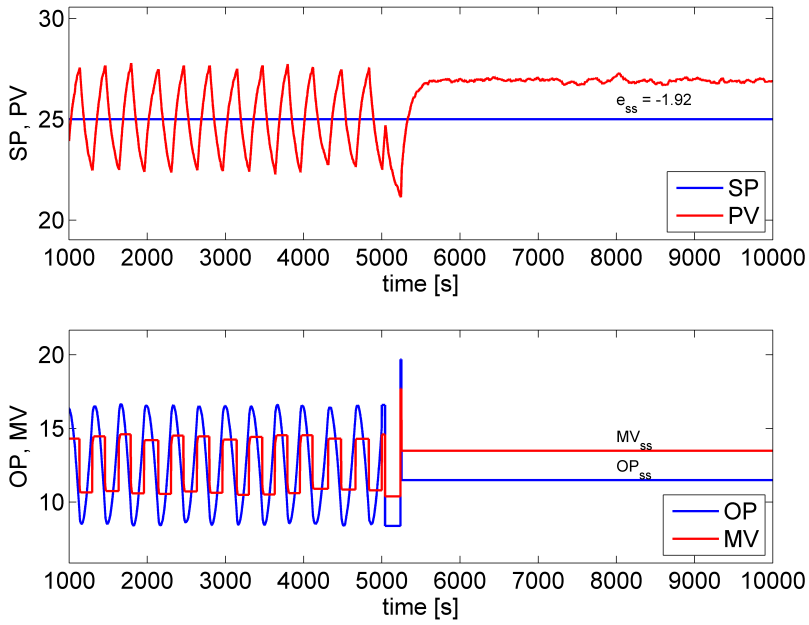

Figure 5.9: Results with 50% mismatch in stiction parameter f_d.

values of the extremes ($\overline{OP}_{max}$, $\overline{OP}_{min}$). However, only the last two extremes of OP could be considered in the case of low level noise. Table 5.1 shows the results obtained with these two different approaches. Figure 5.10 shows the results for one of these MC simulations for a case of $\sigma = 0.05$.

Table 5.1: Impact of noise on stiction compensation.

Noise Level (σ)	Average steady-state error ($\overline{\lvert e \rvert}_{ss}$)	
	mean extremes of OP	last 2 extremes of OP
0	0.001	0.027
0.01	0.035	0.097
0.02	0.066	0.199
0.05	0.160	0.471
0.1	0.331	0.946
0.2	0.584	1.882

Possible limitations. Other possible limitations of the proposed method are listed below. Poor performance could be obtained for the hard case of inhomogeneous stiction. However, when stiction-induced limit cycles arise, the valve operates generally in a small range. Therefore, under closed loop conditions, stiction can reasonably be assumed to be independent of the stem position. Note also that, after the valve is brought to its steady-state position, the minimum time needed for the PV to reach the reference is equal to the settling time of the process, which could be also very long (temperature control loops). Nevertheless, these two issues are common to other open-loop methods [145, 164].

Finally, the proposed method might show poor performance in the cases where perturbations change continuously, e.g. control loops in cascade configuration or in the presence of non-stationary disturbances, and also when perturbations arise exactly during the execution of the compensating moves (5.9).

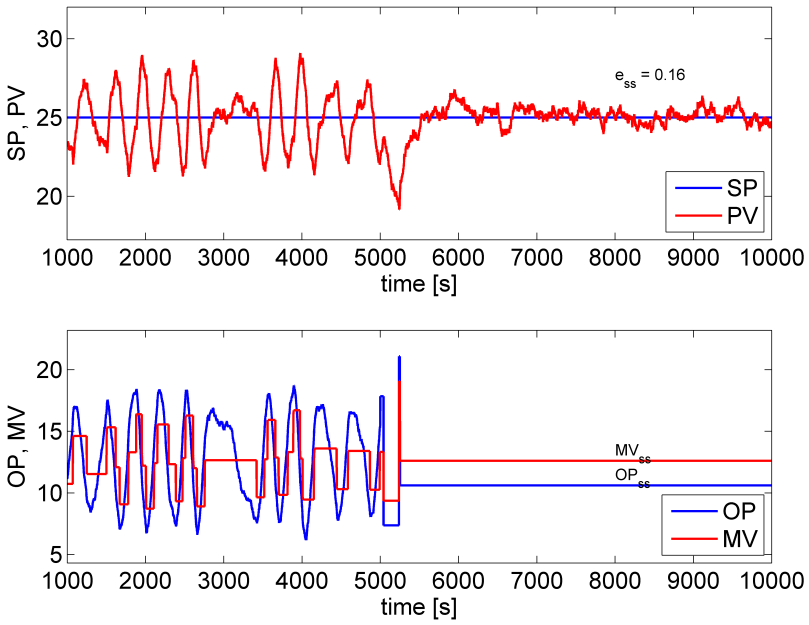

Figure 5.10: Results for a noisy control loop.

5.4 Application to Pilot Plant

The proposed compensation method is then implemented in Laboratory of Process Control at University of Alberta, by Prof. Biao Huang of Department of Chemical and Materials Engineering. Figure 5.11 shows a picture and a schematic of the laboratory facility. The flow rate control loop for Tank1 is studied with a sampling time $T_s = 1$ second.

As shown in Figure 5.12, the compensator is inserted into a MATLAB-Simulink interface between the OPC server and the pilot plant. Valve stiction is introduced by passing the output of a PI controller through the Chen's model before driving the control valve.

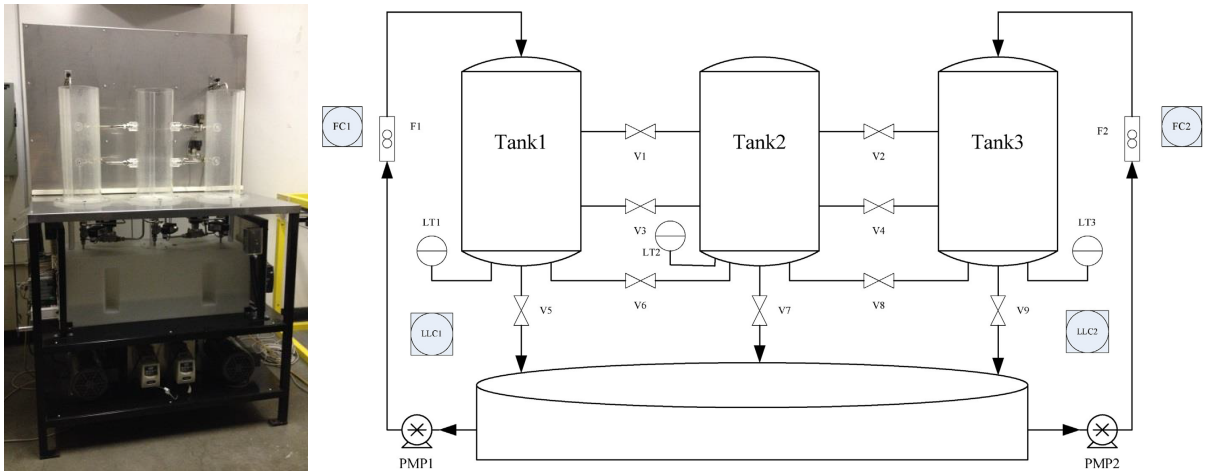

(a) The facility **(b)** The process schematic

Figure 5.11: The pilot plant (called *Hybrid Tank*).

Numerous experiments have been run in order to test the proposed compensation algorithm. Here below only two examples of application are presented. In both cases, controller parameters are set to $C(s) = 9\left(1 + \frac{1}{1.8\,s}\right)$, and stiction parameters are $f_s = 7$, $f_d = 3$.

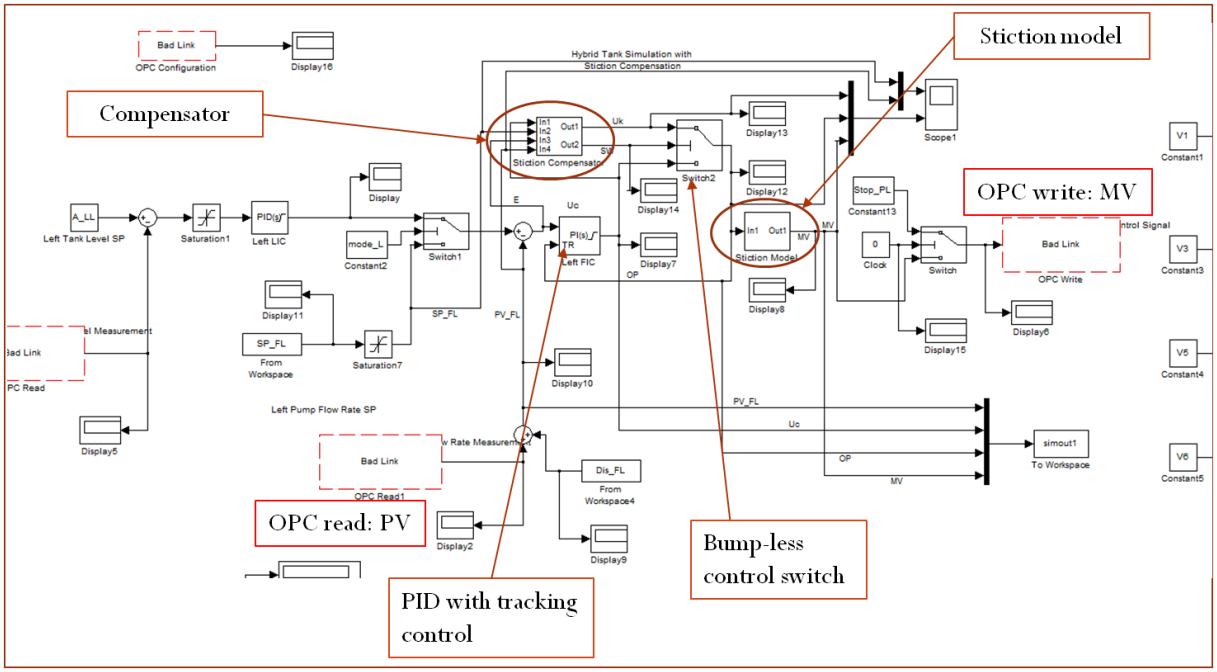

Figure 5.12: The SIMULINK control loop of Tank1.

Test #1: with no additional perturbations. In this first case, no set point and no external disturbance enters the control loop. As shown in Figure 5.13, clear waves of triangular shape are registered on OP, waves of rectangular shape appear on MV and PV. The compensator is activated at time 250 seconds, and the oscillation on PV is removed in about 45 seconds by means of four precise movements. After 300 seconds, the valve input is set to $OP_{ss} = 45\%$ and the valve is kept to its steady position ($MV_{ss} = 48\%$); in the meanwhile, the flow rate reaches in open-loop its reference ($SP = 4l/min$). Note that Figure 5.13 shows also the time trend of u_c, the output signal of PI controller.

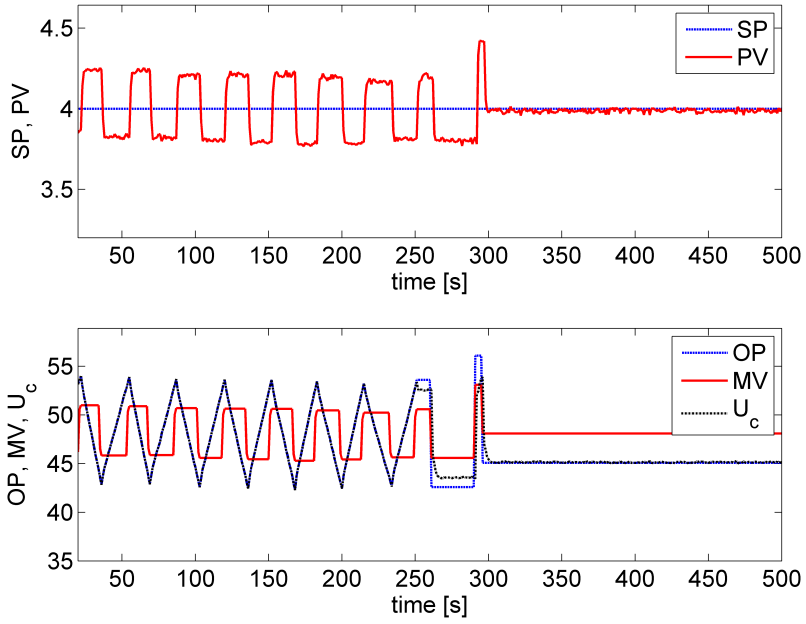

Figure 5.13: Test #1: stiction compensation in the pilot plant.

Test #2: with additional perturbations. In this second example, two set point changes occur at time instants 600 and 1200 seconds. A step disturbance of amplitude $-1\ l/min$ affects the output at time 1800. Figure 5.14 shows the behavior the proposed algorithm. The compensator is activated in four different occasions, and brings each time the flow rate to the correct reference. When perturbations occur the PI controller is resumed by means of the bumpless control switch, as seen in Figures 5.5 and 5.12. The error threshold is set to $e_{lim} = 3\,A_{PV}$, and a time equal to 20 half-periods of sustained oscillation is awaited before each compensation restarts.

Thus, good performances first obtained in simulation has been confirmed on pilot plant data. Further results are omitted for the sake of space limits.

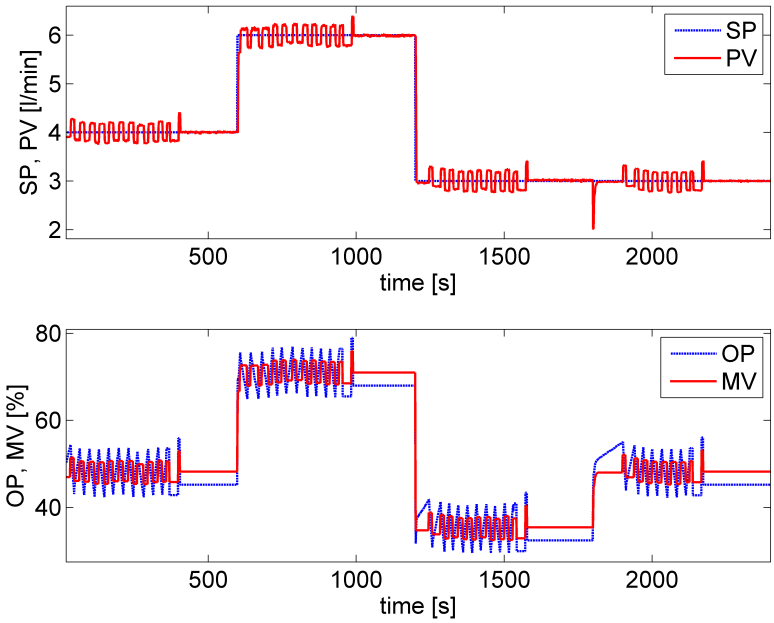

Figure 5.14: Test #2: stiction compensation in the pilot plant.

5.5 Conclusions

In this chapter, a new compensation method for oscillations caused by stiction in control valve is proposed. The technique is based on an improved version of the two-moves method, which is proved to overcome many previous limitations. Four movements in open-loop operation are employed, by causing faster responses as well as complete removal of the oscillation. The control error is monitored to switch to standard PI(D) controller in the case of set point change and in order to reject external disturbances.

The proposed method can be applied in practice without specific assumptions on the valve position and without particular tuning parameters. Anyway, a reliable detection and a solid estimation of stiction are important prerequisites. Numerous simulation examples and pilot plant applications are used to demonstrate the effectiveness of the new method. Our future work might concern implementation of the compensation algorithm on several industrial control loops, and efforts to overcome residual limitations.

Chapter 6

Smart Diagnosis

Abstract [1]

This chapter presents main features of the *advanced PCU*, a performance monitoring system, which, in addition to variables normally registered in industrial plants - controller output (OP), controlled variable (PV) and set-point (SP) - makes use of additional variables made available by intelligent instrumentations and field bus communication systems.

Experimental runs on a pilot plant scale have been carried out in order to introduce different types of valve malfunctions and to define suitable indices (KPI) able to diagnose them. Subsequently, threshold values for the indices have been calibrated and a logic has been developed to assign different performance grades. It is shown how the Travel Deviation allows specific evaluation of valve status and to detect different causes of malfunctioning.

The same logic is implemented in an advanced release of an existing performance monitoring system and advantages in the accuracy of diagnosis are shown. Finally the system has been successfully validated by on line implementation for control loops assessment of an industrial power plant.

[1] This chapter is based on: [31]: *Advanced Diagnosis of Control Loops: Experimentation on Pilot Plant and Validation on Industrial Scale*.

6.1 Introduction

Control loop diagnostics is widely recognized as an important aspect to face in order to improve plant efficiency and then competitiveness; in recent years quite a significant research effort has been devoted to this topics. Usually, control loops assessment and diagnosis is performed by means of the 3 variables which are more commonly acquired in industrial plants, that is: Set Point (SP), Controlled Variable (PV) and Controller Output (OP). The objective is to have a prompt diagnosis of the onset of low performance condition and to be able to distinguish among different causes. Main distinction is among external perturbations, controller tuning and valve problems: for this reason techniques able to characterize different sources have been proposed.

The significance of loop oscillations can be evaluated by means of the technique proposed by Hägglund (known as ODT) [67], by using zero crossings of the error signal ($e = PV - SP$) and calculating the integrated absolute error (IAE) between successive zero crossings. A first characterization of oscillations can be performed by means of Auto Correlation Function (ACF) of Thornhill et al. [157]. Advances and new directions in oscillation detection and diagnosis has been widely reviewed in Thornhill and Horch [156]. Once tuning is detected as cause of low performance in the loop, model free retuning techniques are quite appealing: see for instance Shamsuzzoha and Skogestad [128]. Recently Marchetti et al. [102] proposed a retuning technique for cascade loops based on oscillation trends, which does not require any additional information on the process.

The state of the art and advanced methods for the diagnosis of valve stiction (static-friction) has recently found a comprehensive compendium in the book edited by Jelali and Huang [85], where eight different techniques are illustrated and compared on a benchmark of industrial data. The possibility of diagnosing stiction is included in several closed loop performance monitoring (CLPM) systems, proposed nowadays by major software houses.

Being the valve position (MV) usually not available, a still open problem is the quantification of stiction, by predicting MV from PV and OP values. Quite a lot of techniques appear in literature in the last years: Choudhury et al. [50], Jelali [84], Karra and Karim [90], Farenzena and Trierweiler [61]. The reliability of these techniques is still under exploration, as showed by Qi and Huang [115], Bacci di Capaci and Scali [22].

In new design plants, the adoption of intelligent instrumentation, valve positioner and field bus communication systems increases the number of variables which can be acquired and analyzed by the monitoring system. This fact enlarges the potentialities of performing a more precise diagnosis of valve problems. Causes of malfunctioning in pneumatic valves (see Figure 2.3a), by far the most used in process control, are not only limited to the presence of stiction (and related problems, as deadband, hysteresis, backslash), but can also include other causes (changes in spring elasticity, membrane wear or rupture, leakage in the air supply system).

The positioner itself can also be the source of other specific faults which can upset loop performance. All these malfunctions require specific actions to be counteracted by operators. Therefore it is very important to be able to diagnose and separate different sources. Surprising enough, this topic has not yet been largely addressed in literature; one of the few works is given by Huang and Yu [81]. Other references can be found in Section 2.7.

In the last years, ENEL (the largest Italian Electric company) started a project of advanced diagnostics, in order to enhance the possibility of accurate diagnosis of these sources of perturbations. The starting point was the performance monitoring system, already developed at CPCLab of the University of Pisa, based on the 3 classical variables (SP, PV, OP) and denominated *PCU* (Plant Check Up, [123]).

The first step of this project was devoted to an experimental characterization of anomalies in control valves and was oriented to a fine diagnosis based on additional variables available by intelligent instrumentation. First results are reported in [126]. This chapter includes the con-

tinuation of this activity, which after experimentation and check, has lead to a new architecture of the performance monitoring system, based on 4 or 6 available measurements.

This chapter has the following structure: Section 6.2 describes the experimental plant (pilot scale), its instrumentation and types of reproduced anomalies; Section 6.3 presents the definition of performance indices and the calibration of threshold values; Section 6.4 illustrates the logics of the diagnosis system and a comparison of verdicts based on different variables; Section 6.5 presents results for industrial loops (power plant); conclusions and next steps are reported in Section 6.6.

6.2 The Experimental Pilot Scale Plant

The Idrolab plant is a pilot scale experimental facility having the general scope of testing new technology to improve efficiency and environmental compatibility of thermoelectric power plants. The specific project regards the development of a new architecture of the automatic system for loops performance monitoring and fault diagnosis (*PCU*). Experiments were carried out on the hydraulic module (M1) of the plant, which allows water recirculation between two drums [126] (see Figure 6.1).

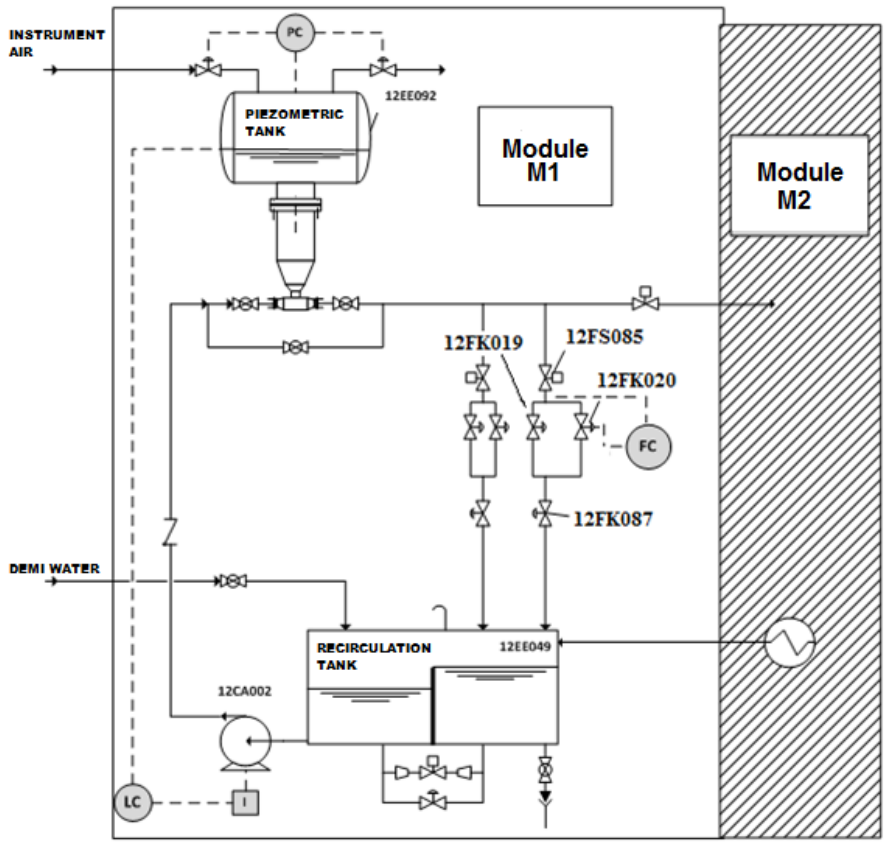

Figure 6.1: The pilot plant Idrolab.

The presence of bypass lines equipped with control valves and the possibility of acting on pressure and level of the higher drum, allows one to carry out experiments in a wide range of operating conditions. By Fieldbus Foundation communication protocol, the control system can collect data from many "intelligent" instruments installed, among which the two pneumatic actuators under test: Fisher Rosemount - DVC5020F type and ABB - TZID type (see Figure 6.2a). The pneumatic actuators are coupled to spherical valves which control the water flow rate in recirculation lines.

The positioner of the pneumatic valve acts as an inner control loop on the valve position

(a) Actuator, valve and positioner **(b)** Modified actuator

Figure 6.2: Pictures of the control valve (DVC5020F type).

and allows one to speed up the response of the valve. A schematic representation of a Flow Control (FC) loop with positioner is reported in Figure 6.3.

In addition to SP, OP and PV, commonly available in an industrial FC loop (C_e), DS, P, MV represent the variables made available by the positioner (for a total of 6 variables). The Drive Signal (DS), is the electric signal generated by the inner controller (C_i) which, through the i/p converter, generates the pressure signal (P) acting on valve membrane (P_i), thus determining the position of the valve stem (MV, also called Valve Travel); P_e indicates the process relating MV with PV.

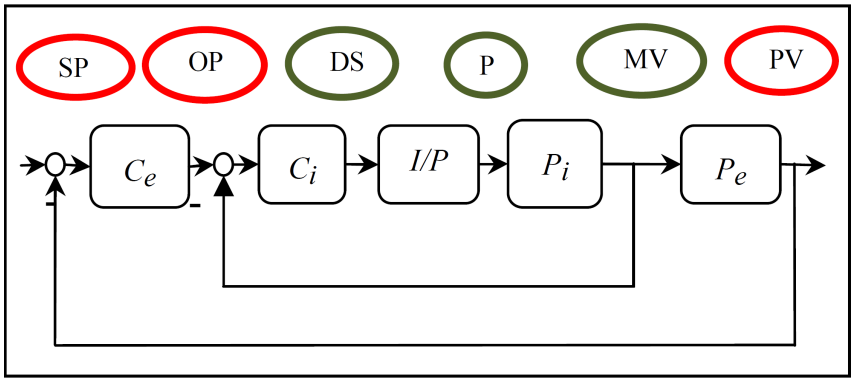

Figure 6.3: Block diagram of a FC loop with positioner.

Different problems have been reproduced in experimental valves by means of a modular item mounted on top of them, as shown in Figure 6.2b. This equipment has allowed one to reproduce common anomalies: static and dynamic friction, air leakage and i/p converter malfunction. Further details about description of valve problems and the ways these anomalies were reproduced are reported in [126].

In this second stage of the project, attention was focused on common sources of oscillation in control loops and on common causes of anomaly in industrial valves. The basic idea is to develop the enhanced system by taking into account indications coming from additional variables made available by intelligent instrumentation, thus originating the improved PCU_N,

with up to $N = 6$ variables.

Many experiments were performed in the allowed operating range of the valves and of perturbations. Experimental runs were carried out with the valve operating in Travel Mode and in Flow Control Mode [126]. In Flow Control Mode, the FC loop acts directly on the valve or the Level Control loop acts as primary loop on FC. Runs were carried out by introducing valve anomalies or loop perturbations in the system operating at steady state (no Set Point changes) and repeated applying step SP changes of the flow rate.

Table 6.1 reports 6 typologies of experiments. They can be considered representative of general behavior of the system, thus allowing to draw general conclusions. The nominal case N does not present any valve malfunction or loop perturbation. In case D there is an external loop disturbance. In the other cases, malfunctions related to stiction, dynamic friction (jamming), air leakage and i/p converter clogging have been reproduced in the actuator.

Table 6.1: List of the cases of study.

Case		Description
N	nominal	no valve anomalies or external disturbance
D	disturbance	external perturbation and no valve anomalies
J	jamming	internal dynamics slowed down
S	stiction	valve static friction
L	leakage	imposed on the air circuit tools
M	i/p converter malfunction	nozzle clogging

Different responses in terms of loop and actuator variables (OP, PV, MV, DS, P) to SP change were characterized for the nominal cases and for the faulty conditions [126]. The availability of MV allows one to introduce a key variable: Travel Deviation, which is defined as the difference between real and desired stem position ($TD = MV - OP$). TD is the most immediate variable for a first distinction between different phenomena. Typical trends of TD in the nominal case and in the presence of different types of malfunction are shown in Figure 6.4.

The following preliminary qualitative observations can be formulated.

- In the nominal case TD has a mean value close to zero and has only low peaks in correspondence with SP variations. An acceptability band for nominal conditions can be easily set: TD_{lim} (in red in Figure 6.4).
- Dynamic friction (jamming) shows to be very similar to nominal case and seems difficult to detect.
- Air leakage determines a clear downward shift of the mean value of TD, which lays for a long time outside its acceptability band.
- Malfunction (clogging) of i/p converter shows a quite similar behavior to air leakage.
- Stiction produces persistent oscillations in TD, even when the SP is constant; TD_{lim} is often trespassed.
- TD oscillations may also be caused by the presence of periodic disturbances (or aggressive tuning controller), but in this case, amplitude peaks are quite small because MV follows OP: this allows one to exclude the presence of stiction.

It is worth to say that these observations are fairly general because they involve malfunctioning of single components of the control loop (in particular valves and pneumatic actuators) and therefore their appearance do not depend on the different characteristics of the process (chemical or physical nature).

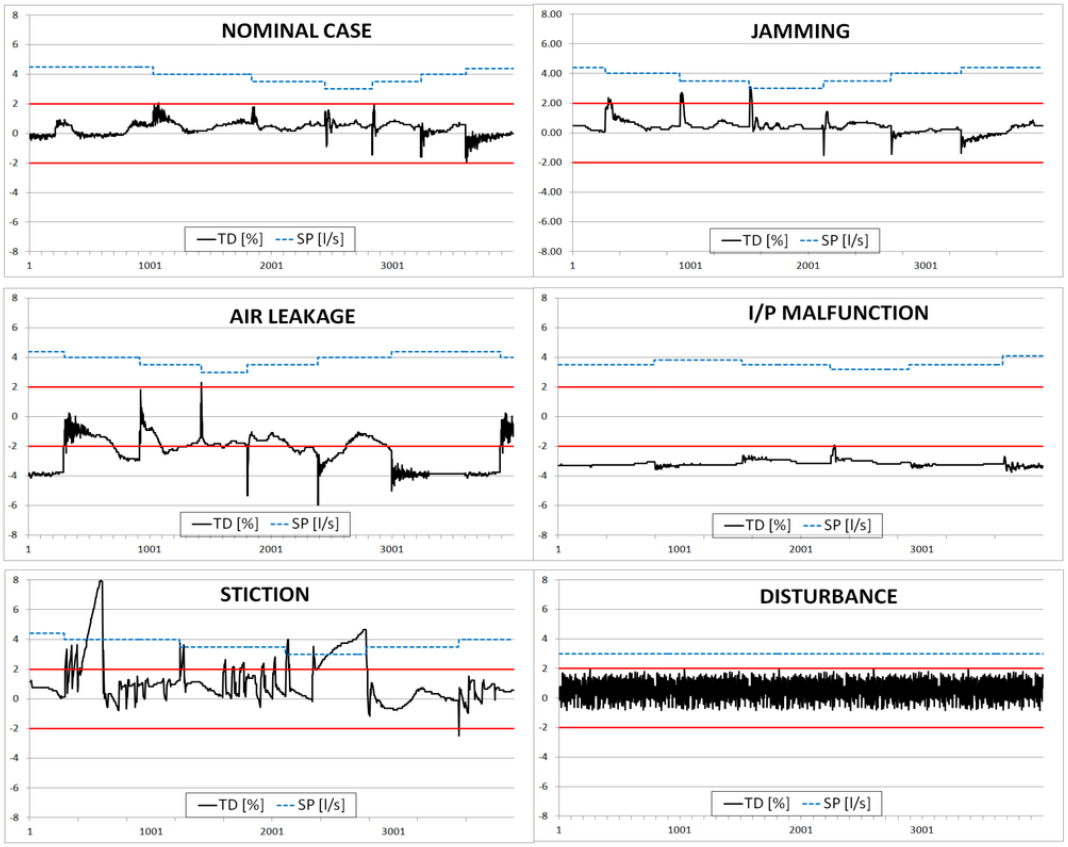

Figure 6.4: TD time trends for nominal case and different malfunctions.

6.3 KPI Definition and Calibration

Data trends have been analyzed with the scope of performing a complete automatic analysis of the actuator using Travel Deviation. The methodology has been overall validated on more than 50 different data sets. Six Key Performance Indices, based on simple metrics of TD, are adopted:

- ***I*_1**, Significant Oscillation Index: number of times TD_{lim} is exceeded (normalized to 1 hour).
- ***I*_2**, Percent Time Out: Time percentage of TD out of its acceptability band.
- ***I*_3**, Mean Travel Deviation: Mean value of TD.
- ***I*_4**, Integral Travel Deviation: Integral of TD (normalized to 1 hour).
- ***I*_5**, Absolute Integral Travel Deviation: Integral of TD absolute value (normalized to 1 hour).
- ***I*_6**, Blockage Index: Numbers of valve stick-slip movements excluding peaks due to SP changes (normalized to 1 hour).

These indices allows a quantitative assessment of the different behaviors between nominal cases and faulty ones. Indices I_3, I_4 and I_5 are defined independently of any other parameters. On the contrary, I_1 and I_2 are based on TD_{lim}, the acceptability band of oscillation of TD. Also I_6 values depend on two secondary parameters which allow one to exclude TD peaks caused by set point changes.

Calibration of the threshold values for the actuator KPI and for the additional parameters was performed afterwards. The threshold calibration allows one to characterize the nominal behavior and to recognize different malfunctions. Range of variation of the different parame-

ters have been tested and consequently the values assumed by the KPI for the cases listed in Table 6.1 have been evaluated. For brevity sake, these results are not reported in this chapter.

For example, high changes in the values of I_6 were observed, and I_1 was always close to zero in nominal cases. Among additional parameters, acceptability band for TD was set to $TD_{lim} = \pm 2$. Obviously, calibration values may depend on the specific equipment and loop; in particular they depend on control operators sensitivity and their level of acceptable performance. Therefore, calibration thresholds can vary for different applications, but qualitative trends, shown in Figure 6.4, remain; illustration of case studies and all details can be found in [125].

Table 6.2 shows the calibrated values of thresholds for actuator indices. Each actuator index is also associated to one or more valve malfunctions: the symbol "&" means anomalies which affect indiscriminately the index, while "OR" indicates anomalies which are discernible one from the other.

Table 6.2: Actuator indices: threshold values and malfunctions.

Index	$I\_i - low$	$I\_i - high$	Detectable Malfunction
I_1	5	10	Stiction & Leakage & i/p Malfunction
I_2	3	6	Stiction OR (Leakage & i/p Malfunction)
I_3	± 1	± 2	Leakage & i/p Malfunction OR Stiction
I_4	± 3000	± 6000	Leakage & i/p Malfunction
I_5	3000	6000	Leakage & i/p Malfunction
I_6	5	12	Stiction

The following quantitative observations can be done:

- Stiction is promptly detectable. On the basis of index I_6 and, in addition, by indices I_1 and I_2.
- Air leakage and i/p malfunction are not clearly separable. They act on the same indices, producing, in particular, the same effects on the indices from 1 to 5. Both cause a loss of pressure – directly due to loss of air or due to the difficult opening of the relay – with the consequent move of the valve stem.
- Jamming (dynamic friction) affects mainly index I_1, but this index is sensitive to all other failures. For this reason, this anomaly does not seem detectable by TD.
- Further experimentations based on DS and P could allow to separate air leakage and i/p malfunction.
- This approach ignores simultaneous type of failures which may happen in practice; this scenario is still object of research and experimentation.

The logic for assignment of verdicts does not require any calibration, once threshold values have been set. Obviously, validations and confirmations by plant operators are necessary to check the reliability of the diagnosis [125].

6.4 Actuator State and New Diagnostic System

The logic of the new *PCU*, which performs actuator analysis, will be presented. Even with the limitations highlighted before, it was possible to set a new logic which allows one to:

- assess the operating condition of actuators with three performance grades:
  1. **Good** (no problems);
  2. **Alert** (incipient deterioration);

3. **Bad** (poor performance).

- indicate the cause when performance is not acceptable (level 2 or 3).

With reference to Table 6.2, two threshold values ($I\_i - low$ and $I\_i - high$) were established:

- below $I\_i - low$ value, the performance is considered similar to the nominal case (good);
- above $I\_i - high$ value, the performance is poor;
- between the two values, $I\_i - low \div I\_i - high$, there is the area of incipient deterioration.

The verdict of actuator state is based on actuator indices compared with their threshold values. The logic follows the combination of the indications reported in Table 6.3.

Table 6.3: Verdict of actuator state.

Actuator State	Conditions on Actuator Indices		
GOOD	All the actuator indices good		$I\_i < I\_i - low$ for $i = 1,...,6$
ALERT	Almost one index overcomes the low threshold	&	$I\_i > I\_i - low$ &
	No indices overcome the high threshold		$I\_i < I\_i - high$ for $i = 1,...,6$
BAD	Almost one index overcomes the high threshold		$\exists\, i : I\_i > I\_i - high$

Therefore it is possible to diagnose three causes of valve malfunction:

1. **Stiction**: it can be diagnosed without any doubt.
2. **Air leakage or i/p malfunction**: they can be diagnosed only together.
3. **Generic Malfunction**: includes all causes not directly recognizable but responsible for actuator fault.

The synthesis of the logic about actuator status is reported in Table 6.4 and illustrated below in the flowchart of Figure 6.5. All indices contribute to define the actuator state, but only I_3 and I_6 determine the cause of failure.

Table 6.4: Conditions for the emission of actuator verdict.

Condition		Source of actuator anomaly
Actuator State	GOOD	–
I_3	BAD	Air leakage or i/p malfunction
I_6	BAD	Stiction
I_3	GOOD or ALERT	
Actuator State	ALERT or BAD	Generic Malfunction

The proposed logic has been included in the new (advanced) performance monitoring system (PCU_4). Figure 6.6 shows the architecture of the system.

The availability of the MV/TD allows one to evaluate the specific KPI indices and to activate a new analysis path oriented to actuator diagnostics (module Act_AIM). Module Act_AIM issues verdicts of state and causes of anomalies of the actuator: Stiction, Air leakage or i/p malfunction and Generic Malfunction. These verdicts are definitive and affect subsequent analyses.

In previous *PCU* (PCU_3) the only possible path of analysis was oriented to loop diagnostics (now indicated as Loop_AIM) to detect presence of external disturbances or controller tuning problems. As main difference, valve anomalies are detected only indirectly and always classified as stiction. More details about different PCU_3 modules can be found in Chapters 3 and 7 (see also [123]). In PCU_4, the loop path is activated subsequently to actuator path and some more accurate tests in Frequency Analysis Module (FAM) and Stiction Analysis Module (SAM) are performed.

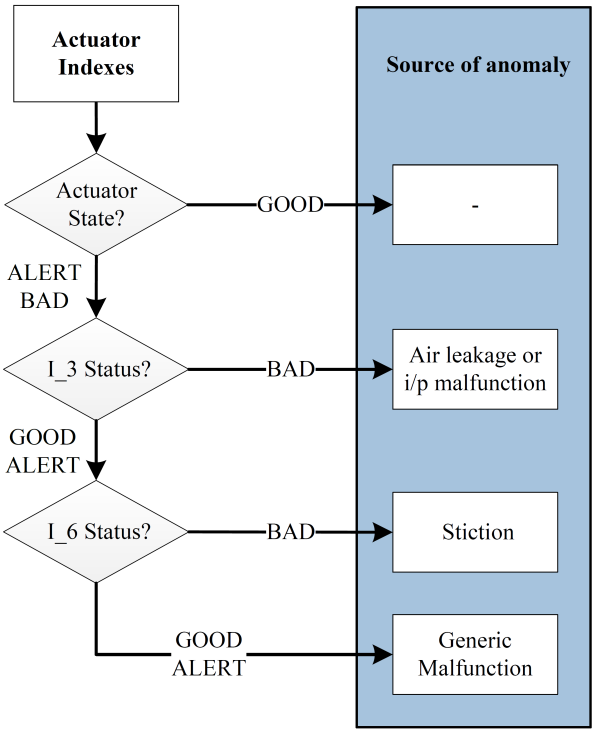

Figure 6.5: Logic for the emission of actuator verdict.

Table 6.5 shows a comparison of the results between the two releases of *PCU* system, based on 3 and 4 variables, applied to the typologies listed in Table 1. Some observations follow.

- In all cases (except D) the PCU_3 is not able to recognize any type of malfunction. No significant oscillation is detected because loop oscillation is considered acceptable on the basis of the threshold value assumed for the Hägglund technique [67].
- On the contrary PCU_4 is able to diagnose malfunctions in the actuator (not yet visible in the loop) and issues correct verdicts (S, L, M). Therefore indices $I\_1 - I\_6$ and the logic of verdict emission are properly set.
- Both *PCU* releases recognize the nominal case (N).
- In case D a disturbance is actually present. The verdict is confirmed by PCU_4, for which the actuator is good and the disturbance is properly indicated in the loop.
- Dynamic friction (case J) is not correctly detected based on previous considerations.
- For cases L and M, PCU_4 detects properly an actuator fault, but it is unable to distinguish between air leakage and i/p converter malfunction. These two causes are detected only together and the loop state is good.
- Case S is emblematic: PCU_4 correctly detects valve stiction, while PCU_3 wrongly emits a verdict of good performance.

It is evident that MV (and then TD) allows a successful diagnosis of malfunctions that are not detectable simply by using OP and PV; that is, the actuator analysis implemented in PCU_4 allows one to recognize serious malfunctions which otherwise would be hidden by loop dynamics. Analogously, the availability of MV would make stiction quantification an easier problem.

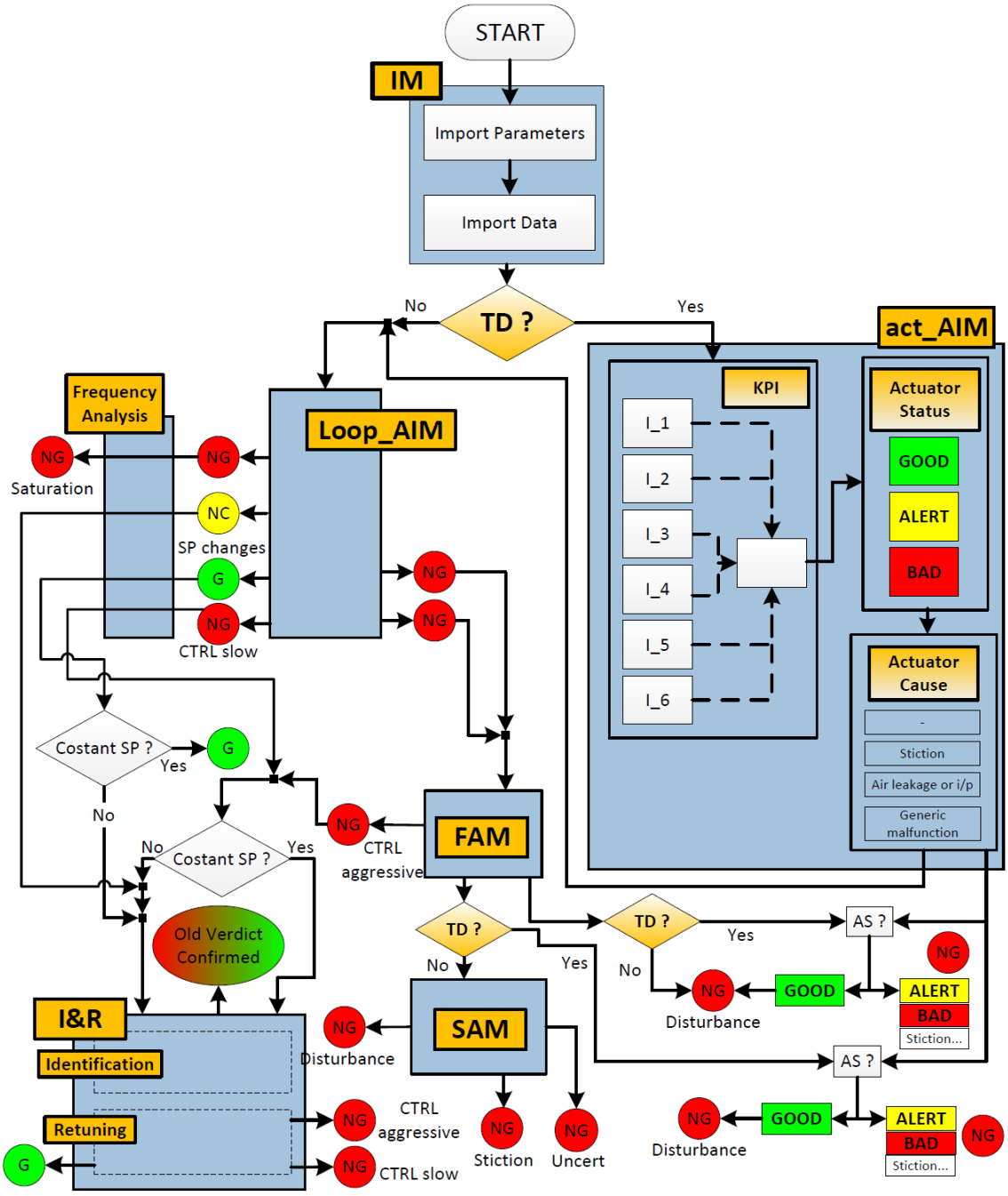

Figure 6.6: Schematic representation of the PCU_4 (MV and TD available).

Table 6.5: Comparison of results on Idrolab data: PCU_3 vs PCU_4.

Case	PCU_3	PCU_4	
	Loop Status	Actuator Status	Loop Status
N	GOOD	GOOD	GOOD
D	BAD [Disturbance]	GOOD	BAD [Disturbance]
J	GOOD	GOOD	GOOD
S	GOOD	BAD [Stiction]	GOOD
L	GOOD	BAD [Air leakage or i/p malfunction]	GOOD
M	GOOD	BAD [Air leakage or i/p malfunction]	GOOD

6.5 Validation on Industrial Data

The ENEL - La Casella (Piacenza), a combined cycle power plant (4 groups), was chosen as first site for PCU_4 validation. Each independent unit is composed of a gas turbine, a heat recovery exchanger for steam generation and a steam turbine. Control loop regulation is performed by pneumatic valves with positioners.

The whole monitoring and assessment system has been implemented on-line (PCU_4_GUI). As shown by Figure 6.7, the system performs scheduling of operations, data acquisition directly from DCS via OPC servers, data analysis and display of results on an user-friendly interface.

The system employs a standard database, which is also used for configuration of loops and servers. The analysis are executed through the MATLAB Runtime which acquires data and parameters of monitored loops in the form of Excel input files. The verdicts of performance and diagnosis are emitted in the form of text files, easily accessible for the users. Figure 6.8 presents a typical page of the interface which plant operators can visualize in control room.

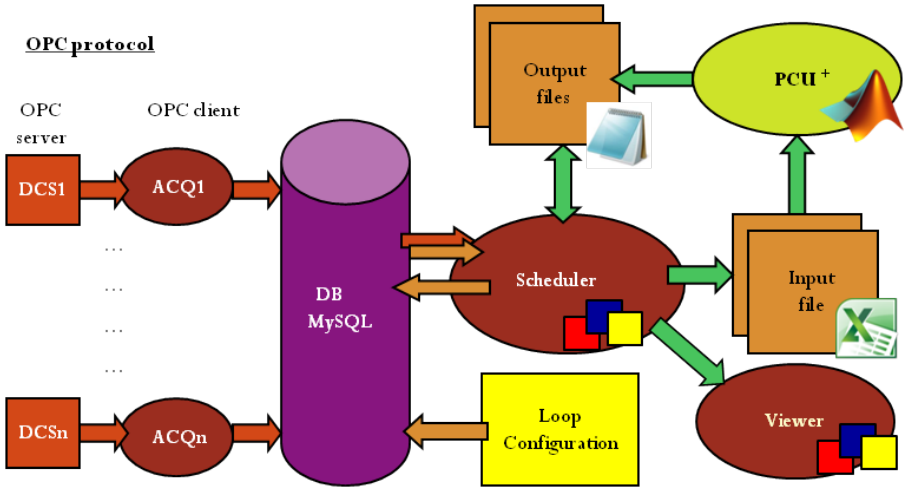

Figure 6.7: Structure, modules e logic of the on-line PCU_4.

Currently, 28 ($7 \cdot 4$) critical loops have been configured in the system and analyzed for months. As results, during the year 2013, the system has allowed to assess:

- 21 loops with good performance;
- 7 loops with bad performance (2 affected by external disturbances; 5 with controller tuning problems);
- 19 valves with good performance;
- 9 valves affected by stiction.

For example, the 4 actuators used for the level control of the high pressure (HP) cylindrical bodies have been constantly diagnosed in stiction. These problems have been confirmed directly by plant operators, who observed heavy wear on valve stems during the plant shutdowns. Figure 6.9 shows time trends for two different loops: a level control (LC) loop for HP cylindrical body and a temperature control (TC) loop for methane preheating.

The LC loop has a valve clearly affected by friction. The TD is particularly oscillating and often trespasses the band of acceptability ($TD_{lim} = \pm 2$). Note that also PV is oscillating. The MV is characterized by continuous stick and slip movements. The values of the actuator indices are respectively: $I\_1 = 46$, $I\_2 = 5.6$, $I\_3 = -0.47$, $I\_4 = -1691$, $I\_5 = 2413$, $I\_6 = 120$; note that I_6 is ten times bigger than its high-level threshold value (compare Table 6.2). Therefore, the verdict on the actuator is stiction. On the contrary, the TC loop has no significant oscillation and shows good performance both in the loop and in the actuator.

Figure 6.8: Viewer of the on-line PCU_4.

6.6 Conclusions

The adoption of additional variables, made available by intelligent instrumentation, allows a more efficient control loops assessment and a more accurate diagnosis of causes. In particular the Travel Deviation, by means of suitable performance indices, is able to detect different types of malfunctioning in pneumatic valves.

Performance indices and the logic of assigning performance grades, defined and calibrated on the pilot plant, has been implemented and successfully validated on a power plant owned by ENEL. Further results of application are reported in technical reports prepared for plant operators, during the periods of testing and validation of the system implemented on-line. Overall, the software *PCU* can be considered reliable in monitoring performance and diagnosing malfunctions.

Further improvements are possible by using additional variables, available only from some types of valve positioners, as the Drive Signal of the positioner and the output Pressure of the i/p converter; future activity will be devoted to their analysis.

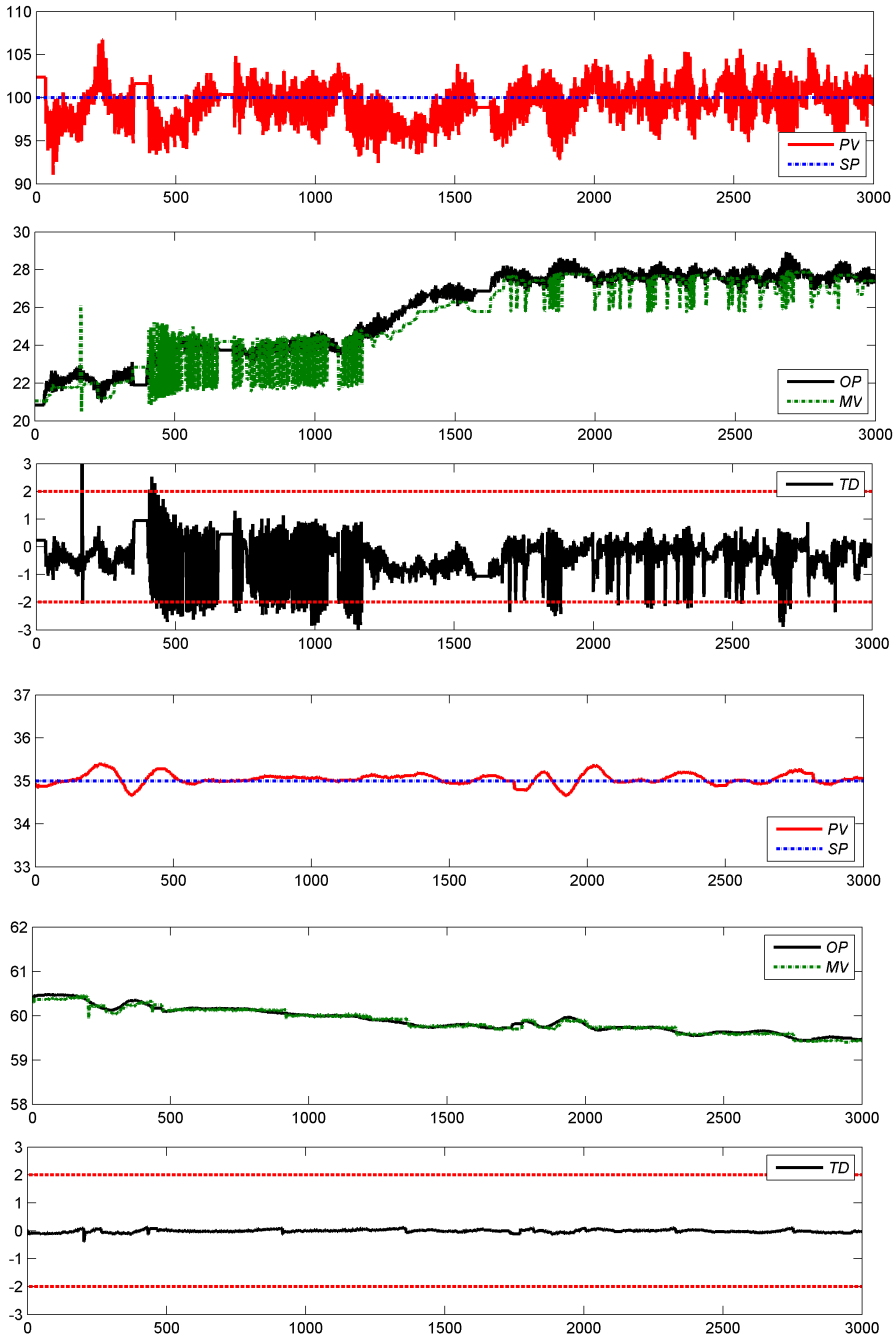

Figure 6.9: Time trends for: top) LC loop with valve stiction; bottom) TC loop with good performance.

Chapter 7

Examples of Applications to Industrial Plants

Abstract [1]

This chapter presents main features of *PCU_CLUI*, a dedicated version of the system *PCU* for monitoring and assessment of control loops. This version has been specifically developed for CLUI-EXERA, an association of industrial users of control systems, and it has been delivered to different companies with the objective of analyzing the most critical control loops of their industrial plants.

The system analyses data recorded by DCS during routine operations and issues automatic verdicts about the performance of basic control loops. Indications of causes of low performance (controller tuning, valves, disturbances) and different strategies to adopt (retuning, valve maintenance, upstream actions) are also given.

This chapter illustrates overall system architecture, with characteristics of the modules which accomplish different tasks of performance analysis, verdicts emission and operator support. A synthesis of the main techniques and algorithms adopted in the system is also given, together with differences among different versions of the system, according to available information on the plant.

In particular, as examples of application of *PCU_CLUI*, this chapter focuses on assessment of numerous control loops of two plants of ENI-Versalis, as a partner of CLUI-EXERA. Examples of results are presented, with illustration of loops performance assessment, and actions suggested by the monitoring system.

[1] This chapter is based on: [31]: *A System for Advanced Performance Monitoring: Application to Complex Plants of the Chemical Industry*.

7.1 Introduction

Control loop performance assessment (CLPA) has been recognized as an important factor to improve profitability of industrial plants. In the last years many techniques have been proposed to allow performance evaluation from routine recorded data and several software packages appeared on the market and are now used as monitoring tools. A control loop performance monitoring system should be able to detect poor performing loops and to indicate different causes, then suggesting appropriate moves to apply on the plant. Main sources of malfunction are external perturbations, poor controller tuning and valve problems.

In Figure 7.1a, the 3 main variables of a control loop are indicated: Set Point (SP), Controlled Variable (PV) and Controller Output (OP). The valve position (MV) is not available in general and malfunctions have to be diagnosed by referring only to these three signals transmitted in 4 – 20 mA current. This constitutes the so-called "standard" diagnostics.

In new design plants, the adoption of intelligent instrumentation, valve positioners and field bus communication systems increases the number of variables which can be acquired and analyzed by a monitoring system (Figure 7.1b). The positioner acts as an inner control loop on the valve position and allows one to speed up the valve response. In addition to SP, OP and PV, DS, P, MV represent the variables typically made available by the positioner (for a maximum of 6 variables). The Drive Signal (DS), is the electric signal generated by the internal controller (C_i) which, through the I/P converter, generates the pressure signal (P) acting on valve membrane, thus determining the position of the stem.

The knowledge of MV allows a more precise diagnosis of loop and valve problems, especially stiction (static-friction), which is known to be the most common cause of performance degradation [85]. Cause of malfunctioning in valves are not only limited to the presence of stiction (and related problems, as deadband, hysteresis, backslash), but can also include other causes: changes in spring elasticity, membrane wear or rupture, leakage in the air supply system, I/P malfunction; details have been reported in Chapter 6 ([126] and [31]).

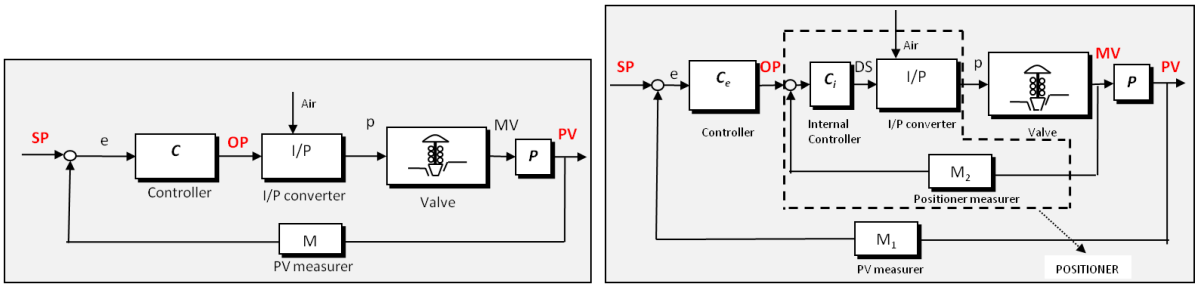

(a) with standard equipment. **(b)** with advanced devices.

Figure 7.1: Reference scheme for different types of control loop.

The research group of the Chemical Process Control Laboratory (CPCLab) of the University of Pisa is active in control loop monitoring systems since many years. The *PCU* (Plant Check Up) is the name of the performance monitoring system now installed on several industrial plants. Different versions of the system are available, depending on the equipment and the measurements available in the plants; periodically new versions of the system are released. The basic version of PCU is now supervising more than 1200 loops of refinery plants.

The system analyses data recorded by the DCS during routine operations and indicates causes of low performance and strategies to adopt using the three "standard" variables. More recently, an advanced version of the diagnostic system has been developed. This version of PCU uses 4 variables (SP, PV, OP and also MV) and grant a more precise - "advanced" - diagnostics. As explained in Chapter 6, this system has been firstly tested on a pilot plant and later implemented in an industrial power plant [31].

This chapter has the following structure: Section 7.2 describes the two main versions of the

performance monitoring system (PCU), giving some details on the whole architecture and the specific modules with the main techniques and algorithms implemented; in Section 7.3 a comparison between the standard and the advanced version of the system is presented; Section 7.4 and 7.5 illustrate problems and results of the off-line application of the system to chemical industrial plants; conclusions and next steps are reported in Section 7.6.

7.2 The System Architecture

A schematic representation of the last version of the "standard" PCU is reported in Figure 7.2a. A full description of the version implemented on-line in a refinery plant is reported in [123]; a synthesis of the latest version is reported below.

The *Initialization Module* (IM) imports parameter values and performs a first check on loop status; if the quality of the data is not good, or a change of configuration is detected, or the valve is operating manually, the analysis is stopped. In these cases, the loop receives a (definitive) label of **NA**: Not Analyzed.

The *Anomaly Identification Module* (AIM) performs a first assignment of performance with verdicts: such as **G** (Good), **NG** (Not Good). Loops subject to excessive set point changes (amplitude or frequency) are temporarily labeled as **NC** (Not Classified) and sent to the *Identification and Retuning Module* (I&R). For loops not in saturation, after a data pre-treatment, tests to detect oscillating or sluggish loops are executed; these tests refer to the Hägglund's approach ([67, 68]), with suitable modifications of internal parameters, based on field calibration [125].

According to Hägglund's criterion [67] an oscillation is considered relevant if its Integral of Absolute Error overcomes an assumed value ($IAE > IAE_{lim}$), for a certain number of times (N_{lim}), in the supervision time window T_{sup}. IAE and IAE_{lim} are defined as:

$$IAE = \int_{t_i}^{t_{i+1}} |e(t)|\, dt \qquad IAE_{lim} = \frac{(2a \cdot RangePV)}{\omega_u} \tag{7.1}$$

where e is the error ($e = PV - SP$), t_i and t_{i+1} are two zero crossing times. IAE_{lim} depends on the range of the controlled variable PV, the amplitude a, and the loop critical frequency $\omega_u = 2\pi/P_u$ (if not known, it can be estimated from the value of the integral time constant (τ_i) of the controller, in the hypothesis of a Ziegler & Nichols tuning: $\tau_i = P_u/1.2$). The technique allows one to detect oscillations in the frequency range of interest (low-middle) and to disregard high frequency oscillations, associated with instrumentation noise.

In the case of both Hägglund's tests resulting negative, the loop is classified as acceptable and a definitive label **G** is assigned. Slow loops can only be caused by the controller: therefore they receive a **NG** label and are sent to I&R Module. Oscillating loops can be caused by aggressive tuning, external disturbance or valve stiction: for this reason, they are primarily sent to FAM, for a frequency analysis.

The *Frequency Analysis Module* (FAM) has the scope of separating irregular oscillations from regular ones on the basis of a power spectrum which computes dominant frequencies; irregular loops are labeled **NG**, without any further inquiry about causes. Regular loops with deteriorating oscillations are sent to the I&R Module, otherwise, in the case of loops showing permanent oscillations, to the SAM for stiction/disturbance detection.

The *Identification & Retuning Module* (I&R) accomplishes process identification and, if successful, controller retuning and evaluation of performance improvements. It receives from the AIM module loops with constant SP labeled as **NG** (Not Good) caused by improper tuning and loops labeled as **NC** (Not Classified) with variable SP. Identification in the case of constant SP is performed using a Simplex based search technique. In the case of variable SP, being typical of secondary loops under cascade control, an ARX process model is identified.

When model identification is successful, new tuning parameters are then calculated. The achievable performance improvement is evaluated by means of suitable upgrading indices and

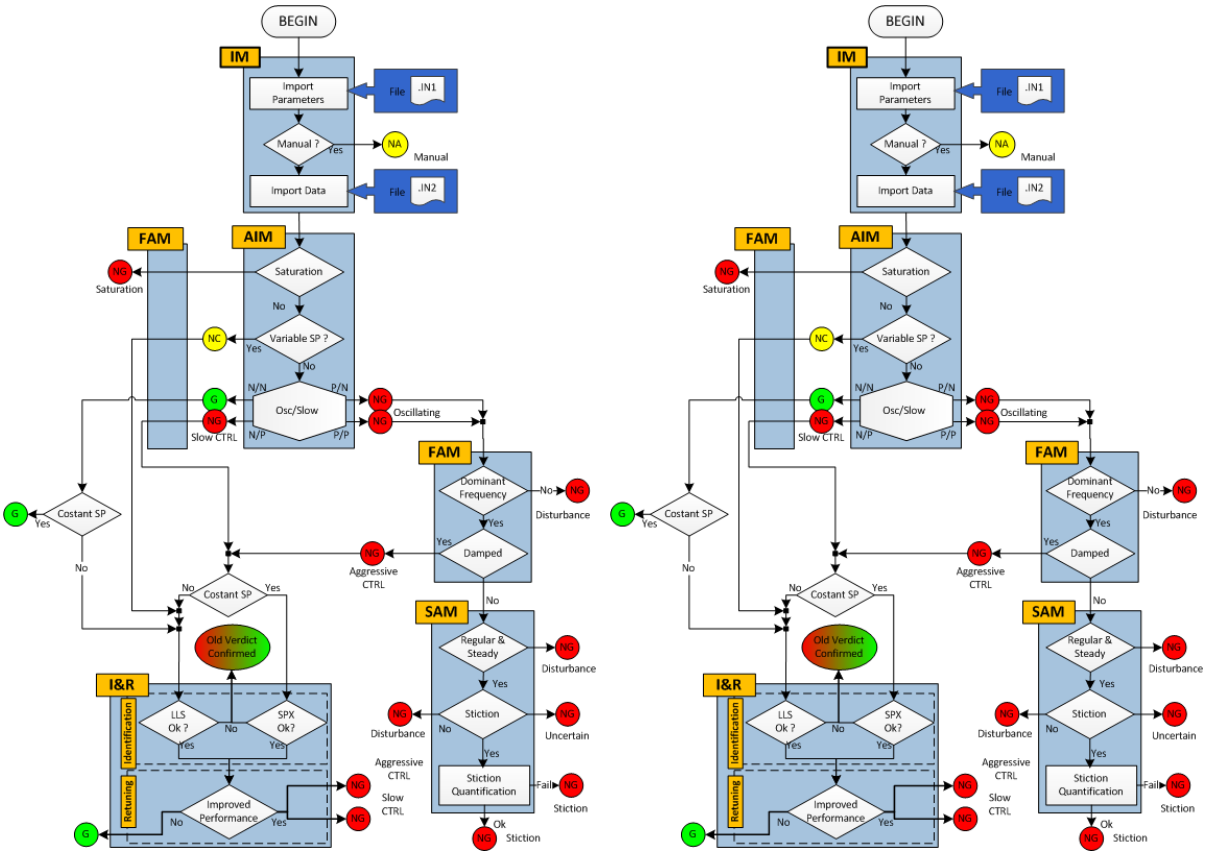

(a) Standard PCU. **(b)** Advanced PCU.

Figure 7.2: Schematic representations of different PCU versions.

new controller settings are proposed. Otherwise, in the case of impossible identification, the previous assigned verdict is confirmed, without any additional suggestion. The nominal performance improvement, predicted on the basis of the identified model, is evaluated by means of the upgrading index ϕ:

$$\phi = \frac{IAE_{Act} - IAE_{Best}}{IAE_{Act} - IAE_{Min}} \tag{7.2}$$

where IAE is the Integral of Absolute Error of the step response for the actual regulator (Act), for the best controller having PI/PID structure ($Best$), and for the optimal regulator (Min). For $\phi \rightarrow 1$, the proposed ($Best$) controller is closed to the optimal one; for any $\phi > 0$ there are improvements, but a threshold has been assumed to implement the new tuning: $\phi = 0.40$, fixed after field validation [123].

The *Stiction Analysis Module* (SAM) analyses data of **NG** oscillating loops and performs different tests to detect the presence of valve stiction and to quantify its amount. This module has been recently improved, as seen in Section 3.5 [23]. About stiction detection, four techniques are applied: the Relay based fitting of values of PV [119], the improved qualitative shape analysis [124], the Cross-Correlation [77] and the Bicoherence [46].

Stiction quantification is performed only on loops clearly indicated as affected. A grid search algorithm with a Hammerstein system identification (a nonlinear stiction model plus a linear ARX model) allows one to estimate the unknown MV signal [22]. To increase the reliability of stiction estimations, data can be divided in sets and the method can be applied separately [23]. As seen in Section 2.8, the possibility of diagnosing, quantifying and compensating stiction is nowadays included in some CLPA systems, proposed by software houses or published in the specific literature [39].

A schematic representation of the "advanced" PCU is reported in Figure 7.2b. A new anal-

ysis path oriented to actuator diagnostics (module Act_AIM) is activated by the availability of MV and TD (Travel Deviation), defined as the difference between real and desired valve position $TD = MV - OP$. Six specific KPI indices and a specific logic of assigning performance grades are implemented. Module Act_AIM issues verdicts of state and causes of anomalies of the actuator: Stiction, Air leakage or I/P malfunction and Generic Malfunction can be diagnosed. These verdicts are definitive and affect the other analyses: the loop path is activated subsequently to actuator path and some more accurate tests in FAM and SAM are performed.

7.3 Comparison of PCU Versions

The knowledge of MV and TD permits a successful diagnosis of malfunctions that are not detectable simply by using OP and PV; that is, the actuator analysis implemented in advanced PCU recognize malfunctions which otherwise would be hidden by loop dynamics. In Section 6.4, a detailed comparison of the results between the two releases of PCU system, based on 3 and 4 variables, applied to the same data, has been presented.

Here, in Table 7.1, only some results are briefly reported. For example, advanced PCU is able to diagnose malfunctions in the actuator (not yet visible in the loop) and issues correct verdicts (Stiction, Leakage, I/P Malfunction), while standard PCU wrongly emits a verdict of good performance.

Table 7.1: Comparison of results on pilot plant data: Standard PCU vs Advanced PCU.

Case		Good	Disturbance	Stiction	Leakage	I/P malfunction
Standard PCU	**Loop Status**	Good	Disturbance	Good	Good	Good
Advanced PCU	**Loop Status**	Good	Disturbance	Good	Good	Good
	Actuator Status	Good	Good	Stiction	Leakage	I/P malfunction

7.4 Application on Industrial Data

CLUI-EXERA is the name of an association of industrial users of control systems, for which a dedicated version of the system *PCU* has been specifically developed. The whole monitoring and assessment system has been delivered to different companies in the form of a lighter version with respect to the one developed for ENEL (see Section 6.5). This specific version, called *PCU_CLUI*, can be easily implemented on-line by plant operators.

As shown by Figure 7.3, the system, similarly to the one of Figure 6.7, performs scheduling of operations, data acquisition directly from DCS via OPC servers, data analysis and display of results via an user-friendly program. Specifically in this version, the software employs a light database, and the analysis are executed through the MATLAB Runtime which acquires data and parameters of monitored loops in the form of Excel input files. Other Excel input files are also used for configuration of loops and servers. The verdicts of performance and diagnosis are emitted in the form of text files, easily accessible for the users. Figure 7.4 presents examples of typical pages of the program, which plant operators can examine in control room.

In the context of these activities, the PCU_CLUI system has been applied off-line to data obtained from numerous control loops of two petrochemical plants of ENI-Versalis: ethylene plant of Porto Marghera and butadiene plant of Ravenna (Italy). The results of this application are briefly illustrated below.

Ethylene is produced by steam cracking from virgin naphtha. The mixture of gas and liquid olefins, obtained in two gas burners, is separated at low temperature and high pressure through a series of columns and reactors: demethanizer, deethanizer, catalytic hydrogenation reactor,

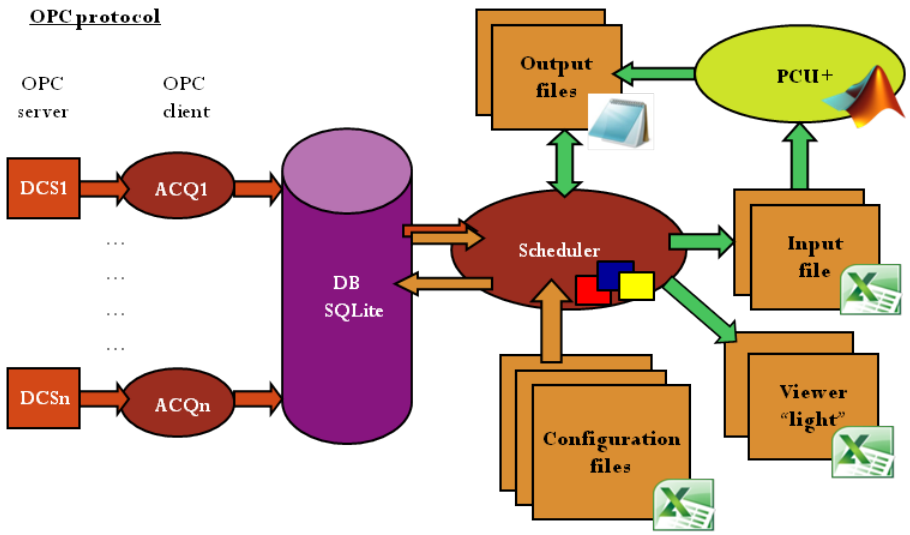

Figure 7.3: Structure, modules e logic of the on-line PCU_CLUI.

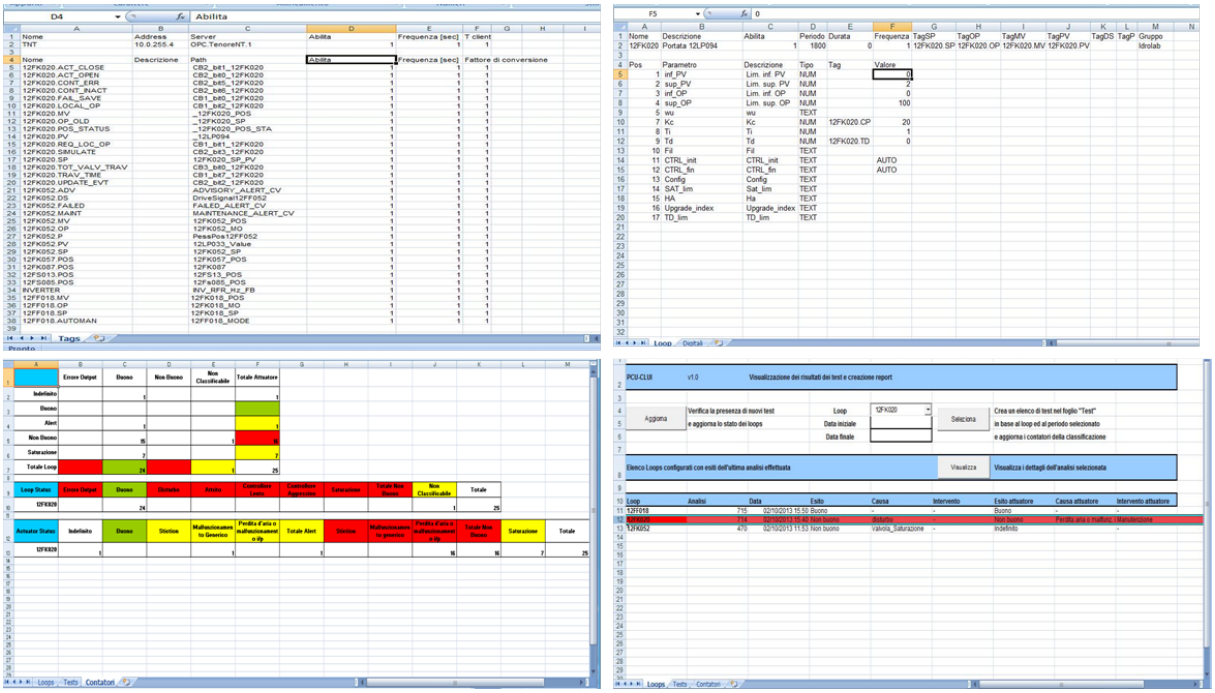

Figure 7.4: Viewer of the on-line PCU_CLUI.

ethylene–ethane splitter and then depropanizer, propylene–propane splitter and debutanizer (see Figure 7.5).

Whereas, butadiene is obtained from crude butane. The plant is composed of a extractive distillation with a specific solvent of a raffinate product, a degassing for the recovery of the solvent and a two-stage distillation to get high purity 1,3-butadiene and other co-products (see Figure 7.6).

Control loop regulation is performed by pneumatic valves with standard equipment, therefore only SP, PV and OP data are available. No valve positioners are used, so the standard version of PCU has been applied (Figure 7.2a). 83 loops of the ethylene plant and 15 loops of the butadiene plant have been assessed respectively. Repeated acquisitions for the same 98 loops have been collected, for a total of 1180 data sets.

On the basis of the more frequent verdict, the system has allowed one to assess:

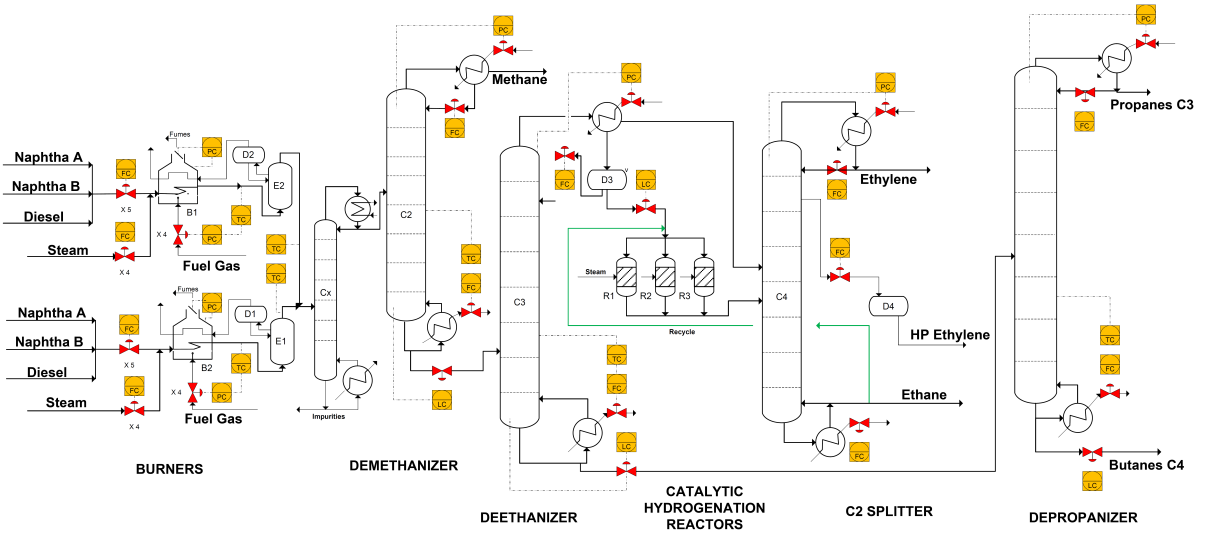

Figure 7.5: A basic flow sheet of the ethylene plant.

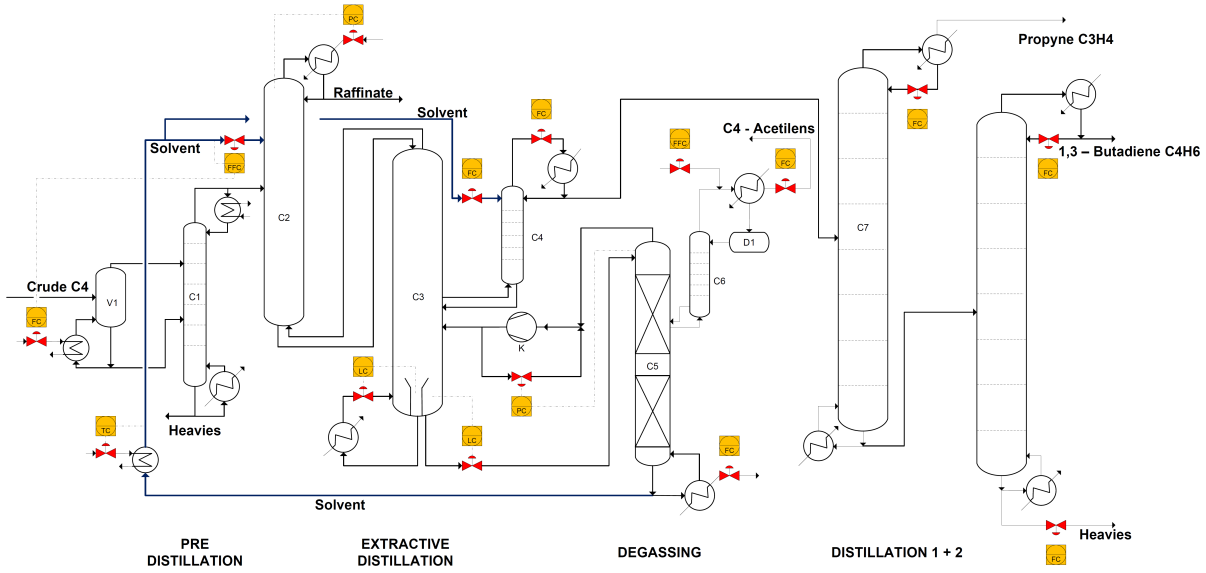

Figure 7.6: A basic flow sheet of the butadiene plant.

- 16 control loops operating in manual (**NA**);
- 36 loops with good performance (**G**);
- 26 loops Not Good (**NG**) with controller tuning problems (5 too aggressive and 21 too sluggish);
- 15 loops **NG** with valve stiction;
- 3 loops **NG** affected by external disturbances;
- 2 loops with low performance (**NG**) but unclear source of malfunction.

A good matching between the verdicts issued by the PCU system and the indications of control operators has been achieved. The system has assessed overall 46 loops with low performance. Only 15 valves are indicated with problems and this will give an economic saving since unnecessary maintenance of the other valves – which does not improve performance – can be avoided.

In addition, 26 loops are reported with controller problems; in 8 cases the retuning is suggested. This allows operators to save time during campaign of retuning since they have precise

suggestions for critical loops.

Therefore, useful indications have been obtained with the standard PCU; a more precise assessment would be possible with the advanced version of the system.

7.5 Example of Results

Three illustrative examples are shown in the sequel as representative of a category of loops.

Loop FC1 This flow rate control loop, obtained from butadiene plant, has PI controller and constant SP. The loop represent a case of initial mismatch between PCU and operator verdicts, for which a recalibration of Hägglund's criterion on oscillating loops is needed. Default values for the parameters are: $2a = 0.02$, $N_{lim} = 10$, $T_{sup} = 50\,P_u$. With a value of $2a = 0.02$, the verdicts from AIM and SAM modules are always **NG**, indicating disturbance as cause of malfunction in 11 out of 12 acquisitions.

On a practical level, indeed, these oscillations – due to their small amplitude (compare Figure 7.7a) – are considered acceptable and the PCU verdicts seem too severe, as a sort of False Alarms (Figure 7.7b). The results obtained with an increased value of Hägglund's parameter ($2a = 0.06$) are completely different (12 cases of **G**) and perfectly aligned to operator indications (Figure 7.7c).

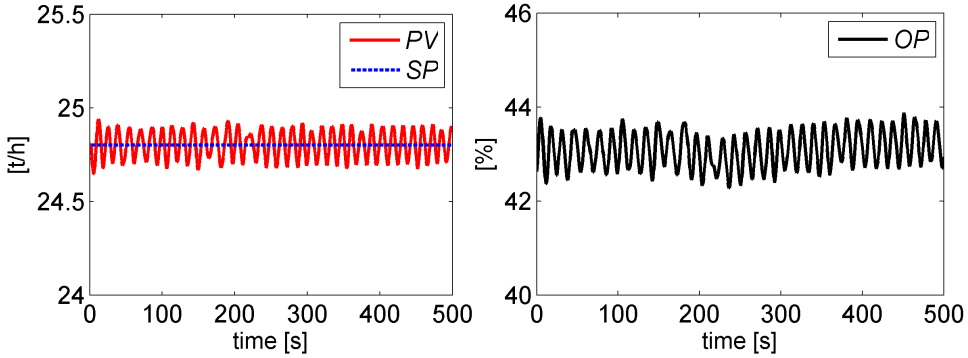

(a) Time trends

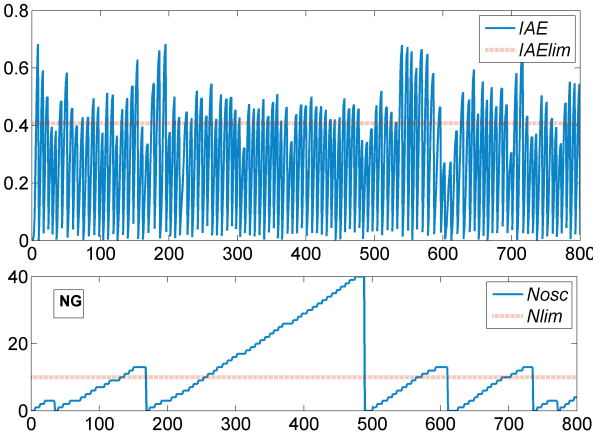

(b) Hägglund's test: **NG** with $2a = 0.02$

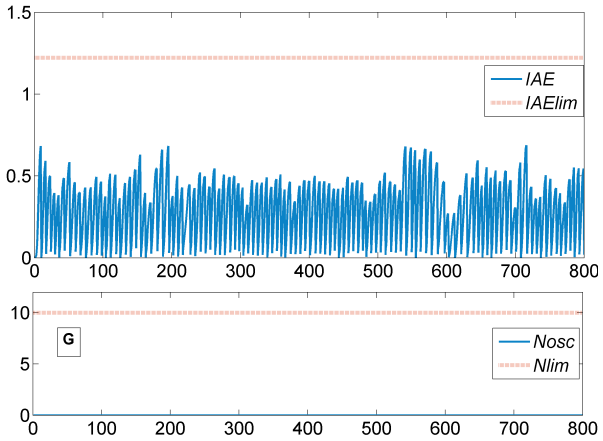

(c) Hägglund's test: **G** with $2a = 0.06$

Figure 7.7: Results for Loop FC1.

Loop FC2 Also this flow rate control loop, obtained from ethylene plant, has PI controller and variable SP. This loop is a clear case of incorrect tuning. The verdicts from AIM and

I&R modules are **NG**, for 10 out of 12 acquisitions, indicating as cause: sluggish controller (Figure 7.8a). The identification is always successful and the old settings ($K_c = 0.4$, $\tau_i = 150$), should be changed to new ones: $K_c = 2.2 - 2.9$, $\tau_i = 30 - 45$. An increase of integral action is then suggested; the upgrade index based on the model (see Section 7.2) is always very high: $\phi = 0.78 - 0.99$ (Figure 7.8b). Future acquisitions will permit to check the predicted improvements obtained with the suggested retuning.

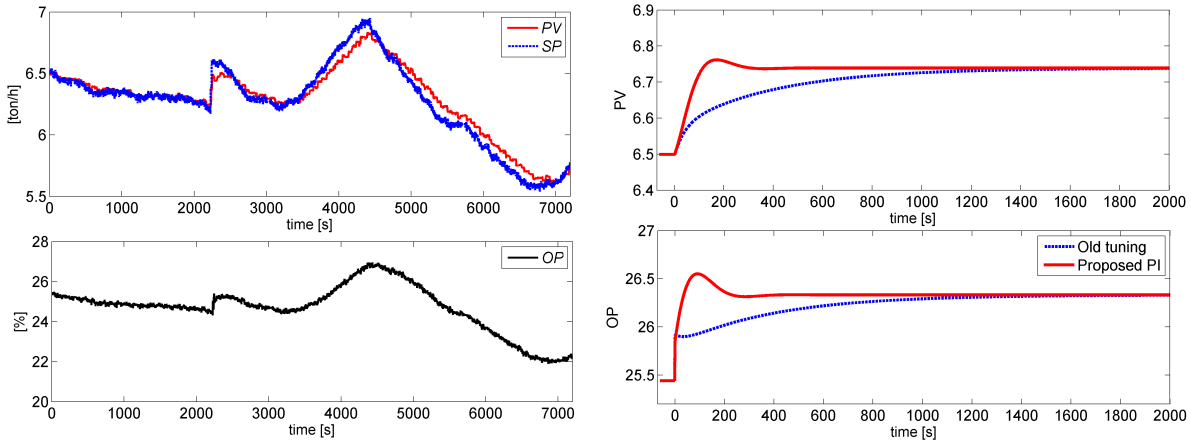

(a) Time trends **(b)** Step responses for computation of ϕ

Figure 7.8: Results for Loop FC2.

Loop FC3 This third flow rate control loop, from ethylene plant, has PI controller and variable SP. It is a typical case of valve malfunction. Indeed, this loop has been indicated as affected by stiction in 11 out 12 acquisitions. The presence of stiction is clearly recognizable by the PV and OP shapes (close to square waves and triangles, respectively in Figure 7.9a). Moreover, the plot of PV(OP) diagram shows evident stiction characteristics (Figure 7.9b) since in FC loops PV is proportional to MV.

About stiction quantification, the S parameter is rather constant for the 11 **NG** acquisitions (see Table 7.2). Note that 1% of stiction is enough to cause performance problems [85]. A good valve maintenance will surely bring to an improvement of performance with an elimination of stiction.

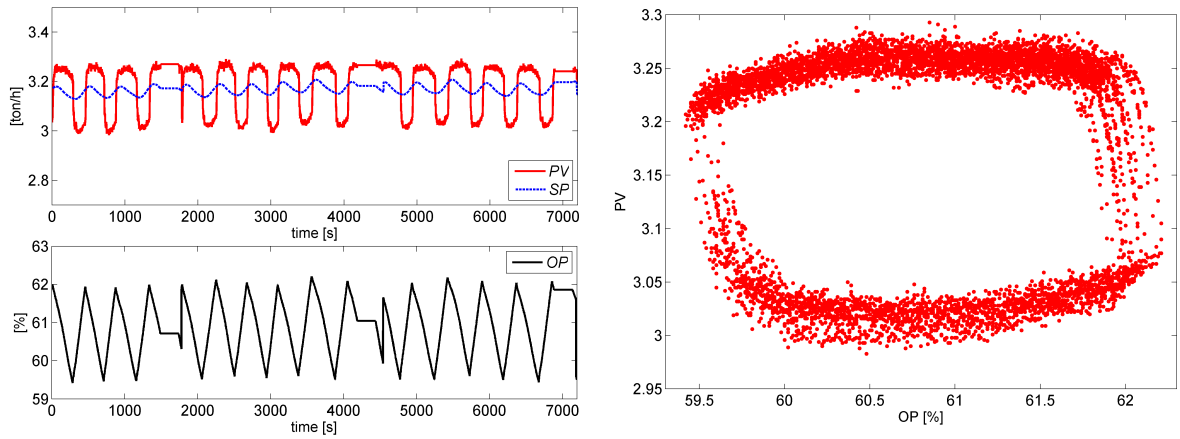

(a) Time trends **(b)** PV(OP) with the typical shape of a sticky valve

Figure 7.9: Results for Loop FC3.

Table 7.2: Loop FC3. Results of stiction quantification, parameter S for different acquisitions.

Acquisition	1	2	3	4	5	6	7	8	9	10	11	mean	std deviation
Stiction S [%]	2.4	2.0	1.8	2.5	2.2	2.4	2.2	2.3	2.0	2.5	1.8	2.2	0.26

7.6 Conclusions

A well-established performance monitoring system (*PCU*) has been described with details about its different versions. As an example, the application of standard version of the system to data obtained from control loops of complex chemical plants have been presented. A good matching between the verdicts issued and the indications of the operators has been achieved. Significant benefits can be obtained: saving costs of unnecessary maintenance (good valves) and saving time following suggestions about retuning of low performing controllers.

Further results have been reported in technical reports prepared for plant operators, during the periods of testing and validation of the system. More precise indications, that is, further distinction of causes and corrections, would be possible with the advanced PCU.

Chapter 8

Conclusions

8.1 Activities and Main Results

Many different activities have been carried out in this PhD thesis; synthetically they include: development of new techniques, their implementations in the monitoring system *PCU*, application on pilot and industrial plants.

Details, improvements with respect to existing methods and future work are reported below, as comments to different chapters.

In Chapter 2, an overall review of recent international researches concerning the topic of friction in control valves has been conducted. The phenomenon has been studied in all its different aspects: modeling, classic detection, advanced (smart) diagnosis, quantification, compensation and implementation in control loop monitoring software. This activity has collected, compared and analyzed pros and cons of a large number of techniques which have recently appeared in the literature.

For what concerns the first line of research – the "standard" diagnosis of control loops – in Chapter 3, a first automatic procedure which allows modeling and quantification of friction in control valves has been developed. This technique employs only data normally stored in DCS of process industry - control action (OP) and process variable (PV) - and allows one to estimate the unknown valve position (MV). The control loop is described as a Hammerstein system: a nonlinear block for valve friction and a linear block (ARX model) for process dynamics. An empirical model based on two simple parameters is used to accurately reproduce the behavior of a sticky valve, while process is identified with the least squares method. A grid method allows one to estimate stiction parameters and, consequently, process parameters.

It has been verified that this estimate of friction can be negatively affected by the inevitable presence of further perturbations on process variables such as set point variations, incorrect tuning of controllers and external disturbances. Therefore, a first methodology has been proposed in order to discard data for which is very likely to get incorrect estimates and in order to limit application to appropriate cases. Simulations indicate that some sources of perturbation can be managed, thus improving the reliability of stiction estimation.

In the perspective of practical implications, estimation and quantification of friction prove to be critical to schedule and check control valves maintenance. To this end, numerous industrial data, which consist in repeated data acquisitions of the same sticky valves, have been analyzed. This allows one to develop a historical trend of valve friction in the same loop, which permits one not only to check, but also to schedule the maintenance of the valve.

In addition, the first algorithm of stiction quantification has been implemented into a new specific analysis module. This module has been included in the latest version of *PCU*, the software for analysis and monitoring of control loops, and a large set of industrial data has been

analyzed.

In Chapter 4, research activities related to stiction quantification have been further developed. In particular, performance of different techniques have been evaluated in terms of accuracy of the estimates in situations of valve friction and simultaneous presence of external disturbances on process variables. The control loop has been identified with Hammerstein models of different types: the linear part as ARX, ARMAX, State Space, Extended-ARX or Extended-ARMAX, and the non-linear part with two well-established data-driven stiction models. Advantages and disadvantages of different techniques have been highlighted, basing on data collected in simulation and on data obtained from a pilot plant.

For this purpose, dedicated experimentation campaigns have been run on the plant facility of IdroLab, owned by ENEL, located in Livorno (Italy). Static friction is introduced into a pneumatic valve by tightening the stem in its seat; the valve stem position is measured in order to directly check the identification of process dynamics and the prediction of unknown MV signal. As a result, extended linear models allow a better identification of process dynamics and a more reliable stiction estimation in the presence of external disturbance superimposed to valve friction. By contrast, simpler linear models are preferable in situations where valve friction is the only source of oscillation.

Later, a further research effort has been done to extend the comparison between techniques of stiction identification and quantification basing on larger sets of data, in particular on a benchmark data set and numerous data obtained from industrial plants. In addition, Appendix C proposes a new comparison of stiction quantification techniques – from literature and personally developed – on another set of industrial data.

In Chapter 5, the issue of stiction compensation has been studied with more attention. In particular, a technique has been developed from a consolidated approach of the literature, called "2-movements". This study was motivated by the fact that current versions of this approach have, indeed, some drawbacks, such as long times of implementation and, most of all, some important assumptions on valve position in oscillation. As a result, the proposed approach improves previous implementations, by overcoming their main limitations.

In detail, using the amplitude of oscillations before the start of the compensation and the estimate of valve friction – obtainable with already developed quantification techniques – it is possible to compute the value of valve input signal to obtain the desired valve position at steady state. This approach, by performing in open loop four precise movements of different amplitude and duration, allows a complete removal of oscillations on the control variable, in shorter time than previous implementations. In addition, reference variations can be tracked and external disturbance can be rejected by monitoring the control error and by switching appropriately back and forth from the friction compensator to the standard PID controller. The effectiveness of this method has been demonstrated through several examples of simulation and subsequently validated by some applications on a pilot plant. In particular, this study has been conducted during the months of abroad research stay, and the activities of experimentation have been carried out in Laboratory of Process Control at University of Alberta.

For what concerns the second line of research – dedicated to the "advanced" diagnosis of control loops – as shown in Chapter 6, numerous experimental tests have been carried out within the pilot plant facility (IdroLab) owned by ENEL. In order to reproduce some typical malfunctions of actuators, specific performance indices able to diagnose such malfunctions have been defined. Subsequently, threshold values for performance indices have been calibrated and a logic of assignment of different degrees of performance has been developed. In particular, it has been verified that valve position error permits a specific assessment of the actuator state and allows one to identify various causes of malfunction.

Later, this diagnostic logic has been implemented in the new system of performance monitoring. Evident advantages in accuracy of diagnosis than previous versions of the program have emerged. For example, at the actuator level, one can separate static friction and dynamic friction from air leakage. Finally, this new version of *PCU* system (PCU_4) was implemented and then successfully validated on the combined cycle energy plant of La Casella - Piacenza, owned by ENEL. An on-line version, which interfaces with the DCS, is currently used to monitor several process control loops.

Finally, as reported in Chapter 7, emphasis on the benefits obtained in loops monitoring from the application of *PCU* system is illustrated. As example and as part of the collaboration with CLUI-EXERA, a large set of data from control loops of two chemical plants owned by ENI-Versalis – ethylene of Porto Marghera and butadiene of Ravenna – has been analyzed. These data revealed some interesting issues and typical malfunctions were assessed: valves with friction, incorrect tuning of controllers, external perturbations.

8.2 Open Issues & Future Developments

Some research issues are still open and possible directions of future works are briefly presented.

Within the new partnership with ENEL Engineering & Research, a new study specifically oriented to the analysis of the performance of control loops during the *transient* phases (start up procedures, load variations, and stop procedures) of electrical units of combined cycle power plants was launched. This need arises from the fact that these energy plants are currently operating in a discontinuous manner with highly variable set points due to the high variability which they are subjected in terms of electrical power to be delivered in the network.

This activity is based on the analysis of data recorded by the advanced monitoring system *PCU* implemented in the plant of La Casella, owned by ENEL, and based on data obtained from the pilot plant IdroLab through new test campaigns specially dedicated. Unfortunately, contingent problems of various kinds, as the scarce availability of new industrial data and the shut-down of the pilot plant, have considerably slowed down this study. The future goal, also during months after the end of this PhD, is to complete such collaborative activities.

At the same time, the possibility of reaching valid results of common interest in completion of the international collaboration undertaken will be tested. In particularly, activities started during the period of visit in Canada by Prof. Huang and concerning Expectation Maximization algorithms applied to valve stiction estimation will be completed with the aim of eventual publication of significant results.

Other future activities could address various issues concerning control loops monitoring and assessment (CLPM/CLPA), and they would be specifically oriented to the development of new algorithms to include in *PCU* software. Among other topics, interesting aspects, at the moment only partially analyzed, may be:

- a new data-driven model of valve friction which could overcome some limitations of models presented so far in the literature;
- revisiting the issue of friction estimation by integrating analysis in frequency and in time domain, and through the use of the descriptive function;
- implementation of new techniques of literature for the detection of significant oscillations (even multiple) to integrate the basic technique of Hägglund [67], the only one currently implemented in *PCU* software.

Appendix A

Stiction Quantification - Additional Issues

Abstract

In this appendix some additional aspects related to issues faced in Chapter 4, but not reported in the corresponding papers [29] and [30], are briefly described.

A.1 Other Sources of Loops Oscillation

In real data, some of the oscillatory behaviors of control loops come from external disturbances and poor controller tuning. The main focus of Chapter 3 and 4 is the identification and quantification of a control loop with valve stiction, possibly with the additional presence of external disturbances, which makes the task much more difficult. Thus, the cases of loop oscillation not due to stiction, that is, only due to aggressive controller or external disturbances or due to both of these sources, have not been extensively considered, neither in the simulation section nor for real data sets.

It is worth to notice that in the industrial practice the proposed identification methods, as almost any stiction quantification method, should be applied only on data where valve stiction has been reliably detected by specific diagnosis techniques. Nevertheless, cases of pure external disturbance and pure aggressive tuning could be used as negative tests, in order to estimate close-to-zero stiction parameters.

Here below two simulation examples are briefly illustrated as negative tests.

A.1.1 Pure external disturbance

A case of pure external disturbance is analyzed first. Valve stiction is not present ($MV = OP$; so that $S = 0$, $J = 0$), while the linear process is the one of Eq.4.23, as well as the external disturbance: $\eta_k = 0.25\big(sin(0.03\,k) + 0.5sin(0.07\,k)\big)$.

Figure A.1 shows the time trends and the estimated signals obtained with EARMAX linear model and Kano's stiction model [87]. Note that PV and MV signals are both well estimated; in particular, $MV_{pre} = OP = MV$, that is, stiction parameters are quantified exactly equal to zero. Also the external nonstationary disturbance is evaluated with good accuracy ($\eta_p \approx \eta$).

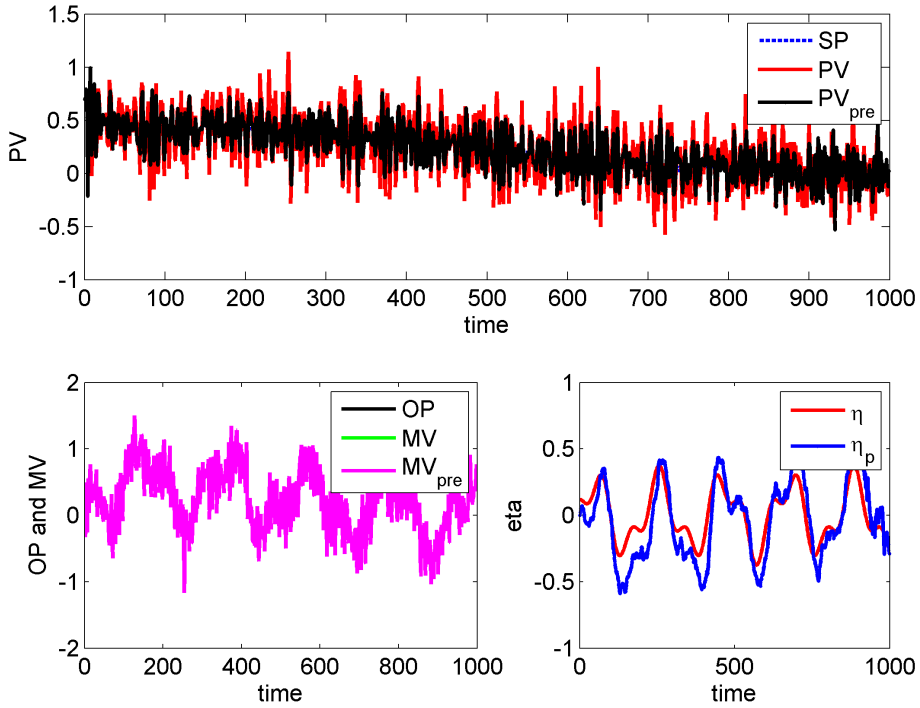

Figure A.1: Simulation data with only external disturbance (no valve stiction).

In addition, note that the Monte-Carlo simulation analysis performed in Section 4.3.1 could be extended, by considering the case of no valve stiction ($S = 0$, $J = 0$). Therefore, x-axis of Figures 4.7 and 4.8 could be enlarged accordingly, and values of fitting indices (E_G and $F_{PV}^{(val)}$) could be extrapolated from the visible points.

Note that these values would be particular small, since the lower is stiction, the higher is the noise-to-signal ratio. This is due to the fact that standard deviation of the stationary disturbance $\{e_k\}$ has been fixed for each simulation, while the amplitude of oscillation (PV) decreases as the amount of stiction, that is, the ratio S/J, decreases. Therefore, a case of no stiction would mean a maximum level of noise-to-signal ratio.

A.1.2 Pure aggressive controller tuning

Then, the same simulation example (Eq.4.23) has been studied in the case of another source of oscillatory behavior, that is, aggressive controller tuning. Valve stiction and external disturbance are not present: $S = 0$, $J = 0$, and $\eta_k = 0 \ \forall \, k$. The controller parameters are set to $K_c = 2$ and $K_i = 1.75$, which represent a very aggressive tuning.

Figure A.2 shows the time trends and the estimated signals obtained with ARMAX linear model and Kano's stiction model. Note that PV and MV signals are both well estimated; in particular, $MV_{pre} = MV$, that is, stiction parameters are quantified exactly equal to zero. Therefore, the identification approach passes the negative test also in the case of aggressive tuning.

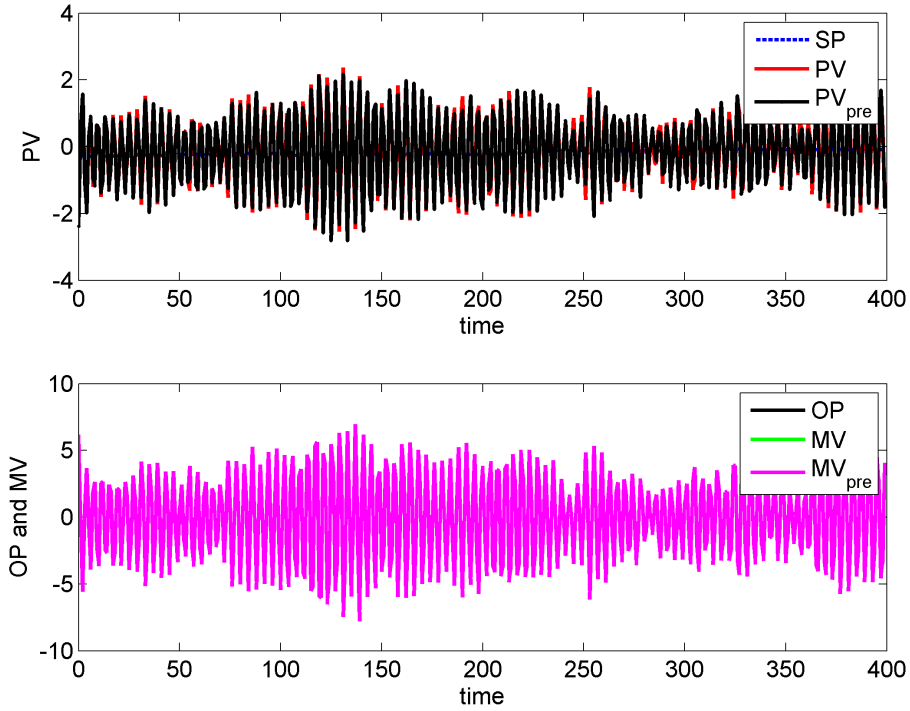

Figure A.2: Simulation data with aggressive controller tuning (no valve stiction and no external disturbance).

A.2 Effect of White Noise Level

It is worth noticing that, in simulation data presented in Section 4.3.1, a white noise with a standard deviation equal to $\sigma = 0.1$ is not actually small if compared with the variance of noise-free PV signal. The noise-to-signal ratio (NSR) is indeed quite large for all the considered simulations, ranging in the following interval: $NSR \in [5\%, 25\%]$. As said before, when the amount of stiction (that is, the ratio S/J) increases, the amplitude of oscillation also increases. Therefore, since the standard deviation of the stationary disturbance $\{e_k\}$ is fixed for each simulation, the higher is stiction, the lower is the noise-to-signal ratio.

As an example, Figure A.3 shows the time trends for a case of simulation with valve stiction (Kano's model, with $S = 5$, $J = 2$) and an external nonstationary disturbance: $\eta_k = a\big(sin(0.03k) +$

$0.5sin(0.07\,k)\big)$. The noise-to-signal ratio on PV is equal to 9.8% in this case.

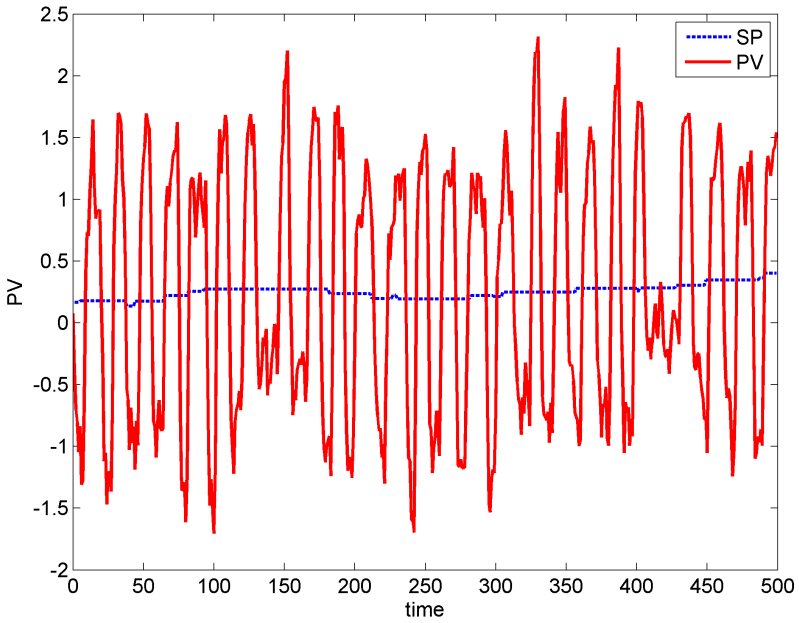

Figure A.3: Simulation data of SP and PV with a significant level of white noise ($\sigma = 0.1$).

A.3 Disturbances with More Complex Behaviors

Here below the effect of disturbances with more complex behaviors (e.g. drift and colored noise) is analyzed. The same linear process of Eq.4.23 is studied, and valve stiction is described by Kano's model.

A.3.1 Drift

Figure A.4 shows the time trends for a case of simulation with $S = 10$, $J = 4$, and an external drift disturbance, which increases linearly with time: $\eta_k = a\,k$. Identification is performed by using Kano's stiction model and EARMAX linear model. Note that PV and MV signals are both well estimated. The estimates of stiction parameters are close to real values: $\hat{S} = 10$, $\hat{J} = 3.8$.

Also the external nonstationary disturbance is evaluated with good accuracy; the estimated bias term (η_p) clearly shows an increasing trend, with a fair fitting error. Therefore, good performance is also possible in the cases of such drift disturbances, provided that an extended linear model (EARMAX or EARX) is used in the identification.

A.3.2 Colored noise

Here the case of colored noise is evaluated. Note that, if assumed as colored noise, the external disturbance (η) is nor slowly-varying neither nonstationary, as in the case of a sum of two sinusoidal waves (as in Eq. 4.19 and 4.24) or a drift signal. On the opposite, as stated by [101], the average output signal of a colored noise is actually stationary, and equal to zero when modeled as the output of a stable filter in response to a white noise.

Therefore, none of the proposed linear structures (extended and not) can properly identify this specific disturbance dynamics. In the case of colored noise, the most appropriate class of linear models would describe the equation error not as a moving average, but as an additional autoregression. Examples are an ARARX model or an ARARMAX model, if an ARMA description of the error is also present.

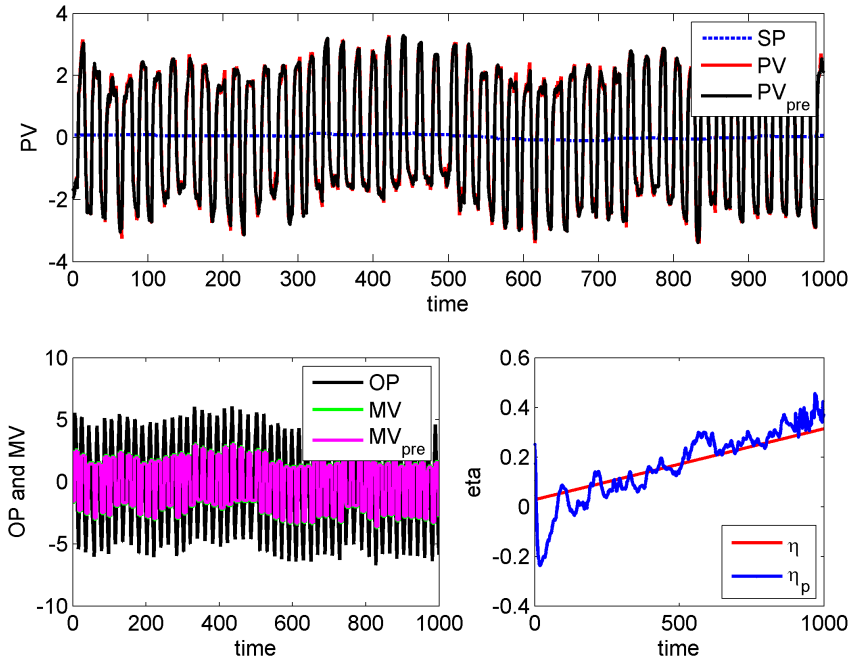

Figure A.4: Simulation data with a drift disturbance.

Figure A.5 shows the time trends for the same case of simulation (Eq.4.23) with $S = 10$, $J = 4$, and an external disturbance (η) which is a colored noise with the following expression: $\eta_k = -a_1\eta_{k-1} - a_2\eta_{k-2} + b_0 v_k + b_1 v_{k-1}$, with $a_1 = 0.1$, $a_2 = 0.8$, $b_0 = 1$, $b_1 = -0.2$, where $\{v_k\}$ is a white noise with variance $\sigma = 0.02$.

The identification is performed by using Kano's stiction model and EARMAX linear model. Note that an important structural mismatch is now present in the linear part of the model; while the most appropriate model would be an ARARMAX model.

Anyway, PV and MV signals are well estimated also in this case. In addition, stiction parameters estimates are close to real values: $\hat{S} = 10$, $\hat{J} = 3.6$. However, the external nonstationary disturbance is evaluated with very low accuracy. Indeed, the estimated bias term (η_p) shows a slower time trend, with a significant fitting error, because of the linear model mismatch.

To conclude, it has to be recalled that in the proposed methodologies only the process is modeled using cause and effect relationship, and the external disturbance is described as a bias on the output. In particular, (η) is assumed to be a slowly-drifting parameter, not a term varying in time with high frequency, as in the case of colored noise [89]. Therefore, in the presence of valve stiction, very good identifications are possible only when the external disturbance varies slower than the oscillation induced by stiction.

A.4 Different Models for the Hammerstein System

In Chapter 3 and 4, only different types of linear plant have been evaluated and the stiction nonlinear behavior has been modeled by the same model used for prediction. It would be nice to use nonlinear plants and more sophisticated stiction models.

First of all, it has to be said that more sophisticated approaches are not new in the literature. For example, a nonlinear process model has been used by [118], who have performed valve stiction estimation in the framework of a Hammerstein-Wiener system. In addition, a non-deterministic stiction model (*Preisach* type) has been recently proposed by [59]. The idea of combining a nonlinear process model and a more sophisticated stiction model is very interesting, but it is far beyond the scope of this thesis.

This approach could interest the future research as stated in Section 4.6: "Furthermore,

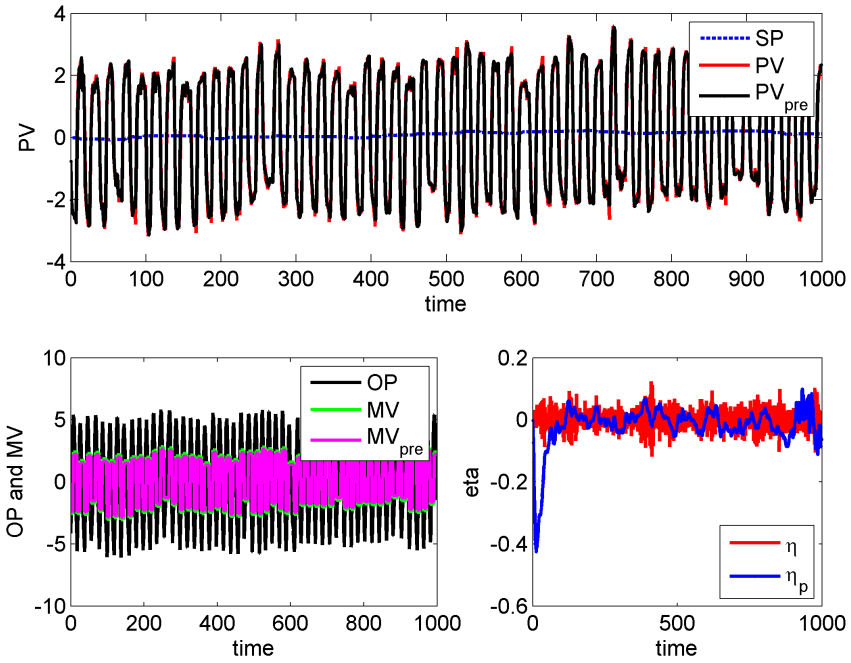

Figure A.5: Simulation data with a colored noise.

more complex and flexible stiction models could be used to describe non uniform friction dynamics in order to obtain more consistent estimates when repeated data registrations are analyzed." In addition, note that this approach tends to be really complex, and might be also impractical for on-line and even off-line industrial applications.

Anyway, it has to be recalled that for the pilot plant experiments presented in Chapter 4, no stiction model is used to generate the data. Conversely, static friction is introduced on purpose in the control valve by tightening the stem in its seat. Therefore, a structural error in the nonlinear part of the Hammerstein model is present, which makes the identification procedure more challenging than in the simulation cases.

A.5 Impact of Process Time Delay

In general, estimation of time delay is an important issue in identification problems. In Chapter 4, for the sake of simplicity, time delay of the linear process models is never estimated in the analysis showed. In particular, time delay is assumed known for the simulation results, and it is fixed a priori for the pilot plant data and the industrial data.

The impact of time delay could be evaluated by considering another grid of possible time delay L, where $L = T_s t_d$ is taken as a multiple of the sampling time (T_s). For every triple (S, J, t_d), the coefficients of the linear model could be then identified. This approach is robust, but obviously heavy in terms of computational load.

Among other standard solutions to estimate the time delay, [95] and [89] have proposed a cross correlation analysis between the input (MV) and the output (PV) sequence. Anyway, this analysis should be repeated for every point of the stiction parameters grid, that is, every candidate sequence of MV.

Here below the impact of time delay is studied by using the same linear process of Eq.4.23, but with a time delay equal to $t_d = 2$:

$$y_k = 0.5215y_{k-1} - 0.0590y_{k-2} + 0.0009y_{k-3} + 0.2836u_{k-1-t_d} + 0.2442u_{k-2-t_d} + 0.0088u_{k-3-t_d} + e_k + 0.5e_{k-1} + 1.0e_{k-2} - 1.0e_{k-3} + \eta_k \quad \text{(A.1)}$$

where (η) is the external disturbance, $\eta_k = a\big(sin(0.03\,k) + 0.5sin(0.07\,k)\big)$, with $a = 0$ for the case of pure valve stiction, and $a = 0.25$ for the case of stiction and disturbance.

One hundred Monte-Carlo (MC) simulations are carried out, by using different realizations of white noise $\{e_k\}$, with Kano's stiction model for both disturbance amplitudes. Note that an appropriate tuning for the process is now $K_c = 0.35$ and $K_i = 0.15$. The time delay presence is taken into account by building a grid of possible delays: $t_d \in [0, t_{d_{max}} = 5]$.

Figure A.6a shows the results of one identification in the case of pure valve stiction (with $S = 5$ and $J = 2$) by using ARX linear model. Figure A.6b reports the results of one identification in the case of same valve stiction plus external disturbance, by using EARMAX linear model. Note that Kano's model is also used in both the identification steps.

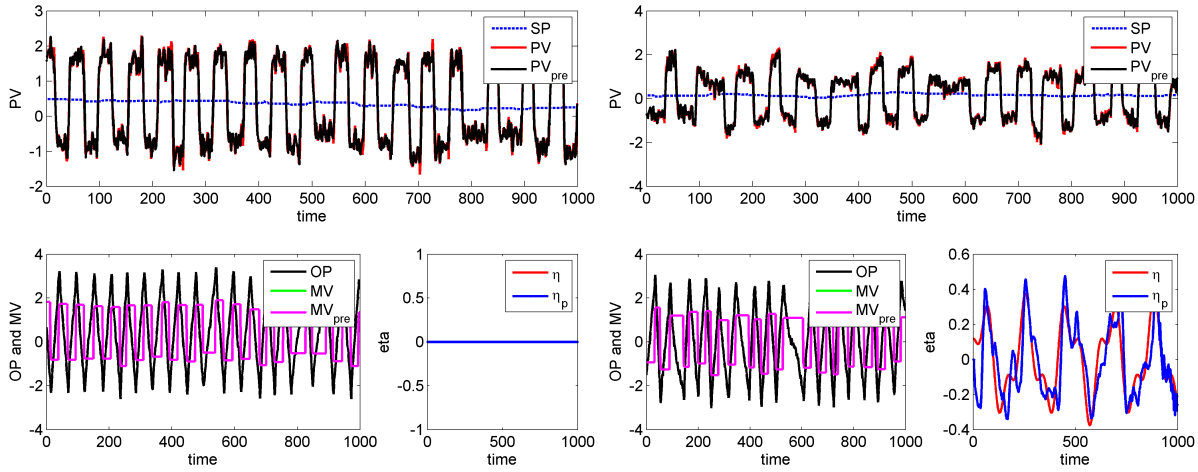

(a) Pure valve stiction, with ARX model. **(b)** Stiction and disturbance, with EARMAX.

Figure A.6: Simulation trends for process with time delay.

Table A.1 shows the overall results for these two different linear process models. Note that similar results can be obtained with the other three models: ARMAX, SS, and EARX. Average estimates of stiction parameters ($\bar{S}$, $\bar{J}$) and time delay ($\bar{t}_d$), with corresponding standard deviations (σ_S, σ_J, σ_{t_d}) are reported. Also average indices of fitting are evaluated: $\bar{F}_{PV}^{(id)}$, $\bar{F}_{PV}^{(val)}$. On the whole, it is possible to assess that time delay has no significant impact on the identification methods.

Table A.1: Effect of time delay for the MC simulations.

LIN model	η	$\bar{S}$	σ_S	$\bar{J}$	σ_J	$\bar{t}_d$	σ_{t_d}	$\bar{F}_{PV}^{(id)}$	$\bar{F}_{PV}^{(val)}$
ARX	no	5.00	0.00	1.97	0.54	1.99	0.10	97.67	97.64
ARX	yes	4.99	0.01	2.26	0.57	1.82	0.39	95.97	95.94
EARMAX	no	4.99	0.04	1.14	0.26	2.01	0.17	98.30	98.25
EARMAX	yes	4.99	0.07	1.82	0.31	1.91	0.29	97.89	97.55

Indeed, the performance of the considered methods are comparable with the ones already presented in Chapter 4 in terms of estimations of stiction parameters and indices of fitting. Average estimated values are close to actual parameters, especially for S parameter. Identification of J is subject to lower accuracy and precision, in particular when a inappropriate linear process model is used, that is, ARX (non extended) model in the case of stiction plus disturbance, and EARMAX (extended) model in the case of pure valve stiction.

Note that this particular effect is not due to the presence of process time delay, but it is due to the structural difficulty lying in the identification problem: Hammerstein system with

internal unknown variable (MV). Note also that time delay is correctly estimated, with small variance, that is, only few cases of error.

A.6 Impact of Controller Tuning Parameters

As stated in Chapter 4, in the case of direct identification methods, as the ones presented in this thesis, the impact of controller tuning parameters on the estimation results is proved to be not particularly significant. Good performances are possible for reasonably large ranges of controller parameters around nominal values, both for nonextended and extended process models. The effect of poor controller tuning has been analyzed by using simulation data in Section 4.3.2. Here below the same analysis is repeated for data obtained from a flow rate control loop installed in a pilot plant.

This plant is different from the facility described in Chapter 4, and belongs to the control laboratory of the University of Alberta (see Figure 5.11). Stiction cannot be introduced by tightening the stem in its seat, but it is simply inserted by passing the output (OP) of the controller through a data-driven stiction model (here, Chen's model [43]), in order to get MV signal.

A case of pure valve stiction, with $S = f_s + f_d = 10$, and $J = f_s - f_d = 4$, is considered; no external disturbance (η) is present. In a first experiment, the controller (PI-type) parameters are set to $K_c = 18$ and $K_i = 10$, which represent an aggressive tuning. Then, in a second experiment, the parameters are changed to $K_c = 6$ and $K_i = 3$, which compose a sluggish tuning. Note that an appropriate tuning for this process should be $K_c = 9$ and $K_i = 5$.

Figure A.7a shows the results of identification for the case of aggressive tuning, by using Kano stiction model and ARMAX linear model. Figure A.7b reports results for the case of sluggish tuning, by using Kano stiction model and EARMAX linear model. In both cases, PV and MV signals are well estimated.

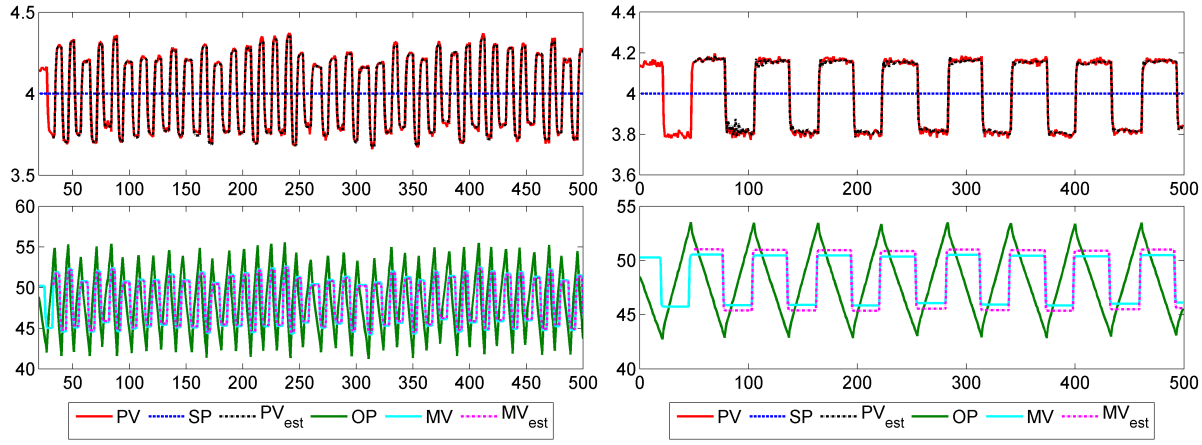

(a) Aggressive tuning. **(b)** sluggish tuning.

Figure A.7: Pilot plant data with different controller parameters.

Similar results have been obtained for the other linear process models, as showed in Tables A.2 and A.3. Therefore, good performance and robustness of the approaches obtained in simulation are confirmed by using pilot plant data.

Note that, as expected, the results for the sluggish tuning are a bit inferior to the ones for the aggressive tuning. Fewer periods of oscillation are registered in the same time interval ($\simeq 500\,s$), and then data are less exciting for the process and less informative, especially for extended linear models. Note also that identification of J parameter is confirmed to be more critical. On the whole, good performance and robustness of the approaches with respect to very different controller tuning parameters have been verified.

Table A.2: Results for data with aggressive tuning.

LIN model	NL model	S	J	$F_{PV}^{(id)}$	$F_{PV}^{(val)}$	F_{MV}
ARX	Kano	10.0	3.7	93.73	93.85	94.95
ARMAX	Kano	10.0	3.7	93.75	93.91	94.95
SS	Kano	10.0	3.7	93.76	93.90	94.95
EARX	Kano	10.0	3.7	94.25	93.63	94.95
EARMAX	Kano	10.0	3.8	94.33	93.77	96.63

Table A.3: Results for data with sluggish tuning.

LIN model	NL model	S	J	$F_{PV}^{(id)}$	$F_{PV}^{(val)}$	F_{MV}
ARX	Kano	10.0	3.5	93.46	-	88.80
ARMAX	Kano	10.0	3.6	93.50	-	91.04
SS	Kano	10.0	3.6	93.50	-	91.04
EARX	Kano	10.0	5.0	90.86	-	77.61
EARMAX	Kano	10.0	5.0	91.68	-	77.61

A.7 Impact of Stiction Grid Dimension

Some details about the grid dimension have been already given in Section 4.2.3. The stiction parameters grid has a triangular shape, since $f_s \geq 0$, $f_d \geq 0$ (or $S \geq J$). Thus, overshoot stiction cases ($J > S$) are excluded; actually waveforms generated for these combinations are rarely observed in practice. The largest value of S (and J) is the OP oscillation span. Therefore, under boundary conditions, when $S = J = \Delta OP$ (the span of OP), the valve jumps between two extreme positions, generating an exactly squared MV signal.

In addition, the step size of stiction parameters plays an obvious key role: small values allow one to increase accuracy, avoiding the effect of local minima, at the expense of higher computational times. A rigorous proof of this statement has been given in [90].

According to the experience and extensive simulation results, by assuming as acceptable an error on the estimation of S and J equal to 0.1 (which is 1/1000 of stroke of valve stem, 0-100%) a step size equal to 0.05 can be considered adequate. For example, for the simulation results of Chapter 4 (Figures 4.5, 4.6, 4.7, 4.8), a grid with a step size equal to 0.1 has been considered. No extra simulation, varying the step size of the grid, is here presented.

Appendix B

Stiction Quantification - Another Approach

Abstract

In this appendix, another possible approach for valve stiction quantification is briefly illustrated. This study has been conducted during the months of abroad research stay at University of Alberta, by Prof. Biao Huang of Department of Chemical and Materials Engineering.

In details, parameters of control loop with sticky valve are identified and estimated by implementing a specific Expectation Maximization (EM) algorithm. The system, previously described in Chapters 3 and 4 with several types of Hammerstein model – a nonlinear block for the sticky valve and linear block for the process dynamics – is now reformulated so that the friction nonlinearity becomes a set of simple linear and parallel relations, thus constituting a sort of "multi-mode" model to be integrated with the linear dynamics of the process, to form an extended model.

Such unknowns parameters are estimated by EM algorithm that employs, among other algorithms, techniques for filtering and smoothing (of Kalman style), and which, starting from known external variables of input and output, simultaneously identifies all system parameters: valve and process. This activity must be considered additional to previous works, in particular to [25] and [30], but it is still at a draft level.

B.1 Introduction

Generally speaking, the expectation maximization (EM) algorithm computes maximum likelihood (ML) estimates of unknown parameters θ in probabilistic models involving latent variables Z [1]. The EM algorithm can be thought as a systematic way of separating one hard problem into two new closely linked problems, each of which is hopefully more tractable than the original problem [127].

This problem separation forms the very heart of the EM algorithm. More pragmatically speaking, the EM algorithm is an iterative method that alternates between computing a conditional expectation and solving a maximization problem, hence the name expectation maximization.

To thoroughly appreciate the EM algorithm, it is important to understand why the above mentioned problem separation indeed results in an ML estimate. It is also worth to notice that EM algorithms can be effectively used for estimating models of dynamic systems, i.e., *system identification*. In particular, EM algorithms can be used for identification of system parameters even in the case of missing variables.

Therefore, EM can be applied in the specific situation extensively faced in this thesis, that is, the case of model-based valve stiction detection and estimation, since the actual valve position (MV) is a variable not typically available. In Chapters 3 and 4, the control loop has been modeled by means of several types of Hammerstein system, that is, a nonlinear block for the sticky valve and a linear block for the process dynamics. In this appendix, the idea is to apply EM algorithm in the framework of such a type of Hammerstein system.

Before giving the problem formulation, the specific literature concerning EM algorithms applied to system identification has been revised. First of all, it is worth to notice that numerous are the papers for linear systems identification using the EM algorithms, and there are also quite a few approaches for nonlinear systems. Nevertheless, very few are the methods specifically oriented for Hammerstein systems. A brief introduction to some of these works is given below.

[165] develops and illustrates a maximum-likelihood based method for the identification of Hammerstein–Wiener model structures, by using a specific EM algorithm. A very general situation is considered wherein multi-variable data, non-invertible Hammerstein and Wiener nonlinearities, and colored stochastic disturbances both before and after the Wiener nonlinearity are all catered for. Anyway, the nonlinearity (or nonlinearities, in the case of MIMO systems) must be *memoryless*, such as saturation, deadzone, polynomial, and piecewise linear functions. In the method of [117], a pure Hammerstein model is identified with EM algorithm, along with a kernel-based identification approach for the linear part. Anyway, the nonlinear part is still a standard function, that is, a static nonlinearity.

Therefore, these two approaches cannot be directly or indirectly applied in the case of valve stiction nonlinearity, which is non-static and has strong features of memory.

Indeed, this issue seems to have been already tackled in [163]: "Hammerstein systems are usually composed of static (memoryless) nonlinearities and linear dynamic components. However, in order to detect the control valve stiction, Hammerstein systems needs to be extended: the input nonlinearity has a hysteretic behavior, instead of being memoryless. Such systems are referred to as *extended* Hammerstein systems. It is worthy to point out that some recent articles [among others, [162]] studied the identification of Hammerstein systems with non-static input nonlinearities. However, these studies are not designed for describing control valve stiction based on oscillatory signals, and consequently are hardly applicable in this case [...]".

[1] The term *latent* variable is adopted from statistics and refers to a variable that is not directly observed. Hence, a latent variable has to be inferred (through a mathematical model) from other variables that are directly observed, i.e., measured. Latent variables are sometimes also referred to as *hidden* variables or *unobserved* variables and, within the EM literature, they are sometimes called the *missing* data or the *incomplete* data.

An useful toolbox is freely available with the objective, among others, of using EM algorithm to identify dynamic systems; the latest version can be found in [110]. Indeed, this toolbox can perform system identification for different types of models (linear, as transfer function or State Space; nonlinear, as Hammerstein–Wiener transfer function, bilinear State Space, general State Space; frequency domain data) by using different techniques (gradient based search, EM algorithm, subspace methods). Nevertheless, the specific combination, that is, Hammerstein system and EM algorithm, which is being sought in this appendix is not directly supported in the toolbox.

This appendix has the following structure: in Section B.2, in order to derive the EM algorithm, the ML problem is clearly defined. Section B.3 gives a basic introduction to the EM algorithm within the setting of dynamic systems. Section B.4 states the problem formulation. Conclusion and future developments are given in Section B.5

B.2 Maximum Likelihood Estimation

The maximum likelihood method is based on the rather natural idea that the unknown parameters should be chosen in such a way that the observed measurements becomes as likely as possible. More specifically, the ML estimate is computed according to:

$$\hat{\theta}^{ML} = \arg\max_{\theta} p_\theta(y_1,...,y_N) \tag{B.1}$$

where y_t denotes the measurement at time t. Furthermore, subindex θ indicates that the corresponding probability density function $p_\theta(y_1,...,y_N)$ is parameterized by the (unknown) parameter θ. The joint density of the observations $p_\theta(y_1,...,y_N)$ can, using the definition of conditional probabilities, be written as:

$$p_\theta(y_1,...,y_N) = p_\theta(y_1)\prod_{t=2}^{N} p_\theta(y_t|Y_{t-1}) \tag{B.2}$$

where $Y_{t-1} := \{y_1,...,y_{t-1}\}$. It is often convenient to consider the so called log-likelihood function:

$$L_\theta(Y) = \log p_\theta(y_1,...,y_N) = \sum_{t=2}^{N} \log p_\theta(y_t|Y_{t-1}) + \log p_\theta(y_1) \tag{B.3}$$

rather than the likelihood function. In the interest of a more compactness, the notation $Y = \{y_1,...,y_N\}$ is introduced. The logarithm is a strictly increasing function, implying that the following problem is equivalent to (B.1):

$$\hat{\theta}^{ML} = \arg\max_{\theta} \sum_{t=2}^{N} \log p_\theta(y_t|Y_{t-1}) + \log p_\theta(y_1) \tag{B.4}$$

This problem can of course be solved using standard methods such as Newton's method or one of its related variants. However, the ML problem can also be solved using the expectation maximization algorithm, an approach that has steadily gained in popularity since its formal birth in 1977 [57].

B.3 Expectation Maximization

The strategy underlying the EM algorithm is to separate the original ML problem (B.4) into two linked problems, each of which is hopefully easier to solve than the original problem. Abstractly speaking this separation is accomplished by exploiting the structure inherent in the probabilistic model.

The *key idea* is to consider the joint log-likelihood function of both the observed variables Y and the latent variables Z:

$$L_\theta(Z,Y) = \log p_\theta(Z,Y) \tag{B.5}$$

and then to assume that the latent variables Z are available. Using the definition of conditional probability:

$$p_\theta(Z|Y) := \frac{p_\theta(Z,Y)}{p_\theta(Y)} \tag{B.6}$$

the following connection between (B.3) and (B.5) can be established:

$$\log p_\theta(Y) = \log p_\theta(Z,Y) - \log p_\theta(Z|Y) \tag{B.7}$$

Let θ_k denote the estimate of the parameter θ from the k^{th} iteration of the algorithm. The problem separation mentioned above is now obtained by integrating (B.7) w.r.t. $p_{\theta_k}(Z|Y)$, resulting in:

$$\begin{aligned}\log p_\theta(Y) &= \int \log p_\theta(Z,Y) p_{\theta_k}(Z|Y) dZ - \int \log p_\theta(Z|Y) p_{\theta_k}(Z|Y) dZ \\ &= \underbrace{E_{\theta_k}\{\log p_\theta(Z,Y)|Y\}}_{:=Q(\theta,\theta_k)} - \underbrace{E_{\theta_k}\{\log p_\theta(Z|Y)|Y\}}_{:=V(\theta,\theta_k)}\end{aligned} \tag{B.8}$$

In the above equation we have used the fact that

$$\int \log p_{\theta_k}(Z|Y) dZ = \log p_{\theta_k}(Y) \tag{B.9}$$

It is worth noticing that the latent variables are here assumed to be continuous. However, there is nothing that prevents one from deriving the EM algorithm for discrete latent variables, the only difference is that the integrals in (B.8) is replaced by summations.

Studying the difference between the log-likelihood function $L_\theta(Y)$ evaluated at two different values θ and θ_k,

$$L_\theta(Y) - L_{\theta_k}(Y) = (Q(\theta,\theta_k) - Q(\theta_k,\theta_k)) + (V(\theta_k,\theta_k) - V(\theta,\theta_k)) \tag{B.10}$$

where the definitions in (B.8) have been used. It is now interesting to consider $(V(\theta_k,\theta_k) - V(\theta,\theta_k))$ in more detail. Straightforward application of the definition of $V(\theta,\theta_k)$ provided in (B.8) results in:

$$\begin{aligned}V(\theta_k,\theta_k) - V(\theta,\theta_k) &= \int \log\left(\frac{p_{\theta_k}(Z|Y)}{p_\theta(Z|Y)}\right) p_{\theta_k}(Z|Y) dZ \\ &= E_{\theta_k}\left\{-\log\left(\frac{p_\theta(Z|Y)}{p_{\theta_k}(Z|Y)}\right)|Y\right\}\end{aligned} \tag{B.11}$$

Note that this means that $V(\theta_k,\theta_k) - V(\theta,\theta_k)$ is the *Kullback-Leibler information distance* [94] between $p_{\theta_k}(Z|Y)$ and $p_\theta(Z|Y)$. Furthermore, the negative logarithm is a convex function, which implies that Jensen's inequality[2] can be used to establish

$$\begin{aligned}E_{\theta_k}\left\{-\log\left(\frac{p_\theta(Z|Y)}{p_{\theta_k}(Z|Y)}\right)|Y\right\} &\geq -\log E_{\theta_k}\left\{\frac{p_\theta(Z|Y)}{p_{\theta_k}(Z|Y)}|Y\right\} \\ &= -\log \int p_\theta(Z|Y) dZ = 0\end{aligned} \tag{B.13}$$

[2] Jensen's inequality states that if f is a convex function then

$$E\{f(x)\} \geq f(E\{x\}), \tag{B.12}$$

provided that both expectations exist.

which effectively proves that

$$V(\theta_k, \theta_k) - V(\theta, \theta_k) \geq 0. \tag{B.14}$$

Hence, if one makes use of this fact in (B.10) and chooses a new parameter θ such that $Q(\theta, \theta_k) \geq Q(\theta_k, \theta_k)$, the likelihood is in fact also increased, or at least is left unchanged:

$$Q(\theta, \theta_k) \geq Q(\theta_k, \theta_k) \quad \Longrightarrow \quad L_\theta(Y) \geq L_{\theta_k}(Y) \tag{B.15}$$

The EM algorithm now suggests itself that if one starts by computing $Q(\theta, \theta_k)$ according to its definition in (B.8), this function can then be maximized with respect to θ in order to obtain a new estimate θ_{k+1}. According to the above analysis, this new estimate will indeed produce a higher or at least the same likelihood as the previous estimate θ_k. This procedure is then repeated until convergence, which is summarized in the algorithm below. It is very important to note that the convergence is only guaranteed to be to a local minima.

Expectation Maximization Algorithm

---

1. Set $k = 0$ and initialize θ_0 such that $L_{\theta_0}(Y)$ is finite.
2. **Expectation (E) step:** Compute

$$Q(\theta, \theta_k) = E_{\theta_k} \log p_\theta(Z, Y) | Y = \int \log p_\theta(Z, Y) p_{\theta_k}(Z|Y) dZ \tag{B.16}$$

3. **Maximization (M) step:** Compute

$$\theta_{k+1} = \arg\max_\theta Q(\theta, \theta_k). \tag{B.17}$$

4. If not converged, update $k := k + 1$ and return to step 2.

The resulting function $Q(\theta,\theta_k)$ acts as a local (about θ_k) approximation of $L_\theta(Y)$. The EM algorithm seeks a maximizer of $L_\theta(Y)$ by computing and seeking maximizers of $Q(\theta,\theta_k)$. The evaluation of $Q(\theta,\theta_k)$ can be thought of as a smoothing step since it involves computing an expectation conditional on the whole observations sequence Y.

There are several ways in which the convergence check in step 4 of the above algorithm can be performed. One common way is to simply monitor the value of the log-likelihood and say that the algorithm has converged whenever the increase falls below a certain threshold $\varepsilon_L > 0$ (a typical default value is $\varepsilon_L = 10^{-6}$):

$$|L_{\theta_{k+1}(Y)} - L_{\theta_k(Y)}| \leq \varepsilon_L \tag{B.18}$$

Another way to check for convergence is to monitor the change in the parameter value between two consecutive iterations and state that the algorithm has converged when

$$\|\theta_{k+1} - \theta_k\|^2 \leq \varepsilon_P \tag{B.19}$$

where $\varepsilon_P > 0$ is some suitably chosen threshold.

The choice of the incomplete data Z is a key design variable in the implementation of the EM-algorithm. In [127] EM algorithm is introduced as a tutorial, and a simple example is provided to show how the EM algorithm can be used to solve the identification problem of a linear state-space model. In this case, the states $X := \{x_1, ..., x_{N+1}\}$ plays the role of latent

variables, due to the fact that if the states were known one could find the parameters simply by solving a linear regression problem.

The aim of this appendix is to suggest an algorithm that finds the θ_N^{ML} that maximizes (B.4) for each N. As a result it cannot be guaranteed that θ_N^{ML} is actually found. This is basically the same situation as when (B.4) can be explicitly maximized by gradient methods, and one cannot guarantee that solution ends up in a local maximum.

B.4 Problem Formulation

In this section the problem formulation is briefly introduced. In this section the problem formulation is briefly introduced. The control loop is modeled by a Hammerstein system as depicted in Figure B.1. In details, x and y are the linear process input and output (that is, MV and PV respectively), u is the controller output (that is, OP), r is the loop set point, w and v are sequences of Gaussian white noise.

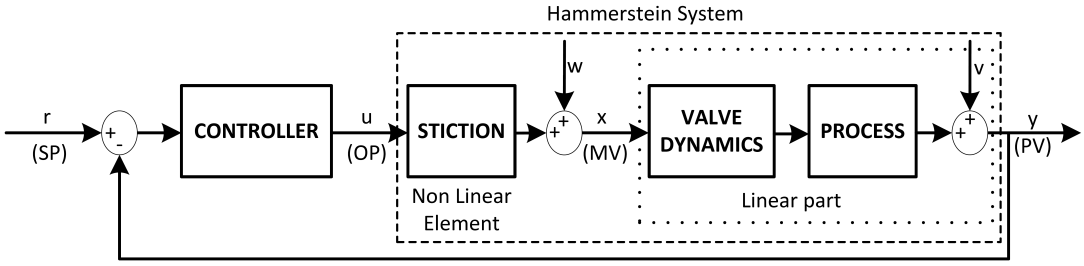

Figure B.1: Hammerstein system representing the (sticky) control valve followed by the linear process, inserted into the closed-loop system.

First of all, an easy method which employ EM algorithm in the problem of valve stiction estimation inside the framework of Hammerstein model is briefly described below. The usual grid of search for the stiction parameters is built up, and an EM algorithm is employed for each grid combination. Only the identification of the linear part of the system is performed, by using process output y and the candidate valve output x. A common data-driven stiction model (e.g., [87, 76]), and a standard linear process model could be used (e.g., ARX, ARMAX, State Space).

To be honest, this approach seems just another interpretation of the typical – almost abused – approach to tackle the problem of valve stiction estimation. It is surely a first solid step to introduce EM algorithms in this context, but it does not seem to be able to produce significant advantages in terms of accuracy, precision and computational times with respect to basic methods, as least squares method with ARX linear model. Moreover, this approach does not exploit the peculiarity of EM algorithm in managing missing variables, that is, in this case, the unmeasurable signal of valve position (x, that is, MV).

Therefore, a full EM-based method has to be introduced. A draft of approach is here proposed.

The following *extended* Hammerstein system is considered. Valve stiction is described with He's model [76], and the linear process dynamics with a simple ARX model.

A flowchart of the data-driven model of He is given in Figure B.2.

The sticky valve has a nonlinear dynamics expressed by the following two simple relations:

$$x_k = \begin{cases} x_{k-1} + [e_k - \text{sign}(e_k) \cdot f_d] & \text{if} \quad |e_k| > f_s \\ x_{k-1} & \text{if} \quad |e_k| \leq f_s \end{cases} \tag{B.20}$$

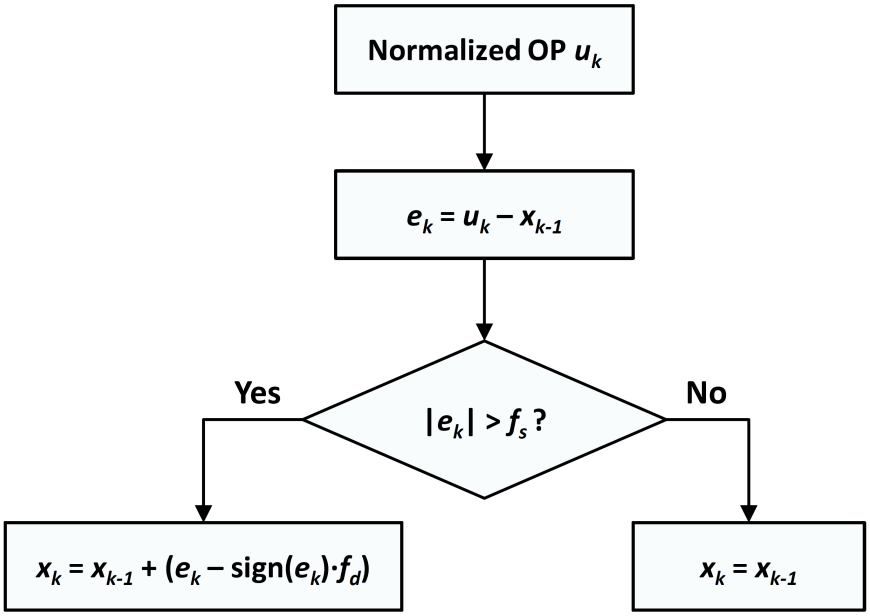

Figure B.2: Flowchart of He's stiction model (redrawn from [74]).

where x is the stem position (valve output), u is the actuator air pressure, that is, the controller output (valve input). Two parameters are involved: f_s the static friction force, and f_d the dynamic friction force. Note that e_k is a sort of valve position error: $e_k = u_k - x_{k-1}$. By substituting e_k, one gets:

$$x_k = \begin{cases} u_k - [\text{sign}(u_k - x_{k-1}) f_d] & \text{if} \quad |u_k - x_{k-1}| > f_s \\ x_{k-1} & \text{if} \quad |u_k - x_{k-1}| \leq f_s \end{cases} \tag{B.21}$$

and then, by separating the nonlinear *sign* function, three different input-output relations for the sticky valve are possible:

$$x_k = \begin{cases} u_k - f_d & \text{if} \quad |u_k - x_{k-1}| > f_s \quad \& \quad u_k - x_{k-1} > 0 \\ u_k + f_d & \text{if} \quad |u_k - x_{k-1}| > f_s \quad \& \quad u_k - x_{k-1} < 0 \\ x_{k-1} & \text{if} \quad |u_k - x_{k-1}| \leq f_s \end{cases} \tag{B.22}$$

The linear part is a standard ARX model:

$$\begin{aligned} y_k &= \sum_{j=1}^{n} -a_j \cdot y_{k-j} + \sum_{j=1}^{m} b_j \cdot x_{k-j-L} + v_k \\ &= \theta_y \varphi_y + \theta_x \varphi_x + v_k \end{aligned} \tag{B.23}$$

where a_j and b_j are the coefficients for the autoregressive and exogenous part, respectively. Linear parameters can also be expressed by vectors θ_y, θ_x, with $\varphi_y = [y_{k-1}, ..., y_{k-n}]^T$ and $\varphi_x = [x_{k-1}, ..., x_{k-m}]^T$. For simplicity, the orders (n,m) and the time-delay units L are assumed known.

The Hammerstein system (see Figure B.1) is now reformulated so that the friction nonlinearity becomes a set of simple linear and parallel relations (B.22), thus constituting a switching "multi-mode" model to be integrated with the linear dynamics of the process, to form an extended model.

Therefore, a switching state variable I has to be introduced. This variable can assume only three natural values for all time samples: $I_k = 1, 2, 3 \, \forall k$. The valve dynamics can be then summarized as:

$$x_k^i = A^i x_{k-1}^i + B^i u_k + F_d^i + w_k \quad \text{with} \;\; i = 1, 2, 3 \tag{B.24}$$

where $A = [0, 0, 1]$, $B = [1, 1, 0]$, and $F_d = [-f_d, f_d, 0]$.

The problem to be solved has the following features:

- $C_{obs} := \{U, Y\}$: the observed variables are the sequence of valve input $U := \{u_1, ..., u_N\}$, and the sequence of process output $Y := \{y_1, ..., y_N\}$, where N is the total number of time samples.
- $C_{mis} := \{X, I\}$: the missing variables are the sequence of valve output $X := \{x_1, ..., x_N\}$, and the sequence of state variable $I := \{I_1, ..., I_N\}$.
- $\theta := \{f_d, f_s, \theta_{lin}, \sigma_v^2, \sigma_w^2\}$: the set of parameters to be identified, where $\theta_{lin} = [\theta_y, \theta_x]$ is the set of parameters for the linear part of the system, and σ_v^2, σ_w^2 are the variances of the two Gaussian noises.

The Q function can be written as:

$$Q(\theta, \theta_k) = E_{\theta_k} \log p_\theta(C_{mis}, C_{obs}) | C_{obs} = \int \log p_\theta(C_{mis}, C_{obs}) \cdot p_{\theta_k}(C_{mis} | C_{obs}) \mathrm{d}C_{mis} \tag{B.25}$$

By substituting corresponding variables in (B.25), the joint probability $\log p_\theta(I, X, Y, U)$ is:

$$\log p_\theta \left(I_N, x_N, y_N, u_N | I_{1:N-1}, X_{1:N-1}, Y_{1:N-1}, U_{1:N-1}\right) \cdot p(I_{1:N-1}, X_{1:N-1}, Y_{1:N-1}, U_{1:N-1}) \tag{B.26}$$

By applying the chain rule, one gets:

$$\log \prod_{k=1}^{N} p_\theta \left(I_k, x_k, y_k, u_k | I_{1:k-1}, X_{1:k-1}, Y_{1:k-1}, U_{1:k-1}\right) \tag{B.27}$$

By looking at graph for the system of Figure B.3, the generic k^{th} term of (B.27) can be written as the product of three probabilities:

$$p_\theta(y_k | x_k, y_{k-1:k-n}) \cdot p_\theta(x_k | I_k = i, u_k, x_{k-1}) \cdot p_\theta(I_k | u_k, x_{k-1}) \tag{B.28}$$

The first term of (B.28), with respect to process output y, has a Gaussian (normal) distribution

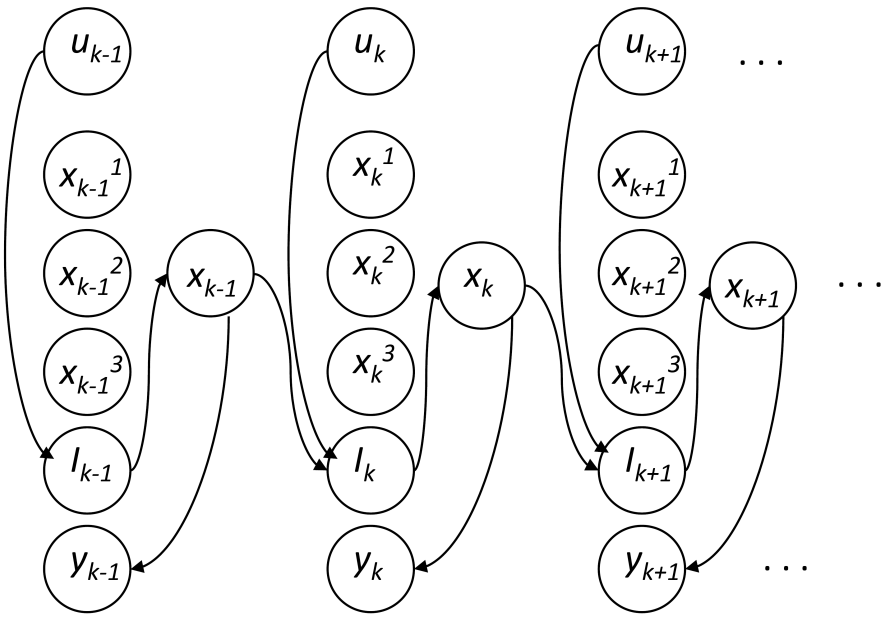

Figure B.3: Graph of the system.

with zero-mean and variance σ_v^2:

$$y_k - \theta_y \varphi_y - \theta_x \varphi_x := F_y = v_k \sim N(0, \sigma_v^2) \tag{B.29}$$

$$p(F_y) = \frac{1}{\sigma_v\sqrt{2\pi}} \exp\left(\frac{-\left(F_y - 0\right)^2}{2\sigma_v^2}\right) \tag{B.30}$$

Also the second term, with respect to the valve output x, has a Gaussian (normal) distribution with zero-mean and variance σ_w^2:

$$x_k^i = A^i x_{k-1}^i - B^i u_k - F_d^i := F_x^i = w_k \sim N(0, \sigma_w^2) \tag{B.31}$$

$$p(F_x^i) = \frac{1}{\sigma_w\sqrt{2\pi}} \exp\left(\frac{-\left(F_x^i - 0\right)^2}{2\sigma_w^2}\right) \tag{B.32}$$

The third term, with respect to the switching variable state I, is a discrete probability with two different switching terms:

$$\begin{aligned} P(I_k = 1,2) &= P(|u_k - x_{k-1}| > f_s) = P(e_k < -f_s \vee e_k > f_s) \\ P(I_k = 3) &= P(|u_k - x_{k-1}| \leq f_s) = P(-f_s \leq e_k \leq f_s) \end{aligned} \tag{B.33}$$

so that $\sum_{i=1}^{3} P(I_k = i) = 1$.

These probabilities can be expressed by means of the cumulative distribution function (CDF). Figure B.4 shows a probability density function (PDF) and a CDF for a Gaussian with mean $\mu = 0.2$, variance $\sigma = 1$, and static friction $f_s = 1.5$. Since in general $P(e_k \leq E_a) = CDF(E_a)$ and $P(E_a \leq e_k \leq E_b) = CDF(E_b) - CDF(E_a)$, one gets:

$$\begin{aligned} P(e_k < -f_s \vee e_k > f_s) &= P(e_k < -f_s) + P(e_k > f_s) = CDF(-f_s) + (1 - CDF(f_s)) \\ P(-f_s \leq e_k \leq f_s) &= P(e_k \leq f_s) - P(e_k \leq -f_s) = CDF(f_s) - CDF(-f_s) \end{aligned} \tag{B.34}$$

Indeed, the two switching probabilities sum to 1.

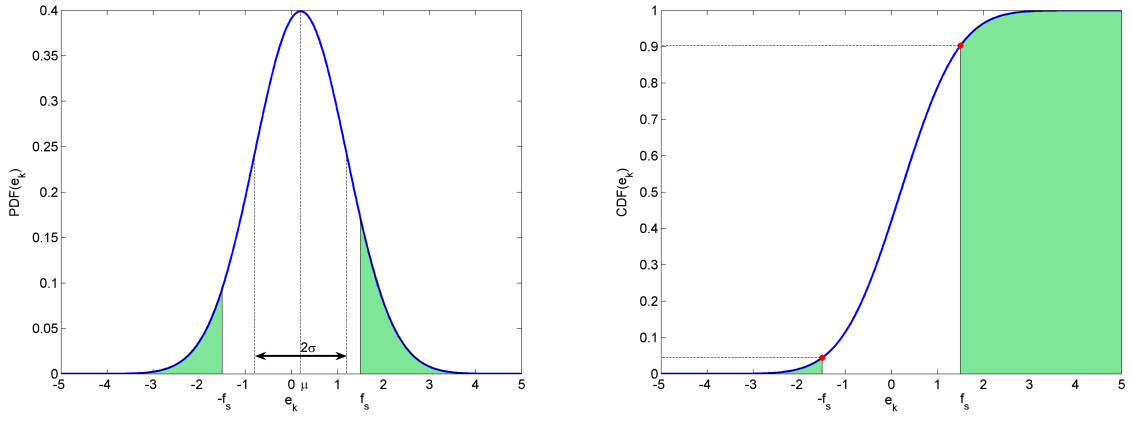

(a) Probability Density function. **(b)** Cumulative Density Function.

Figure B.4: Probability plots.

The CDF for the Gaussian distribution of e_k has the following expression:

$$CDF(e_k) = \frac{1}{2}\left[1 + \text{erf}\left(\frac{e_k - \mu}{\sigma\sqrt{2}}\right)\right] \tag{B.35}$$

with $z_k = \frac{e_k - \mu}{\sigma\sqrt{2}}$ and $\text{erf}(z_k) = \frac{2}{\sqrt{\pi}} \int_0^{z_k} \exp(-t^2)\,dt$. Thus, numerical values of probability can be computed.

B.5 Conclusions and Future Developments

This appendix has presented a draft of method which applies Expectation Maximization algorithm to the problem of valve stiction estimation in control loops. A introduction to EM algorithms and maximum likelihood (ML) problems has been given within the setting of dynamic systems. The specific formulation of problem has been stated, but the procedure has not been yet fully derived. Future activity will imply a complete derivation of the algorithm, and then applications to simulation examples and real data from pilot facilities and industrial plants.

Appendix C

Stiction Quantification - Further Applications

Abstract [1]

This appendix completes the study of scientific approaches and related techniques regarding estimation of valve stiction. Chapter 2 was mainly devoted to an overview of features of different techniques proposed for modeling, detection, quantification, and compensation of friction in control valves.

In this appendix, in the perspective of a very practical approach, performance of some well-established methods for stiction quantification are compared by application on the same industrial datasets of different origin, in order to show how discrepancies may arise and possible causes of error, thus giving indications of next research work to carry out.

[1] This appendix is based on [26]: *Comparison of Techniques for Valve Stiction Quantification*.

C.1 Introduction

Chapter 2 has reviewed existing literature and techniques appeared in recent years about different issues of valve stiction. It was put into evidence that, while several aspects can be considered to have reached a mature level of knowledge, stiction quantification should deserve further research efforts. This happens because the knowledge of stiction amount is a very important issue in order to follow stiction evolution in time and to be able to predict valve maintenance. Techniques presented up to date usually have been validated on few industrial data and therefore, according to the author's opinion, there is room for improvements in order to obtain larger reliability of predictions.

In this appendix, performance of some well-established methods for stiction quantification are compared by application on different industrial datasets. The text is organized as indicated in the sequel. In section C.2, some recent techniques, selected on the basis of their characteristics, are illustrated with some more details. Afterwards, they are compared on industrial datasets, having different origin. A first dataset, analyzed in section C.3, derives from a benchmark made available in [85], while a second dataset, presented in section C.4, has been created during a multiannual plant implementation of a performance monitoring and valve diagnostic system developed by the authors [123]. This opportunity is to be considered a distinctive aspect of this study, as it allows one to put into evidence the real practical significance of different techniques, very often presented and tested only in simulation or on a limited number of industrial data. Finally, overall conclusions and future trends of research activity are reported in section C.5.

C.2 Stiction Quantification Techniques

As discussed in Chapter 4, the main difficulty in stiction detection and quantification is that the actual valve stem position (MV) is not available in the most of industrial plants [25]. Furthermore, the *true* value of valve stiction is not known a priori and cannot be measured through specific invasive tests. Therefore, the validation of a proposed technique on a single set of industrial data can be useless. This is confirmed by the fact that different detection and quantification techniques can strongly disagree when applied on the same data.

In [85] different techniques for stiction detection and quantification can yield different and inconsistent results when applied on the benchmark data used as bed of comparison. In Chapter 4 it was also underlined that stiction estimation may fail in the case of simultaneous presence of external process disturbances. Repeating system identification and stiction estimation for different acquisitions for the same valve allows one to follow the evolution of stiction values in time and to disregard anomalous cases, which result as *outliers* with respect to the main trend [25]. Afterwards, control operators, by comparing stiction with acceptable thresholds, may be able to schedule valve maintenance or, if the case, to perform on-line stiction compensation.

In this appendix, the focus is on stiction detection and estimation. A large number of industrial data is used to compare several different stiction quantification techniques in order to establish their strengths and weaknesses.

Firstly, 8 quantification methods are compared on a large set of the benchmark data available in [85]. Then, 4 of these techniques are selected to be further applied on a industrial data set obtained from Italian refinery plants, which consists of different acquisitions for the same valves for long times.

The stiction quantification methods here compared are:

- the original method of Chapter 3 ([22, 25]), based on grid search and Hammerstein system identification (Kano's stiction [87] model plus ARX linear model), here called HAM1;

- the method of Chapter 4 ([29, 30]) based on grid search and Hammerstein identification (Kano's stiction model plus State Space model), here called HAM2;
- the method of Chapter 4 ([29, 30]) based on grid search and Hammerstein identification (He's stiction model [76] plus E(xtended)-ARX model), here called HAM3;
- the original technique of He and Wang [75], based on their semiphysical stiction model [74] and simplifying assumptions on signal oscillations, here called He; [2]
- the Hammerstein system identification method proposed by Karra and Karim [90], here called K&K;
- the method of Lee et al. [95], based on constrained optimization and contour map, here called Lee;
- the method of Jelali [85], based on global search algorithms, here called Jelali;
- the Hammerstein-Wiener identification approach of Romano and Garcia [118], here called R&G.

These quantification techniques have been chosen for different reasons: Jelali, K&K and Lee methods are now considered well-established techniques of the literature, and their results are easily accessible. R&G is an interesting example of Hammerstein-Wiener identification, which models the process as nonlinear. He method is a novel simplified approach which has shown recent appealing results. The other three Hammerstein methods have been developed in Chapter 3 and 4, and can now be considered robust methodologies validated on a large set of data obtained from pilot and industrial plants.

C.3 Benchmark Data

In [86] an exhaustive comparative study of 11 methods for detecting stiction in control valves was presented. This study involved 93 different data sets from different process industries, including power plants (POW), chemical plants (CHEM), pulp and paper mills (PAP), commercial buildings (BAS), mining (MIN) and metal processing (MET).

This dataset is now a well-known benchmark useful for validation of novel techniques concerning control loop performance assessment. In the same [86], a brief comparison of the results of three stiction quantification techniques were also presented: Karra and Karim [90], Lee et al. [95], and Jelali [84] methods were compared on some of these industrial loops.

In [75] the authors compared their stiction quantification method with other 4 published methods using 20 industrial loops. In the present appendix, an even more comprehensive comparison of an higher number (8) of stiction quantification methods is shown. A thorough discussion of the results is then provided, explaining the (possible) reasons of success and failure of the methods in different cases.

Table C.1 provides stiction quantification results on 29 industrial loops of the benchmark [86]. The real root causes of malfunction for these loops are known. The estimated values of the two stiction parameters are reported in different columns: S (dead band + stick band), and J (slip-jump).

The results of the first three Hammerstein methods (HAM1, HAM2, HAM3) are obtained by using fixed parameters: the time-delay and the orders of the linear process models are, respectively, $t_d = 0$, and $(n; m) = (2; 2)$ for HAM1 (ARX) and HAM3 (EARX), $n = 2$ for HAM2 (State Space). The step size of 2-D grid of stiction parameters is $h_S = h_J = 0.1$ (compare Chapter 4).

Results of the He method are obtained using the codes provided by the authors with default values of parameters. Note that this method naturally estimates dynamic friction f_d by simply using the span of oscillation of controller output signal (OP) and information of the true time

[2] *Acknowledgment*: the author thank Dr. He providing his MATLAB codes used in this study.

delay θ. This methods requires also information of the process gain K_p to estimate values of static friction f_s. Here, in the sake of simplicity, for all the loops, the model time delay is fixed to $\theta = 0$, and, in Table C.1, the results of He method are reported only in the form of parameter S. Nevertheless, $f_d (\approx S/2)$ can provide by itself a good picture of the stiction severity, and f_s could be assumed slightly greater than f_d.

The results of the other four methods (K&K, Lee, Jelali, and R&G) are taken directly from the literature. The cells filled with a short dash (-) indicate that the loop was not analyzed in the original publication.

It worth to recall that S, which is equal to $f_s + f_d$, or approximately to $2f_d$, is more easy to be identified and usually provide a significant measure of stiction. On the opposite, J, equal to $f_s - f_d$, or approximately to $2(f_s - f_d)$, is much more difficult to be estimated since it is usually very small and hidden by field noise in industrial data [29, 50].

Table C.1: Benchmark data: comparison of stiction quantification techniques.

loop	stic ?	HAM1		HAM2		HAM3		He	K&K		Lee		Jelali		R&G	
		S	J	S	J	S	J	S	S	J	S	J	S	J	S	J
CHEM 1	yes	0.7	0.5	0.7	0.4	0.9	0.0	0.82	0.5[a]	0.5[a]	0.39	0.04	-	-	-	-
CHEM 2	yes	3.3	0.1	3.6	0.0	0.4	0.0	8.35	4.0	0.0	2.52	0.65	-	-	-	-
CHEM 3	no	0.1	0.0	0.0	0.0	0.1	0.0	1.52	0.0[a]	0.0[a]	0.0[b]	0.0[b]	-	-	-	-
CHEM 4	no	7.9	7.4	4.7	1.5	7.5	3.4	13.4	3.5	2.5	0.03	0.02	-	-	-	-
CHEM 5	yes	0.4	0.0	0.3	0.1	0.4	0.0	0.39	0.4	0.0	0.26	0.09	-	-	-	-
CHEM 6	yes	0.0	0.0	0.0	0.0	0.0	0.0	0.31	0.2	0.2	0.01	0.01	-	-	-	-
CHEM10	yes	1.8	1.7	1.8	1.7	1.7	0.9	1.93	1.85	0.05	1.77	1.73	-	-	-	-
CHEM 11	yes	0.0	0.0	0.1	0.0	0.0	0.0	1.76	0.48	0.06	0.24	0.06	-	-	-	-
CHEM 12	yes	1.6	0.6	1.5	0.3	1.8	0.0	1.89	0.5	0.5	1.42	0.14	-	-	-	-
CHEM 13	no	0.5	0.0	0.6	0.0	0.4	0.0	2.11	2.0	2.0	0.04[c]	0.04[c]	-	-	-	-
CHEM 14	no	1.5	0.0	1.8	0.3	1.7	0.2	2.57	1.6	0.0	0.76[c]	0.28[c]	-	-	-	-
CHEM 15	no (?)	0.0	0.0	1.7	1.0	0.0	0.0	2.41	0.5	0.2	0.18[d]	0.11[d]	-	-	-	-
CHEM 16	no (?)	0.1	0.1	0.1	0.1	0.5	0.4	2.97	0.0	0.0	0.10[d]	0.10[d]	-	-	-	-
CHEM 23	yes	0.2	0.1	0.4	0.0	24.8	0.1	27.8	9.0	9.0	21.57	0.28	-	-	-	-
CHEM 24	yes	8.1	0.0	0.9	0.7	16.0	0.0	19.3	23.0	1.0	20.64[e]	1.07[e]	22.9	0.81	-	-
CHEM 25	yes	2.0	0.2	1.4	0.2	1.8	0.3	1.92	1.8	0.3	1.62[f]	1.62[f]	1.8	0.59	1.59	0.44
CHEM 26	yes (?)	0.1	0.0	0.7	0.1	0.1	0.1	5.16	0.6	0.6	4.11	1.59	-	-	-	-
CHEM 28	yes (?)	0.9	0.1	0.7	0.3	6.0	0.0	4.76	1.4	0.4	1.63	0.35	-	-	1.59	0.87
CHEM 29	yes	3.4	0.0	3.4	0.0	3.5	0.0	11.25	3.2[a]	0.2[a]	5.35[g]	0.51[g]	-	-	9.2	0.0
CHEM 32	yes	7.4	1.5	6.5	0.2	13.0	0.0	22.1	15.0[h]	4.0[h]	12.28	0.08	-	-	-	-
PAP 2	yes	2.6	0.0	2.6	0.0	2.7	0.0	3.49	2.6	1.8	2.52[i]	2.52[i]	3.0	0.84	0.42	0.0
PAP 4	no	2.3	0.3	2.4	0.0	17.3	0.0	15.0	1.0	0.3	4.27	0.12	-	-	-	-
PAP 5	yes	0.0	0.0	0.0	0.0	0.4	0.0	0.41	0.0	0.0	0.01[j]	0.01[j]	-	-	0.07	0.0
PAP 7	no	0.0	0.0	0.0	0.0	0.1	0.0	0.21	0.0[k]	0.0[k]	0.07	0.07	-	-	-	-
PAP 9	no	0.0	0.0	0.1	0.1	3.9	0.1	3.81	2.0[h]	2.0[h]	0.0	0.0	-	-	-	-
MIN 1	yes	1.0	0.0	1.1	0.1	1.7	0.0	1.63	1.2[k]	1.2[k]	1.16	1.16	1.02	0.96	1.0*	1.0*
BAS 7	yes	1.2	0.0	1.2	0.0	1.4	0.0	1.67	1.6	0.1	0.61	0.53	-	-	-	-
POW 2	yes	8.4	0.4	8.4	0.4	9.9	0.4	9.88	12.0[a]	12.0[a]	1.15	0.87	11.47	1.10	5.08	0.01
POW 4	yes	0.9	0.0	1.0	0.3	1.4	0.0	3.73	3.6[a]	1.2[a]	0.58	0.39	4.49	2.49	-	

a: applied on the first 1000 samples; *b*: on the data window 100-900 samples; *c*: on the data window 100-700 samples;
d: on the data window 800-1200 samples; *e*: on the data window 100-800 samples; *f*: on the data window 100-350 samples;
g: on the data window 2000-2500 samples; *h*: on the data window 1-600 samples; *i*: on the first 450 samples; *j*: on the first 3000 samples;
k: on the first 2000 samples; *: results from Choudhury et al. [50]

In general, as it results from Table C.1, different methods can deliver very different values for the stiction parameter estimates. Note that the exact stiction estimates are clearly dependent on several issues. In addition to some general aspects (e.g., the dataset used in identification, choice of objective function, identification algorithm), in the case of Hammerstein system identification with grid search algorithm, also the following issues are important: type, order, and time-delay of the process linear model; type of the stiction model; step size of the search grid. Furthermore, the identification results can be sensitive to the initialization of the Kano's stiction model. This issue could seem a negligible aspect, but in reality, it has been verified to

play an important role [30].

It should be also noted that, except for HAM3 and K&K methods, which use extended process linear models, the other techniques do not differentiate other causes from stiction. In other words, the estimation could be misleading for the case of oscillation not caused by stiction, or for the case of simultaneous presence of stiction and external disturbance. Therefore, it is not only preferable, but also necessary to confirm stiction by detection methods before quantifying its amount. Detailed comments about the results of Table C.1 are reported in the next subsection.

C.3.1 Results on benchmark data

As stated before, it is clear that different methods can yield different values for the stiction parameter estimates. However, little discrepancies in the numerical values are to be tolerated in order to regard as consistent the results of all the selected methods. In this view, according to the homogeneity of the estimates, the benchmark data can be divided in three categories:

- *Inconsistent Loops*: data with very inhomogeneous results (e.g., some values close to zero vs. some significant values of stiction, or very different non zero values);
- *Partially Consistent Loops*: data with only 1 or 2 inconsistent estimates which appear as wrong values with respect to the average amount (*outliers*);
- *Consistent Loops*: data with (very) homogeneous results among all the selected methods.

This classification is based on basic statistics according to the following procedure. For each benchmark loop, mean values ($\bar{S}$, $\bar{J}$) and standard deviations (σ_S, σ_J) are computed between all the available estimates of stiction parameters. Two regularity factors are then computed:

$$R_S = f\left(\frac{\bar{S}}{\sigma_S}\right) = \frac{1}{3}\cdot\frac{\bar{S}}{\sigma_S} \qquad R_J = f\left(\frac{\bar{J}}{\sigma_J}\right) = \frac{1}{3}\cdot\frac{\bar{J}}{\sigma_J} \tag{C.1}$$

These two indices give a simple measure of the homogeneity of the estimates, in analogy to what presented by [157] for the regularity index of oscillation period in time trends. The threshold value for both R factors is fixed as unitary, according to what suggested in [157]. Afterwards, for the sets of values with $R_S < 1$, the number of inconsistent estimates (*outliers*) is assessed.

An estimate (S_i) is here considered an *outlier* with respect to the whole set if its distance from the mean value is bigger than the standard deviation of the set:

$$|S_i - \bar{S}| > \sigma_S \tag{C.2}$$

Now, mean values ($\bar{S}^{II}$) and standard deviations (σ_S^{II}) are recomputed without the *outliers* only for the estimates of S. Finally, a second regularity factor can be defined:

$$R_S^{II} = \frac{1}{3}\cdot\frac{\bar{S}^{II}}{\sigma_S^{II}} \tag{C.3}$$

Also the threshold value for R_S^{II} factor is fixed to unitary. The whole classification criterion is schematically reported in Table C.2. It worth to notice that R_J factor is not considered in the classification, since the estimation of J parameter is a more difficult task. As a matter of fact, the sets of J estimates result typically much more variable than sets of S: $R_J < R_S$.

Note also that the proposed regularity factors prove to be very low as the average value of estimates approaches zero ($\bar{S}^{II} \to 0$); that is, when a negligible amount of stiction is quantified. Therefore, the previous criterion has to be relaxed for these low-stiction cases in order to properly assess which set of estimates are fairly consistent. As a consequence, a low-level threshold for the second mean value of S is fixed ($\bar{S}_{tr}^{II} = 0.5$) and a corrected regularity factor is computed: $R_{S_{co}}^{II} = 1/3 \cdot (\bar{S}_{tr}^{II}/\sigma_S^{II})$.

Table C.2: Criterion for the classification of benchmark data.

Category	Regularity factor	N° of outliers	Regularity factor without outliers
Consistent Loops (C)	$R_S > 1$	-	-
Partially Consistent Loops (P-C)	$R_S < 1$	1 or 2	$R_S^{II} > 1$ or $R_{S_{co}}^{II} > 1$
Inconsistent Loops (I)	$R_S < 1$	2 or more	$R_S^{II} < 1$ & $R_{S_{co}}^{II} < 1$

Applying the previous criterion of Table C.2 to the benchmark data, the following result is obtained:

- 11 (out of 29) are considered as *Inconsistent Loops*: CHEM 4, CHEM 11, CHEM 13, CHEM 15, CHEM 16, CHEM 23, CHEM 26, CHEM 32, PAP 4, PAP 9, and POW 4.
- 12 are the *Partially Consistent Loops*: CHEM 2, CHEM 3, CHEM 6, CHEM 12, CHEM 14, CHEM 24, CHEM 28, CHEM 29, PAP 2, PAP 5, PAP 7, and POW 2.
- 6 are the *Consistent Loops*: CHEM 1, CHEM 5, CHEM 10, CHEM 25, MIN 1, and BAS 7.

Overall results are reported in Table C.3, while details for each loop are given in the following subsections.

Table C.3: Classification results.

loop	stic ?	# of	With all methods						# of	Without outliers				Category
		Methods	$\bar{S}$	σ_S	$\bar{J}$	σ_J	R_S	R_J	Outliers	$\bar{S}^{II}$	σ_S^{II}	R_S^{II}	$R_{S_{co}}^{II}$	
CHEM 1	yes	6	0.67	0.19	0.29	0.25	1.16	0.39	-	-	-	-	-	C
CHEM 2	yes	6	3.70	2.61	0.15	0.28	0.47	0.18	2	3.36	0.63	1.79	-	P-C
CHEM 3	no	6	0.29	0.61	0.00	0.00	0.16	-	1	0.04	0.05	0.24	3.04	P-C
CHEM 4	no	6	6.17	4.56	2.96	2.78	0.45	0.36	2	5.90	2.14	0.92	-	I
CHEM 5	yes	6	0.36	0.06	0.04	0.05	1.92	0.24	-	-	-	-	-	C
CHEM 6	yes	6	0.09	0.14	0.04	0.09	0.21	0.16	2	0.003	0.01	0.17	33.33	P-C
CHEM10	yes	6	1.81	0.08	1.22	0.74	7.80	0.55	-	-	-	-	-	C
CHEM 11	yes	6	0.43	0.68	0.02	0.03	0.21	0.24	1	0.16	0.20	0.27	0.82	I
CHEM 12	yes	6	1.45	0.50	0.31	0.25	0.97	0.41	1	1.64	0.20	2.76	-	P-C
CHEM 13	no	6	0.94	0.88	0.41	0.89	0.36	0.15	2	0.39	0.24	0.53	0.68	I
CHEM 14	no	6	1.66	0.58	0.16	0.15	0.95	0.35	2	1.67	0.15	3.64	-	P-C
CHEM 15	no (?)	6	0.80	1.02	0.26	0.42	0.26	0.21	1	0.48	0.71	0.22	0.23	I
CHEM 16	no (?)	6	0.63	1.16	0.14	0.15	0.18	0.31	1	0.16	0.19	0.27	0.85	I
CHEM 23	yes	6	13.96	12.37	1.90	3.97	0.38	0.16	3	18.46	8.35	0.74	-	I
CHEM 24	yes	7	15.83	8.36	0.60	0.49	0.63	0.40	1	18.32	5.64	1.08	-	P-C
CHEM 25	yes	8	1.74	0.19	0.52	0.50	2.99	0.34	-	-	-	-	-	C
CHEM 26	yes (?)	6	1.80	2.24	0.48	0.66	0.27	0.24	2	0.38	0.32	0.39	0.52	I
CHEM 28	yes (?)	7	2.43	2.08	0.34	0.30	0.39	0.37	2	1.24	0.42	0.99	-	P-C*
CHEM 29	yes	7	5.61	3.29	0.12	0.21	0.57	0.19	2	3.77	0.89	1.41	-	P-C
CHEM 32	yes	6	12.71	5.66	1.16	1.70	0.75	0.23	2	11.92	6.07	0.65	-	I
PAP 2	yes	8	2.49	0.90	0.74	1.04	0.93	0.24	2	2.67	0.17	5.19	-	P-C
PAP 4	no	6	7.05	7.17	0.14	0.15	0.33	0.32	2	2.49	1.35	0.62	-	I
PAP 5	yes	7	0.13	0.19	0.00	0.00	0.22	0.14	2	0.02	0.03	0.17	5.47	P-C
PAP 7	no	6	0.06	0.08	0.01	0.03	0.25	0.15	1	0.03	0.05	0.24	3.49	P-C
PAP 9	no	6	1.64	1.88	0.44	0.87	0.29	0.17	2	0.53	0.98	0.18	-	I
MIN 1	yes	8	1.23	0.28	0.63	0.57	1.45	0.37	-	-	-	-	-	C
BAS 7	yes	6	1.28	0.38	0.13	0.23	1.12	0.18	-	-	-	-	-	C
POW 2*	yes	8	8.29	3.59	2.17	4.35	0.77	0.17	2◇	8.86	2.17	1.36	-	P-C
POW 4	yes	7	2.24	1.63	0.73	0.93	0.46	0.26	2	2.52	1.59	0.53	-	I

*: basically on the threshold value. ◇: outliers are assessed by using distance from real values - here known - of stiction.

C.3.2 Loops with Inconsistent results

The level control (LC) loop CHEM 4 is known to suffer from controller tight tuning and to have no stiction problems. It shows clear sinusoidal trends in the controlled variable signal (PV),

and in the controller output signal (OP) (Figure C.1a), and an elliptical limit cycle on PV(OP) diagram (Figure C.1b). The level set point (SP) is actually constant. Lee method correctly detects no stiction ($S = 0.03$, $J = 0.02$); on the contrary, all the other methods (K&K, HAM1, HAM2, HAM3, and He) indicate the presence of significant stiction ($S \geq 3.5$; $J \geq 2.5$), which results as false alerts.

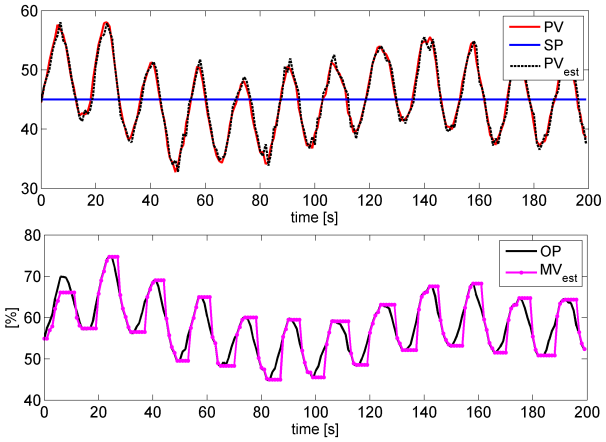

(a) time trends - PV and MV estimated with HAM1 method.

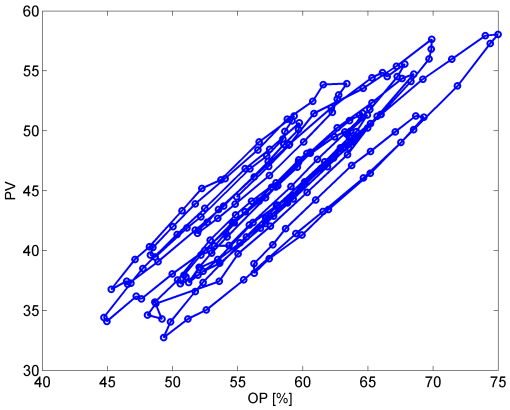

(b) elliptic-shaped limit cycle on PV(OP) plot.

Figure C.1: Results for loop CHEM 4.

For the flow control (FC) loop CHEM 11, which suffers from stiction, K&K and Lee methods estimate a little amount of stiction ($S < 0.5$; $J < 0.5$). On the contrary, the other three Hammerstein models give zero values of stiction; while He method yields a higher amount ($S = 1.76$).

The CHEM 13 is an analyzer control (AC) loop with a faulty steam sensor and no stiction problems. Lee method gives the most appropriate estimate ($S = 0.04$, $J = 0.04$); while the other three Hammerstein methods (HAM1, HAM2, HAM3) yield low amount of stiction ($S \approx 0.5$). K&K and He methods give significant values: $S = 2.0$, $J = 2.0$, and $S = 2.11$, respectively.

The pressure control (PC) loop CHEM 15 (likely) suffers from oscillation induced by other loops and has no stiction problems. HAM1 and HAM3 methods agree and estimate zero values of stiction; Lee and K&K yield very low values ($S < 0.5$; $J < 0.2$); while HAM2 and He methods estimate significant amounts of stiction: $S = 1.7$, $J = 1.0$, and $S = 2.41$, respectively.

Also the PC loop CHEM 16 (likely) suffers from interaction and has no stiction problems. Here 6 methods yield negligible amount of stiction ($S < 0.1$, $J < 0.1$). HAM3 gives a slightly higher amount of stiction ($S = 0.5$, $J = 0.4$); while He method wrongly gives a significant amount of stiction ($S = 2.97$).

The FC loop CHEM 23 is an example of evident stiction visible in the measured signals (Figure C.2a): triangular shapes in OP trend and rectangular shapes in PV signal, to be considered proportional to MV signal. Also the PV(OP) plot has the very typical pattern of loops with sticky valve (Figure C.2b). However, this loop generates very inconsistent outcomes. HAM1 and HAM2 methods agree and wrongly estimate very low values of stiction ($S \leq 0.4$; $J \leq 0.1$). On the contrary, HAM3, Lee and He methods yield very large amount of stiction: $S \in [21.57; 27.8]$, $J \in [0.1; 0.28]$; while K&K technique gives a lower amount of stiction ($S = 9.0$, $J = 9.0$).

For the LC loop CHEM 26, which (likely) suffers from stiction, only Lee and He methods give a significant amount of stiction, respectively: $S = 4.11$, $J = 1.59$, and $S = 5.16$. Conversely, HAM2 and K&K methods yield very low values ($S \in [0.6; 0.7]$, $J \in [0.1; 0.6]$); while HAM1 and HAM3 methods estimate close to zero values.

The FC loop CHEM 32 suffers from valve stiction. All the methods give significant amount of stiction, but the specific values are different. HAM3, K&K (applied on the first 600 samples),

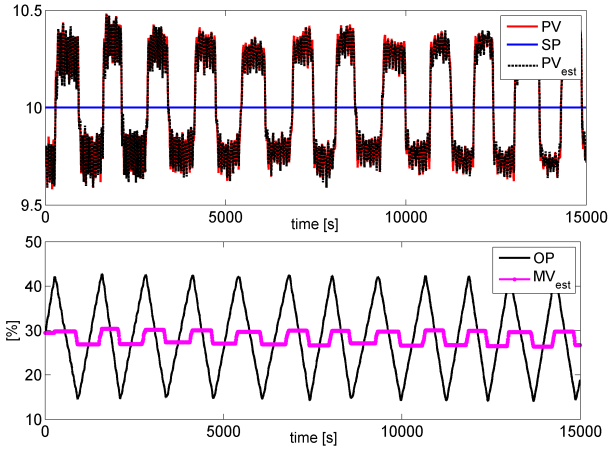

(a) time trends - PV and MV estimated with HAM3 method.

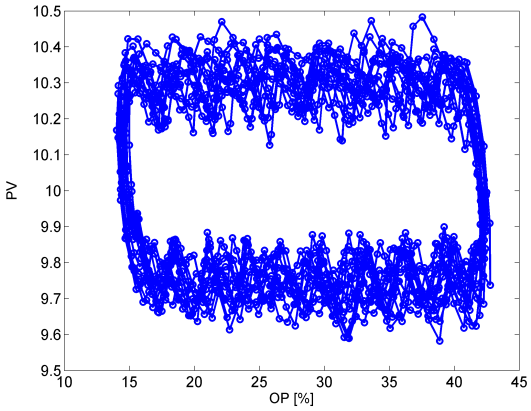

(b) parallelogram-shaped limit cycle on PV(OP) plot.

Figure C.2: Results for loop CHEM 23.

and Lee methods yield very close values: $S \in [12.28; 15.0]$, $J \in [0.0; 4.0]$. HAM1, HAM2 give lower values: $S \in [6.5; 7.4]$, $J \in [0.2; 1.5]$; while He method estimates the highest amount ($S = 22.1$).

The PAP 4 is a concentration control (CC) loop which is said to be affected by dead zone and tight tuning, and not by stiction. Triangular shapes in OP and PV trends are registered; a narrow elliptic-shaped PV(OP) plot is obtained (Figure C.3). However, 3 out of 6 stiction detection techniques indicate stiction as the source of oscillation [85]. Similarly, all the quantification methods yield significant amounts of stiction. Different numerical values are obtained: HAM3 and He methods give the highest value ($S = 17.3$, $J = 0.0$, and $S = 15.0$, respectively); Lee estimates a stiction of medium amount ($S = 4.27$, $J = 0.12$), while HAM1 and HAM2 yield similar lower values: $S \in [2.3; 2.4]$, $J \in [0.0; 0.3]$. Finally, K&K obtains the lowest amount: $S = 1.0$, $J = 0.3$.

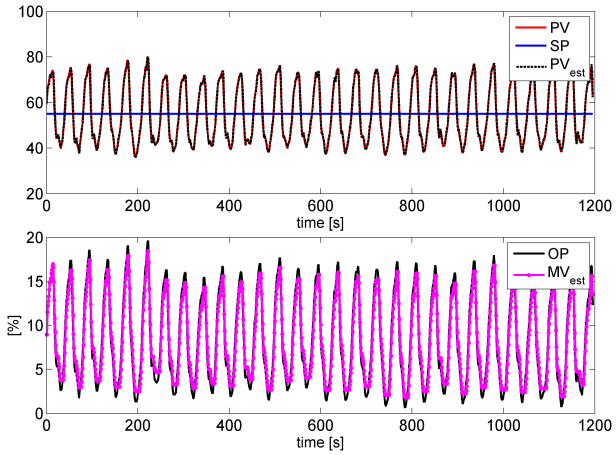

(a) time trends - PV and MV estimated with HAM2 method.

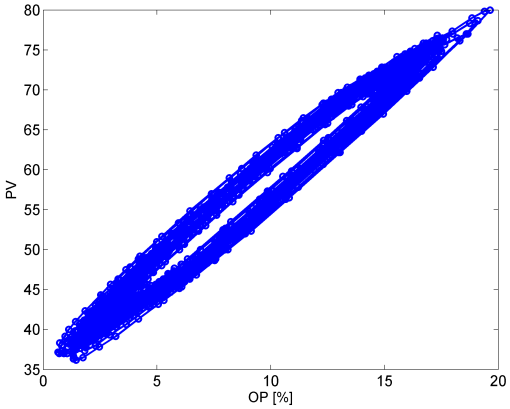

(b) elliptical limit cycle on PV(OP) plot.

Figure C.3: Results for loop PAP 4.

For the temperature control (TC) loop PAP 9 the oscillation is not induced by stiction and a typical sinusoidal trend is registered in OP signal (Figure C.4). HAM1, HAM2, and Lee methods correctly estimate negligible values of stiction. Conversely, HAM3 method and K&K technique (basing only on the first 600 samples) yield significant amounts of stiction: $S \in$

[2.0;3.9], $J \in [0.1;2.0]$. This loop seems a case where the specific use of an extended linear model alters stiction estimation. Also He method wrongly gives significant amount of stiction ($S = 3.81$).

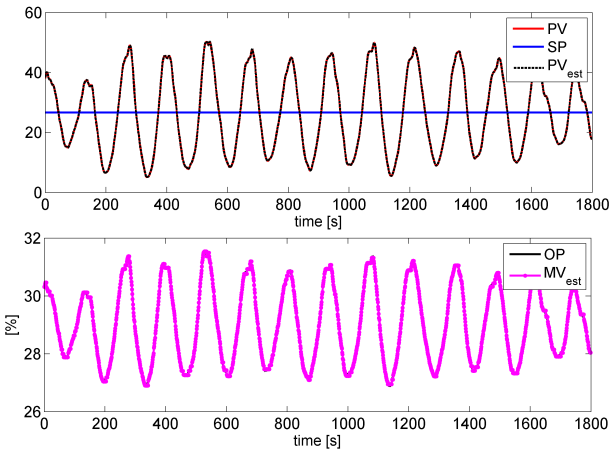

(a) time trends - PV and MV estimated with HAM2 method.

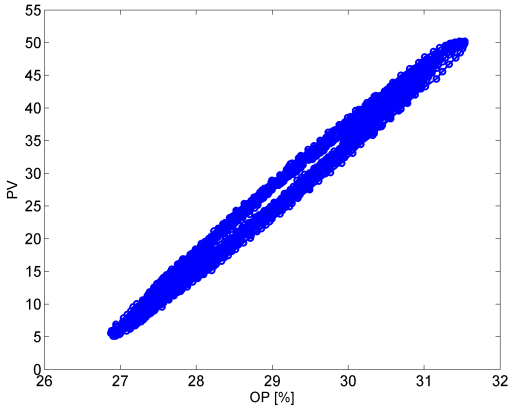

(b) narrow elliptical limit cycle on PV(OP) plot.

Figure C.4: Results for loop PAP 9.

Also for the LC loop POW 4, which is known to suffer from valve problems, different amounts of stiction are estimated. HAM1, HAM2, HAM3, and Lee methods estimate medium amount of stiction: $S \in [0.58;1.4]$, $J \in [0.0;0.58]$; while K&K method (basing on the fist 1000 samples) and Jelali technique give higher values: $S = 3.6$, $J = 1.2$, and $S = 4.49$, $J = 2.49$, respectively. Also He method gives a significant amount of stiction ($S = 3.73$).

C.3.3 Loops with Partially Consistent results

The FC loop CHEM 2 presents only two cycles of oscillation induced by stiction. All the selected methods estimate stiction, but the numerical values are quite different. Four techniques agree and estimate stiction of medium amount: $S \in [2.5;4.0]$, $J \in [0;0.65]$. Two methods seem to give outliers: HAM3 method, which yields a much lower amount of stiction ($S = 0.4$, $J = 0$), and He method, which yields an higher value ($S = 8.35$).

For the FC loop CHEM 3, quantization is the known problem and no valve stiction is present. Six techniques agree and properly estimate negligible amounts of stiction ($S \approx 0$, $J \approx 0$). Only He method gives an evident outlier: a significant amount of stiction ($S = 1.52$).

Also the FC loop CHEM 6 is known to suffer from stiction. Here, all the six techniques agree, but they all estimate stiction of very low amount ($S \approx 0$, $J \approx 0$). He method yields the highest amount: $S = 0.31$.

The FC loop CHEM 12 is clearly affected by stiction: triangular shapes in OP trend and rectangular shapes in PV signal are registered (Figure C.5a). Also the PV(OP) plot has the typical parallelogram shape of a sticky valve (Figure C.5b). HAM1, HAM2, HAM3, and Lee methods estimate consistent values of stiction: $S \in [1.42;1.8]$, $J \in [0;0.6]$; also He technique gives a similar amount ($S = 1.89$). Only K&K method yields an evident outlier by estimating lower values of stiction: $S = 0.5$, $J = 0.5$.

The FC loop CHEM 14 is said to suffer from faulty steam sensor and not from stiction. However, 5 stiction detection techniques indicate stiction as the source of oscillation [85]. Similarly, all the compared quantification methods yield significant values of stiction. Furthermore, five methods obtain very close values: $S \in [1.6;1.8]$, $J \in [0;0.3]$. Two estimates result as outliers: Lee method, yielding a lower amount of stiction ($S = 0.76$, $J = 0.28$) basing on a specific data window (100 - 700 samples), and He method, by giving the highest amount ($S = 2.57$).

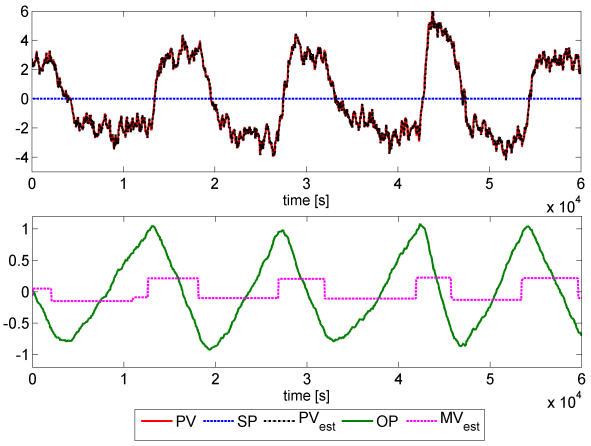

(a) time trends - PV and MV estimated with HAM1 method.

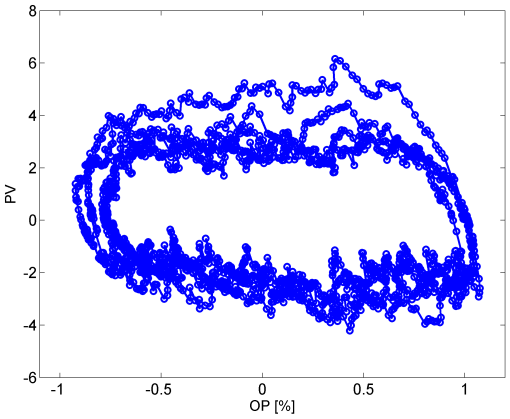

(b) limit cycle on PV(OP) plot.

Figure C.5: Results for loop CHEM 12.

The FC loop CHEM 24 suffers from valve stiction and shows significant set point oscillations. Lee, K&K, He, and Jelali methods yield very similar values for the stiction estimates: $S \in [19.3; 23.0]$, $J \in [0.81; 1.07]$. Conversely, HAM1 e HAM3 methods give lower values: $S \in [8.1, 16]$, $J = 0$. HAM2 method yield a clear outlier, by estimating near to zero values of stiction.

The TC loop CHEM 28 is (likely) affected by stiction. The estimates of 5 out of 7 methods are rather close and show a middle amount of stiction: $S \in [0.7; 1.63]$, $J \in [0.1; 0.87]$. On the contrary, two seem the outliers: HAM3 and He methods, which yield a higher amount: $S = 6.0$, $J = 0$, and $S = 5.7$, respectively.

The FC loop CHEM 29 suffers from stiction. All the methods give significant amount of stiction, but the specific numerical values are quite different. HAM1, HAM2, HAM3, and K&K methods give very similar values: $S \in [3.2; 3.5]$, $J \in [0.0; 0.2]$. Lee method, applied on a specific data window (2000 - 2500 samples), gives slightly higher values: $S = 5.35$, $J = 0.51$. Two estimates result as outliers. R&G and He methods, which give higher parameters: $S = 9.2$, $J = 0.0$, and $S = 11.2$, respectively.

For the FC loop PAP 2, which is affected by stiction, the estimates with 4 out of 8 methods (HAM1, HAM2, HAM3, Jelali) are really close: $S \in [2.52; 3.0]$, $J \in [0.0; 0.84]$. K&K method and Lee technique (basing only on the first 450 samples) yield similar estimates of S (2.6; 2.52) and higher values of J. Also He method gives quite a similar amount of stiction ($S = 3.49$). For this loop, only R&G method estimates a lower amount ($S = 0.41, J = 0.0$), which proves to be a clear outlier.

The CC loop PAP 5 is said to suffer from stiction and that is confirmed by 5 out of 6 detection techniques [85]. Four methods seem to give wrong - but consistent - estimation, since they obtain close to zero or very low amounts of stiction ($S < 0.01$, $J = 0.0$). However, this might simply due to the fact that the span of oscillation of OP signal is actually very small: $\Delta OP = 0.8$. He and HAM3 methods give higher values of stiction: $S = 0.41$, and $S = 0.40$, $J = 0.0$, respectively, which result as outlier according to Eq. C.2.

The FC loop PAP 7 has oscillation induced by an external disturbance. In this case, all the methods correctly estimate negligible amounts of stiction ($S < 0.07$, $J < 0.07$). Once again He method gives a (small) outlier: $S = 0.21$.

For the LC loop POW 2, which is clearly affected by stiction, all the methods estimate significant amount of stiction, but the specific values of S and J are quite different (Figure C.6). Since MV data are available for this loop [50], giving $S \approx 11.25$ and $J \approx 1$, it can be concluded that Jelali method delivers the most accurate values ($S = 11.47$, $J = 1.1$). Note that K&K method

also yields a good estimate of deadband plus stickband ($S = 12$), but not of the slip-jump ($J = 12$). The estimate of He method seems acceptable ($S = 9.88$); also HAM1, HAM2, HAM3 methods obtain good stiction estimations: $S \in [8.4; 9.9]$, $J = 0.4$. On the opposite, Lee and R&G techniques give two outliers: very low amount of stiction: $S = 1.15$, and $S = 5.08$, respectively.

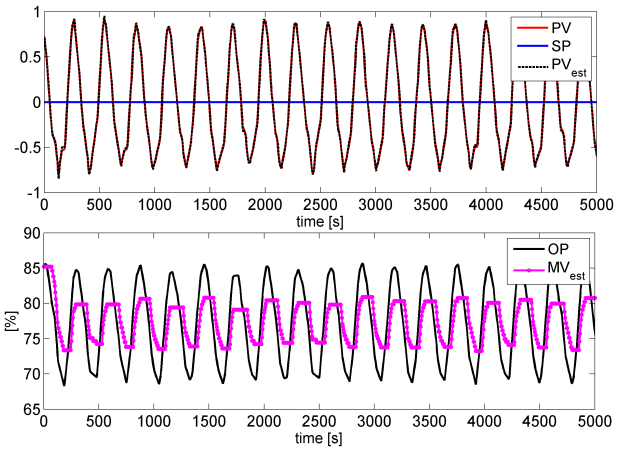

(a) time trends - PV and MV estimated with HAM3 method;

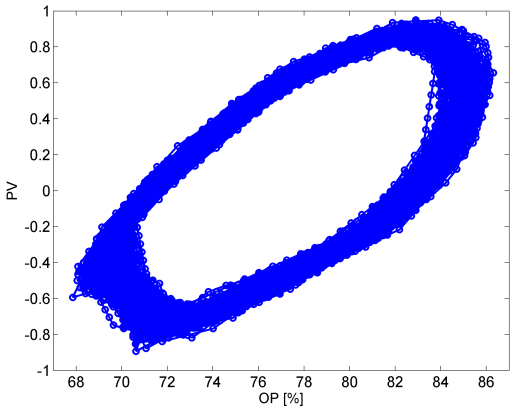

(b) elliptical limit cycle on PV(OP) plot.

Figure C.6: Results for loop POW 2.

C.3.4 Loops with Consistent results

The two FC loops CHEM 1 and CHEM 5 are known to suffer from valve stiction. All the techniques agree and estimate stiction of low amount. Overall results for S parameter are: $\bar{S} = 0.67$, $\sigma_S = 0.19$, with a regularity factor of $R_S = 1.16$, for CHEM 1, and $\bar{S} = 0.36$, $\sigma_S = 0.06$, with $R_S = 1.92$, for CHEM 5.

The PC loop CHEM 10 (Figure C.7a) is a typical case of stiction: OP shows ideally triangular pattern, PV trend is of the saw-tooth type, and PV(OP) plot has a clearly elliptical shape (Figure C.7b). Indeed, an ellipse can be fitted to this plot, giving a middle amount of apparent stiction: $S \approx 1.78$ [85]. Here all the selected techniques are in very good agreement: $\bar{S} = 1.81$ with $\sigma_S = 0.08$, and $R_S = 7.80$. The estimates are very close for HAM1, HAM2, and HAM3 methods: $S \in [1.7; 1.9]$, $J \in [0.9; 1.7]$. Also Lee obtains very similar values of S and J, while K&K yields a similar value of S, but a smaller value of slip-jump ($J = 0.05$). Also He method gives a similar amount of stiction ($S = 1.93$).

For the PC loop CHEM 25, which (very likely) suffers from stiction, the estimates with all 8 methods are close: $S \in [1.4; 2.0]$, $J \in [0.2; 0.59]$, with $R_S = 2.99$. Only Lee method, applied on a specific data window (100 - 350 samples), gives a higher value of slip-jump ($J = 1.62$).

For the TC loop MIN 1, which is clearly affected by stiction, the results of all 8 methods are in good agreement: $S \in [1.0; 1.7]$ and $J \in [0.0; 1.2]$, with $R_S = 1.45$. Values of S are really very close; while more variability lies in J values. Here K&K method has been applied on the first 2000 samples. The couple ($S = 1$, $J = 1$), reported in Table C.1 under R&G, has been actually obtained by [50]. Also He method is very aligned to the others ($S = 1.63$).

Also for the TC loop BAS 7, which suffers from stiction, the results of 6 methods are in good agreement: $S \in 1.2; 1.6]$ and $J \in [0.0; 0.3]$, with $R_S = 1.12$. Also He method is really consistent ($S = 1.67$). Lee method yields slightly different parameters: a lower value of stick band + dead band ($S = 0.61$) and a higher slip-jump ($J = 0.53$). Triangular shapes in OP trend are registered, and an elliptic-shaped PV(OP) plot is obtained (Figure C.8).

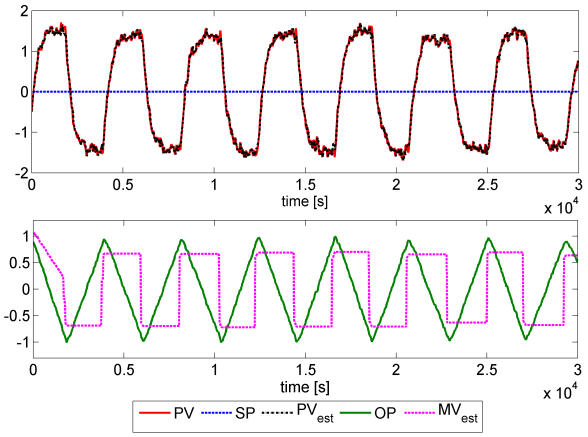

(a) time trends - PV and MV estimated with HAM1 method;

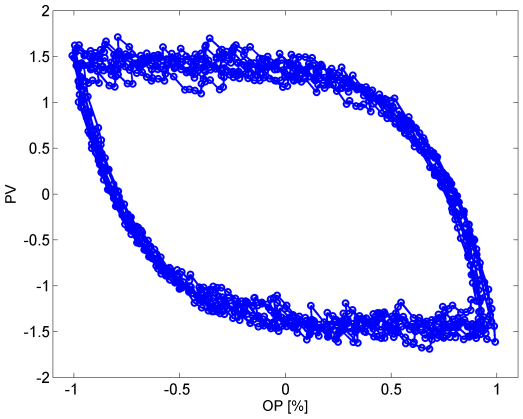

(b) pattern on PV(OP) plot.

Figure C.7: Results for loop CHEM 10.

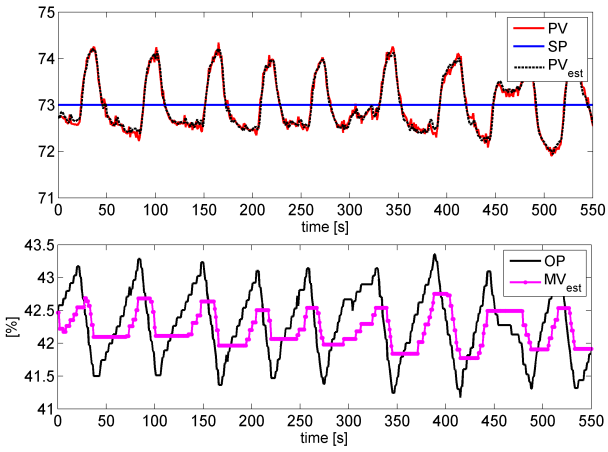

(a) time trends - PV and MV estimated with HAM2 method;

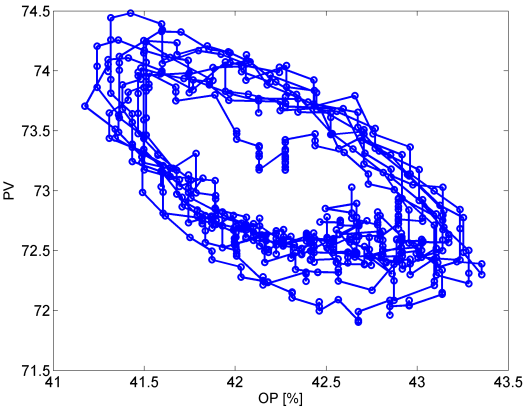

(b) pattern on PV(OP) plot.

Figure C.8: Results for loop BAS 7.

C.3.5 Overall considerations on results on benchmark data

An overall comparison of the eight stiction quantification techniques is shown in Table C.4. The number of applications (stiction and no stiction cases), the number of false negatives and false positives, the number of highest and lowest estimates, and the number of outliers according to Eq. C.2 are reported in different rows. Note that a false positive is assessed when an estimate $S > 0.5$ arises for a case of no stiction; while a false negative when an estimate $S < 0.5$ arises for a case of stiction. Here the verdicts reported in [86] are assumed as true situations.

Specific comments are needed about He method. This technique can be considered the simplest solution, since it does not perform any system identification, but it gives partially consistent results in the overall comparison. The advantages of its simplicity apply only to cases where stiction is known to be the root cause of oscillation (e.g., CHEM 10, 12, 25, MIN 1, BAS 7), where the estimated values of S are in good agreement with the other methods. However, it should be noticed that this method tends typically to give the highest amounts of stiction with respect to other estimates (e.g., CHEM 2, 28, 29, and 32), which then prove to be outliers (19 times).

In addition, for cases of no stiction caused oscillations, this method yields misleading results – with non zero, or even significant, values of stiction – which result as false positives in 8

Table C.4: Comparison of overall performance of different techniques.

Method		HAM1	HAM2	HAM3	He	K&K	Lee	Jelali	R&G	Total
	Total	29	29	29	29	29	29	6	7	187
Tests	Stiction	20	20	20	20	20	20	6	7	133
	No stiction	9	9	9	9	9	9	0	0	54
False Negatives		6	5	6	3	2	5	0	0	27
False Positives		3	5	4	8	5	2	0	0	27
Highest estimates (S)		2	0	6	19	4	0	0	0	31*
Lowest estimates (S)		9	9	5	0	7	10	0	2	42$^{\diamond}$
Outliers		1	3	5	19	3	5	0	2	38

*: 1 case of triple parity. $^{\diamond}$: 5 cases of double parity (2 for $S \neq 0$, 3 for $S = 0$), and 4 cases of triple parity ($S = 0$)

times out of 9 (e.g., CHEM 3, 4, 3, 14, 15, 16, PAP 4, 9). Therefore, this method must be necessarily applied only once that stiction is clearly detected as the main source of loop oscillation. All the other techniques show comparable results in terms of false positives, false negatives, and outliers. Finally, note that Hammerstein methods which use a simple linear model for the process (HAM1, HAM2, and Lee) tend to obtain lower stiction values with respect to techniques which implement an extended model (HAM3, K&K).

At the end of this extended comparison it is confirmed that different stiction quantification techniques can strongly disagree: inconsistent verdicts or different estimations can be obtained, even when stiction is clearly detected. Therefore, a more reliable stiction assessment should be based on a weighted combination of selected methods.

C.4 Industrial Data

In this section, other industrial examples are used to further compare performance of the selected methods. As already pointed out, repeating system identification and stiction quantification for different acquisitions for the same valve allows one to obtain a more reliable assessment of the stiction amount. Following the evolution of stiction values in time, and disregarding - if the case - anomalous cases (outliers) are useful practices to obtain effective scheduling and checking of valves maintenance.

Four of the previous selected stiction quantification techniques are now applied to three datasets obtained from Italian process industries [123, 23]. Data refer to repeated registrations (of PV, OP, SP) for the same loops. The source of malfunction is known to be stiction, but the actual MV signals are not available. Trends of values of parameter S are reported for each method: HAM1, HAM2, HAM3, and He (Figure C.9). Values of J are not reported since their estimate, as said earlier, is less significant and reliable.

C.4.1 Industrial Loop I

These data are from a pressure control loop installed in a refinery plant. The controller has PI algorithm and the SP is variable. Six different registrations, collected during a month, are available just before the valve maintenance. Four well-established detection techniques [77, 46, 119, 124] always indicate the loop as affected by stiction. Therefore, rather constant stiction values, though unknown, are expected. In Figure C.9, pretty uniform values of stiction are actually obtained for each method; therefore all techniques prove to be sufficiently reliable. In details, HAM1 and HAM3 methods give very similar values: $S \in [4; 4.9]$; also HAM2 and He methods obtain constant stiction trends, but with higher average amounts: $\bar{S} = 5.36$, and $\bar{S} = 5.95$, respectively. Figure C.10 shows registered time trends of SP, PV, OP and the estimated values of PV and MV (PV_{est}, MV_{est}) for two different acquisitions.

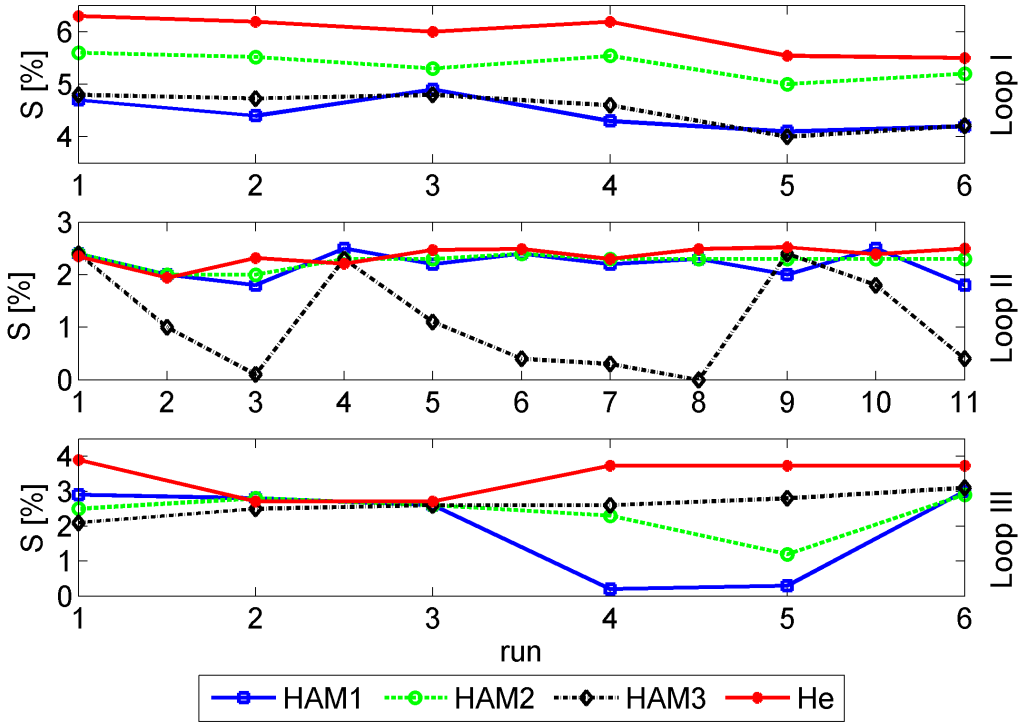

Figure C.9: Trends of stiction parameter S using different methods. Top panel) industrial Loop I; central) Loop II; bottom) Loop III.

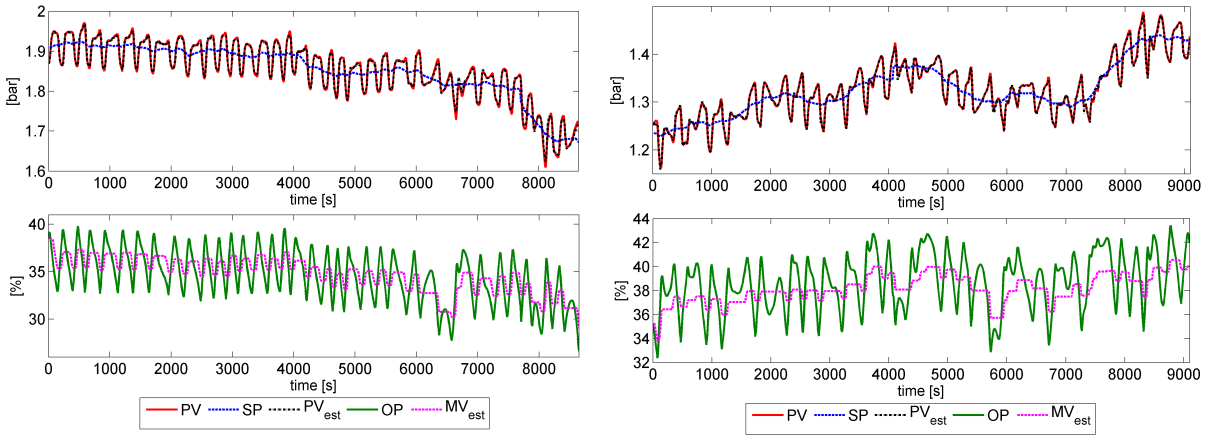

(a) registration # 1 - PV and MV are estimated with HAM3.

(b) registration # 4, estimation performed with HAM2.

Figure C.10: Results for Loop I.

C.4.2 Industrial Loop II

These data are from a flow control loop installed in an ethylene plant. The controller has PI algorithm and the SP is variable. The presence of stiction is clearly recognizable by the PV and OP shapes being close to square and triangular waves, respectively (Figure C.11a). Moreover, the PV(OP) diagram shows evident stiction characteristics (Figure C.11b), since in FC loops PV is proportional to MV. The same four detection techniques [77, 46, 119, 124] indicate this loop as affected by stiction in 11 acquisitions registered along two consecutive days. Therefore, nearly constant stiction values, though unknown, are expected. From Figure C.9, rather uniform values of stiction ($S \in [1.8; 2.5]$) are quantified by HAM1 and HAM2, methods which use a non-extended linear process model. Also He method yields very uniform amounts of stiction. The lowest variability is given by HAM2 ($\sigma_S = 0.14$) with a mean value $\bar{S} = 2.26$. Conversely,

an excessively high variability is obtained using HAM3, which implements an extended linear process model (EARX). Therefore, HAM3 method proves to be not sufficiently reliable for this application: a really inconsistent trend is estimated and sometimes even zero values of stiction are obtained, since loop oscillation is not associated with valve stiction but wrongly with a significant external disturbance.

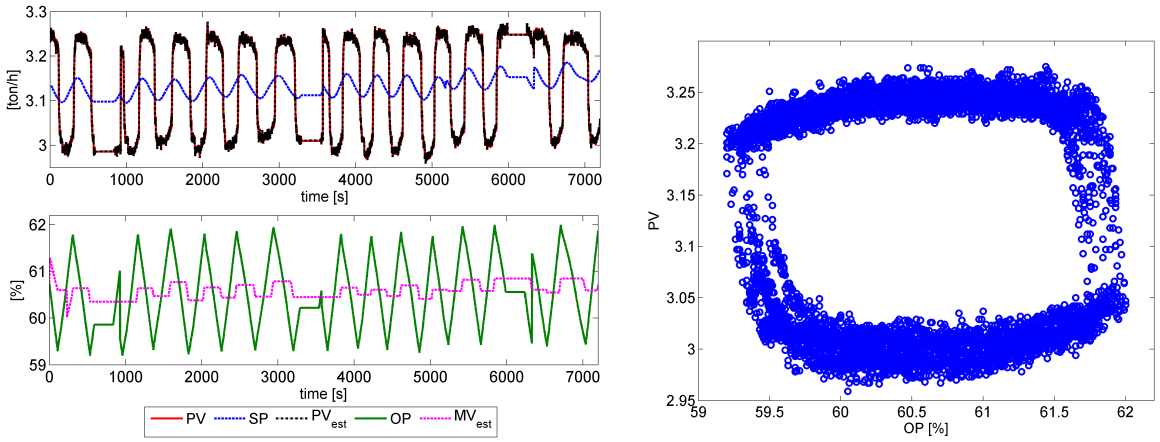

(a) time trends - PV and MV estimated with HAM1. **(b)** limit cycle on PV(OP) diagram.

Figure C.11: Results for Loop II, registration # 8.

C.4.3 Industrial Loop III

These data are from a flow control loop installed in a refinery plant. The controller has a PID algorithm and the SP is variable since the loop is the inner part of a cascade control. The same four detection techniques [77, 46, 119, 124] indicate the presence of stiction in 6 registrations collected along four months. Therefore, a nice trend of stiction - constant or increasing - is expected. Once again stiction is clearly recognizable by the shapes of PV and OP signals, being close to square and triangular waves, respectively (Figure C.12a). For this loop, HAM3 estimates a consistent trend of stiction: $\bar{S} = 2.62$ with $\sigma_S = 0.33$. Also He method yields quite uniform values: $\bar{S} = 3.42$ with $\sigma_S = 0.55$.

Conversely, for registration # 4, using HAM1, and for # 5, using both HAM1 and HAM2, very low ($S \approx 0$) or low values of stiction are estimated. These estimates appear incorrect since they result as outliers with respect to the main trend (Figure C.9). In these two registrations, an external disturbance might act simultaneously with valve stiction. The PV signal does not clearly show a singular frequency of oscillation (Figure C.12b) and the external disturbance can alter stiction estimation. Therefore, for this third industrial application, HAM3 with EARX linear process model, is to be preferred since it is able to manage the cases of simultaneous presence of valve stiction and external disturbance. Methods with non-extended linear process models are not sufficiently reliable as they can estimate inconsistent values of stiction.

This second comparison, about stiction quantification techniques on repeated acquisitions for the same valves, should be considered a more reliable test about efficiency of different techniques.

As first, He method gives accurate results being all three cases affected by large stiction amounts (as pointed out above, it may give wrong results in cases of absent or negligible stiction).

About the other three Hammerstein-based techniques, the comparison indicates that simpler linear process models (ARX in HAM1, and SS in HAM2 method) can be the best choice for stiction quantification, when stiction is the only source of loop oscillation. Conversely, an extended model (as EARX in HAM3 method), which incorporate an additive time-varying non-

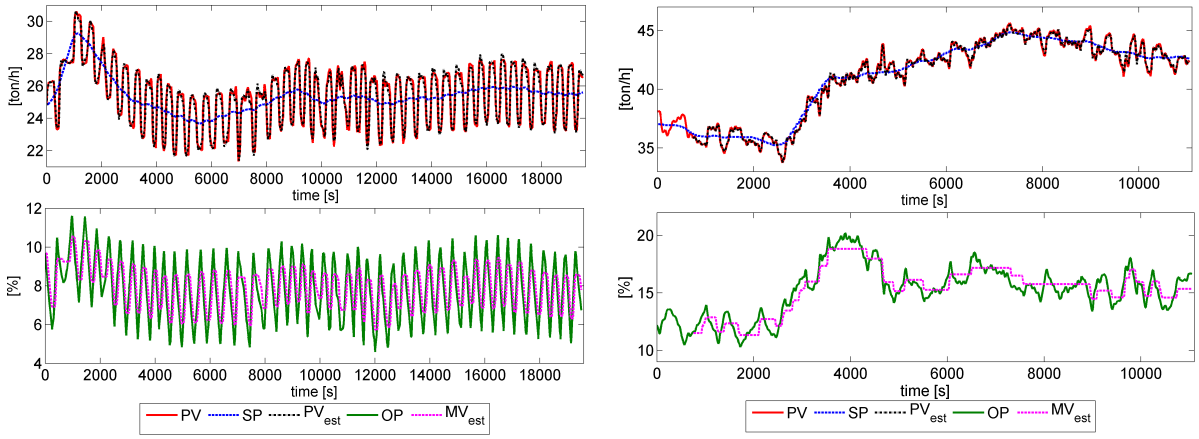

(a) registration # 1.

(b) registration # 4.

Figure C.12: Results for Loop III. In both cases PV and MV are estimated with HAM3 method.

stationary disturbance, confirm to yield a more accurate stiction estimation in the case of disturbance acting simultaneously with stiction, while can give wrong indications (false negative) when disturbance are not actually present. This conclusion is an extension and a confirmation of previous results reported in Chapter 4.

C.5 Conclusions

This comprehensive study has compared several emerging techniques of stiction quantification. Once more we underline that application of a technique on a single data set is not a guarantee of its efficiency and reliability in the light of valve maintenance prediction, ultimate interest of the industrial user.

The comparison on the same dataset confirmed discrepancies on stiction values computed by means of different techniques, already pointed out in other research works. This fact can be imputed to different causes, as the use of different stiction and process models, simultaneous presence of external nonstationary disturbances, and inhomogeneous amounts of stiction along the valve stroke. Stiction quantification is certainly the stage where all mathematical complications and error sources related to modeling and detection sum up with possible unreliable predictions.

For this reason, the comparison of identification techniques with/without disturbance models is appropriate and shows that the added complexity of extended models can be rewarded by better results in cases of simultaneous presence of disturbances and stiction, while it is not worth when stiction is the only source of oscillation.

Therefore, a future research trend can be indicated in the development of techniques to assess the presence of simultaneous disturbances; another point to be proposed can be the adoption of flexible nonparametric stiction models. In perspective of improving the reliability of stiction quantification techniques proposed up to date, analogously to the problem of stiction detection, a practical solution to recommend is to combine and weight verdicts obtained by different methods.

List of Tables

List of Figures

Bibliography

[1] Aspen Tech, Aspen Watch Performance Monitor. http://www.aspentech.com/products/aspen-watch.aspx. accessed on 15 December 2014.

[2] Ciengis, Plantstreamer Portal. http://www.ciengis.com/products/plantstreamer-portal/. accessed on 15 December 2014.

[3] Control Arts, Controller Performance Assessment for Industrial Control Loops. http://www.controlartsinc.com/ControlMonitor/ControlMonitor.html. accessed on 15 December 2014.

[4] ControlSoft, INTUNE. http://www.controlsoftinc.com/intune5plus.shtml. accessed on 15 December 2014.

[5] Emerson Process Management, Control Performance Tools. http://www2.emersonprocess.com/en-US/brands/processautomation/consultingservices/ProcessImprovementOptimization/ControlPerformanceServices/Pages/ControlPerformanceTools.aspx. accessed on 15 December 2014.

[6] Expertune, PlantTriage. http://www.expertune.com/plantTriage.aspx. accessed on 15 December 2014.

[7] Flowserve, Monitoring and Controls. http://www.flowserve.com/Products/Monitoring-and-Controls. accessed on 15 December 2014.

[8] Honeywell, Loop Scout. http://www.loopscout.com/. accessed on 15 December 2014.

[9] Matrikon-Honeywell, Matrikon Control Performance Monitor. http://www.matrikon.com/controlperformance-monitoring/controlperformance-monitor.aspx. accessed on 15 December 2014.

[10] Paprican, Process Control Automatic Control Loop Monitoring and Diagnostics. http://www.paprican.ca/wps/portal/paprican/Technologies_Available/Technologies_for_Licensing/Process_Control?lang=en. accessed on 15 December 2014.

[11] PAS, Control Loop Optimization. http://www.pas.com/Solutions/Operations-Management/Control-Loop-Performance-Management.aspx. accessed on 15 December 2014.

[12] M. Ahammad and M. A. A. S. Choudhury. A simple harmonics based stiction detection method. In *Proceedings of the 9th IFAC DYCOPS*, pages 671–676, Leuven, Belgium, 5–7 July, 2010.

[13] S. Ahmed, S. L. Shah, and B. Huang. Maintenance issues in oil and gas processes: Detection of valve stiction. In *Proceedings of the 1st Annual Gas Processing Symposium*, pages 202–210, Doha, Qatar, 10–12 January, 2009.

[14] M. Ale Mohammad and B. Huang. Frequency analysis and experimental validation for stiction phenomenon in multi-loop processes. *Journal of Process Control*, 21:437–447, 2011.

[15] M. Ale Mohammad and B. Huang. Compensation of control valve stiction through controller tuning. *Journal of Process Control*, 22:1800–1819, 2012.

[16] A. P. Araujo, C. J. Munaro, and M. R. Filho. Quantification of valve stiction and dead band in control loops based on the harmonic balance method. *Industrial & Engineering Chemistry Research*, 51:14121–14134, 2012.

[17] B. M. S. Arifin, C. J. Munaro, M. A. A. S. Choudhury, and S. L. Shah. A model free approach for online stiction compensation. In *Proceedings of 19th IFAC World Congress*, pages 5957–5962, Cape Town, South Africa, 24–29 August, 2014.

[18] B. Armstrong-Hèlouvry, P. Dupont, and C. Canudas de Wit. A survey of models, analysis tools and compensation methods for the control of machines with friction. *Automatica*, 30:1083–1138, 1994.

[19] S. Arumugam and R. C. Panda. Control valve stiction identification, modeling, quantification and control – A review. *Sens. Transducers J.*, 132:14–24, 2011.

[20] S. Arumugam, R. C. Panda, and V. Velappan. A simple method for compensating stiction nonlinearity in oscillating control loops. *International Journal of Engineering and Technology*, 6:1846–1855, 2014.

[21] R. Bacci di Capaci and E. Bartaloni. Diagnostica dei loop di regolazione. *Automazione Oggi*, 366:140–141, 2013.

[22] R. Bacci di Capaci and C. Scali. Valve stiction quantification: A robust methodology to face most common causes of loop perturbations. *Chemical Engineering Transactions*, 32:1201–1206, 2013.

[23] R. Bacci di Capaci and C. Scali. A performance monitoring tool to quantify valve stiction in control loops. In *Proceedings of the 19th IFAC World Congress*, pages 6710–6716, Cape Town, South Africa, 24–29 August, 2014.

[24] R. Bacci di Capaci and C. Scali. Processi industriali sotto controllo: Monitoraggio delle prestazioni e diagnostica dei sistemi di controllo dei processi industriali. *Chimica-Ambiente*, 1:27–29, 2014.

[25] R. Bacci di Capaci and C. Scali. Stiction quantification: A robust methodology for valve monitoring and maintenance scheduling. *Industrial & Engineering Chemistry Research*, 53:7507–7516, 2014.

[26] R. Bacci di Capaci and C. Scali. Comparison of techniques for valve stiction quantification. To be submitted as soon as possible, 2016.

[27] R. Bacci di Capaci and C. Scali. Evolution from classical to advanced valve stiction diagnosis. To be submitted as soon as possible, 2016.

[28] R. Bacci di Capaci, C. Scali, and B. Huang. A revised technique of stiction compensation for control valves. Submitted to 11th IFAC DYCOPS, 2016.

[29] R. Bacci di Capaci, C. Scali, and G. Pannocchia. Identification techniques for stiction quantification in the presence of nonstationary disturbances. In *Proceedings of 9th IFAC ADCHEM*, pages 629–634, Whistler, BC, Canada, 7–10 June, 2015.

[30] R. Bacci di Capaci, C. Scali, and G. Pannocchia. System identification applied to stiction quantification in industrial control loops: A comparative study. Submitted to Journal of Process Control, 2016.

[31] R. Bacci di Capaci, C. Scali, D. Pestonesi, and E. Bartaloni. Advanced diagnosis of control loops: Experimentation on pilot plant and validation on industrial scale. In *Proceedings of 10th IFAC DYCOPS*, pages 589–594, Mumbai, India, 18–20 December, 2013.

[32] R. Bacci di Capaci, C. Scali, D. Pestonesi, and E. Bartaloni. Diagnostica avanzata di valvole di regolazione. *Automazione e Strumentazione*, 62:68–73, 2014.

[33] R. Bacci di Capaci, C. Scali, E. Rossi, F. Gomiero, and A. Pagano. A system for advanced performance monitoring: Application to complex plants of the chemical industry. *Chemical Engineering Transactions*, 43:1369 –1374, 2015.

[34] M. Z. Bartyś and J. M. Kościelny. Application of fuzzy logic fault isolation methods for actuator diagnosis. In *Proceeding of the 15th IFAC World Congress*, pages 21–26, Barcelona, Spain, 21–26 July, 2002.

[35] M. Z. Bartyś, R. Patton, M. Syfert, S. de las Heras, and J. Quevedo. Introduction to the DAMADICS actuator FDI benchmark study. *Control Engineering Practice*, 14:577–596, 2006.

[36] M. Bauer, A. Horch, L. Xie, M. Jelali, and N. Thornhill. The current state of control loop performance monitoring – A survey of application in industry. *Journal of Process Control*, 38:1–10, 2016.

[37] P. Belli, N. Bonavita, and R. Rea. An integrated environment for industrial control performance assessment, diagnosis and improvement. In *Proceedings of the International Congress on Methodologies for Emerging Technologies in Automation*, Roma, Italy, 13–15 November, 2006.

[38] W. L. Bialkowski. Dream versus reality: a view from both sides of the gap. *Pulp and Paper Canada*, 94:19–27, 2003.

[39] A. S. R. Brásio, A. Romanenko, and N. C. P. Fernandes. Modeling, detection and quantification, and compensation of stiction in control loops: The state of the art. *Industrial & Engineering Chemistry Research*, 53:15020–1504014, 2014.

[40] A. S. R. Brásio, A. Romanenko, and N. C. P. Fernandes. Stiction detection and quantification as an application of optimization. In *Proceedings of the 14th International Conference on Computational Science and Its Applications ICCS*, pages 169–179, Guimarães, Portugal, 30 June–3 July 2014, 2014.

[41] A. S. R. Brásio, A. Romanenko, and N. C. P. Fernandes. Detection of stiction in level control loops. In *Proceedings of the 9th IFAC-ADCHEM*, pages 421–426, Whistler, BC, Canada, 7–10 June, 2015.

[42] C. Canudas de Wit, H. Olsson, K. Åström, and P. Lischinsky. A new model for control of systems with friction. *IEEE Trans. Autom. Control*, 40:419–425, 1995.

[43] S. L. Chen, K. K. Tan, and S. Huang. Two-layer binary tree data-driven model for valve stiction. *Industrial & Engineering Chemistry Research*, 47:2842–2848, 2008.

[44] S. B. Chitralekha, S. L. Shah, and J. Prakash. Detection and quantification of valve stiction by the method of unknown input estimation. *Journal of Process Control*, 20:206–216, 2010.

[45] M. A. A. S. Choudhury, V. Kariwala, N. F. Thornhill, H. Douke, S. L. Shah, H. Takada, and J. F. Forbes. Detection and diagnostics of plant-wide oscillations. *The Canadian Journal of Chemical Engineering*, 85:208–2019, 2007.

[46] M. A. A. S. Choudhury, S. L. Shah, and N. F. Thornhill. Diagnosis of poor control loop performance using higher order statistics. *Automatica*, 40:1719–1728, 2004.

[47] M. A. A. S. Choudhury, S. L. Shah, and N. F. Thornhill. Modeling valve stiction. *Control Engineering Practice*, 13:641–658, 2005.

[48] M. A. A. S. Choudhury, S. L. Shah, and N. F. Thornhill. *Diagnosis of Process Nonlinearities and Valve Stiction: Data Driven Approaches*. 1st ed., Springer-Verlag: Berlin, Heidelberg, Germany, 2008.

[49] M. A. A. S. Choudhury, S. L. Shah, N. F. Thornhill, and D. S. Shook. Automatic detection and quantification of stiction in control valves. *Control Engineering Practice*, 16:1395–1412, 2006.

[50] M. A. A. S. Choudhury, S. L. Shah, N. F. Thornhill, and D. S. Shook. Stiction - definition, modeling, detection and quantification. *Journal of Process Control*, 18:232–243, 2008.

[51] M. A. d. S. L. Cuadros, C. Munaro, and S. Munareto. An improved algorithm for automatic quantification of valve stiction in flow control loops. In *Proceedings of the IEEE International Conference on Industrial Technology*, pages 173–178, Valparaiso, Chile, 14–17 March, 2010.

[52] M. A. d. S. L. Cuadros, C. Munaro, and S. Munareto. Improved stiction compensation in pneumatic control valves. *Computers & Chemical Engineering*, 38:106–114, 2012.

[53] M. A. d. S. L. Cuadros, C. Munaro, and S. Munareto. Novel model-free approach for stiction compensation in control valves. *Industrial & Engineering Chemistry Research*, 51:8465–8476, 2012.

[54] M. A. Daneshwar and N. M. Noh. Valve stiction in control loops – A survey on effective methods of detection and compensation. In *Proceedings of the IEEE International Conference on Control System, Computing and Engineering*, pages 155–159, Penang, Malaysia, 23–25 November, 2012.

[55] M. A. Daneshwar and N. M. Noh. Identification of a process with control valve stiction using a fuzzy system: A data-driven approach. *Journal of Process Control*, 24:249–260, 2014.

[56] M. A. Daneshwar and N. M. Noh. Detection of stiction in flow control loops based on fuzzy clustering. *Control Engineering Practice*, 39:23–34, 2015.

[57] A. Dempster, N. Laird, and D. Rubin. Maximum likelihood from incomplete data via the EM algorithm. *Journal of the Royal Statistical Society, Series B*, 39:1–38, 1977.

[58] D. B. Ender. Process control performance: Not as good as you think. *Pulp and Paper Canada*, 9:180–190, 1993.

[59] L. Fang and J. Wang. Identification of Hammerstein systems using Preisach model for sticky control valves. *Industrial & Engineering Chemistry Research*, 54:1028–1040, 2015.

[60] M. Farenzena and J. O. Trierweiler. Modified PI controller for stiction compensation. In *Proceedings of 9th IFAC DYCOPS*, pages 791–796, Leuven, Belgium, 2010.

[61] M. Farenzena and J. O. Trierweiler. Valve stiction evaluation using global optimization. *Control Engineering Practice*, 20:379–385, 2012.

[62] M. Farenzena and J. Q. Trierweiler. Valve backlash and stiction detection in integrating processes. In *Proceedings of the 8th IFAC-ADCHEM*, pages 320–324, Singapore, 10–13 July, 2012.

[63] K. Forsman and A. Stattin. A new criterion for detecting oscillations in control loops. In *Proceedings of the European Control Conference*, pages 155–159, Karlsruhe, Germany, 31 August–3 September, 1999.

[64] C. Garcia. Comparison of friction models applied to a control valve. *Control Engineering Practice*, 16:1231–1243, 2008.

[65] J. Gerry and M. Ruel. How to measure and combat valve stiction on line. In *Proceedings of the ISA International Fall Conference*, pages 750–755, Houston, TX, USA, 10–12 September, 2001.

[66] Z. Guo, L. Xie, A. Horch, Y. Wang, H. Su, and X. Wang. Automatic detection of non-stationary multiple oscillations by an improved wavelet packet transform. *Industrial & Engineering Chemistry Research*, 53:15686–15697, 2014.

[67] T. Hägglund. A control-loop performance monitor. *Control Engineering Practice*, 3(11):1543–1551, 1995.

[68] T. Hägglund. Automatic detection of sluggish control loops. *Control Engineering Practice*, 7:1505–1511, 1999.

[69] T. Hägglund. A friction compensation for pneumatic control valves. *Journal of Process Control*, 12:897–904, 2002.

[70] T. Hägglund. Industrial implementation of on-line performance monitoring tools. *Control Engineering Practice*, 13:1383–1390, 2005.

[71] T. Hägglund. Automatic on-line estimation of backlash in control loops. *Journal of Process Control*, 17:489–499, 2007.

[72] T. Hägglund. A shape-analysis approach for diagnosis of stiction in control valves. *Control Engineering Practice*, 19:782–789, 2011.

[73] Y. Haoli, S. Lakshminarayanan, and V. Kariwala. Confirmation of control valve stiction in interacting systems. *The Canadian Journal of Chemical Engineering*, 87:632–636, 2009.

[74] Q. P. He and J. Wang. Valve stiction modeling: First-principles vs. data-drive approaches. In *Proceedings of the 7th American Control Conference*, pages 3777–3782, Baltimore, MD, USA, 30 June–2 July, 2010.

[75] Q. P. He and J. Wang. Valve stiction quantification method based on a semiphysical valve stiction model. *Industrial & Engineering Chemistry Research*, 53:12010–12022, 2014.

[76] Q. P. He, J. Wang, M. Pottmann, and S. Qin. A curve fitting method for detecting valve stiction in oscillating control loops. *Industrial & Engineering Chemistry Research*, 46:4549–4560, 2007.

[77] A. Horch. A simple method for detection of stiction in control valves. *Control Engineering Practice*, 7:1221–1231, 1999.

[78] A. Horch. *Benchmarking Control Loops with Oscillation and Stiction, In Process Control Performance Assessment, 1st ed., Ordys, A.W., Uduehi, D., Johnson, M.A.* Springer-Verlag, London, UK, 2006.

[79] A. Horch. *Stiction detection based on cross-correlation and signal shape, In Detection and Diagnosis of Stiction in Control Loops: State of the Art and Advanced Methods, 1st ed.; Jelali, M., Huang, B.* Springer-Verlag, London, UK, 2010.

[80] X. Huang, J. Liu, and Y. Niu. *Fault Detection of Actuator with Digital Positioner Based on Trend Analysis Method, In Fault Detection, 1st ed.; Zhang, W.* InTech, Rijeka, Croatia, 2010.

[81] X. Huang and F. Yu. A simple method for fault detection of industrial digital positioners. In *Proceedings of the 7th World Congress on Intelligent Control and Automation*, pages 6863–6866, Chongqing, China, 25–27 June, 2008.

[82] L. Z. X. Ivan and S. Lakshminarayanan. A new unified approach to valve stiction quantification and compensation. *Industrial & Engineering Chemistry Research*, 48:3474–3483, 2009.

[83] M. Jelali. An overview of control performance assessment technology and industrial applications. *Control Engineering Practice*, 14:441–466, 2006.

[84] M. Jelali. Estimation of valve stiction in control loops using separable last square and global search algorithms. *Journal of Process Control*, 18:632–642, 2008.

[85] M. Jelali and B. Huang. *Detection and Diagnosis of Stiction in Control Loops: State of the Art and Advanced Methods*. Springer-Verlag, London, 2010.

[86] M. Jelali and C. Scali. *Comparative Study of Valve Stiction Detection Methods. In Detection and Diagnosis of Stiction in Control Loops, 1st ed., Jelali, M., Huang, B.* 1st ed., Springer, London, UK, 2010.

[87] M. Kano, M. Hiroshi, H. Kugemoto, and K. Shimizu. Practical model and detection algorithm for valve stiction. In *Proceedings of 7th IFAC DYCOPS*, Boston, USA, 5–7 July, 2004. Paper ID n. 54.

[88] D. Karnopp. Computer simulations of stick-slip friction in mechanical dynamics systems. *Trans. ASME J. Dyn. Syst., Meas., Control*, 107:100–103, 1985.

[89] S. Karra and M. N. Karim. Alternative model structure with simplistic noise model to identify linear time invariant systems subjected to non-stationary disturbances. *Journal of Process Control*, 19:964–977, 2009.

[90] S. Karra and M. N. Karim. Comprehensive methodology for detection and diagnosis of oscillatory control loops. *Control Engineering Practice*, 17:939–956, 2009.

[91] D. Karthiga and S. Kalaivani. A new stiction compensation method in pneumatic control valves. *Int. J. Electron. Comput. Sci. Eng.*, 1:2604–2612, 2012.

[92] A. Kayihan and F. J. Doyle. Friction compensation for a process control valve. *Control Engineering Practice*, 8:799–812, 2000.

[93] J. Koj. The fault sources of pneumatic servo-motor control valve assembly. In *Proceedings of the 3rd Polish National Conference on Diagnostic of Industrial Processes*, pages 415–419, Jurata, Poland, 7–10 September, 1998.

[94] S. Kullback and R. A. Leibler. On information and sufficiency. *The Annals of Mathematical Statistics*, 22:79–86, 1951.

[95] K. H. Lee, Z. Ren, and B. Huang. Novel closed-loop stiction detection and quantification method via system identification. In *Proceedings of the 3rd ADCONIP*, pages 341–346, Jasper, Alberta, Canada, 2008.

[96] K. H. Lee, E. C. Tamayo, and B. Huang. Industrial implementation of controller performance analysis technology. *Control Engineering Practice*, 18:147–158, 2010.

[97] C. Li, M. A. A. S. Choudhury, B. Huang, and F. Qian. Frequency analysis and compensation of valve stiction in cascade control loops. *Journal of Process Control*, 24:1747–1760, 2014.

[98] C. Li, F. Qian, M. A. A. S. Choudhury, and W. Du. Stiction quantification based on time and frequency domain criterions. In *Proceedings of 9th IFAC ADCHEM*, pages 635–640, Whistler, BC, Canada, 7–10 June, 2015.

[99] X. Li, J. Wang, B. Huang, and S. Lu. The DCT-based oscillation detection method for a single time series. *Journal of Process Control*, 20(5):609–617, 2010.

[100] X. C. Li, S. L. Chen, C. S. Teo, K. K. Tan, and T. H. Lee. Data-driven modeling of control valve stiction using revised binary-tree structure. *Industrial & Engineering Chemistry Research*, 54:330–337, 2015.

[101] L. Ljung. *System identification: theory for the user (2nd ed.)*. Prentice Hall, New Jersey, USA, 1999.

[102] E. Marchetti, A. Esposito, and C. Scali. A refinement of cascade tuning to improve control performance without requiring any additional knowledge on the process. *Industrial & Engineering Chemistry Research*, 52(18):6193–6200, 2013.

[103] T. Matsuo, H. Sasaoka, and Y. Yamashita. Detection and diagnosis of oscillations in process plants. In *Knowledge-Based Intelligent Information and Engineering Systems*, volume 2773 of *Lect. Notes Comput. Sci.*, pages 1258–1264. Springer Berlin Heidelberg, 2003.

[104] L. F. Mendonça, J. M. C. Sousa, and M. G. J. Sá da Costa. An architecture for fault detection and isolation based on fuzzy methods. *Expert Syst. Appl.*, 36:1092–1104, 2009.

[105] T. Miao and D. Seborg. Automatic detection of excessively oscillatory feedback control loops. In *Proceedings of the IEEE International Conference on Control Applications*, pages 359–364, Kohala Coast, HI, USA, 22–27 August, 1999.

[106] P. Mishra, V. Kumar, and K. P. S. Rana. A novel intelligent controller for combating stiction in pneumatic control valves. *Control Engineering Practice*, 33:94–104, 2014.

[107] P. Mishra, V. Kumar, and K. P. S. Rana. An online tuned novel non linear pi controller for stiction compensation in pneumatic control valves. *ISA Transactions*, 58:434–445, 2015.

[108] E. Naghoosi and B. Huang. Automatic detection and frequency estimation of oscillatory variables in the presence of multiple oscillations. *Industrial & Engineering Chemistry Research*, 53:9247–9438, 2014.

[109] U. Nallasivam, B. Srinivasan, and R. Rengaswamy. Stiction identification in nonlinear process control loops. *Computers & Chemical Engineering*, 34:1890–1898, 2010.

[110] B. Ninness, A. Wills, and A. Mills. UNIT: A freely available system identification toolbox. *Control Engineering Practice*, 21:631–644, 2013.

[111] B. Ould Bouamama, K. Medjaher, M. Bayart, A. Samantaray, and B. Conrard. Fault detection and isolation of smart actuators using bond graphs and external models. *Control Engineering Practice*, 13:159–175, 2005.

[112] G. Pannocchia and M. Calosi. A predictor form PARSIMonious algorithm for closed-loop subspace identification. *Journal of Process Control*, 20:517–524, 2010.

[113] M. A. Paulonis and J. W. Cox. A practical approach for large scale controller performance assessment diagnosis and improvement. *J. Proc. Control*, 13:155–168, 2003.

[114] O. Pozo Garcia, V.-M. Tikkala, A. Zakharov, and S.-L. Jämsä-Jounela. Integrated FDD system for valve stiction in a paper board machine. *Control Engineering Practice*, 21:818–828, 2013.

[115] F. Qi and B. Huang. Estimation of distribution function for control valve stiction estimation. *Journal of Process Control*, 21:1208–1216, 2011.

[116] R. Rengaswamy, T. Hägglund, and V. Venkatasubramanian. A qualitative shape analysis formalism for monitoring control loop performance. *Eng. Appl. Artif. Intell.*, 14:23–33, 2001.

[117] R. S. Risuleo, G. Bottegal, and H. Hjalmarsson. A kernel-based approach to Hammerstein system identification. In *Proceedings of the 17th IFAC Symposium on System Identification*, pages 1011–1016, Beijing, China, 19–21 October, 2015.

[118] R. A. Romano and C. Garcia. Valve friction and nonlinear process model closed-loop identification. *Journal of Process Control*, 21:667–677, 2011.

[119] M. Rossi and C. Scali. A comparison of techniques for automatic detection of stiction: Simulation and application to industrial data. *Journal of Process Control*, 15:505–514, 2005.

[120] M. Ruel. Stiction: The hidden menace. `http://www.expertune.com/articles/RuelNov2000/stiction.htm`, 2000. accessed on 15 December 2014.

[121] K. Salahshoor, I. Karimi, E. N. Fazel, and H. Beitari. Practical design and implementation of a control loop performance assessment package in an industrial plant. In *Proceedings of the 30th Chinese Control Conference*, pages 5888–5893, Yantai, China, 22–24 July, 2011.

[122] T. I. Salsbury and A. Singhal. A new approach for ARMA pole estimation using higher-order crossings. In *Proceedings of the 24th American Control Conference*, pages 4458–4463, Portland, OR, USA, 8–10 June, 2005.

[123] C. Scali and M. Farnesi. Implementation, parameters calibration and field validation of a closed loop performance monitoring system. *Annual Reviews in Control*, 34:263–276, 2010.

[124] C. Scali and C. Ghelardoni. An improved qualitative shape analysis technique for automatic detection of valve stiction in flow control loops. *Control Engineering Practice*, 16:1501–1508, 2008.

[125] C. Scali, S. Marraccini, and M. Farnesi. Key parameters calibration and benefits evaluation of a closed loop performance monitoring system. In *Proceedings of the 9th IFAC-DYCOPS 2010*, pages 683–688, Louvain, Belgio, 5–7 July, 2010.

[126] C. Scali, E. Matteucci, D. Pestonesi, A. Zizzo, and E. Bartaloni. Experimental characterization and diagnosis of different problems in control valves. In *Proceedings of the 18th IFAC World Congress*, pages 7334–7339, Milano, Italy, 28 August–2 September, 2008.

[127] T. B. Schön. An explanation of the expectation maximization algorithm.

[128] M. Shamsuzzoha and S. Skogestad. The setpoint overshoot method: A simple and fast closed-loop approach for PID tuning. *J. of Process Control*, 20:1220–1234, 2010.

[129] Q. L. Shang, J. J. Li, and S. E. Yu. Stiction characteristics identification of pneumatic control valve. *Inf. Technol. Journal*, 12:4790–4796, 2013.

[130] Y. Shardt, Y. Zhao, F. Qi, K. Lee, X. Yu, B. Huang, and S. L. Shah. Determining the state of a process control system: Current trends and future challenges. *Can. J. Chem. Eng.*, 90:217–245, 2012.

[131] B. C. Silva and C. Garcia. Comparison of stiction compensation methods applied to control valves. *Industrial & Engineering Chemistry Research*, 53:397–3984, 2014.

[132] A. Singhal and T. I. Salsbury. A simple method for detecting valve stiction in oscillating control loops. *Journal of Process Control*, 15:371–382, 2005.

[133] S. Sivagamasundari and D. Sivakumar. Estimation of valve stiction using particle swarm optimization. *Sens. Transducers J.*, 129:149–162, 2011.

[134] S. Sivagamasundari and D. Sivakumar. Quantification of nonlinear valve stiction model using compound evolution algorithms. *Int. J. Eng. Res. Appl.*, 2:932–938, 2012.

[135] S. Sivagamasundari and D. Sivakumar. A new methodology to compensate stiction in pneumatic control valves. *Int. J. Soft Comput. Eng.*, 2:480–484, 2013.

[136] B. Srinivasan, U. Nallasivam, and R. Rengaswamy. Multiple root cause analysis of linear oscillatory closed-loop single-input single-output (siso) systems. In *Proceedings of the 4th ADCONIP Conference*, pages 36–41, Thousand Islands Lake, Hangzhou, China, 23–26 May 2011, 2011.

[137] B. Srinivasan, U. Nallasivam, and R. Rengaswamy. Root cause analysis of linear closed-loop oscillatory chemical process systems. *Industrial & Engineering Chemistry Research*, 51:13712–13731, 2012.

[138] B. Srinivasan, U. Nallasivam, and R. Rengaswamy. An integrated approach for oscillation diagnosis in linear closed loop systems. *Chem. Eng. Res. Des.*, 93:483–495, 2015.

[139] B. Srinivasan and R. Rengaswamy. Automatic oscillation detection and characterization in closed-loop systems. *Control Engineering Practice*, 20(8):733–746, 2012.

[140] B. Srinivasan, T. Spinner, and R. Rengaswamy. A reliability measure for model based stiction detection approaches. In *Proceedings of the 8th IFAC-ADCHEM*, pages 750–755, Singapore, 10–12 July, 2012.

[141] B. Srinivasan, T. Spinner, and R. Rengaswamy. A new measure to improve the reliability of stiction detection techniques. *Industrial & Engineering Chemistry Research*, 54:7476–7488, 2015.

[142] R. Srinivasan and R. Rengaswamy. Apparatus and method for stiction compensation in a process control system. 2007/0088446 A1.

[143] R. Srinivasan and R. Rengaswamy. Stiction compensation in process control loops: A framework for integrating stiction measure and compensation. *Industrial & Engineering Chemistry Research*, 44:9164–9174, 2005.

[144] R. Srinivasan and R. Rengaswamy. Techniques for stiction diagnosis and compensation in process control loops. In *Proceedings of the American Control Conference*, pages 2107–2117, Minneapolis, MN, USA, 14–16 June, 2006.

[145] R. Srinivasan and R. Rengaswamy. Approaches for efficient stiction compensation in process control valves. *Computers & Chemical Engineering*, 32:218–229, 2008.

[146] R. Srinivasan, R. Rengaswamy, and R. Miller. Control loop performance assessment. 1. A qualitative approach for stiction diagnosis. *Industrial & Engineering Chemistry Research*, 44:6708–6718, 2005.

[147] R. Srinivasan, R. Rengaswamy, and R. Miller. A modified empirical mode decomposition (EMD) process for oscillation characterization in control loops. *Control Engineering Practice*, 15(9):1135–1148, 2007.

[148] R. Srinivasan, R. Rengaswamy, S. Narasimhan, and R. Miller. Control loop performance assessment 2. Hammerstein model approach for stiction diagnosis. *Industrial & Engineering Chemistry Research*, 44:6719–6728, 2005.

[149] A. Stenman, F. Gustafsson, and K. Forsman. A segmentation-based method for detection of stiction in control valves. *Int. J. Adapt. Control and Signal Process*, 17:625–634, 2003.

[150] M. Stockmann, R. Haber, and U. Schmitz. Pattern recognition for valve stiction detection with principal component analysis. In *Proceedings of the 7th IFAC Symposium on Fault Detection, Supervision and Safety of Technical Processes*, pages 1438–1443, Barcelona, Spain, June 30–July 3, 2009.

[151] P. Subbaraj and B. Kannapiran. Fault detection and diagnosis of pneumatic valve using adaptive neuro-fuzzy inference system approach. *Appl. Soft Comput.*, 19:362–371, 2014.

[152] L. Tang, L. Fang, J. Wang, and Q. Shang. Modeling and identification for pneumatic control valves with stiction. In *Proceedings of the 17th IFAC Symposium on System Identification*, pages 1244–1249, Beijing, China, 19–21 October, 2015.

[153] L. Tang and J. Wang. Estimation of the most critical parameter for the two-movement method to compensate for oscillations caused by control valve stiction. *IEEE Transaction on Control Systems Technology*, 2016.

[154] N. F. Thornhill. Finding the source of nonlinearity in a process with plant-wide oscillation. *IEEE Trans. Control Syst. Technol.*, 13:434–443, 2005.

[155] N. F. Thornhill and T. Hägglund. Detection and diagnosis of oscillation in control loops. *Control Engineering Practice*, 5:1343–1354, 1997.

[156] N. F. Thornhill and A. Horch. Advances and new directions in plant-wide disturbance detection and diagnosis. *Control Engineering Practice*, 15:1196–1206, 2007.

[157] N. F. Thornhill, B. Huang, and H. Zhang. Detection of multiple oscillations in control loops. *Journal of Process Control*, 13(1):91–100, 2003.

[158] V.-M. Tikkala, A. Zakharov, and S.-L. Jämsä-Jounela. A method for detecting non-stationary oscillations in process plants. *Control Engineering Practice*, 32:1–8, 2014.

[159] N. Ulaganathan and R. Rengaswamy. Blind identification of stiction in nonlinear process control loops. In *Proceedings of the American Control Conference*, pages 3380–3384, Seattle, WA, USA, 11–13 June 2008, 2008.

[160] G. Wang and J. Wang. Quantification of valve stiction for control loop performance assessment. In *Proceedings of the 16th International Conference on Industrial Engineering and Engineering Management*, pages 1189–1194, Beijing, China, 21–23 October, 2009.

[161] J. Wang. Closed-loop compensation method for oscillations caused by control valve stiction. *Industrial & Engineering Chemistry Research*, 52:13006–13019, 2013.

[162] J. Wang, A. Sano, T. Chen, and B. Huang. Identification of Hammerstein systems without explicit parameterisation of non-linearity. *International Journal of Control*, 82:937–952, 2009.

[163] J. Wang and Q. Zhang. Detection of asymmetric control valve stiction from oscillatory data using an extended Hammerstein system identification method. *Journal of Process Control*, 24:1–12, 2014.

[164] T. Wang, L. Xie, F. Tan, and H. Su. A new implementation of open-loop two-move compensation method for oscillations caused by control valve stiction. In *Proceedings of 9th IFAC ADCHEM*, pages 433–438, Whistler, BC, Canada, 7–10 June, 2015.

[165] A. Wills, T. B. Schön, L. Ljung, and B. Ninness. Identification of Hammerstein–Wiener models. *Automatica*, 49:70–81, 2013.

[166] L. Xie, Y. Cong, and A. Horch. An improved valve stiction simulation model based on ISA standard tests. *Control Engineering Practice*, 21:1359–1368, 2013.

[167] Z. Xu, C. Q. Zhan, and S. Zhang. Non-invasive valve stiction detection using wavelet technology. In *Proceedings of the Joint 48th IEEE Conference on Decision and Control and the 28th Chinese Control Conference*, pages 4939–4944, Shanghai, China, 16–18 December, 2009.

[168] Y. Yamashita. An automatic method for detection of valve stiction in process control loops. *Control Engineering Practice*, 14:503–510, 2006.

[169] Y. Yamashita. Diagnosis of oscillations in process control loops. In *Proceedings of the 16th Europe Symposium Computer Aided Process Engineering and 9th International Symposium Process System Engineering*, pages 1605–1610, Garmisch-Partenkirchen, Germany, 9–13 July, 2006.

[170] Y. Yamashita. Diagnosis and quantification of control valves. In *Proceedings of the 47th SICE International Conference on Instrumentation, Control and Information Technology*, pages 2108–2111, Tokyo, Japan, 20–22 August, 2008.

[171] H. Zabiri, A. Maulud, and N. Omar. NN-based algorithm for control valve stiction quantification. *WSEAS Trans. Syst. Control*, 4:88–97, 2009.

[172] H. Zabiri and N. Mazuki. A black-box approach in modeling valve stiction. *World Academy of Science, Engineering and Technology*, 68:264–271, 2010.

[173] H. Zabiri and M. J. Ramasamy. Nlpca as a diagnostic tool for control valve stiction. *Journal of Process Control*, 19:1368–1376, 2009.

[174] H. Zabiri and Y. Samyudia. MIQP-based MPC in the presence of control valve stiction. *Chem. Product Process Model*, 4:85–97, 2009.

[175] H. Zabiri, Y. Samyudia, and W. N. W. M. Zainudin. Neural network modeling of valve stiction dynamics. In *Proceedings of the World Congress on Engineering and Computer Science (WCECS)*, San Francisco, USA, 24–26 October, 2007.

[176] A. Zakharov and S.-L. Jämsä-Jounela. Robust oscillation detection index and characterization of oscillating signals for valve stiction detection. *Industrial & Engineering Chemistry Research*, 53:5973–5981, 2014.

[177] A. Zakharov, E. Zattoni, L. Xie, O. P. Garcia, and S.-L. Jämsä-Jounela. An autonomous valve stiction detection system based on data characterization. *Control Engineering Practice*, 21:1507–1518, 2013.

Acknowledgments

The other day, reading the acknowledgments of my Master Thesis, I have been flattened by a sense of deja-vu of unbearable heaviness. Four years have passed, but the (short) considerations to be made at the end of this PhD work are - alas - a natural continuation of the stream of thoughts that flowed at that time.

I keep running my frantic race on the edge, poised between an utopian desire for aesthetic-conceptual perfection and a totally unjustified feeling of cosmic depression. And moreover, I have to note that also this thesis seems to fall in conjunction with another sliding door of my life.

Again, this page only contains so-called "proper thanks", thus excluding other thanks, comments, remarks, considerations and maybe worthlessness and obviousness which I could write at the end of this new sweaty work. Therefore, may be questionable, I will confine myself only to thank those people who have actively contributed to the drafting of this text.

My first thank goes - of course - to Prof. Scali for the time and the passion he has dedicated to me. His support, his critical sense and his psychological incitement have been once again truly remarkable. I have great respect for him and I admire his sympathy and his sarcasm.

The second mention goes to Prof. Pannocchia for the practical help he provided me in the processing of computer codes, and for his natural ability in dissolving all my small and great doubts. And he continues to prove to be *Guru*.

Another thank you goes to Prof. Huang, who kindly welcomed me into his research group in distant and (after all, not so) cold Edmonton. This allowed me to compare myself with other nice young students and researchers working in process control, and to run experiments in his laboratory. Paraphrasing, over there, they seem to practice a "different sport".

Again, a special thank to Prof. Vatistas for his jovial and affectionate manners.

Also thank to the people of the group of ENEL Engineering & Research with whom I collaborated. In particular, thank you to Daniela - organizer and superheroine, Evaldo - who seems to solve all troubles in the pilot plant (IdroLab), and Marco B. for his availability and kindness.

Finally, I thank Marco V. for his willingness to clarify all my doubts and curiosities about the magical world of LaTeX, skills in which he excels despite being a *lake guy*.